PARTIAL MASS RECOVERY FROM DNAPL SOURCE ZONES:

CONTAMINANT MASS FLUX REDUCTIONS AND REDUCTIVE

DECHLORINATION OF RESIDUAL DNAPL

A Thesis
Presented to
The Academic Faculty

by

Eric John Suchomel

In Partial Fulfillment
of the Requirements for the Degree
Doctor of Philosophy in Environmental Engineering in the
School of Civil and Environmental Engineering

Georgia Institute of Technology
December 2006

PARTIAL MASS RECOVERY FROM DNAPL SOURCE ZONES:

CONTAMINANT MASS FLUX REDUCTIONS AND REDUCTIVE

DECHLORINATION OF RESIDUAL DNAPL

Approved by:

Dr. Kurt D. Pennell, Advisor
School of Civil and Environmental
Engineering
Georgia Institute of Technology

Dr. William J. Koros
School of Chemical Engineering
Georgia Institute of Technology

Dr. Joseph B. Hughes
School of Civil and Environmental
Engineering
Georgia Institute of Technology

Dr. Frank E. Löffler
School of Civil and Environmental
Engineering
Georgia Institute of Technology

Dr. Ching-Hua Huang
Civil and Environmental Engineering
Georgia Institute of Technology

Date Approved: August 10, 2006

To my parents
Tom and Sue Suchomel
for their constant love and support

ACKNOWLEDGEMENTS

As my time as a graduate student draws to a close, I would like to acknowledge the many people who made this endeavor such a wonderful experience. First and foremost, I wish to say thank you to my family for their constant love and support over the past five years. No one has done more for me than Mom, Dad, and Heather, and I hope they are as proud of me as I am grateful to them.

Dr. Kurt Pennell, my advisor, has been a constant source of advice and encouragement, both professional and academic, over the past five years. His has pushed me to achievements beyond what I hoped were possible, and his door has always been open to me as a mentor and friend. As I leave Tech I look forward to continuing to interact with him, both personally and professionally.

Dr. Frank Löffler has provided much support and professional advice as a member of my doctoral committee. Perhaps more importantly, he has been an invaluable collaborator on a great deal of the research presented in this dissertation. I would like to express heartfelt gratitude for having had the opportunity to work with him and move my research in unexpected and exciting directions.

I wish to thank Dr. Joseph Hughes for taking time out of his extremely busy schedule to serve on my committee. His support, constructive criticism, and expertise in my research field have all been much appreciated. I also thank Dr. William Koros for serving as a minor advisor on my committee. I am especially grateful for his continued interest in a research project so unlike his own work. Finally, thanks to Dr. Ching-Hua

TABLE OF CONTENTS

LIST OF TABLES

LIST OF FIGURES

LIST OF SYMBOLS AND ABBREVIATIONS

<u>Acronyms</u>

AATDF	Advanced Applied Technology Demonstration Facility
BDI	Bio-Dechlor INOCULUM
CB	chlorobenzene
CMC	critical micelle concentration
CT	carbon tetrachloride
DCE	dichloroethene
DMD	density modified displacement
DNAPL	dense non-aqueous phase liquid
ELSD	evaporative light scattering detector
EO	ethylene oxide
EOR	enhanced oil recovery
FID	flame ionization detector
GAC	granular activated carbon
GC	gas chromatograph
GTP	ganglia-to-pool ratio
HLB	hydrophile-lipophile balance
HOC	hydrophobic organic compound
HRC™	Hydrogen Release Compound
IFT	interfacial tension
ISCO	in situ chemical oxidation
LNAPL	light non-aqueous phase liquid
LT	light transmission
MCL	maximum concentration level
MSR	molar solubilization ratio
NAPL	non-aqueous phase liquids
NRC	National Research Council
PCE	tetrachloroethene
PCR	polymerase chain reaction
PITT	partitioning inter-well tracer test
PV	pore volume
RGB	red, green, and blue color vector
RMSE	root mean-square error
RTm PCR	real time polymerase chain reaction
SDWA	Safe Drinking Water Act
SEAR	surfactant enhanced aquifer remediation
SOC	synthetic organic compound
TCE	trichloroethene
USEPA	United States Environmental Protection Agency
USGS	United States Geological Survey
VC	vinyl chloride
VOC	volatile organic compound
WSR	weight solubilization ratio

Symbols

a_o	specific interfacial area
b	ratio of adsorption and desorption rates
C	concentration
C^a	effluent contaminant concentration
$C^{a, eq}$	equilibrium contaminant concentration
$C^{a, t=0}$	effluent contaminant concentration prior to dissolution
C_C	aqueous concentration of organic compound
$C_{C,sat}$	solubility of organic compound
C_o	initial concentration
C_S	aqueous surfactant concentration
C^S_a	aqueous phase concentration of surfactant
$C_{S,CMC}$	surfactant critical micelle concentration
D_L	free liquid diffusivity
d_{50}	mean grain diameter
g	gravitational constant
h_b	porous media bubbling pressure
K	porous media hydraulic conductivity
K_L	mass transfer coefficient
k	mass transfer coefficient
k_i	intrinsic permeability
k_r	relative permeability
k_{rw}	relative permeability of aqueous phase
M/M^0	fraction of initial contaminant mass remaining in source zone
MF	mass flux
MF_o	initial mass flux
N_A	aggregation number
N_B	Bond number
N_{Ba}	bank number
N_{Ca}	capillary number
N_T	total trapping number
n	porosity
P_c	capillary pressure
P_i, P_o	pressures on concave, convex sides of interface
q_w	aqueous phase Darcy velocity
R_1, R_2	radii of curvature
$R_{F,Lang}$	Langmuir retardation factor
R_{vg}	viscous-to-gravity ratio
Re	Reynolds number
r_p	media pore radius
S	saturation
$S^S_{m,max}$	maximum amount of surfactant sorbed
S_{nwr}	non-wetting fluid residual saturation
S_s	maximum water saturation
S_{wi}	irreducible water saturation
s_a	aqueous phase saturation

t_h	time scale for horizontal NAPL displacement
t_v	time scale for vertical NAPL displacement
U	pore water velocity
U_i	coefficient of uniformity
Z_n	NAPL pool height

Greek Symbols

$\Delta\rho$	difference between aqueous and organic densities
α	angle of system flow to horizontal
γ	interfacial tension
γ_a	organic phase surface tension
γ_{ab}	interaction energy across organic-aqueous phase interface
γ_{aw}	air-water interfacial tension
γ_b	aqueous phase surface tension
γ_{ow}	organic-aqueous phase interfacial tension
θ	contact angle
μ_w	aqueous phase viscosity
ρ_b	bulk density of porous media
ρ_n	NAPL density
ρ_w	water density
τ	angle of displacement for mobilized organic liquid

SUMMARY

Surfactant enhanced aquifer remediation (SEAR) is an *in situ* flushing process where surfactants are used to overcome the limitations associated with pump-and-treat remediation of dense non-aqueous phase liquid (DNAPL) source zones. Efficient treatment of DNAPL source zones, including tetrachloroethene (PCE) and trichloroethene (TCE) DNAPLs, by physicochemical remediation technologies such as SEAR has been demonstrated at both the laboratory and pilot (field) scales. While some studies have reported estimated DNAPL mass recoveries in excess of 90% during SEAR, it is now accepted that some (potentially significant) fraction of initial DNAPL mass present within a source zone will persist following treatment. Recent field studies suggest that DNAPL mass recoveries on the order of 60-70% are more typical for surfactant (and cosolvent) flushing. As a consequence, it is likely that dissolved-phase contaminant concentrations, both within and emanating from, a DNAPL source zone will exceed drinking water standards for long periods of time, even with aggressive treatment. It is therefore reasonable to question what (if any) benefit incomplete or partial mass removal provides with respect to protection of human health and the environment.

A promising strategy for the efficient detoxification and recovery contaminant mass present following partial mass removal is the use of metabolic microbial reductive dechlorination as a tertiary treatment. Reductive dechlorination is an anaerobic process during which PCE is sequentially reduced to the following chlorinated ethenes: TCE, *cis*-dichloroethene (*cis*-DCE), vinyl chloride (VC), and ethene. It was long believed that toxic effects would preclude reductive dechlorination at aqueous PCE concentrations near

saturation or within PCE-DNAPL source zones. However, recent experiments have demonstrated PCE dechlorination in batch systems at both high aqueous PCE concentrations and in the presence of PCE-DNAPL. Dechlorination activity has also been observed in one-dimensional columns (1-D), although activity stalled at *cis*-DCE or VC. While complete dechlorination is a primary goal of reductive dechlorination, partial dechlorination may enhance DNAPL dissolution rate, thereby decreasing source zone longevity. Dissolution enhancement did occur during the column experiments, although technical obstacles such as column bio-clogging, partitioning of dechlorination products into the DNAPL, and pH toxicity effects were apparent.

The primary objective of this research was to further the understanding of the consequences of partial mass recovery from DNAPL source zones. Particular attention was paid to impact of surfactant-based remediation strategies on post-treatment effluent contaminant concentrations and mass flux as well as the applicability of microbial reductive dechlorination as an efficient polishing mechanism for residual DNAPL present in source zones following aggressive physicochemical treatment. Two dimensional (2-D) experimental results indicated that, for some DNAPL compounds (e.g., TCE), recovery by surfactant-enhanced solubilization using the surfactant Tween 80 is comparable to that observed with low interfacial tension (IFT) solutions designed to mobilize the DNAPL. Hence, Tween 80 (or similar surfactants) should be considered for remediation of TCE source zones, particularly if combined with bioremediation of residual contamination.

The effects of partial mass removal on dissolved-phase contaminant flux were investigated in a 2-D aquifer cell containing a PCE source zone and down-gradient plume region. The aquifer cells were flushed with sequential pulses of a 4% Tween™ 80

surfactant solution to achieve incremental PCE mass removal. DNAPL distribution in the source zone was quantified using a light transmission system and expressed in terms of a ganglia-to-pool mass ratio (GTP), which varied from 1.6 (61.5% ganglia) to 0.16 (13.8% ganglia). GTP values decreased with increasing mass recovery, consistent with the observed preferential dissolution of ganglia. Mass flux reductions occurred only after depletion of ganglia mass and were followed by prolonged lower-level mass flux in low-GTP systems containing persistent high-saturation pools. Subsequent experiments revealed similar mass flux reductions with mobilization-based flushing strategies requiring lower volumes of surfactant; however, care must be taken during system design to minimize potential for uncontrolled downward contaminant migration.

Experiments assessing microbial reductive dechlorination in a one dimensional 1-D soil column containing a 10 cm NAPL source zone and a 50 cm down-gradient plume region were also conducted. Activity and distribution of S*ulfurospirillum multivorans*, a PCE-to-*cis*-DCE dechlorinating organism, was evaluated in the presence of either a mixed NAPL (0.25 mol/mol PCE in hexadecane) or pure PCE-DNAPL. PCE to *cis*-DCE dechlorination was observed in the mixed NAPL column, with enhanced PCE dissolution (~4X) and 53% mass recovery after 18 days of operation. Quantitative PCR analysis confirmed a correlation between *S. multivorans* and enhanced PCE dissolution in the source zone. In contrast, minimal reductive dechlorination was observed in the column containing pure PCE-DNAPL. Similar enhancement was observed in a column containing a mixed PCE to ethene dechlorinating consortium; however dechlorination stalled at *cis*-DCE and VC. Results suggest that enhanced dissolution of PCE in NAPL source zones is feasible provided that PCE concentrations remain below toxic levels.

CHAPTER 1

INTRODUCTION AND OBJECTIVES

The presence of dense non-aqueous phase liquids (DNAPLs), particularly the chlorinated organic solvents trichloroethene (TCE) and tetrachloroethene (PCE), in the subsurface has been the subject of a great deal of attention in recent years. Use of these solvents in a variety of settings, ranging from dry cleaning to metal degreasing, has resulted in their widespread release into the environment, through both accidental spills and improper disposal. Once released, DNAPL compounds tend to migrate through the unsaturated zone until encountering the water table, at which point their infiltration into the saturated zone is governed by a number of factors, including the volume of DNAPL spilled, DNAPL viscosity and interfacial tension (IFT), and wettability of the porous media (Mercer and Cohen 1990). Interactions between these factors produce DNAPL source zones, containing complex mixtures of organic-phase ganglia entrapped at or below residual DNAPL saturation and regions of pooled DNAPL at locally high saturations, and capable of producing long-term groundwater contamination (NRC 1997).

It is now widely recognized that conventional pump-and-treat approaches, in which groundwater is extracted from the subsurface and treated above ground to remove dissolved phase contaminants, are ineffective for recovering appreciable fractions of contaminant mass from DNAPL source zones (Mackey and Cherry 1989, MacDonald and Kavanaugh 1994). A number of innovative strategies for source zone treatment have been developed, including *in situ* chemical oxidation, thermal treatment, and cosolvent and/or surfactant flushing. One of the most promising approaches for efficient DNAPL

mass recovery is surfactant enhanced aquifer remediation (SEAR), an *in situ* flushing process utilizing surfactants to overcome many of the limitations associated with pump-and-treat remediation. DNAPL recovery by SEAR is primarily accomplished via two mechanisms: miscible displacement (i.e., solubilization) and/or low interfacial tension (IFT) immiscible displacement (i.e., mobilization). Solubilization increases the aqueous solubility of DNAPL compounds due to contaminant partitioning into the hydrophobic core of surfactant micelles, a process that minimizes the risk of uncontrolled DNAPL migration but may be rate limited and can require large volumes of flushing solution (Taylor et al. 2001). In contrast, mobilization, or displacement of DNAPL free product via IFT reduction, has been shown to be effective (recoveries greater than 80%) with as little as one to two pore volumes of surfactant flushing (Dwarakanath et al. 1999). However, uncontrolled mobilization of DNAPL can result in downward migration of the organic liquid, leading to the contamination of previously unaffected aquifer regions (Ramsburg and Pennell 2001). In an effort to realize the benefits of mobilization while mitigating downward migration of DNAPL free product, the density modified displacement (DMD) method, in which *in situ* alcohol partitioning is used to convert the DNAPL into a light non-aqueous phase liquid (LNAPL) prior to mobilization, was recently developed and tested in two-dimensional (2-D) aquifer cells (Ramsburg and Pennell 2002a, 2002b).

Surfactant-based treatment strategies have been reported to achieve DNAPL recoveries in excess of 90% at several field sites (see e.g., Abriola et al. 2001, Abriola et. 2003, Hasegawa et al. 2000, Londergan et al. 2001). However, it is now generally accepted that some fraction of DNAPL mass initially present within a source zone will

persist following treatment, regardless of the flushing-based strategy employed (Stroo et al. 2003, NRC 2004). Dissolved-phase contaminant concentration within, and emanating from, DNAPL source zones may exceed drinking water standards for long periods of time (on the order of years to decades) following aggressive source zone treatments. It is therefore reasonable to question the benefits of partial mass recovery with regards to protection of human health (Cherry et al. 1997). While it is critically important to understand the impact of partial mass recovery on post-treatment contaminant discharge, assessments to date have been based almost exclusively on mathematical model predictions of DNAPL dissolution. These results have led to conflicting interpretations on the importance of partial mass recovery (e.g., Rao and Jawitz 2003, McWhorter and Sale 2003), and demonstrated that a number of factors, including aqueous-phase flow field and DNAPL distribution, play critical roles in determining post-treatment discharge from DNAPL source zones.

Given that complete dissolution of DNAPL source zone mass remaining after treatment may not occur within reasonable time frames (Christ et al. 2005b), focus has shifted to developing tertiary (or polishing) source zone treatment technologies such as microbial reductive dechlorination. During reductive dechlorination, PCE is sequentially reduced to less-chlorinated daughter products such as *cis*-dichloroethene (*cis*-DCE), vinyl chloride (VC), and ethene, a non-toxic endpoint. A number of column studies have demonstrated that reductive dechlorination performance is possible at relatively high aqueous PCE concentrations or in the vicinity of DNAPL (see e.g., Cope and Hughes 2001, Yang and McCarty 2002), with observed liquid-liquid (DNAPL-water) mass transfer enhancements ranging from 3- to 6-fold. In these studies, PCE dechlorination

stalled at *cis*-DCE or VC rather than complete detoxification to ethene. In addition, system-specific factors such as non-uniform DNAPL distributions, bio-clogging, partitioning of dechlorination products from the aqueous phase into the DNAPL, and toxic effects due to pH reductions make it difficult to apply the column results to other experimental systems.

The overall objective of this research was to evaluate the benefits of partial mass recovery from DNAPL source zones via surfactant flushing, focusing on post-treatment reductions in effluent contaminant concentrations and mass flux, and the potential for coupling microbial reductive dechlorination as a tertiary treatment to surfactant flushing. An understanding of contaminant recoveries expected by surfactant flushing is necessary for evaluating post-treatment plume development. As such, experiments were conducted to evaluate TCE mass recovery as a function of surfactant-based treatment strategy and source zone TCE-DNAPL distribution. Results from these experiments (along with similar experiments previously conducted for PCE) were subsequently used in studies designed to measure post-treatment effluent concentrations and mass flux as a function of contaminant mass recovery, initial DNAPL distribution, and surfactant-based DNAPL recovery mechanism. Since partial source zone mass recovery is unlikely to reduce effluent contaminant concentrations to regulatory limits (i.e., maximum concentration levels or MCLs), column studies were also conducted to evaluated reductive dechlorination performance and distribution of pure and mixed microbial consortia in the vicinity of a PCE-NAPL source zone.

This document begins with a literature review of the processes governing NAPL infiltration and current technologies employed during source zone treatment (Chapter 2).

Also included in Chapter 2 are detailed descriptions of SEAR technologies and recovery mechanisms, and discussions of the limitations associated with source zone treatments (i.e., partial mass recovery) and the feasibility of microbial reductive dechlorination as a tertiary source zone treatment. The materials, experimental equipment and protocols, and analytical methods employed during this research are described in sufficient detail to allow replication of this work (Chapter 3). This is followed by five sections (Chapters 4-8) describing experimental results for each of the specific objectives of this research, and a discussion of the overall conclusions, along with recommendations for related and extended research (Chapter 9). The specific objectives (Chapter 4-8) of this research were:

1. Compare the effectiveness of SEAR-based flushing strategies for remediation of TCE-DNAPL contaminated source zones. Miscible displacement (solubilization), immiscible displacement (mobilization), and density modified displacement approaches were all considered, with the results evaluated on the basis of TCE mass recovery, volume of surfactant solution required, and the occurrence and direction of NAPL displacement. (Chapter 4)

2. Assess the benefits of partial DNAPL mass removal from a contaminated source zone. Even under optimal conditions, aggressive source zone treatment technologies are unlikely to achieve complete contaminant mass recovery. Therefore, reductions in aqueous-phase contaminant effluent concentrations and mass flux were monitored as a function of DNAPL mass recovery via miscible displacement-based surfactant flushing for source zone DNAPL distributions ranging from pool-dominated to ganglia-dominated. (Chapter 5)

3. Evaluate the effects of SEAR-based recovery mechanisms on post-treatment aqueous-phase contaminant effluent concentrations and mass flux. Miscible, immiscible, and density modified displacement can produce radically different post-treatment DNAPL distributions, impacting subsequent aqueous-phase contaminant plume development. Plume development following partial and complete immiscible displacement and density modified displacement of and PCE-DNAPL were monitored and compared to the baseline miscible displacement results described in Chapter 5. (Chapter 6)

4. Evaluate reductive dechlorination activity of *Sulfurospirillum multivorans*, a PCE to *cis*-DCE dechlorinator, in the vicinity of a residual PCE-NAPL source zone. Given that complete NAPL mass removal using physicochemical methods such as SEAR is unlikely, the subsequent use of microbes to enhance mass transfer of residual PCE to accelerate contaminant recovery has been suggested. *S. multivorans* viability both in and near pure PCE-DNAPL (plume concentration of 1,200 μM) and mixed PCE/hexadecane NAPL (plume concentration 300 of μM) source zones was evaluated. (Chapter 7)

5. Assess activity and distribution of a mixed microbial consortium capable of complete dechlorination of PCE to ethene (Bio-Dechlor INOCULUM, BDI) in the vicinity of a mixed PCE/hexadecane source zone. In addition to accelerated mass recovery, a primary goal of bioaugmentation and/or biostimulation is the conversion of PCE to a non-toxic end product (i.e., ethene). Ethene (as well as other PCE dechlorination daughter product) concentrations and the distribution of key *Dehalococcoides* populations capable of ethene production were monitored in a one-dimensional column containing a residual NAPL source zone. (Chapter 8)

CHAPTER 2

LITERATURE REVIEW

2.1 Introduction

Groundwater is a vital natural resource that is used by over 75% of American cities as a drinking water supply (USGS 1998). As early as the 1970s, the presence of synthetic organic contaminants (SOCs) in natural waters was observed. However, the widespread nature of the problem was not recognized until requirements for groundwater monitoring were expanded in the early 1980s (Schwille 1988). Upon recognition of the extent of groundwater contamination in the United States, the U.S. Congress amended the Safe Drinking Water Act (SDWA) in 1986, requiring monitoring of 14 volatile organic compounds (VOCs) in addition to 35 other synthetic organics (Letterman 1999).

In the past, VOCs were often improperly disposed of, either through accidental discharge or intentional release into the subsurface, leading to their widespread presence in groundwater. A survey conducted by the United States Environmental Protection Agency (USEPA) found that SOCs were present in 17% of small-scale and 28% of large-scale public drinking water treatment facilities using groundwater as their water source (USEPA 1990). The SOCs found in groundwater are often characterized by relatively low aqueous solubility values (i.e., less than 1000 mg/L), allowing for their existence as a distinct organic phase in the subsurface if present in sufficient quantity. If a separate organic phase is present, contaminant dissolution from the organic phase into the aqueous phase may provide a long-term source of groundwater contamination. Liquid-liquid mass transfer limitations and contaminant dilution during groundwater flow often prevent the aqueous phase concentration of the contaminant from reaching the aqueous solubility.

However, even if dilution and mass transfer are accounted for, the maximum concentration level (MCL) of these compounds as specified by the USEPA is often greatly exceeded, implying that a distinct organic phase, if present, acts as a source for long-term groundwater contamination.

2.2 Non-Aqueous Phase Liquids

When present in the subsurface as a distinct liquid phase, organic compounds are designated as non-aqueous phase liquids (NAPLs). NAPLs are further subcategorized on the basis of their density relative to aqueous phase (i.e., water); as light non-aqueous phase liquids (LNAPLs) if the organic phase is less dense than the aqueous phase or as dense non-aqueous phase liquids (DNAPLs) if the organic phase has a greater density than the aqueous phase. Table 2.1 lists the physical properties of several DNAPL compounds that are commonly present as subsurface contaminants.

Table 2.1: Properties (at 25°C) of organic compounds that exist as DNAPL contaminants.

Compound Name	Molecular Weight (g/mol)	Aqueous Solubility (mg/L)[a]	Density (g/cm^3) (20°C)[a]	Dynamic Viscosity (cP)[b]	MCL (mg/L)[c]
Chloroform	119.4	8,500	1.48	0.56	-
Carbon Tetrachloride (CT)	153.8	850	1.59	0.85 (30°C)	0.005
Trichloroethene (TCE)	131.4	1,100	1.46	0.53	0.005
Tetrachloroethene (PCE)	165.8	150	1.68	0.80 (30°C)	0.005
Chlorobenzene (CB)	112.6	450	1.11	0.72 (30°C)	0.100

a: Schwarzenbach et al. 2003
b: Riddick and Bunger 1970
c: Ramsburg 2002

Upon release into the subsurface, organic compounds tend to migrate downward through the unsaturated zone until the water table is encountered. Once the water table is reached, LNAPLs will tend to pool along the top of the water table whereas DNAPLs will continue to migrate downward through the saturated zone until a low permeability confining layer is reached, or the organic liquid source exhausted. In addition, capillary forces in the subsurface will act to entrap residual NAPL droplets within the porous medium during migration. The specific behavior of a NAPL during infiltration is influenced by several factors specific to the NAPL as well as the porous media, including viscosity, interfacial tension (IFT), and wettability of the porous media (Mercer and Cohen 1990). The complexity of interactions between these variables in the subsurface, as well as the effects of scale, has led to observations of local entrapped NAPL saturations ranging from 1% up to 50% (Schwille 1988, Lenhard et al. 1993).

2.2.1 Interfacial Tension

The interfacial tension (γ), or IFT, between two fluids arises from the fact that when fluids are in contact with one another a free energy develops due to inward (i.e., away from the interface) molecular attractions between fluid molecules located at the interface (Bear 1972). In order to minimize the free energy present in the system the molecules along the interface attempt to contract, resulting in the generation of a force at the interface. Interfacial tension can be related to the force developed at the interface by dividing the magnitude of the force by a characteristic length, and is typically reported in units of dyne/cm (equivalent to g/s^2). Interfacial tension is dependent on the properties of the two fluids in contact and can be related to the pressure difference across the fluid-fluid interface by the Young-Laplace Equation (Middleman 1998):

9

$$P_c = \gamma \left(\frac{1}{R_1} + \frac{1}{R_2} \right) \qquad (2.1)$$

In Equation 2.1, P_c is the capillary pressure (in units of dyne/cm^2) and R_1 and R_2 are the radii of curvature of the interface in cm (see Figure 2.1). The capillary pressure is equal to the pressure difference across the interface and may be described using $P_c = P_i - P_o$, where P_i and P_o are the respective pressures on the concave and convex sides of the interface. Residual NAPL droplets are entrapped within the aquifer pore space due to the
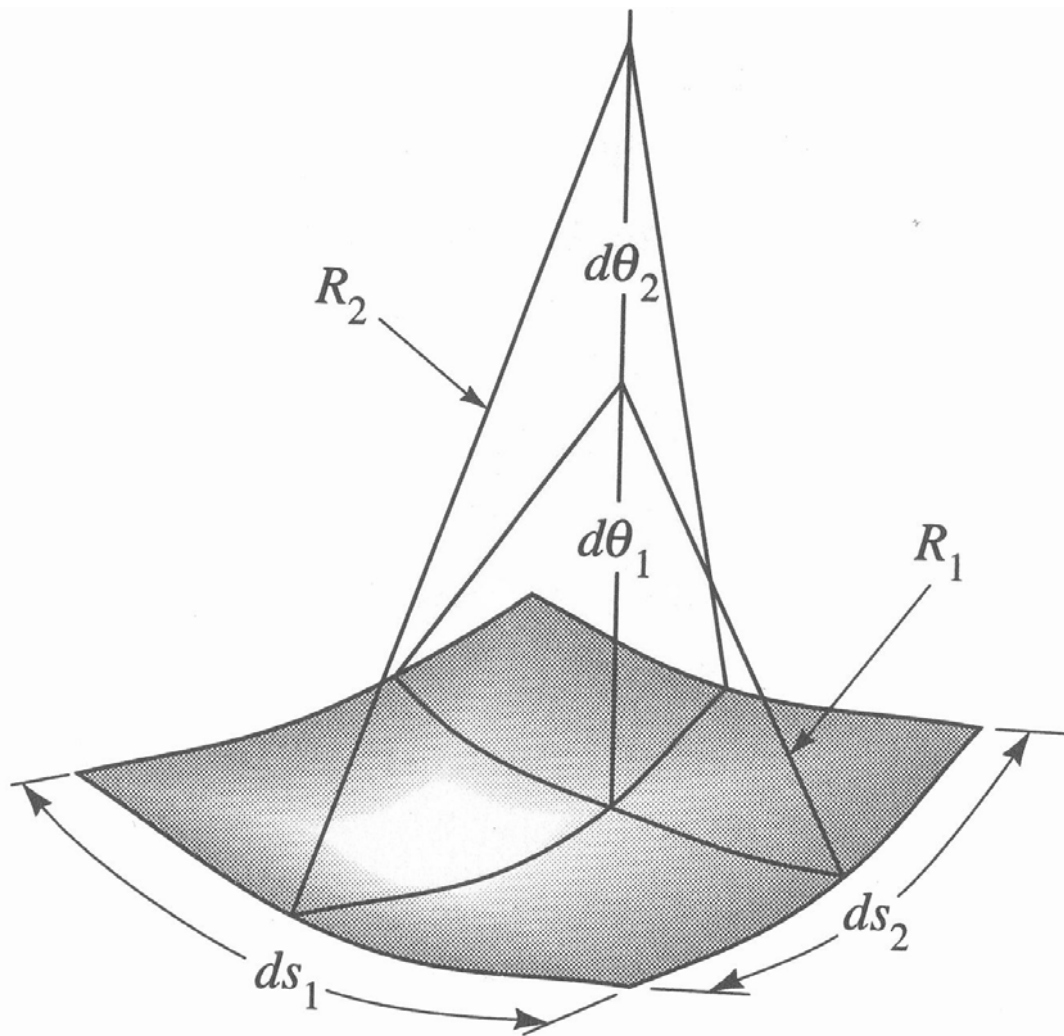
Figure 2.1: Conceptual model of interface between two fluids (Middleman 1998).

tendency of aquifer solids to be coated with water (i.e., water-wetting). The resulting liquid-liquid interface produces a capillary pressure which may be sufficient, depending on the radius of the pore space and the interfacial tension between the organic and aqueous fluids, to cause portions of the NAPL to break off and become entrapped within the porous matrix of the subsurface as discrete globules, or interconnected ganglia.

2.2.2 Wettability

The preferential coating (also known as wetting) of a solid particle by one fluid in the presence of a second, immiscible fluid is referred to as the wettability of a porous media (Morrow 1990). Wettability of a media is generally quantified through use of a water-solid particle contact angle that is measured by placing a drop of organic liquid onto a solid surface in the presence of water. A contact angle of less than 60º indicates a water-wetting surface, while an angle of greater than 120º indicates an oil-wetting (or organic-wetting) surface. Contact angles between 60º and 120º are generally most common and indicate surfaces having intermediate (i.e., neither water- nor oil-) wetting. Solid particles that are considered to be oil-wetting and water-wetting based on this definition are shown in Figure 2.2. Wettability can alternately be determined by placing a drop of water onto a surface in the presence of air, with a contact angle of less than 60º indicating a water-wetting surface. In most research applications (see e.g., Mercer and Cohen 1990, Bradford and Leij 1995) it is typically assumed that the soil matrix was either strongly water-wetting (contact angle less than 60º) or oil-wetting (contact angle less than 120º). Morrow (1990), however, observed that wettability is actually a complex phenomenon dependent on several factors including mineralogy, water chemistry, organic phase chemistry, and soil surface roughness.

In the subsurface, wettability of a porous media has been shown to significantly affect the infiltration and entrapment behavior of NAPL. Assuming a similar particle size distribution, residual NAPL saturation in an intermediate or oil-wetting system will generally be greater than NAPL saturation in a completely water-wetting system (Morrow 1990). In addition, natural systems may contain particles with both water- and oil-wetting characteristics, along with regions of fractional wettability where both water- and oil-wetting particles are present together. In regions of fractional wettability, NAPL saturation tends to be dependent on the relative number of oil-wetting particles present, with an increase in the number of oil-wetting particles resulting in an increase in NAPL saturation (Bradford and Leij 1995).
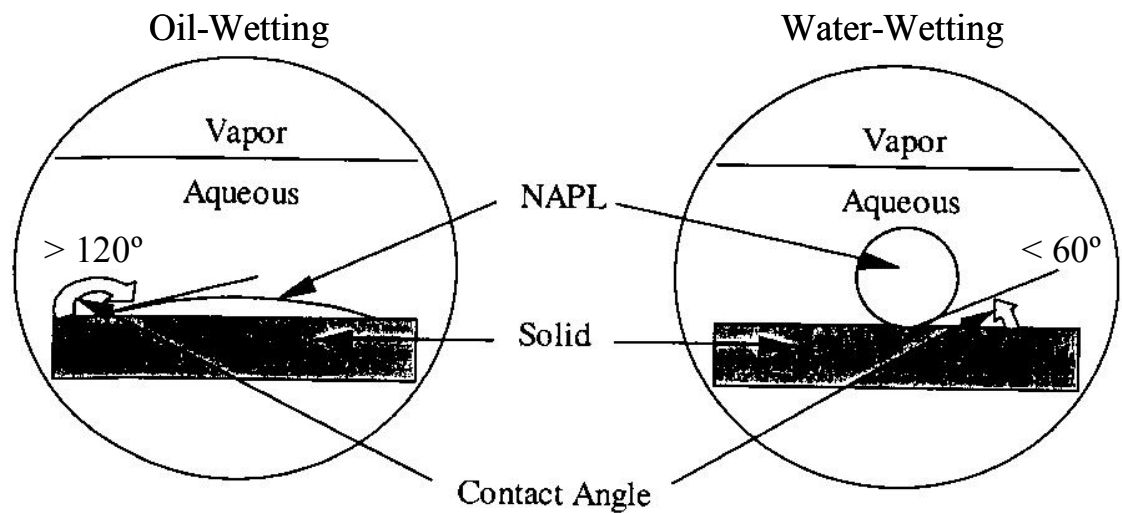
Figure 2.2: Oil-wetting (left) and water-wetting (right) contact angles (Ramsburg 2002).

2.2.3 Capillary Pressure-Saturation

NAPL saturation can be generally related to capillary pressure through use of a capillary pressure-saturation curve (Figure 2.3). Capillary pressure-saturation (P_c-S)

curves are specific to an individual porous medium and are hysteretic in nature, meaning that the P_c-S relationship for increasing water saturation (imbibition) is not the same as the relationship for decreasing water saturation (drainage). Hysteretic behavior is caused by a number of factors, including the geometric shape of a pore causing a lower pressure being required to drain water from the pore than to fill it (known as the "ink bottle" effect), and differences in the water-porous media contact angle during advancement (imbibition) and retreat (drainage) (Fetter 1999).

S_w	=	Wetting Phase Saturation
S_{nw}	=	Nonwetting Phase Saturation
S_{wr}	=	Residual Wetting Phase
S_{nwr}	=	Residual Nonwetting Phase
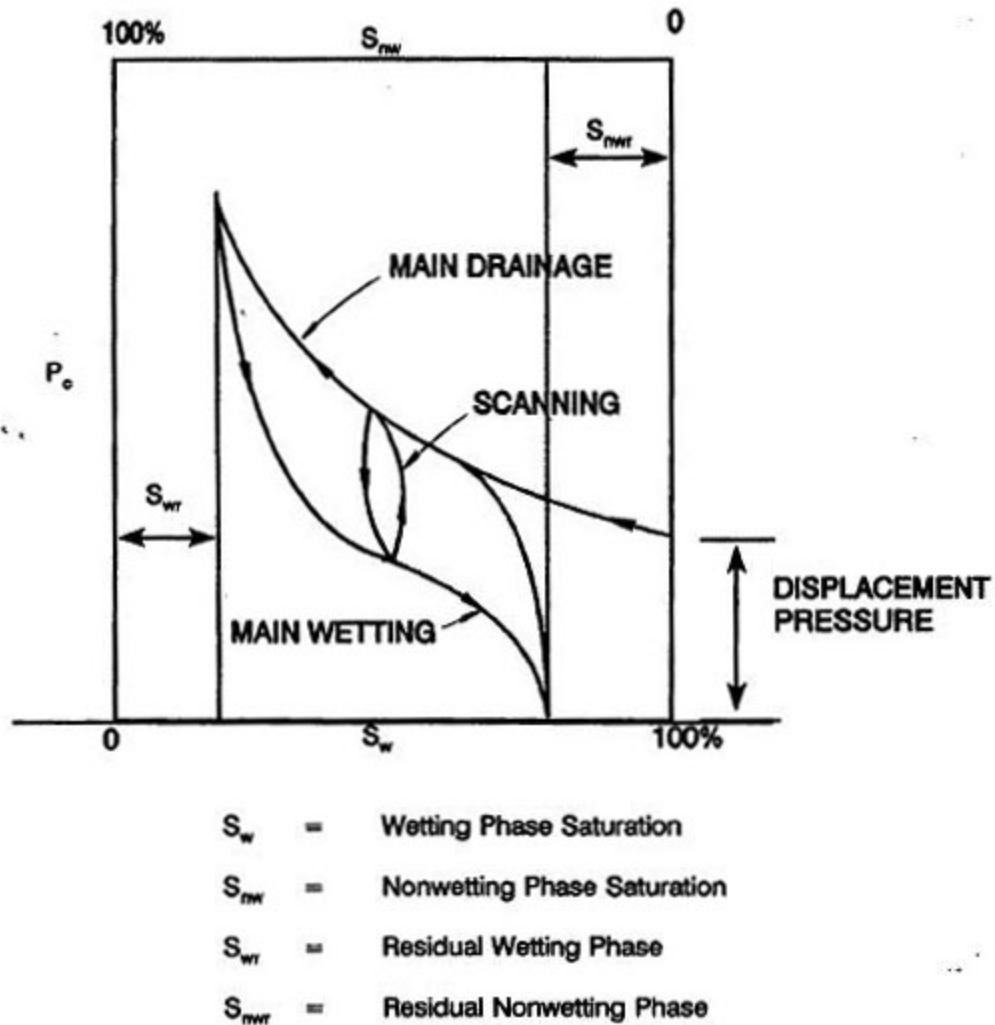
Figure 2.3: General capillary pressure-saturation relationship showing hysteresis (Pankow and Cherry 1996).

13

Empirical models such as the van Genuchten (1980) relationship (Equation 2.2) are typically used to describe the P_c-S relationship. In Equation 2.2, S_{wi} is the residual water saturation, S_s is the maximum water saturation, h_b is the porous media bubbling pressure, and n, m, and α are empirical constants.

$$S = S_{wi} + \frac{S_s - S_{wi}}{\left[1 + (\alpha P_c)^n\right]^m}$$

$$n = \frac{1}{1 - m} \qquad (2.2)$$

$$\alpha = \frac{1}{h_b}\left(2^{1/m} - 1\right)^{1-m}$$

In general, Equation 2.2 can accurately describe the P_c-S behavior for air-water systems; however, it is often unable to adequately describe the behavior for systems containing organic liquids. Hence, a number of studies have attempted to predict the capillary pressure-saturation relationships for both two-phase (oil-water) and three-phase (oil-air-water) systems. The effect of porous medium wettability on P_c-S relationships was investigated by Bradford and Leij (1995, 1996), using interfacial tension (γ) and contact angle (θ) ratios to the scale the air-NAPL capillary pressure-saturation curve. The scaling relationship is shown in Equation 2.3, where the subscripts 1 and 2 represent the two-phase systems being scaled.

$$P_{c1} = \frac{\gamma_1 \cos\theta_1}{\gamma_2 \cos\theta_2} P_{c2} \qquad (2.3)$$

The above relationship is able to scale P_c-S curves reasonable well, provided that the porous media is strongly water wetting (contact angle less than 50º) (Amyx et al. 1960). Based on these promising results, Bradford and Leij (1995, 1996) were the first attempt to predict P_c-S behavior for a fractionally (i.e., not strongly water-wetting) wetting

14

system. Results from these studies suggest that porous media wettability may play a key role in describing multi-phase flow behavior in some systems.

In general for fractionally wetting systems (i.e., not strongly water-wetting), residual saturation increases with decreasing particle size (Bradford et al. 1999). In addition, mass transfer of the contaminant from the organic to the aqueous phase is increased due to an increase in the interfacial area. It was hypothesized by Hassanizadeh and Gray (1990) that the hysteretic nature of the P_c-S curve is an artifact resulting from projection of the three-dimensional capillary pressure-saturation-interfacial area relationship onto the two-dimensional capillary pressure-saturation plane. However, it was demonstrated by Reeves and Celia (1996) that, although there is a relationship between capillary pressure, interfacial area, and saturation, the relationship postulated by Hassanizadeh and Gray (1990) could not explain P_c-S hysteresis.

While the previously described P_c-S relationships are true static systems, Bradford and Leij (1995, 1996) also observed that dynamic properties such as the relative NAPL permeability also play a key role in describing multi-phase flow behavior. Aqueous (wetting phase) flow in a two-phase flow can be described using a modified version of Darcy's law (Equation 2.4, Schwille 1984), where q_w is the wetting phase Darcy velocity, ρ_w is the wetting fluid density, μ_w is the wetting fluid viscosity, and dh_w/dl is the head gradient of the wetting fluid.

$$q_w = \frac{-k_r k_i \rho_w}{\mu_w} \frac{dh_w}{dl} \qquad (2.4)$$

A similar expression may also be written for the organic wetting (i.e., NAPL) phase. In general, the presence of entrapped NAPL in the subsurface will result in a reduction in the permeability of the porous medium. This reduction is described through use of the

relative permeability (k_r), the ratio of the permeability for a fluid (either NAPL or water) at a given saturation to the intrinsic permeability of the porous media (k_i). This relationship can be shown graphically thorough use of relative permeability curves (Figure 2.4). In Figure 2.4, the water content at which the wetting fluid (typically water) no longer flows is the irreducible water saturation (S_{wi}). A similar value, the residual saturation (S_{nwr}) can be used to describe the saturation below which the non-wetting fluid (typically NAPL) no longer flows.
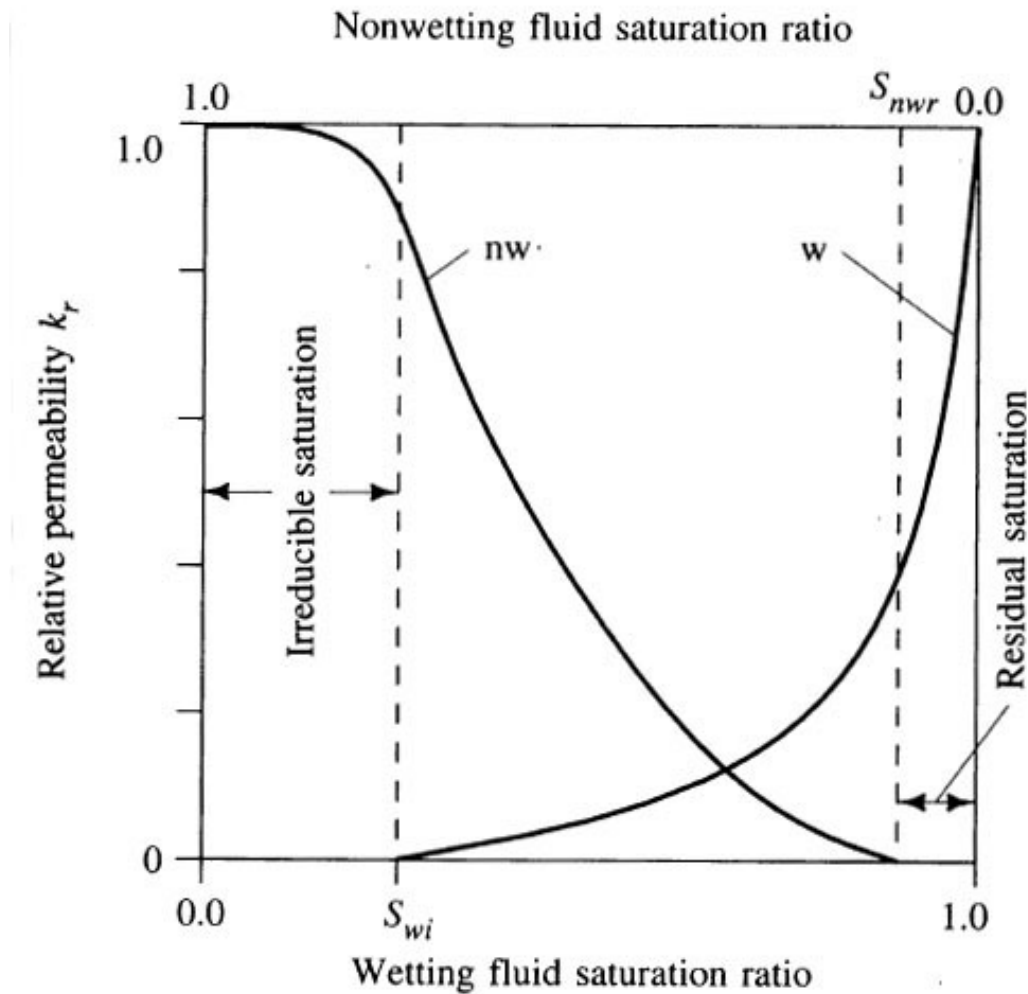
Figure 2.4: Relative permeability curves for a two-phase system (Fetter 1999).

In a two-phase aqueous-organic system during NAPL infiltration, the organic phase will tend to take the path of least resistance, preferentially flowing through subsurface regions of high permeability. If a region of low permeability is encountered, lateral spreading of the NAPL will occur. When the area available for lateral spreading is limited, NAPL pooling, characterized by areas of locally high NAPL saturation (i.e., greater than residual), will occur above regions of low permeability. The presence of NAPL pools can increase the pressure head exerted on the low permeability regions; if the pressure head exceeds the entry pressure of the porous media, infiltration of the NAPL into the low permeability region can occur. The pressure head required for NAPL infiltration into subsurface regions of low permeability was expressed by Cohen and Mercer (1993) and Pankow and Cherry (1996) in units of NAPL pool height as:

$$Z_n = \frac{2\gamma \cos\theta}{r_p g \rho_n} \qquad (2.5)$$

where Z_n is the NAPL pool height, γ is the interfacial tension between the organic and aqueous phases, θ is the contact angle, r_p is the pore radius of the low permeability media, g is the gravitational constant, and ρ_n is the NAPL density. Alternately, McWhorter and Nelson (1979) developed an empirical correlation (Equation 2.6) to describe the entry pressure of a NAPL pool when pore radius data is unavailable.

$$Z_n = 9.6 \left(\frac{\rho_w}{\rho_n - \rho_w} \right) \left(\frac{\gamma}{\gamma_{aw}} \right) \left(\frac{K}{n} \right)^{-0.403} \qquad (2.6)$$

In Equation 2.3, ρ_w is the density of water, γ_{aw} is the air-water interfacial tension (usually assumed to be 65 dynes/cm), K is the hydraulic conductivity of the porous media in units of cm/s, and n is the media porosity.

2.2.4 NAPL Dissolution

DNAPLs, when entrapped and/or pooled in the subsurface, can act as long-term sources of groundwater contamination. The region of an aquifer where entrapped or pooled DNAPL exists is known as the source zone. As previously uncontaminated water moves through the source zone, dissolution of contaminant from the NAPL into the aqueous phase occurs, resulting in down-gradient movement of the contaminant. This aqueous phase contamination is generally referred to as the groundwater plume; contaminant concentration within the plume can be no greater than the aqueous solubility of the contaminant and is generally much lower.

Contaminant dissolution is often rate limited by mass transfer from the organic to aqueous phase due to a variety of factors, including subsurface heterogeneity. The presence of heterogeneity in source zone may create zones of bypassing and/or limited contact where there is little opportunity for mass transfer from the organic to the aqueous phase (Powers et al. 1991). In addition, DNAPL distribution (i.e., interfacial area) can limit contaminant mass transfer, with regions of extensive DNAPL pooling exhibiting lower mass transfer rates than regions primarily characterized by entrapped DNAPL globules at residual saturation (Rathfelder et al. 2001). Contaminant mass transfer from the organic phase into the aqueous phase is conceptually described in Figure 2.5, where $C^{a,eq}$ is the equilibrium solubility of the contaminant, C is the bulk aqueous phase contaminant concentration, and δ is the film thickness. Based on this conceptual model, NAPL dissolution rate has been described using a linear driving force expression (Equation 2.7, see e.g., Powers et al. 1991, Taylor et al. 2001), where q is the Darcy velocity, k is the mass transfer coefficient and a_o is the specific surface area of the NAPL.

$$q\frac{dC}{dt} = ka_o\left(C^{a,eq} - C\right) \qquad (2.7)$$

The parameters k and a_o are often combined into a lumped mass transfer constant that can be related to the modified Sherwood number (Equation 2.8).

$$Sh' = \frac{ka_o(d_{50})^2}{D_L} \qquad (2.8)$$

A number of empirical correlations have been developed for estimation of the modified Sherwood number. A representative one, incorporating the aqueous phase Reynolds number and median grain size (d_{50}) and uniformity index (U_i) of the porous media is given below (Equation 2.9, Powers et al. 1991).

$$Sh' = 57.7\,\text{Re}^{0.61}\,d_{50}^{0.64}U_i^{0.41} \qquad (2.9)$$

While the empirical correlations described above are useful, care must be taken when employing them, as they are system specific and will not adequately describe conditions for scenarios such as flow interruptions (Taylor et al. 2001).
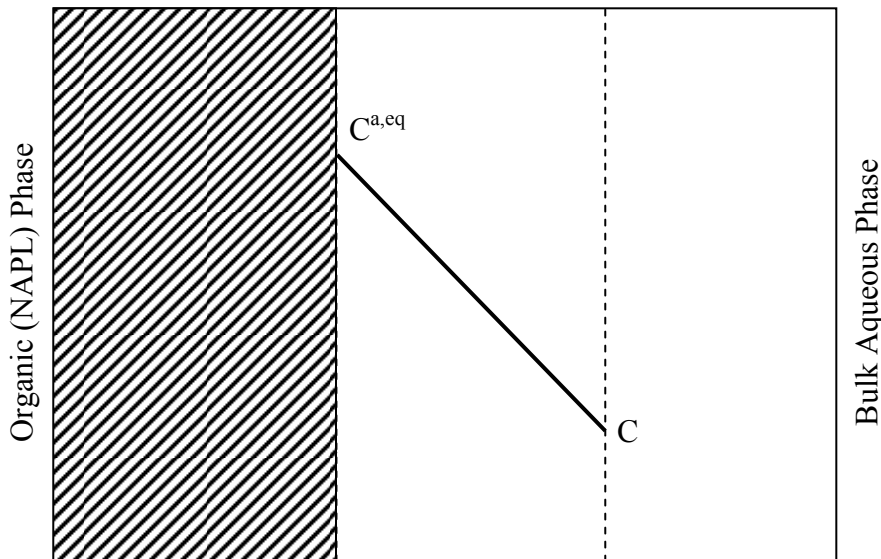
Figure 2.5: Conceptual description of mass transfer from organic phase (NAPL) to bulk aqueous phase.

Local mass transfer from NAPL compounds to the aqueous phase will generally be at equilibrium (i.e., bulk concentration equal to solubility), unless aqueous flow in the system is at a very high rate (Powers et al. 1991). Despite this observation, contaminant concentrations within the aqueous plume will nonetheless be low due to flow bypassing and dilution, usually on the order of mg/L (ppm); however, even these low concentrations greatly exceed the MCL for many contaminants (typically μg/L or ppb level, see Table 2.1). As a result, the presence of a DNAPL source zone can render large quantities of groundwater unsuitable for use. In addition, many currently employed source zone remediation technologies rely on DNAPL dissolution to achieve contaminant removal and are therefore of limited use in cases where the contaminant has a low aqueous solubility. Taken together, these issues present a great a challenge with respect to removal of source zone contaminants and restoration of contaminated aquifers to required water quality standards.

2.3 Source Zone Remediation Technologies

In the past, pump-and-treat was the most commonly applied method for treatment of DNAPL contaminated aquifers. During pump-and-treat, contaminated groundwater is extracted to the surface where it is treated to the MCL, usually by either air stripping to remove VOCs or contaminant adsorption onto granular activated carbon (GAC), and then either released back into the subsurface, released to surface waters, or discharged to a treatment facility. Because the pump-and-treat process focuses solely on the aqueous phase, successful source zone remediation is dependent on contaminant dissolution into the aqueous phase. Pump-and-treat remediation is an effective means for plume containment and dissolved phase recovery, and is economically attractive due to its

relatively low initial cost compared to other technologies (Ramsburg and Pennell 2001). However, for DNAPL source zones, particularly in areas of subsurface heterogeneity, pump-and-treat has been shown to be unsuccessful at removing significant fractions of contaminant mass in reasonable time frames (years to decades) and operational, maintenance, and monitoring costs are prohibitive (Mackey and Cherry 1989, MacDonald and Kavanaugh 1994, NRC 1997).

The efficiency of pump-and-treat remediation of DNAPL source zones is limited by both the low aqueous solubility of many DNAPL compounds as well as mass transfer limitations that often arise in the subsurface. As a result, dissolution of DNAPL mass in the subsurface can be a time intensive process, regardless of its distribution. In an effort to increase the efficiency and effectiveness of DNAPL source zone treatment, a number of innovative technologies have been developed, including chemical oxidation, thermal treatment, and cosolvent flushing, and surfactant flushing. The first three technologies are briefly described in subsections below. The fourth (surfactant flushing) is the primary *in situ* source zone treatment used in this research. Surfactant flushing was selected for a number of reasons, including flexible potential recovery mechanisms (i.e., miscible displacement versus immiscible displacement), potential for coupling with post-treatment bioremediation (see e.g., Christ et al. 2005a), and general low cost and toxicity of surfactants. Surfactant flushing is described in detail in section 2.4, focusing on recovery mechanisms and the potential for coupling with bioremediation.

2.3.1 *In Situ* Chemical Oxidation

The objective of *in situ* chemical oxidation (ISCO) is to transform potentially toxic contaminants into benign daughter products. The most common oxidant used in

subsurface remediation is Fenton's reagent, in which a concentrated hydrogen peroxide solution (10-50%) is used in conjunction with a ferrous iron catalyst (e.g., iron sulfide) to produce highly reactive hydroxyl radicals (Equation 2.10, Zoh and Stenstrom 2002).

$$H_2O_2 + Fe^{2+} \rightarrow Fe^{3+} + OH^- + OH^{\bullet} \qquad (2.10)$$
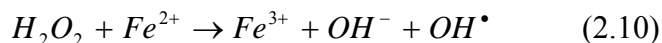
Hydroxyl radicals (along with radicals produced during side reactions such as $O_2^{\cdot}$) are powerful, non-specific oxidants that are able to react with a variety of volatile organic compounds. As a result, they have been widely investigated as a means for remediation of contaminants typical to DNAPL source zones (e.g., Chen et al. 2001, Teel et al. 2001). Other potential oxidants such as permanganate have also been investigated (e.g., Schroth et al. 2001, MacKinnon and Thomson 2002); however, Fenton's reagent offers the highest potential for oxidation at a reasonable cost (Basel and Nelson 2000). In addition to extensive laboratory investigation, a limited number of chemical oxidation field studies have been performed to date using a variety of chemical oxidants (see e.g., USEPA 1998, USEPA 2000). Results have generally been comparable to those observed for the test cell at Cape Canaveral, Florida. During the test, contaminant mass recovery/destruction estimates ranged from 62-84%; however, DNAPL migration to regions outside the test cell was observed (Battelle 2001, Stroo et al. 2003).

Chemical oxidation is attractive because it transforms the contaminant, which can alleviate the need for post-treatment contaminant disposal that is often required by other technologies. In addition, oxidation reaction rates are rapid, potentially shortening required remediation times. The major drawback of ISCO is that it is a nonspecific technology that allows for oxidation of all subsurface carbon, including microorganisms and soil organic matter, potentially negatively altering the subsurface composition (Basel

and Nelson 2000). This can also result in consumption of the oxidant prior to its reaching the target areas of contamination. Additionally, chemical oxidation is most appropriate as a dissolved phase treatment, limiting its potential value in source zone remediation (Chen et al. 2001). Also, the ferric iron and permanganate species present during chemical oxidation will precipitate should the subsurface pH increase above very acidic values (less than 3), with the resulting solid precipitates potentially reducing the porous media permeability, resulting in flow bypassing (Chen et al. 2001, Schroth et al. 2001).

2.3.2 Thermal Treatment

The objective of thermal remediation is to vaporize and/or displace contaminants from both the saturated and unsaturated zones of the subsurface. Displaced contaminants are recovered as a distinct organic liquid or vapor for subsequent above-ground treatment and disposal. The heating of the subsurface required for thermal remediation can be achieved through a variety of techniques, including electrical heating, steam injection, and radio frequency heating. A limited number of laboratory-scale experiments have demonstrated the potential for successful remediation when steam injection is employed (e.g., Hunt et al. 1988, She and Sleep 1999). Thermal treatments in general, and steam flushing in particular, are attractive because they may potentially be effective with a wide variety of compounds. However, steam flushing can be a highly energy intensive process, and the low interfacial tension (IFT) between the steam and NAPL can lead to uncontrolled downward DNAPL migration (Schmidt et al. 2002). Successful mitigation of downward DNAPL displacement has been reported at laboratory-scale through employment of co-injected steam and air (Schmidt et al. 2002, Kaslusky and Udell 2002).

In addition, a limited number of field-scale thermal remediation studies have been conducted utilizing both steam injection and electrical heating (see e.g., USEPA 1995, USEPA 2000). Field tests focusing on steam injection to recover pentachlorophenol and heating oil have reported recoveries ranging from 65-86% (Soga et al. 2004). Heron and coworkers (2005) conducted a test at the Young-Rainey STAR Center, Largo, Florida using a combination of steam extraction and electrical resistance heating. Recovery of a mixed DNAPL was estimated to exceed 99% over a 4.5 month operational period. Recent demonstrations of six-phase heating (Battelle 2001) for DNAPL recovery were characterized by more moderate mass reductions (approximately 90%) as well as possible DNAPL penetration into a previously uncontaminated lower confining layer.

2.3.3 Cosolvent Flushing

During cosolvent flooding a concentrated alcohol solution, typically comprised of up to 80-95% alcohol with the balance water, is injected into the subsurface. At high concentrations, alcohol solutions will act as cosolvents, greatly increasing the aqueous solubility of many organic-phase contaminants due to the miscibility of the alcohol-NAPL system. In addition, highly concentrated alcohol solution may also lower the interfacial tension (IFT) between the aqueous and organic phases, resulting in low-IFT displacement (mobilization) of the NAPL. Taken together, these factors make cosolvent flooding a potentially very attractive remediation technology. Laboratory studies (Imhoff et al. 1995, Lunn and Kueper 1997) have demonstrated the effectiveness of this technology in remediation of NAPL source zones. Lunn and Kueper (1997) reported efficient recovery of greater than 90% of the PCE initially present in a 2-D aquifer cell during flushing with a 90% ethanol cosolvent formulation. Effluent PCE concentrations

of nearly 100,000 mg/L were observed, and no DNAPL displacement was observed. Conversely, while PCE recovery with a 90% 1-propanol cosolvent was also high (up to 96%), the primary contaminant recovery mechanism was PCE mobilization.

In addition, several field-scale demonstrations of cosolvent flushing have been conducted, most notably at Dover Air Force Base and the former Sage's dry cleaner site in Jacksonville, Florida (see e.g., Rao et al. 1997, Falta et al. 1999, Jawitz et al. 2000). The preliminary cosolvent flushing study conducted at the Dover Site demonstrated recovery of approximately 64% of PCE mass initially present in a contained test cell (Rao et al. 1997). A second study in Jacksonville, Florida was able to achieve similar PCE mass recovery (62-65%) without test cell confinement; down-gradient aqueous PCE concentrations were reduced by up to 92% following cosolvent flushing (Jawitz et al. 2000). While cosolvent flushing holds potential as a subsurface remediation technology, it has a number of possible drawbacks, including downward DNAPL migration during displacement, density override of the less dense alcohol solution, relatively high costs associated with concentrated alcohol solutions (approximately $1/gallon for ethanol), and safety hazards arising from the flammability of many alcohols (particularly ethanol).

2.4 Surfactant Enhanced Aquifer Remediation

Surfactant enhanced aquifer remediation (SEAR) is a source zone remediation technology closely related to cosolvent flushing. The term SEAR is generally used to describe any *in situ* flushing process in which surfactants are used in an effort to overcome the limitations associated with pump-and-treat remediation of contaminant source zones. Remediation is achieved by utilizing surfactant solutions to either increase the apparent aqueous solubility of a contaminant and/or displace (mobilize) and recover

the DNAPL as a distinct liquid phase. In both cases, the time required for treatment is greatly reduced when compared to pump-and-treat. A potential drawback of displacement-based SEAR, however, is the possibility of decreased interfacial tension between the aqueous and organic phases leading to downward DNAPL migration. Also, the equipment requirements for SEAR-based remediation (e.g., injection and effluent treatment systems), as well as surfactant costs (e.g., $1.50/gallon of Tween 80), can result in initial capital costs for SEAR that are significantly greater than those of conventional pump-and-treat systems (Ramsburg and Pennell 2001). However, since SEAR-based technologies can achieve source zone remediation much more efficiently than pump-and-treat systems, these increased capital costs can be offset by reductions in both the time required for source zone remediation and the volume of effluent requiring above-ground treatment. Ramsburg and Pennell (2001) conducted a cost comparison between surfactant flushing and pump-and-treat, observing that fixed capital and chemical costs were greater for the former ($330,000 versus $120,000). However, pump-and-treat remediation time was 4,400 days compared to 36 days for surfactant flushing, resulting in increased operation and maintenance costs and a much greater total cost, $1,170,000 for pump-and-treat as opposed to $380,000 for surfactant flushing.

SEAR-based source zone remediation strategies rely on two primary mechanisms for DNAPL removal; miscible and immiscible displacement. Miscible displacement (also referred to as solubilization) is based on an increase in the aqueous solubility of a contaminant in the presence of a surfactant due to the formation of surfactant micelles. During miscible displacement the DNAPL remains relatively stationary in the subsurface. Immiscible displacement, or mobilization, relies on a reduction in the IFT between the

organic (DNAPL) and aqueous phases resulting from accumulation of surfactant molecules at the interface between the two phases. The resulting decrease in IFT allows for entrapped and pooled DNAPL to be mobilized/released, resulting in formation of a bank of organic phase contaminant that is subsequently recovered as free product. Immiscible displacement can also result in significant DNAPL migration and redistribution within the subsurface. It is important to note that miscible and immiscible displacement are not mutually exclusive – they may be observed simultaneously, with contaminant recovery attained via mobilization often resulting in additional significant DNAPL solubilization.

2.4.1 Surfactants

Surfactants, or surface active agents, are an important class of chemicals that are widely used in products ranging from detergents, pharmaceuticals, and food products to fuel additives. In solution, surfactants molecules will generally preferentially accumulate at surfaces or interfaces due to their molecular structure. The molecular structure of a typical surfactant consists of two distinct moieties, hydrophobic and hydrophilic, that act to create the features unique to this class of chemical. Generally, the hydrophobic region of a surfactant is comprised of a long chained alkane, while the composition of the hydrophilic moiety varies. Differences in the hydrophilic moiety structure are used to categorize surfactants into four classes: zwitterionic, cationic, anionic, and nonionic (Rosen 1989). Substitution of native subsurface cationic species with cationic surfactants has been investigated in the past as a means for increasing *in situ* contaminant sorption capacity (Xu and Boyd 1995). However, cationic surfactant toxicity as well as the high costs associated with these compounds has led to abandonment of this approach; current

SEAR research is focused nearly completely on anionic and nonionic surfactant species. Table 2.2 lists several anionic and nonionic surfactants, many of which have been investigated for use in SEAR-based remediation, and Figure 2.6 shows representative nonionic and anionic surfactant structures.

Table 2.2: Anionic and nonionic surfactants that have been used in SEAR.

Trade Name	Chemical Name	Manufacturer
Anionic		
Aerosol AY100	Sodium diamyl sulfosuccinate	Cytec Industries
Aerosol MA80-I	Sodium dihexyl sulfosuccinate	Cytec Industries
Aerosol OT100	Sodium dioctyl sulfosuccinate	Cytec Industries
Alfoterra 145-4 PO Sulfate	Propoxylated alcohol ether sulfate	Custom
Dowfax 8390	Hexadecyl diphenyloxiide disulfonate	Dow Chemical
Hostapur SAS	Sodium secondary alkane sulfonate	Hostapur
Rexophos 25/97	Phosphated alkyl phenol ethoxylate	Emkay Chemical
Nonionic		
Brij 97	Polyoxyethylene 10 oleyl ether	Uniqema
Span 80	Sorbitan monooleate	Uniqema
Tergitol 15-S-12	Secondary alcohol ethoxylate	Union Carbide
Triton X-100	Octylphenol ethoxylate	Union Carbide
Tween 80	Polyoxyethylene 20 sorbitan monooleate	Uniqema
Witconol 2722	Polyoxyethylene 20 sorbitan monooleate	Witco
Witconol NP-100	Nonylphenol ethoxylate	Witco
Witconol SN-120	Linear alcohol ethoxylate	Witco

Anionic surfactants are characterized by a hydrophilic moiety that carries a negative charge. They may be further subcategorized by the type of functional group that comprises the hydrophilic moiety (e.g., sulfate, carboxylate, or phosphate). Most anionic surfactants are relatively inexpensive and as a result have been widely employed as detergents and for enhanced oil recovery (EOR) (Shah and Schecter 1977). Salt addition to anionic surfactant formulations can alter the resulting phase behavior of the organic

and aqueous phases, allowing anionic formulations to be easily modified to optimize contaminant recovery (Dwarakanath et al. 1999). As a result, a number of studies have investigated this surfactant class for use in SEAR-based remediation (e.g., Pennell et al. 1994, Dwarakanath et al. 1999).

While uncharged, the hydrophilic moieties of nonionic surfactants remain highly polar, generally due to the presence of multiple ethylene oxide (EO) functional groups within the molecule. Nonionic surfactants are excellent emulsifying agents (Rosen 1989) and many are easily biodegraded and have thus seen widespread use in a variety of household products (Pennell et al. 1997). While a number of nonionic surfactants may have the potential to adversely affect human health (e.g., Triton X-100 and alkylphenols) others, including the Tween and Witconol groups, are relatively nontoxic in nature and have been employed in food-grade applications. As a result, a great deal of research has focused on the possibility of utilizing these compounds in aquifer remediation (e.g., Shiau et al. 1994, Taylor et al. 2001, Ramsburg and Pennell 2001).

Surfactants, when present at sufficient concentration, tend to self-aggregate to form micelles due to their unique molecular structure. Micelles are formed as a result of interactions between either the hydrophobic or hydrophilic moieties of individual surfactant monomers (Attwood and Florence 1983). Under aqueous conditions such as those typically found in the subsurface, micelle formation results from interactions between the hydrophobic moieties of surfactant monomers. These micelles may be visualized as having a hydrophobic core that is surrounded by a hydrophilic mantle or shell (Figure 2.7). Although the micelle depicted in Figure 2.7 is an idealized sphere,

actual micelle shapes vary from this based on the structure of the surfactant monomers
(Attwood and Florence 1983).

w + x + y + z = 20
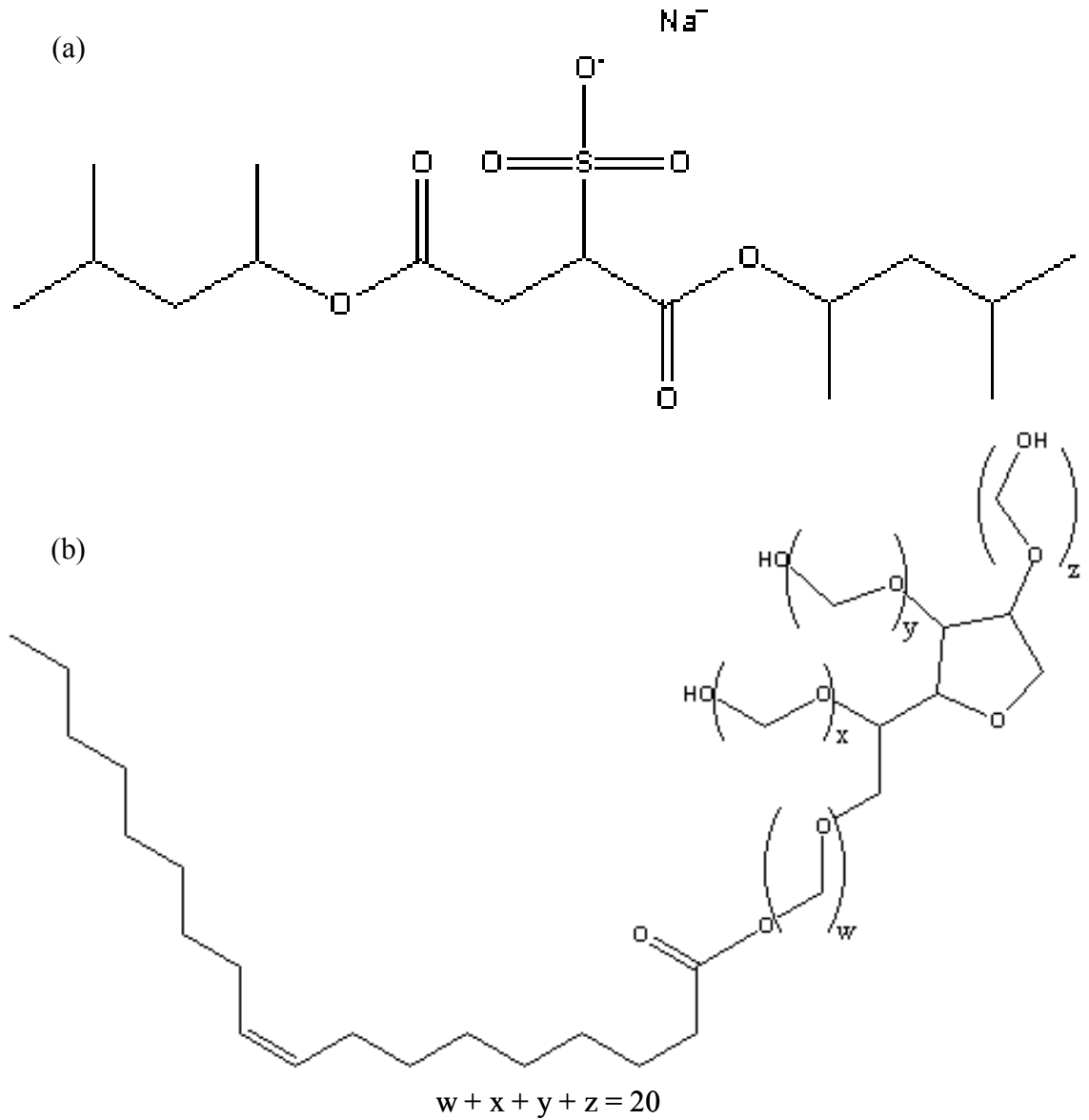
Figure 2.6: Representative structures for an (a) anionic (Aerosol MA, molecular weight:
388 g/mol) and (b) nonionic (Tween 80, molecular weight: 1310 g/mol) surfactant.
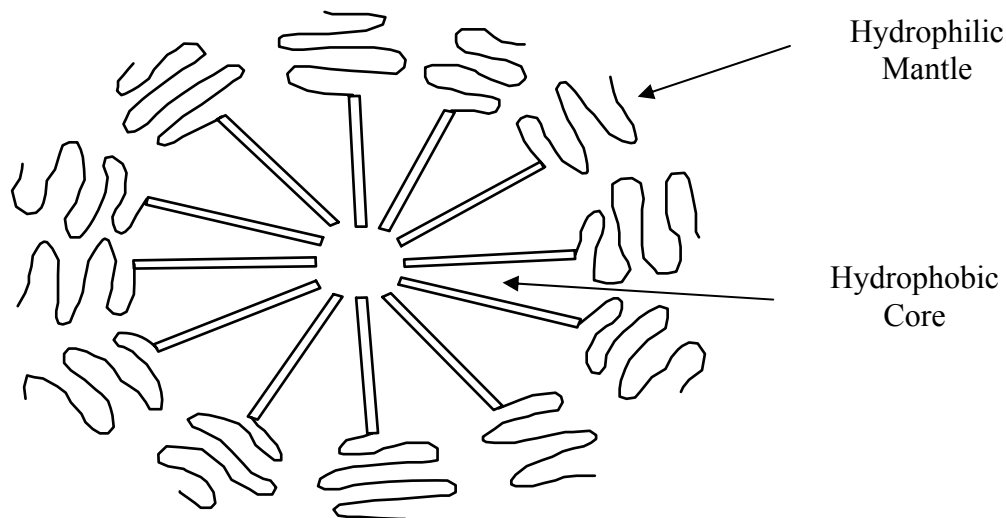
Figure 2.7: Structure of idealized nonionic surfactant micelle in an aqueous system.

The surfactant concentration at which self-aggregation to form micelles occurs is referred to as the critical micelle concentration, or CMC. At concentrations greater than the CMC, the number of surfactant monomers (i.e., molecules not associated with a micelle) present in solution will remain constant, while the number of micelles will increase with increasing surfactant concentration. The aggregation number (N_A), or number of surfactant molecules that comprise an individual micelle, does not generally change with changing surfactant concentration under normal conditions (Pennell and Abriola 1997). However, alterations to physical conditions such as electrolyte addition (anionic or nonionic surfactants) or changing temperature (nonionic surfactants) may affect the phase behavior of the surfactant solution, altering micelle composition (Pennell and Abriola 1997). The CMC of a surfactant may be indirectly estimated based on the surface tension of the surfactant solution, or the interfacial tension at the air-surfactant

solution interface (Rosen 1989). At concentrations below the CMC, surfactant monomers preferentially accumulate at the air-aqueous solution interface, thereby acting to lower the surface tension. Upon reaching the CMC, surfactant sorption at the interface reaches a maximum and surface tension reaches a minimum, with no further changes in either the surface tension or amount of surfactant adsorbed occurring with further increases in the aqueous surfactant concentration. The effects of surfactant concentration on aqueous phase surface tension and surfactant sorption at the aqueous phase-air interface are summarized in Figure 2.8.
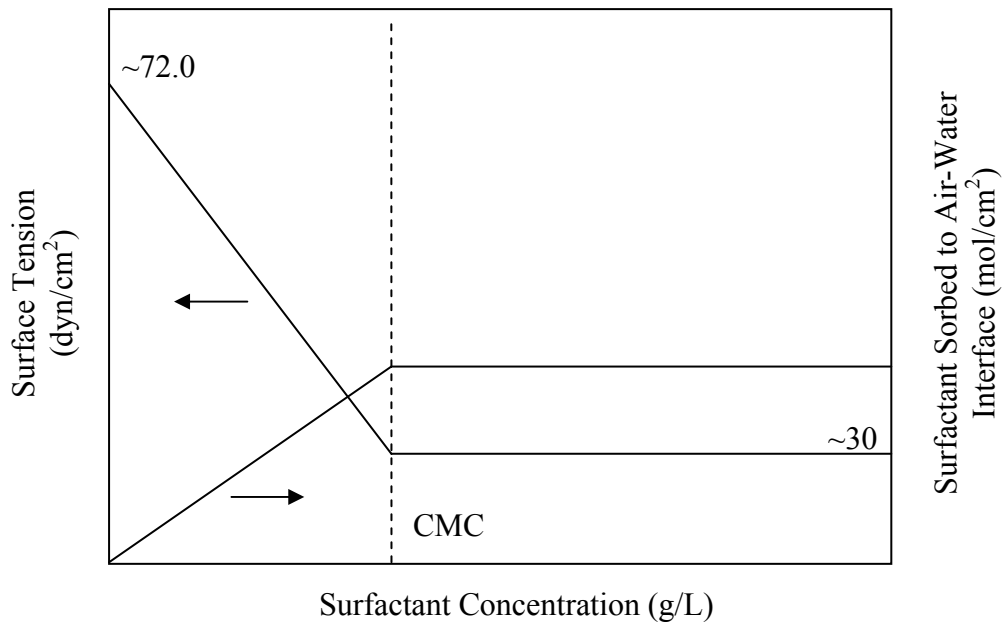
Figure 2.8: Idealized surface tension and interfacial surfactant sorption as a function of surfactant concentration.

When present in a system, surfactants can markedly reduce the interfacial tension between aqueous and organic liquids through the process of interfacial adsorption. The relationship between interfacial tension and aqueous surfactant concentration can be

explained in light of the fact that surfactant molecules as a class tend to accumulate at interfaces. Interfacial tension and surfactant concentration can be related to surfactant sorption (or accumulation) at the organic-water interface through use of the Gibbs surface excess, Γ_s (Equation 2.11, Pennell and Abriola 1997).

$$\Gamma_s = - RT \frac{d\gamma}{d \ln C_S} \qquad (2.11)$$

In Equation 2.11, R is the gas constant, T is the temperature, γ the interfacial tension, and C_S the surfactant molar concentration. Interfacial adsorption is generally greater for organic-water systems compared to air-water systems, resulting in larger IFT reductions for the former. For example, IFT values between PCE and surfactant solutions range from 1-5 dyne/cm (see e.g., Pennell et al. 1994, Taylor et al. 2001), compared to surface tension values between air and surfactant solutions of approximately 30 dyne/cm. Organic-water IFT values can be further reduced, particularly in the case of anionic surfactants, by addition of electrolytes to the system to increase surfactant hydrophobicity. Electrolyte addition to anionic surfactant formulations can decrease IFT to the ultra-low values (less than 10^{-3} dyne/cm) desired for enhanced oil recovery (EOR) applications (Bourrel and Schechter 1988).

Rosen (1989) developed Equation 2.12 as alternative description of the interfacial tension between two liquids in the presence of a surfactant.

$$\gamma_{ow} = \gamma_a + \gamma_b - 2\gamma_{ab} \qquad (2.12)$$

In Equation 2.12, γ_{ow} is the organic-aqueous phase interfacial tension, γ_a is the surface tension of the organic phase, γ_b is the surface tension of the aqueous phase, and γ_{ab} is the interaction energy across the organic-aqueous phase interface per unit length. Examining Equation 2.12, it can be inferred that interfacial adsorption of surfactants effects the

organic-aqueous phase interfacial tension by altering the interaction energy across the interface. As surfactant molecules accumulates at the interface, the similarity of the organic and aqueous liquid phases (i.e., phases a and b) increases, resulting in an increase in the interaction energy across the interface. Assuming that the surface tensions of the two liquid phases remain constant, an increase in the interaction energy will therefore result in a reduction of the organic-aqueous phase IFT.

2.4.2 Miscible Displacement

Surfactant micelle formation is of critical importance for flushing strategies designed to achieve miscible displacement of organic-phase contaminants. In aqueous solutions, surfactant micelles are characterized by a core in which the hydrophobic moieties of the surfactant monomers are grouped (Figure 2.7). This hydrophobic core exhibits properties that can be considered similar to that of a liquid hydrocarbon (Attwood and Florence 1983). When micelles exist in the presence of hydrophobic organic compounds (HOCs), partitioning or incorporation of HOC molecules into the hydrophobic core of surfactant micelles has been observed (Pennell and Abriola 1997). In general, the amount of HOC partitioning into surfactant micelles increases as the aggregation number of the surfactant increases or as the aqueous concentration of surfactant increases. Recall that when above the CMC, an increase in surfactant concentration corresponds to an increase in the quantity of surfactant micelles present. As a result of HOC partitioning into aqueous-phase surfactant micelles, the apparent aqueous-phase solubility of hydrophobic contaminants (often of the type that from DNAPLs) can be greatly increased, thereby reducing the flushing volume required for treatment.

Above the CMC, the apparent aqueous-phase solubility of an organic compound will increase with increasing aqueous surfactant concentration in an approximately linear fashion, as demonstrated in Figure 2.9. The increase in aqueous solubility with increasing surfactant concentration can be described using the weight solubilization ratio, or WSR:

$$WSR = \frac{C_C - C_{C,sat}}{C_S - C_{S,CMC}} \qquad (2.13)$$

where C_C is the aqueous-phase concentration of the organic compound in a surfactant solution of concentration C_S, $C_{C,sat}$ is the solubility of the compound in pure water, and $C_{S,CMC}$ is the critical micelle concentration of the surfactant. When the organic and surfactant concentrations are expressed on a molar, rather than mass, basis, Equation 2.13 becomes the molar solubilization ratio (MSR). While the WSR implies that highly concentrated surfactant solutions will result in greater organic-phase contaminant recoveries, other design factors such as IFT and viscosity must also be taken into account when designing surfactant formulations for miscible displacement applications.

An alternative method for describing aqueous-phase solubility of an organic contaminant in the presence of a surfactant is the solubilization parameter (S). The solubilization parameter has units of mL organic/mL surfactant and may be easily determined from the WSR using the respective densities of the organic compound and surfactant. Using the Chun-Huh equation (Equation 2.14, Huh 1979), the solubilization parameter may be directly related to the interfacial tension between the aqueous (i.e., surfactant solution) and organic phases.

$$\gamma = C / S^2 \qquad (2.14)$$

In Equation 2.14, γ is the interfacial tension (dyne/cm) and C is an empirical constant that is has been determined to approximately equal 0.3 when the organic phase is comprised of chlorinated solvents such as PCE and TCE (Pope and Wade 1995). From the Chun-Huh equation it can be inferred that an increase in the solubilization parameter (and therefore the aqueous solubility of a contaminant) will be accompanied by a reduction in the interfacial tension between the aqueous and organic phases. As a result, care must be taken when designing solubilization-based surfactant formulations to avoid decreasing the IFT to values sufficient for the onset of organic-phase displacement, a consideration discussed in greater detail below. The idealized IFT-solubilization parameter relations described by the Chun-Huh equation is shown in Figure 2.10 and physical properties of representative surfactant formulations used in previous SEAR studies are summarized in Table 2.3.
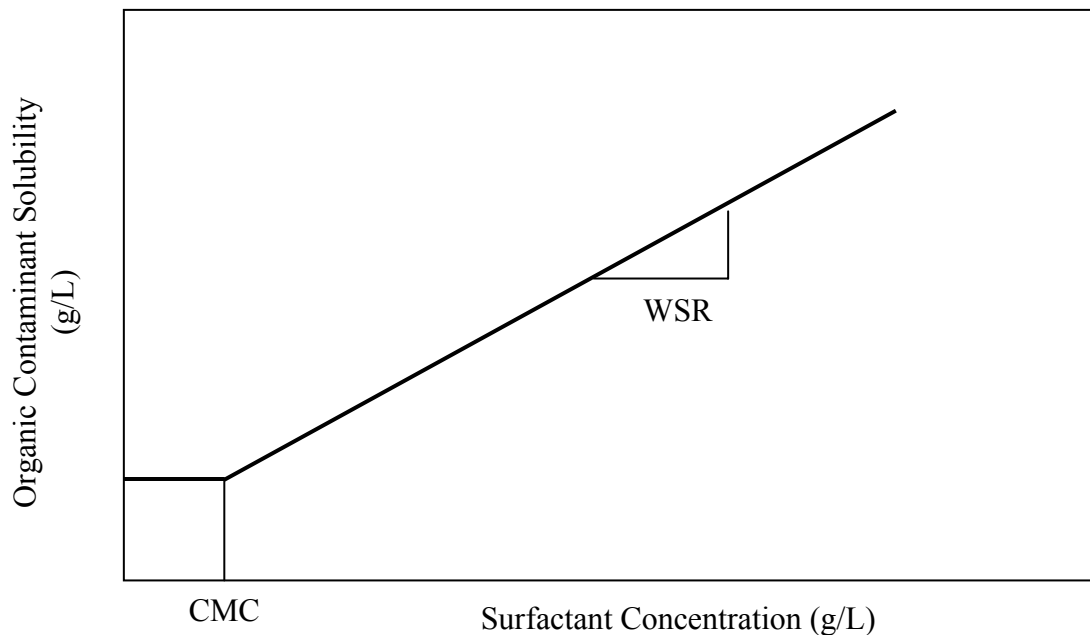
Figure 2.9: Idealized relationship between aqueous phase compound solubility and surfactant concentration.

Fountain et al. (1991) were among the first to investigate the applicability of surfactant-based miscible displacement for DNAPL source zone remediation. They screened approximately 120 surfactants for PCE recovery based on parameters including IFT reduction, magnitude of solubility increase, and emulsion formation. Based on the screening results, a 2% mixture (1:1) of nonylphenol ethoxylate (Witconol NP-100) and a phosphate ester of nonylphenol ethoxylate (Rexophos 25/97) was selected for further study. A series of one-dimensional column experiments investigating removal of residual PCE using this surfactant formulation yielded promising initial results, although problems such as spontaneous formation of viscous surfactant emulsions and low overall recovery (approximately 45%) were encountered.
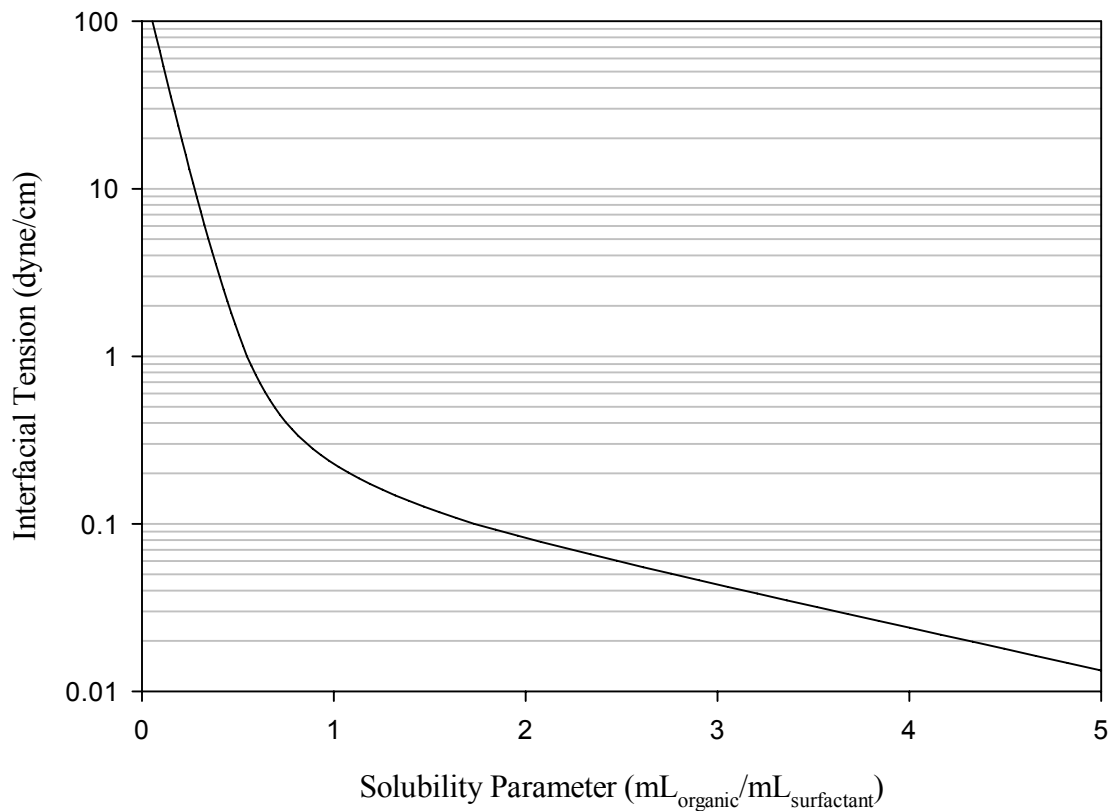
Figure 2.10: Idealized relationship between solubilization parameter (S) and interfacial tension (IFT).

Table 2.3: Physical properties of representative surfactant formulations employed during SEAR.

Reference	Surfactant Formulation	NAPL	IFT (dyne/cm)	S (mL/mL)	MSR (mol/mol)	Aqueous Solubility (mg/L)
Taylor et al. 2001	4% Tween 80 + 500 mg/L $CaCl_2$ (nonionic)	PCE	4.90	0.45	5.41	26,000
Fountain et. al. 1991	1% Rexophos 25/97 (nonionic)	PCE	3.2	0.58	2.55	9,500
Ramsburg and Pennell 2001	8% Aerosol MA + 8% 2-Propanol + 15 g/L NaCl + 1 g/L $CaCl_2$ (anionic)	PCE	0.160	1.18	2.29	76,300
Dwarakanath et al. 1999	4% SDS + 25 g/L NaCl (anionic)	PCE	0.14	0.89	3.40	58,000
Childs et al. 2004	5% Aerosol MA + 4% 2-Propanol + 8 g/L $CaCl_2$ (anionic)	PCE	0.08	0.76	2.90	62,000
West 1992	1% (wt.) Brij 30 (nonionic)	TCE	2.4 (Est.)	0.35	1.39	5,100
West 1992	1% (wt.) Triton X-100 (nonionic)	TCE	3.3 (Est.)	0.30	1.23	4,400
West 1992	1% (wt.) Tergitol NP-10 (nonionic)	TCE	2.4 (Est.)	0.35	15.18	5,100
Dwarakanath et al. 1999	4% SDS + 8% 2-Propanol + 4 g/L NaCl (anionic)	TCE	0.19	0.67	2.28	39,000
Dwarakanath et al. 1999	4% SDS + 8% 2-Propanol + 9.3 g/L NaCl (anionic)	TCE	.02	8.82	38.1	516,000

The solubilization and recovery of residual dodecane from soil columns using a surfactant formulation comprised of 4% polyoxyethylene (20) sorbitan monooleate (Witconol 2722) was investigated by Pennell et al. (1993). While dodecane concentrations in the aqueous effluent increased by five orders-of-magnitude in the presence of the surfactant solution, effluent concentrations remained significantly lower than the equilibrium solubility of dodecane in a 4% Witconol 2722 solution, indicating rate-limited contaminant mass transfer. This effect was initially modeled by Abriola et al. (1993) as a linear driving force expression. Later research incorporated the effects of soil texture on rate-limited solubilization and predicted mass transfer coefficients using a Sherwood correlation that incorporated soil uniformity and mean grain size (Abriola et al. 2000). Subsequent two-dimensional aquifer cell studies conducted by Taylor and coworkers (2001) demonstrated increased PCE effluent concentrations following flow interruption, indicating that rate-limited solubilization has an effect on the recovery of PCE-DNAPL. However, aquifer cell effluent concentrations during flow interruption were significantly lower than those observed in homogeneous column systems, indicating that factors such as subsurface heterogeneity and dilution were more important factors impacting PCE recovery.

Factors beyond solubilization capacity and kinetics may influence performance of surfactant-based solubilization strategies. Rathfelder et al. (2001) were able to accurately predict contaminant mass recovery and effluent concentrations for two-dimensional (2-D) aquifer cell experiments, provided that pore-scale mass transfer limitations were included in the model. However, extensive soil heterogeneity and NAPL distribution information that may not be available at the field scale were required for accurate model predictions.

Additional 2-D surfactant flushing simulations by Dekker and Abriola (2000a, 2000b) for PCE solubilization in heterogeneous porous media demonstrated the potential for density-induced plunging of PCE-laden surfactant solutions. Downward migration of the solubilization plume may have long term impacts on site remediation, especially if penetration of the plume into zones of low permeability porous media occurs.

Surfactant sorption to aquifer material may also affect surfactant-enhanced solubilization performance. For nonionic surfactants, previous research (see e.g., Pennell et al. 1993, Adeel and Luthy 1995, Taylor et al. 2001) has demonstrated that surfactant sorption to porous media with a low organic carbon content exhibits Langmuir behavior (Equation 2.15).

$$S_m^S = \frac{b S_{m,\text{max}}^S C_a^S}{1 + b C_a^S} \qquad (2.15)$$

In Equation 2.15, S_m^S is the amount of surfactant sorbed (mg/g), $S_{m,\text{max}}^S$ is the maximum amount of surfactant sorbed (mg/g), b is the ratio of the adsorption and desorption rates (L/g), and C_a^S is the aqueous phase concentration of the surfactant (g/L). Nonionic surfactant sorption is expected to reach the maximum value (i.e., $S_{m,\text{max}}^S$) when the aqueous surfactant concentration is near the CMC (Pennell et al. 1993). Maximum surfactant sorption for nonionic surfactants is generally low for systems with low organic carbon content, ranging from 0.13 to 0.2 mg/g (Pennell et al. 1993, Taylor et al. 2001). As a result, surfactant losses to porous media will generally be moderate unless sold organic content is high. Anionic surfactant sorption to silica materials with low organic carbon content is also generally not a significant source of surfactant loss (Dwarakanath

et al. 1999) due to anion-anion interactions between silica groups and the hydrophilic head of the surfactant.

Another potential limitation of surfactant-enhanced solubilization is surfactant partitioning (loss) into the organic phase. This is of particular importance for surfactants that tend to partition strongly into the organic phase (e.g., surfactants characterized by low EO numbers), with partitioning occurring more readily when the organic phase is aromatic (Butler and Hayes 1998) or has a relatively low IFT (Zimmerman et al. 1999). Using a series of ethyoxylated nonionic surfactants, Pennell et al. (1997) observed an increase in the minimum surfactant concentrations required for solubilization of PCE and dodecane, indicating surfactant partitioning into the NAPL. Later experiments by Zimmerman et al. (1999) demonstrated partitioning of mixed nonionic surfactants into several pure NAPL of differing composition (e.g., PCE and TCE) based on inconsistencies in the MSR. MSR values calculated based on measured aqueous phase surfactant concentrations were found to differ substantially from those calculated assuming that no partitioning had occurred. For TCE, the MSR calculated assuming that no partitioning occurred was approximately 2.5 while the actual MSR based on measured surfactant concentrations was determined to be 1.0. By lowering the MSR of a surfactant solution, surfactant partitioning into a NAPL may decrease the aqueous phase contaminant concentrations in a surfactant solution, leading to an increase in the treatment volume required. This increase in required treatment volume can be mitigated by using surfactant solutions of higher concentration in order to overcome the MSR reduction.

Cyclodextrins have been investigated as alternative solubilizing agents at the laboratory scale. Cyclodextrins are not surfactants, but are instead comprised of several glucose molecules that form a toroidal structure with a hydrophobic core. Although cyclodextrins do not form micelles, VOC partitioning into the hydrophobic cyclodextrin core can increase their apparent aqueous solubility, much like the case of micellar solubilization (Boving et al. 1999). Contaminant solubilization is accompanied by an IFT reduction comparable to those observed in surfactant formulations with similar solubilization parameters. Boving and Brusseau (2000) compared TCE solubilization efficiency of hydroxypropyl-β-cyclodextrin to a number of surfactants. Solubilization efficiency with hydroxypropyl-β-cyclodextrin was comparable to that when a surfactant solution containing Dowfax 8390 was employed; however, both solutions were less effective than surfactant formulations employing dodecyl sulfate (SDS). Methyl-β-cyclodextrin has also been investigated as a solubilization agent (Boving et al. 1999, Boving and Brusseau 2000). Unlike hydroxypropyl-β-cyclodextrin however, use of this cyclodextrin resulted in an IFT reduction sufficient to mobilize both PCE- and TCE-DNAPL, limiting its attractiveness in remediation strategies. In addition, cyclodextrins can be relatively expensive, costing in excess of $5 per pound.

2.4.3 Immiscible Displacement

If the surfactant formulation used in SEAR is able to reduce the IFT between the aqueous and organic phases a sufficient amount, immiscible displacement, or mobilization, of the organic phase may result. The process of immiscible displacement is generally envisioned as discrete NAPL ganglia, present in the subsurface at residual organic-phase saturation, being released, or "mobilized", from the pore space they

occupy. The mobilization of NAPL entrapped in the subsurface by use of low interfacial tension flushing solutions is an idea with origins in the field of enhanced crude oil recovery (EOR). Mobilization presents an advantage over miscible displacement technologies in that it is generally a much more efficient procedure, often requiring smaller amounts of surfactant solution to achieve mass recovery (Dwarakanath et al. 1999). In addition, significant NAPL solubilization is a frequently observed side effect of mobilization, as the process that results in mobilization (a reduction in IFT) is often related to the high solubilization capacity of surfactant solutions. Significant contaminant mass recovery by solubilization has been observed as a side effect during a number of experiments designed to investigate miscible NAPL displacement (see e.g., Fortin et al. 1997, Dwarakanath et al. 1999).

Mobilization of organic liquids entrapped in porous media is governed by the relative influences of the buoyant, viscous, and capillary forces acting on NAPL ganglia. Pennell et al. (1996) described the ratio of the viscous forces to the capillary forces through use of the dimensionless capillary number, N_{Ca}:

$$N_{Ca} = \frac{q_w \mu_w}{\gamma_{ow} \cos \theta} \qquad (2.16)$$

where q_w is the Darcy velocity of the aqueous phase, μ_w is the aqueous phase viscosity, γ_{ow} is the interfacial tension between the organic and aqueous phases, and θ is the contact angle. Subsurface systems are generally assumed to be completely water wetting and the contact angle therefore typically assumed to be zero.

The dimensionless Bond number (N_B) is employed to describe the ratio of the buoyant forces to capillary forces in a system. It typically takes the form of (Pennell et al. 1996):

43

$$N_B = \frac{\Delta \rho g k_i k_{rw}}{\gamma_{ow} \cos \theta} \qquad (2.17)$$

In Equation 2.17, $\Delta \rho$ is the difference between the aqueous and organic phase densities (i.e., $\rho_w - \rho_o$), g is the gravitational constant, k_i is the intrinsic permeability of the porous media, and k_{rw} is the relative permeability of the aqueous phase. The Bond and capillary numbers were combined by Pennell et al. (1996) in development of the dimensionless total trapping number:

$$N_T = \sqrt{N_{Ca}^2 + 2N_{Ca}N_B \sin \alpha + N_B^2} \qquad (2.18)$$

where α is the angle the system flow makes with the horizontal axis. For flushing strategies employing horizontal flow, α is equal to 0°, and Equation 2.18 becomes:

$$N_T = \sqrt{N_{Ca}^2 + N_B^2} \qquad (2.19)$$

A series of column experiments were conducted by Pennell et al. (1996) to quantify the total trapping number during PCE-DNAPL mobilization. Experiments were conducted using several different surfactant solution formulations injected at varying flow rates to allow for variation of the PCE-aqueous phase interfacial tension. In addition, the porous media used in the experiments was varied to evaluate the effects of medium permeability on PCE mobilization. For all porous media investigated, PCE mobilization was observed to begin above a critical N_T value ranging from 2×10^{-5} to 5×10^{-5}, with complete PCE displacement occurring as N_T approached approximately 1×10^{-4}, as shown in Figure 2.11.
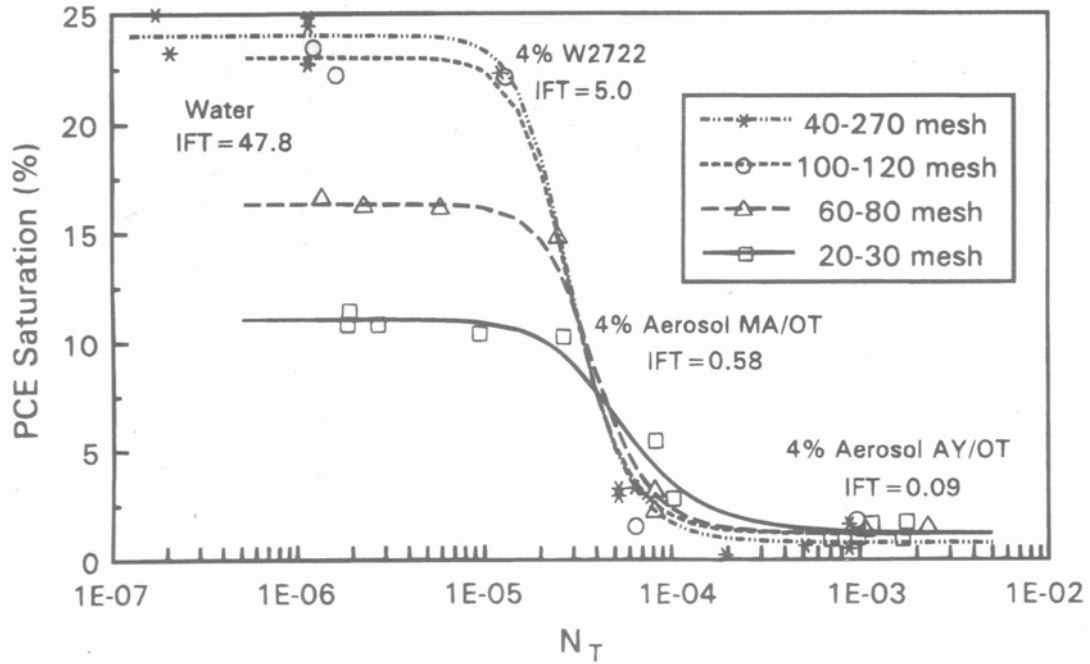
Figure 2.11: PCE mobilization as a function of total trapping number (Pennell et al. 1996).

While immiscible displacement can be an extremely efficient method for DNAPL recovery, vertical displacement of the mobilized organic-phase may lead to downward DNAPL migration and possible contamination of pristine aquifer regions. For horizontal aqueous-phase flow, the angle of displacement for mobilized organic liquid relative to the x-axis (τ) may be predicted from the ratio of the Bond and capillary numbers using Equation 2.20:

$$\tau = \arctan\left(\frac{N_B}{N_{Ca}}\right) \qquad (2.20)$$

Based on Equation 2.20 and the definition of τ, a τ value of 0° is indicative of horizontal displacement and a value of 90° indicates vertical, or downward in the case of a DNAPL, displacement. The alternative concept of the bank number (N_{Ba}), a dimensionless number relating the forces acting on NAPL ganglia parallel to the direction of flow to

45

those acting perpendicular to flow, was introduced by Willson et al. in 1999. Based on the previously developed capillary and Bond numbers and the angle of aqueous-phase flow, α, the bank number may be written as:

$$N_{Ba} = \frac{N_{Ca} + N_B \sin \alpha}{N_B \cos \alpha} \qquad (2.21)$$

When aqueous flow is horizontal, the bank number reduces to the ratio of the capillary number to the Bond number. During 2-D aquifer cell experiments conducted by Willson et al. (1999) with horizontal aqueous phase flow, DNAPL was observed to mobilize perpendicular to the aqueous flow direction (i.e., downward) at low bank numbers ($N_{Ba} \leq$ 0.8), while at high bank number values ($N_{Ba} \geq 3$) most of the DNAPL moved through the flow cell parallel to the direction of aqueous flow with little downward migration, resulting in the formation of a steep bank of organic liquid. In cases where the bank number fell within these two extremes, NAPL behavior became significantly more complex with either shallow bank formation or no bank formation generally observed.

Dwarakanath et al. (1999) performed a series of 1-D column experiments to evaluate the effects of surfactant selection on DNAPL remediation performance by low-IFT surfactant solutions capable of miscible contaminant displacement with high solubilization capacities (solubilization + mobilization). The surfactants Aerosol MA-80, Aerosol AY, and Aerosol OT were compared on the basis of overall NAPL recovery from the column. Very high NAPL recoveries (> 90%) were observed for selected surfactant formulations (primarily Aerosol MA-80); however, significant mobilized free product was observed during all the experiments, indicating the potential for uncontrolled DNPAL migration. Ramsburg and Pennell (2001) conducted a two-dimensional aquifer cell experiment utilizing a similar Aerosol MA surfactant solution formulation to achieve

solubilization + mobilization of a PCE-DNAPL. Following the introduction of 3 pore volumes of surfactant solution, overall contaminant mass recovery was 78% the PCE initially released. Significant downward DNAPL migration was observed during the Aerosol MA flood, with PCE-DNAPL entry into a previously uncontaminated low permeability confining layer.

To be of practical use in field settings, immiscible displacement technologies for DNAPL recovery must be designed to address the potential for downward migration of free organic product. Sabatini et al. (2000) suggested use of gradients in influent solution properties to enhance surfactant solubilization capacity and NAPL stability during solubilization, allowing for an increase in surfactant-based miscible displacement efficiency while minimizing the onset of NAPL displacement. A gradient in electrolyte concentration is used to increase solubilization solution capacity as a function of time. This acts to maximize NAPL recovery by continually increasing solubilization capacity in order to offset decreases in the interfacial area of entrapped NAPL ganglia as their size and number are decreased due to dissolution. Increasing the electrolyte concentration also results in a decrease in organic-aqueous phase IFT, however, the decreases in local organic phase saturation can offset the IFT reduction and prevent NAPL mobilization. Alternately, the synergistic relationship between alcohols and surfactants for NAPL solubilization and recovery has been explored. Martel et al. (1998a, 1998b) developed a surfactant solution containing Hostapur SAS (a secondary alkane sulfonate), 1-butanol, *d*-limonene, and toluene that was subsequently able to recover up to 95% of a complex mixed DNAPL present at a site near Ville Mercier, Quebec, Canada (Martel et at. 1998c).

Several additional techniques for minimizing DNAPL migration have been investigated. Longino and Kueper (1995) employed vertical (upward) flushing in 1-D column studies to minimize downward migration. Using a surfactant formulation of 2% (1:1) Witconol NP-100 and Rexophos 25/97, they were able to successfully recover PCE-DNAPL without significant mobilization against the direction of flow (i.e., downward). An alternative approach suggests flushing DNAPL contaminated aquifers with a 60% aqueous solution of sodium iodide, which has a density of 1.8 mg/L (Miller et al. 2000). This approach has been shown to successfully displace and recover TCE-DNAPL in laboratory studies with no downward TCE migration, but was unable to removal residual DNAPL from the porous media. In addition, both this approach as well as vertical flushing can only be successfully applied in completely confined systems that are unlikely to exist in the field. A third method for mitigating DNAPL migration is density modification through use of a partitioning alcohol. Density modified displacement, which makes use of this phenomenon to immiscibly recover DNAPL that has been converted into an LNAPL, is described below.

2.4.4 Density Modified Displacement

A novel technology for mitigating downward DNAPL migration during immiscible displacement is the Density Modified Displacement (DMD) technique, patented by Pennell (2000). The DMD method as patented is a two step procedure. In the first step, an alcohol cosolvent preflood is used as a chemical means for reducing NAPL density *in situ* without organic phase mobilization. After conversion from a dense NAPL to a neutrally buoyant or light NAPL, a low interfacial tension surfactant flood is subsequently employed to mobilize the organic phase.

During the first step of the DMD process, alcohol partitioning from the aqueous phase into the organic phase is used to affect density change (Lunn and Kueper 1999a, 1999b). The concept of using alcohol partitioning in the subsurface originated with the use of partitioning inter-well tracer tests (PITT) to estimate DNAPL saturations and volumes in contaminated aquifers. Partitioning tracer solutions employed during PITT are generally formulated by dissolving several alcohols characterized by differing partition coefficients in water at relatively low concentrations (<1000 mg/L). As the alcohol tracer solution is swept through the DNAPL source zone, each of the different alcohols will partition into the organic phase based on its affinity for the organic, with non-partitioning alcohols transported through the swept zone at the velocity of the pore water (Taylor 1999). Separation of the partitioning and non-partitioning alcohol tracers is a function of partition coefficients of the alcohols, as well as the volume of DNAPL present in the swept zone. Breakthrough curves for the partitioning alcohols may then be analyzed to estimate the volume of DNAPL present in the swept volume (see e.g., Jin et al. 1995, Annable et al. 1998).

In general, the alcohols employed in PITT are branched and of relatively high molecular weight (Dwarakanath 1997), resulting in many of them being relatively insoluble in water (i.e., on the order of milligrams per liter). These alcohols therefore are not directly applicable to DMD, since their low aqueous solubility would necessitate a sizable increase in the number of pore volumes of flooding required to deliver sufficient alcohol to achieve *in situ* density conversion. In an effort to overcome this limitation, Lunn and Kueper (1997, 1999a, 1999b) investigated the density reduction of PCE using two high solubility alcohols: 1-propanol and 2-butanol. During these studies, successful

density conversion of PCE from a DNAPL to an LNAPL was achieved, with the organic phase density reduced from 1.62 g/mL to 0.95 g/mL. Alcohol partitioning was further investigated by Loverde (1997) using 1-butanol and 1-pentanol. Upon encountering the anionic surfactant solutions used to mobilize the density converted DNAPL, the 1-pentanol formed a highly viscous gel, rendering it unsuitable for use in the DMD method. Conversely, 1-butanol was able to achieve density conversion without adverse phase behavior in the presence of surfactants in both columns and 2-D aquifer cells for several DNAPL compounds (chlorobenzene and 1,2-dichlorobenzene).

Based on these findings, Ramsburg (2002) selected 1-butanol for use in the alcohol preflood (both aqueous and emulsion) step of DMD. The selection of 1-butanol was based on a need for a compromise between the solubility of the partitioning alcohol in the delivery medium (i.e., water) and the tendency of the alcohol to partition into DNAPL. Compared to higher molecular weight alcohols, 1-butanol has large aqueous solubility (approximately 6.5% (wt.)), yet maintains a tendency to partition strongly into any organics that may be present. When compared to many other alcohols, 1-butanol offers the additional advantages of no detrimental phase behavior (i.e., gel formation) as well as potential compatibility with post-surfactant flushing bioremediation schemes.

The behavior of the NAPL-water-1-butanol (BuOH) three component system was investigated by Ramsburg and Pennell (2002a) for three representative DNAPLs (PCE, TCE, and CB). They observed that the partitioning behavior of an alcohol in a three component system (e.g., TCE-water-1-butanol) can be best described using a ternary phase diagram (Figure 2.12). For several DNAPL contaminants typically of interest in SEAR-based remediation (e.g., PCE, TCE, and CB), Type II phase behavior is observed.

In systems exhibiting Type II phase behavior, two partially miscible pairs (in this case DNAPL-water and 1-butanol-water) and one completely miscible pair (DNAPL-1-butanol) are present. As a result of this behavior, two distinct single phase regions (aqueous and organic) can be observed in the ternary phase diagram. In Figure 2.12, an aqueous phase is present at the lower right-hand corner; however, it is too small to be distinguished at the scale presented. Tie lines, or lines of constant composition within a two-phase region, can be used to determine the composition of aqueous and organic phases present at equilibrium. For example, based on the data used to generate Figure 2.12, an aqueous solution with respective TCE, 1-butanol, and water mole fractions of 1.276×10^{-4}, 0.0139, and 0.9859 mol/mol would be in equilibrium with an organic phase having a composition of 0.238 mol TCE/mol, 0.500 mol 1-butanol/mol and 0.262 mol water/mol. Tie lines are a potentially useful concept in the DMD method, as it allows determination of the single tie line corresponding to the organic phase 1-butanol mole fraction at which density conversion from DNAPL to LNAPL will occur. The tie line at which density conversions occurs for TCE when 1-butanol is employed as the partitioning alcohol is shown in Figure 2.12 (Ramsburg and Pennell 2002a).

Ramsburg and Pennell (2002b) performed a series of two-dimensional aquifer cell experiments to evaluate the feasibility of using the DMD method for remediation of CB- and TCE-contaminated aquifer material. The preflood used in these experiments was an aqueous solution of 6% (wt.) 1-butanol. Both CB and TCE were successfully converted from DNAPL to LNAPL, and overall contaminant recovery was high (> 90%). In addition, PCE recovery via DMD with an aqueous preflood in a 2-D aquifer cell was investigated by Ramsburg et al. (2004a) and determined to also be high, with successfully
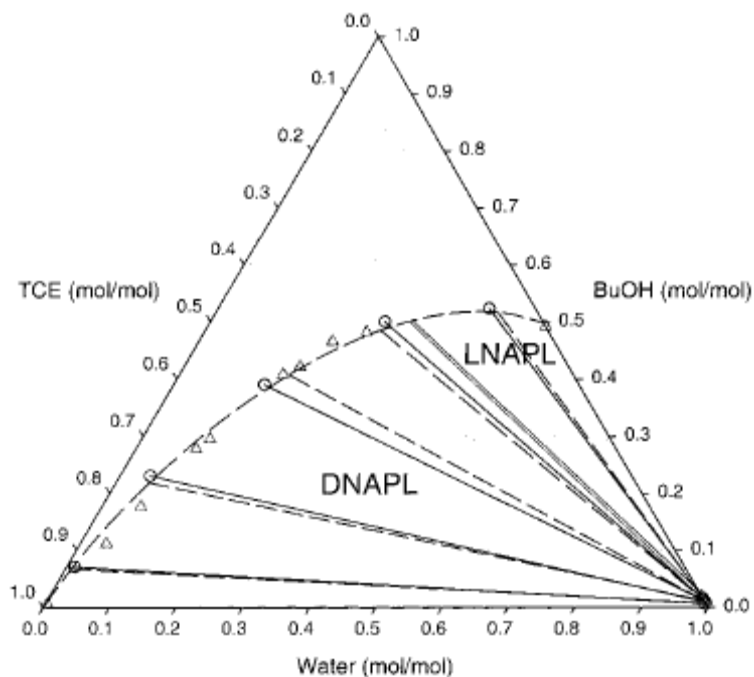
Figure 2.12: TCE, water, and 1-butanol ternary phase diagram (Ramsburg and Pennell 2002a).

DNAPL to LNAPL conversion. However, significant volumes of the aqueous preflood solution were required for density conversion, especially for TCE and PCE (i.e., 6.5 pore volumes of the 6% 1-butanol solution to convert PCE). This factor potentially limits the attractiveness of DMD when compared to other flushing technologies. In an effort to lower the volume of preflood solution required to achieve density conversion, Ramsburg et al. (2003, 2004a) investigated use of surfactant-stabilized emulsions for 1-butanol delivery to TCE- and PCE-DNAPL. The preflood solution used in these experiments was comprised of 4.7% (vol.) Tween 80 + 1.3% (vol.) Span 80 + 15% (vol.) 1-butanol, formulated as a macroemulsion. Successful conversion of both TCE and PCE from DNAPL to LNAPL was reported, and recoveries following the displacement flood were high (> 90%), with significant contaminant solubilization occurring during the emulsion

52

preflood.   In addition, the flushing volume required for conversion to LNAPL was significantly lowered when the emulsion was employed, with approximately 1.2 pore volumes of emulsion preflood required to achieve PCE density conversion.

2.5 Post-Treatment Plume Development and Mass Flux

While the SEAR-based source zone treatment technologies described above have been shown to be highly effective under controlled laboratory conditions, field scale applications have yielded mixed results. DNAPL recoveries from several demonstrations of surfactant flushing are summarized in Table 2.4. In addition, a limited number of cosolvent flushing demonstrations are included in Table 2.4 since post-treatment contaminant mass flux data is available for these sites and discussed below. In some cases (e.g., Bachman, Alameda Point, and the 1996 test cell at Hill Air Force Base OU2) greater than 90% of source zone mass initially estimated to be present was recovered. It should be noted, however, that these mass recovery estimates often do not incorporate the uncertainties inherent in the initial estimations DNAPL mass present in the source zone. In addition, aggressive source zone treatments can significantly alter the distribution and physicochemical properties of any remaining DNAPL, further confounding estimations of contaminant recovery (Stroo et al. 2003).   Generally speaking, it is now widely accepted that some (potentially significant) fraction of initial DNAPL mass present within a source zone will persist following treatment (see e.g., Stroo et al. 2003, NRC 2004).

A number of well controlled, field-scale tests of both surfactant and cosolvent flushing suggest that DNAPL recoveries in the range of 60-70% may be expected (e.g., Brooks et al. 2004, Holzmer et al. 2000, Jawitz et al. 2000, Rao et al. 1997, Soga et al.

Table 2.4: Field demonstrations of surfactant and co-solvent flushing.

Year	Site	Technology	DNAPL	Recovery (%)	References
2000	Bachman Road Oscoda, MI	Surfactant	PCE	90+	Abriola et al. 2001, Abriola et. 2003
1999	Alameda Point, CA	Surfactant	PCE, TCE, DCA, DCE	97	Hasegawa et al. 2000
1999	Camp Lejeune, Marine Corps Base	Surfactant	PCE	~72	Holzmer et al. 2000, Delshad et al. 2000
1997	Hill Air Force Base OU2	Surfactant	TCA, TCE	~90	Meinardus et al. 2002
1996	Hill Air Force Base OU1	Surfactant	Jet Fuel, Chlorinated Solvents	72	Jawitz et al. 2001
1996	Hill Air Force Base OU2	Surfactant	TCE, TCE, PCE, CT	98.5	Londergan et al. 2001
1996	Hill Air Force Base OU1	Surfactant	Jet Fuel, Chlorinated Solvents	58	Knox et al. 1999
1995	Thouin Sand Quarry, Quebec, Canada	Surfactant	TCE, PCE, Waste Oil	95	Martel et at. 1998c
1990	Canadian Forces Base Borden	Surfactant	PCE	69.2	Fountain et al. 1996
1998	Jacksonville, FL	Cosolvent	PCE	64	Jawitz et al. 2000
1997	Dover Air Force Base	Cosolvent	PCE	65	Rao et al. 1997

2004). A number of reasons have been postulated for the limited mass recoveries observed at the field scale, including aqueous phase flow bypassing of contaminated regions and limited access of flushing solutions to DNAPL mass due to contaminant pooling (i.e., mass transfer limitations). As a consequence, dissolved-phase contaminant concentrations within, and emanating from, DNAPL source zones are likely to exceed drinking water standards (e.g., MCLs) for considerable periods of time, even with aggressive treatment strategies (Sale and McWhorter 2001, Soga et al. 2004). It is

therefore reasonable to question the benefits of incomplete or partial mass removal with respect to protection of human health and the environment (Cherry et al. 1997, Freeze 2000, U.S. EPA 2003), and it is of critical importance to understand the impact of the partial, or limited, DNAPL mass recovery that is likely to occur in the field on contaminant mass discharge from a source zone following treatment.

Even in cases where DNAPL source zones can be reasonably well characterized and treated via physicochemical methods to achieve greater than 60% mass removal, questions remain regarding the ability of source zone treatment to improve down-gradient groundwater quality. To date, critical assessments of partial mass removal from NAPL source zones have been based almost exclusively on mathematical predictions of dissolution, often leading to conflicting interpretations (e.g., Rao and Jawitz 2003, McWhorter and Sale 2003). Using an analytical solution for dissolution of DNAPL ganglia and pools in a uniform aqueous flow field, along with limited experimental data, Sale and McWhorter (2001) demonstrated that even removal of high percentages (up to 90%) of a DNAPL source may not result in significant reductions in down-gradient contaminant concentrations. The behavior described by Sale and McWhorter is shown with Line 1 in Figure 2.13, where the percentage reduction in mass discharge (i.e., concentration or mass flux) remains relatively flat until a critical source zone mass recovery point is reached, at which time contaminant mass discharge begins to dramatically decrease. An implication of this behavior is that nearly complete mass removal is required to approach regulatory drinking water standards, and partial mass reduction will provide only minimal improvements in groundwater quality in the short term.
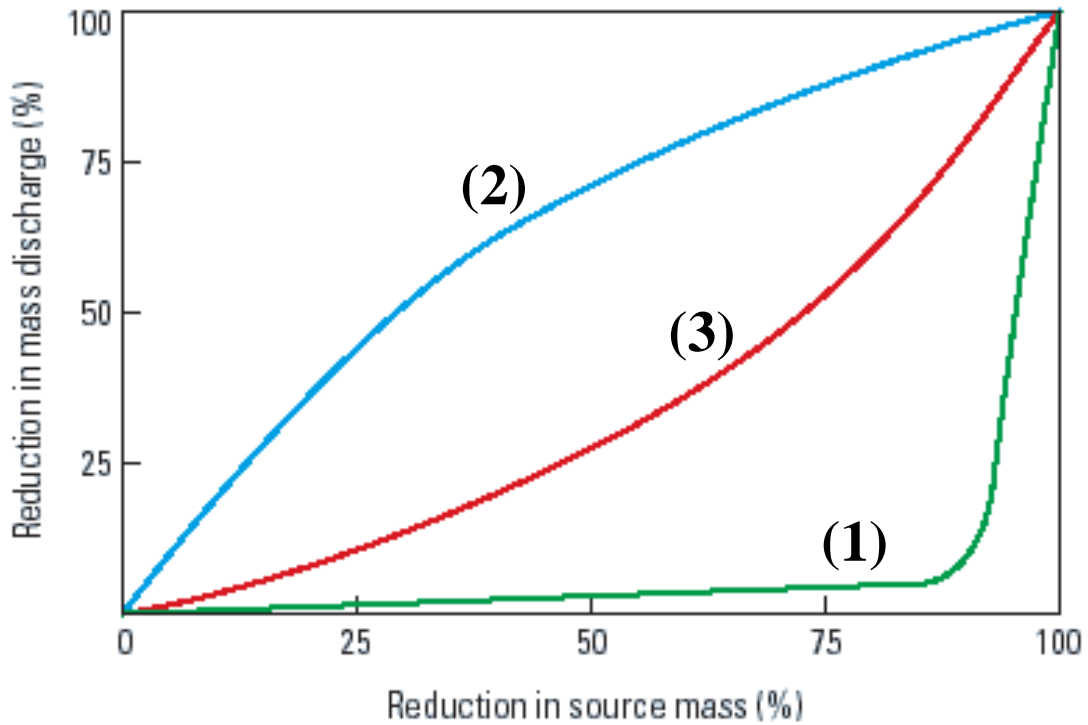
Figure 2.13: Reduction in contaminant mass discharge as a function of source zone mass removal (Stroo et al. 2003).

Conversely, Rao and Jawitz (2003) investigated source zone mass discharge as a function of contaminant recovery using an analytical model consisting of "stream tubes" containing a uniform DNAPL distribution subject to non-uniform flow. Source zone mass discharge reductions (C/C_0) were related to source mass reductions (M/M_0) using a power-law function (Equation 2.22), where Γ is a fitting parameter dependent on source zone conditions including aqueous flow field and DNAPL distribution.

$$C/C_o = M/M_o^{\Gamma} \qquad (2.22)$$

Results from this model indicated that up to 80% reductions in dissolved-phase contaminant mass flux may be possible with only 50% DNAPL mass removal (Figure 2.13, Line 2). The initial results of Rao and Jawitz therefore imply that source zone mass

recovery can be accompanied by significant decreases in mass discharge and source zone treatment in some situations may positively impact groundwater quality (although not necessarily to regulatory endpoints). However, the analytical model as formulated has some limitations. First, non-uniform DNAPL distributions that are expected in the field were not considered. Second, the model does not incorporate the mass reduction arising from stream tubes with only partial (as opposed to complete) mass removal. This could lead to underestimation of mass reductions that accompany (or are required to achieve) a specified flux reduction.

The preliminary work of Rao and Jawitz (2003) was later extended by Jawitz et al. (2005) who adapted the stream tube analytical framework to include both DNAPL distribution non-uniformity and partial mass removal from stream tubes. Jawitz and collaborators were able to combine variability in both the DNAPL distribution and the porous media permeability field (expressed as the stream tube travel time) into a single variable describing the overall spatial variability of the source zone. Within this framework, they determined that as the source zone spatial variability decreases, the amount of mass removal required to achieve a given reduction in contaminant mass flux is increased. For systems similar to that described by Sale and McWhorter (2001) (i.e., uniform NAPL distribution and flow fields that result in low spatial variability), contaminant discharge predicted by the model of Jawitz et al. (2005) was not significant until large amounts of source zone mass reduction had occurred. The converse behavior is also true in the model, with more spatially variable source zones requiring less mass removal to achieve desired flux reductions. However, for such cases, source zone

longevity is increased due either to flow bypassing of DNAPL or mass transfer limitations.

In reality, field-scale reductions in source zone mass discharge as a function of source removal is likely to fall within the extremes described by the simplified analytical models described above. Line 3 of Figure 2.13 was extrapolated by Rao et al. (1997) from data measured during the Dover Air Force Base field demonstration of cosolvent flushing. Though not a surfactant flood, the results are illustrative as post-treatment mass flux behavior is expected to be similar for both surfactant and cosolvent flushing. The extrapolated line is consistent with source mass removal characterized by preferential dissolution of DNAPL ganglia and small pools, with larger pools remaining present in the source zone to act as long-term contaminant sources. Under this scenario, mass discharge reductions may be limited until a large fraction of the DNAPL ganglia present in the source zone are depleted. Following ganglia depletion, a rapid decrease in mass discharge is observed as the remaining low interfacial-area pools are removed. Wood et al. (2005), using a stream tube modeling approach similar to that of Jawitz et al. (2005), evaluated cosolvent flushing of a mixed NAPL test cell at Hill Air Force Base. The evaluation results predicted that 60% source zone mass removal would result in an 80% reduction in contaminant mass flux, corresponding to a log reduction in flux-averaged concentration.

In addition to the analytical models described above, limited numerical simulations have been performed to evaluate mass flux reductions as a function of source zone removal. Parker and Park (2004) evaluated dissolution of non-uniform DNAPL distributions in a homogenous porous medium. In this scenario, dissolution rate was

found to be strongly dependent on DNAPL distribution, with mass recovery significantly limited when the source zone was characterized by laterally extensive (i.e., pooled) DNAPL lenses. Lemke et al. (2004) performed a series of numerical simulations of dissolution of a non-uniform PCE-DNAPL distribution in a statistically homogeneous, non-uniform sandy aquifer. Results from the model realizations predicted mass removals ranging from 60 to 99% and two order-of-magnitude reductions in dissolved-phase concentration and mass flux. These results demonstrated the potential variability in mass removal versus mass flux relationships, even for relatively homogeneous systems, prompting Lemke et al. (2004) to caution that predictions based on simplified conceptual models of DNAPL source zone architecture and flow may not accurately capture reductions in contaminant flux resulting from partial mass removal.

While Figure 2.13 shows mass discharge behavior for up to and including 100% reductions in source zone mass for a number of scenarios, complete mass recovery from a DNAPL source zone is unlikely to occur under realistic conditions that can be expected in the field (see Table 2.4). Some amount of continuing mass discharge is therefore expected following source zone treatment and it is important to consider the possible behaviors of the developing post-treatment contaminant plume. Figure 2.14 (from Soga et al. 2004) demonstrates differing conceptual scenarios (Cases A-C) for aqueous-phase contaminant concentration behavior at a receptor down-gradient from the source zone following treatment. For Case A, contaminant concentrations increase (rebound) following remediation; treatment is therefore defined to be unsuccessful. The Case A scenario can result from a variety of factors: plume shrinkage during treatment that is not accompanied by a corresponding decrease in source zone mass or interfacial area,

59

changes in source zone architecture arising from DNAPL mobilization during treatment (i.e., an increase in interfacial area), or changes in the mass transfer rate from the source zone. The post-treatment contaminant behavior conceptualized in Cases B and C may both be considered successful, when success is defined as down-gradient concentrations remaining below the site-specific target level. However, the maximum concentration level (MCL) is often the target level of regulatory interest. For those scenarios, Case C is preferred (over Case B), as it represents further decreases in contaminant concentrations, which in time may reach the MCL. This can be achieved through physicochemical means, should the reduction in source zone mass resulting from treatment be enough to significantly reduce the DNAPL volume and interfacial area available for mass discharge (Soga et al. 2004). However, physical dissolution of the source zone contaminant mass remaining post-treatment can still require up to several years, with the rate of dissolution dependent on several factors, including post-treatment DNAPL distribution within the porous medium (Christ et al. 2005b). In an effort to more efficiently remove residual mass present in the source zone post-treatment, recent research has focused on developing tertiary source zone treatment technologies. One of the most promising is coupling microbial reductive dechlorination (as the tertiary treatment) to SEAR-based source zone treatments.
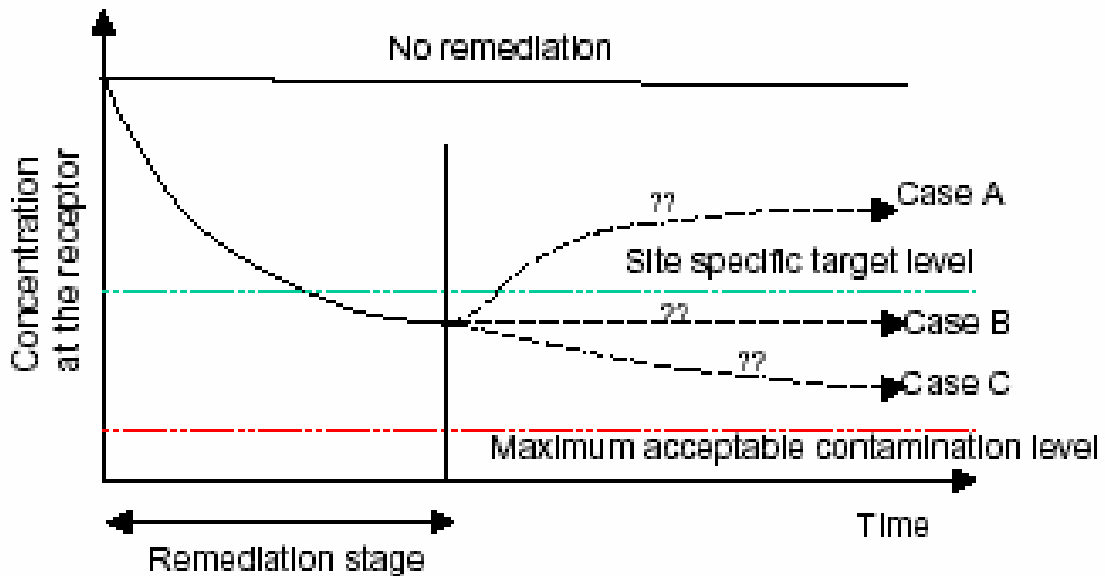
Figure 2.14: Potential aqueous-phase contaminant behavior following source zone treatment (Soga et al. 2004).

2.6 Combined Remedies: Reductive Dechlorination and Source Zone Treatment

The link between degradation of chlorinated hydrocarbons and microbial metabolism has been recognized since the early 1980's (Higgins et al. 1980). It is now recognized that biological oxidation and reduction of chlorinated hydrocarbons are possible, both metabolically and co-metabolically. Of the various biological processes associated with chlorinated hydrocarbon biotransformation, the most relevant with regards to remediation of DNAPL contaminated source zones and down-gradient plume regions is microbial reductive dechlorination. During reductive dechlorination, PCE and TCE are reduced sequentially to less-chlorinated daughter products such as *cis*-dichloroethene (*cis*-DCE), vinyl chloride (VC), and ethene (Figure 2.15), with

hydrochloric acid generated as a side product. The reductive dechlorination process may

occur via either metabolic or co-metabolic pathways under anaerobic conditions.
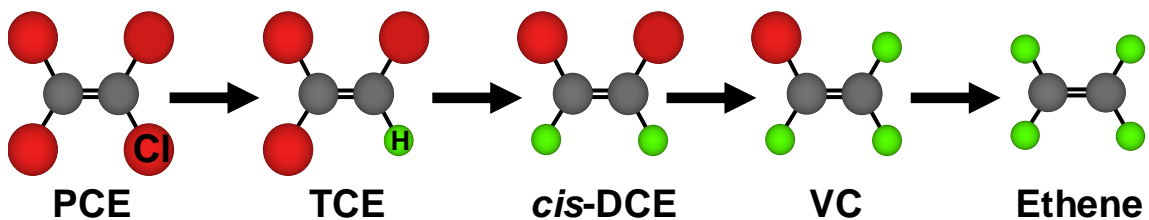
Figure 2.15: Sequential reductive dechlorination of tetrachloroethene to ethene. Figure courtesy of Ben Amos.

PCE dechlorination by anaerobic co-metabolism has been observed under a

number of conditions, including methanogenic, acetogenic, and sulfidogenic (see e.g.,

Fathepure and Boyd 1988, Cole et al. 1995); however slow reaction rates and incomplete

dechlorination make this process unlikely to significantly contribute to source zone

detoxification. Recent studies have focused on the process of chlororespiration, where

chlorinated compounds serve as metabolic electron acceptors (see Figure 2.16) for energy

generation (Löffler et al. 1996, 1999). The chlororespiration process (also referred to as

metabolic reductive dechlorination) is strictly anaerobic and requires introduction of an

electron donor to provide reducing equivalents. Nonetheless, discovery of this pathway

was a promising development for bioremediation of PCE- and TCE-contaminated sites,

implying that efficient dechlorination to ethene, a non-toxic end product, may be possible

(He et al. 2003a, 2003b).
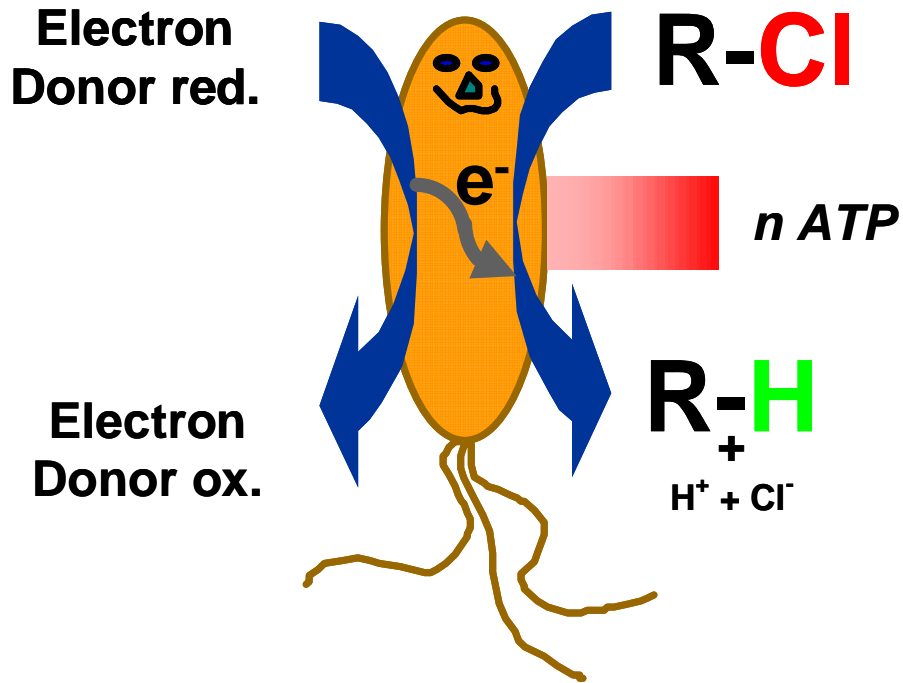
Figure 2.16: Conceptual model of metabolic reductive dechlorination by microorganism. Figure courtesy of Ben Amos.

Use of chlorinated ethenes as growth-supporting (i.e., metabolic) electron acceptors is distributed among a number of bacterial populations. These populations have been divided into a number of phylogenetic groups (see Christ et al. 2005a for a complete listing), including *Dehalobacter*, *Sulfurospirillum*, *Desulfuromonas*, *Desulfitobacterium*, *Clostridium*, and *Dehalococcoides*. While the range of organisms capable of metabolic reductive dechlorination is encouraging, most of the isolated organisms are not capable of complete detoxification to ethene (Löffler et al. 2003). This can result in accumulation of toxic intermediates, particularly dichloroethene and vinyl chloride, within the subsurface environment. However, recent studies have linked the presence of *Dehalococcoides* species and complete dechlorination of parent compounds to ethene (see e.g., Ritalahti et al. 2001, He et al. 2003a, 2003b). *Dehalococcoides*

ethenogenes strain 195 was the first reported isolate capable of dechlorination to ethene, but the final dechlorination step (vinyl chloride-to-ethene) was co-metabolic and therefore slow (Maymo-Gatel et al. 1997). A recent breakthrough was the isolation and identification of *Dehalococcoides* species strain BAV1 (He et al. 2003a, 2003b), an organism capable of using all DCE isomers and vinyl chloride metabolically as growth-supporting electron acceptors.

It was initially believed that reductive dechlorination at high aqueous PCE concentrations (i.e., near saturation) or within a PCE-DNAPL source zone would not occur due to toxicity effects (Robertson and Alexander 1996). In recent years, however, this paradigm has come under increasing scrutiny. Using a consortium of dechlorinating microorganisms, Nielson and Keasling (1999) reported complete reductive dechlorination of PCE at saturation to ethene in a batch system. In addition, inhibition of methanogenic populations in the consortium was observed, presumably due to toxicity effects arising from the high chlorinated ethene concentrations. Yang and McCarty (2000) also reported PCE dechlorination under batch conditions with PCE concentrations approaching solubility, and dechlorination activity in batch systems containing PCE-DNAPL was demonstrated by Carr et al. (2000).

In addition to batch studies, a number of column experiments have been conducted to evaluate reductive dechlorination at high aqueous phase contaminant concentrations and/or in the vicinity of DNAPL. In a series of 1-D column experiments, Yang and McCarty (2000, 2002) evaluated dissolution enhancement from a non-uniformly distributed (and variable between experiments) pure PCE-DNAPL distributions using several electron donor amending strategies. Under these experimental

conditions, PCE-DNAPL dissolution enhancement factors ranging from 3-fold to 5-fold were reported. Cope and Hughes (2001) evaluated PCE dissolution enhancement from 1-D columns uniformly imbibed with mixed NAPL, comprised of 0.13 mol/mol PCE in tridecane and having an aqueous solubility of 26 mg/L (150 μM). The columns were continuously fed with varying levels of the electron donor pyruvate, and dissolution enhancement ranged from 5-fold to 6.5-fold. In both of the above cases dechlorination with a mixed culture capable of converting PCE to ethene was observed; however, stalling of dechlorination at vinyl chloride (Cope and Hughes 2001) and *cis*-DCE (Yang and McCarty 2002) were respectively reported. PCE dissolution enhancement has also been evaluated in a 2-D aquifer cell containing a PCE-DNAPL source zone (Sleep et al. 2006). Following bioaugmentation with a culture capable of complete PCE dechlorination, ethene was detected in the aquifer cell effluent. However, concentrations were relatively low compared to observed levels of *cis*-DCE and VC. PCE dissolution ranged from 2-fold to 3-fold, although performance decreased over time due to reduced flow through the NAPL source zone caused by bioclogging. While the primary objective of microbial reductive dechlorination is complete conversion of chlorinated ethenes to ethene, the observed production of *cis*-DCE and VC may nonetheless be of remedial benefit since it is often accompanied by an enhancement in the DNAPL dissolution rate and reduction in source zone longevity. In addition, *cis*-DCE and vinyl chloride are more accessible to organisms capable of aerobic dechlorination that may be located in aerobic zones down-gradient of the DNAPL source zone (Coleman et al. 2002a, 2002b).

While the column experiments investigating dechlorination of DNAPL source zones demonstrate its promise as a tertiary treatment strategy, experimental results also

present a number of potential obstacles. The experiments reported by Yang and McCarty (2002) were characterized by DNAPL distribution non-uniformity that resulted in competition for nutrients and bio-clogging of the columns due to excessive growth of non-dechlorinating organisms. These factors may be mitigated through use of slow-release electron donors, although modeling results indicate that electron donor limitations may result in formation of biofilms around the DNAPL (Chu et al. 2003). Presence of these biofilms may act to reduce contaminant dissolution rates and impede the supply of electron donor to dechlorinating microbial populations. In addition, partitioning of dechlorination products (i.e., TCE, *cis*-DCE, vinyl chloride) from the aqueous phase into PCE-DNAPL may act to limit further dechlorination (Adamson et al. 2004). Finally, decreases in system pH associated with the generation of hydrochloric acid as a reductive dechlorination product may have toxic effects on some microbial populations (Cope and Hughes 2001).

Results from batch and column studies imply that, although dechlorination to cis-DCE is not uncommon, the presence of active *Dehalococcoides* species is required for complete detoxification of chlorinated ethenes (Ritalahti et al. 2001). This is an important consideration in the design and implementation of bioremediation technologies in the field, either as a direct source zone treatment or as a tertiary polishing step. Field studies have demonstrated the successful application of bioaugmentation with *Dehalococcoides* species both for plume containment (Major et al. 2002) as well direct source zone treatment (Adamson et al. 2003). For reductive dechlorination to be sustained, a source of electron donor must be supplied to the treatment area. Once added, the parent electron donor is transformed through activity of fermentative organisms into

66

hydrogen or acetate, two compounds capable of supporting reductive dechlorination (He et al. 2002). A number of compounds, including ethanol, lactate, propionate, butyrate, and oleate have been shown to be capable of supporting dechlorinating populations (see e.g., Carr and Hughes 1998, He et al. 2002, Yang and McCarty 2002). Other research has focused on using slow-release, non-soluble electron donor substrates such as olive oil, chitin, or the commercial product HRC™ (Hydrogen Release Compound, Regenesis Bioremediation Products, San Clemente, California) (Koenigsberg and Farone 1999, Yang and McCarty 2002). Because most dechlorinating organisms are highly efficient hydrogen users (Löffler et al. 1999), use of electron donor compounds that more slowly release hydrogen may be advantageous by maximizing dechlorination usage of available reducing equivalents (He et al. 2002).

To date, little work has been conducted directly evaluating the coupling of physicochemical source zone treatments with biostimulation or bioaugmentation in the field. However, limited evidence indicating the potential success of this approach has been observed during recent pilot-scale studies. At the Sages site in Jacksonville, Florida (see Table 2.4), an alcohol cosolvent (95% ethanol, 5% water) was flushed through a PCE-DNAPL source zone. A total of 43 L of PCE were recovered during the flood, with approximately 92% ethanol recovery (Jawitz et al. 2000). Some PCE-DNAPL remained in the source zone following treatment, and long-term monitoring (350 days following cosolvent flushing) indicated PCE concentrations in the source zone rebounded to pre-treatment levels and ethanol concentrations were greater than 160 μM (Mravik et al. 2003). In general, elevated alcohol concentrations, such as those observed during the Sages study, have the potential to negatively impact microbial activity. However,

elevated hydrogen and acetate concentrations were observed during additional long-term (3 years following cosolvent flushing) monitoring of the treated area, suggesting that biological activity may rebound with decreasing alcohol concentrations (Mravik et al. 2003). In addition, *Dehalococcoides* populations have been observed in down-gradient soil core samples (Mravik et al. 2003). Distribution and activity of dechlorinating populations in the source zone remains unclear; however, observation of *cis*-DCE within the source implies that dechlorination is ongoing.

A pilot-scale surfactant flushing test was conducted at the Bachman Road site in Oscoda, Michigan (Table 2.4), using a flushing solution comprised of 6% (wt.) Tween 80, a biodegradable, food-grade, nonionic surfactant, and designed for PCE recovery via miscible displacement. Surfactant recovery was greater than 95%, with 19 L of PCE recovered. Down-gradient contaminant concentrations were reduced by two orders-of-magnitude and did not rebound based on long-term (450 days) monitoring (Ramsburg et al. 2004b). No reductive dechlorination was observed in the Bachman Road source zone prior to surfactant flushing. However, PCE degradation products (primarily *cis*-DCE, limited VC) were observed in the source zone following the surfactant flood, along with elevated levels of acetate and formate that were attributed to fermentation of residual Tween 80 (Ramsburg et al. 2004b).

While, the above case studies indicate that coupling of physicochemical and biological remediation approaches may be an efficient source zone treatment strategy, particularly for SEAR, the fate of surfactants not recovered during flushing and their impact on bioremediation remains unclear. Evidence suggests that many nonionic surfactants can be fermented in the subsurface (Yeh et al. 1999), providing an indirect

source of electron donor for reductive dechlorination. However, presence of residual surfactants may also affect contaminant bioavailablity (Pennell et al. 2001). The bioavailability of hexachlorobenzene in the presence of the nonionic Tween surfactant series was investigated by Yeh et al. (1999). At low Tween concentrations (below 10 mg/L), hexachlorobenzene dechlorination rate and extent were unchanged. However, dechlorination rate decreased with increasing surfactant concentration, and complete inhibition was observed at concentrations about 1,000 mg/L. Inhibition was attributed to toxic effects due to high surfactant concentrations. Similar results were reported with a PCE dechlorinating consortium exposed to anionic, nonionic, and cationic surfactants (McGuire and Hughes 2003). Dechlorination rate was least impacted by the nonionic surfactants, and complete dechlorination of PCE to ethene was still possible. In general however, further research is required to more completely evaluate the potential impacts (both positive and negative) of residual surfactants on reductive dechlorinating microbial communities.

CHAPTER 3

MATERIALS, EXPERIMENTAL PROTOCOLS, AND

ANALYTICAL METHODS

A number of different experimental apparatus were employed as part of the research described here. Two aquifer cells were used to evaluate the effect of NAPL composition and distribution on the recovery efficiency of surfactant-based remediation strategies. The first cell, used in Chapters 4 and 6, was a comprised of only a source zone region, while the second cell (used in Chapters 5) was a larger cell containing both a source zone and a dissolved-phase plume region. In addition a one-dimensional column was employed to study microbial reductive dechlorination in the immediate vicinity of a PCE-NAPL (Chapters 7 and 8). These experimental apparatus are described in detail in this chapter, along with experimental materials and analytical methods used in this work.

3.1 Materials

3.1.1 Organic Liquids

The research described herein focused on two representative chlorinated solvents, tetrachloroethene (PCE) and trichloroethene (TCE). These compounds were selected due to widespread presence as NAPLs in the subsurface and their significantly different densities and solubilities, allowing for evaluation of the impact of NAPL composition on remediation efficiency. Both solvents were purchased from Fisher Scientific (Fair Lawn, NJ) as HPLC-grade chemicals. Hexadecane (99% purity) was obtained from Sigma-Aldrich (Milwaukee, WI) and used as an organic carrier phase for experiments requiring reduced aqueous-phase PCE concentrations. For visualization purposes, organic liquids

were colored red at a concentration of 4×10^{-4} M using Oil-Red-O, an organic soluble dye obtained from Fisher Scientific. At relatively low concentrations ($\sim 10^{-4}$ M), the presence of Oil-Red-O has not been observed to significantly affect NAPL physical properties, including interfacial tension, surface tension, density, and viscosity (Taylor et al. 2001).

During experiments employing the density modified displacement (DMD) process, 1-butanol was selected for use as the partitioning alcohol. Extensive research (see e.g., Ramsburg 2002, Ramsburg and Pennell 2002a, Ramsburg and Pennell 2002b) has demonstrated that 1-butanol strikes an appropriate balance between aqueous alcohol solubility and the tendency for the alcohol to partition into DNAPL. In addition, 1-butanol offers a number of additional advantages, including the absence of gel formation when mixed with surfactants and the potential to serve as an electron donor in post-treatment bioremediation. HPLC-grade 1-butanol was purchased from Fisher Scientific and used without additional purification. In addition, optima grade 2-propanol was purchased from Fisher Scientific and employed in selected surfactant solution formulations. Relevant chemical and physical properties of the organic compounds employed in this research are summarized in Table 3.1.

Table 3.1: Relevant properties of organic chemicals used at 25°C.

Chemical	Molecular Weight (g/mol)	Aqueous Solubility (mg/L)[a]	Liquid Density (g/cm³)[a]	Interfacial Tension (dyne/cm)[b]	Dynamic Viscosity (cP)[c]
Tetrachloroethene	165.83	150	1.62	47.4	0.80
Trichloroethene	131.39	1,100	1.47	35.2	0.53
Hexadecane	226.44	Insoluble	0.77	43.4	0.80
1-Butanol	74.12	74,500	0.81	24.6	2.94
2-Propanol	60.12	Miscible	0.78	N/A	1.98

a: Schwarzenbach et al. 2003
b: Ramsburg 2002 (22°C)
c: Ramsburg and Pennell 2002a

The nonionic surfactant polyoxyethylene (20) sorbitan monooleate (Tween 80, provided by Uniqema, New Castle, DE) was selected for use in experiments requiring surfactant-enhanced solubilization or density modified displacement. Tween 80 was selected because is an effective solubilizing agent for use in surfactant enhanced aquifer remediation (e.g., Pennell et al. 1993, Pennell et al. 1997, Ramsburg and Pennell 2001, Taylor et al. 2001). It is also relatively nontoxic (Pennell et al. 1993) and may serve as a source of reducing equivalents for post-treatment reductive dechlorination (Christ et al. 2005a). An additional nonionic surfactant, sorbitan monooleate (Span 80, provided by Uniqema), was also used during density modified displacement due to its synergistic emulsifying relationship with Tween 80. Structurally, Tween 80 is composed of a sorbitan ring derived from the sugar alcohol sorbitol, connected to the oleic acid derivative oleate via an ester linkage. To the sorbitan-oleate structure, ethylene oxide groups (numbering 20 on average) are added at various locations on the sorbitan side of the ester linkage. Span 80 is structurally similar, but lacks any ethylene oxide groups, making it considerably more hydrophobic. The structures of Tween 80 and Span 80, along with a listing of their important physical and chemical properties are provided in Figures 3.1.
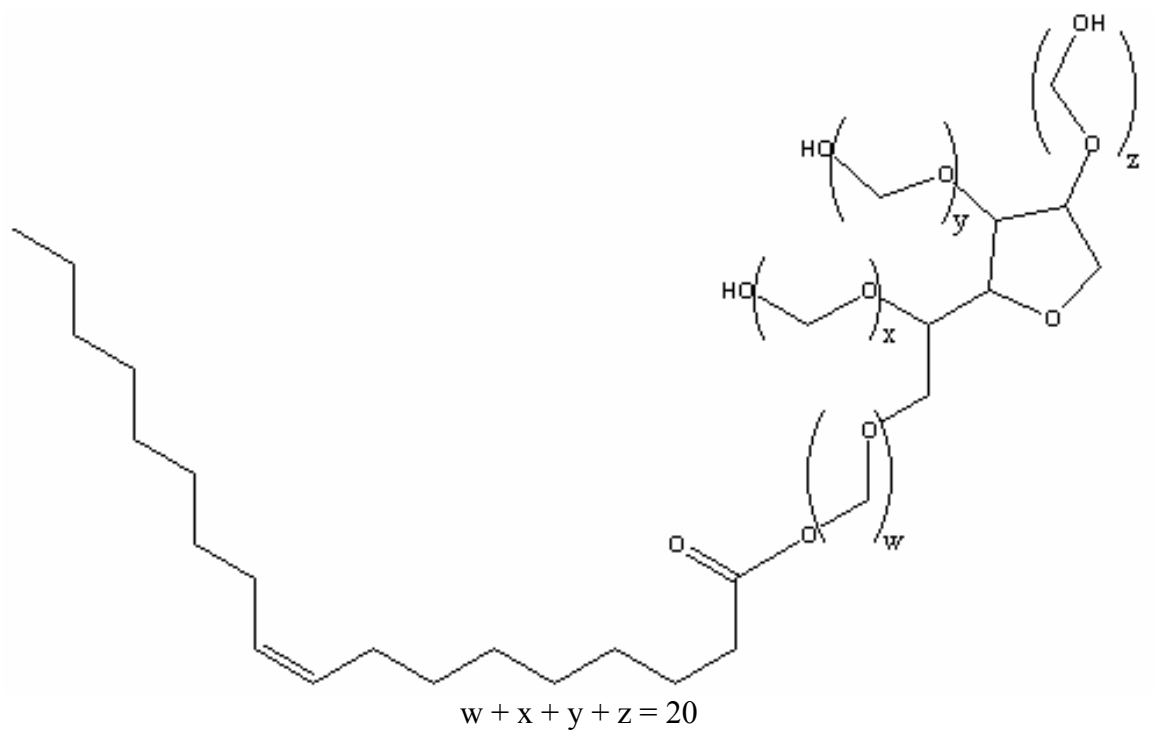
$$w + x + y + z = 20$$

Average Molecular Weight (g/mol)	Hydrophile-Lipophile Balance	Aggregation Number	Critical Micelle Concentration (g/L)
1310	15	110	0.013 (in water)

Data from Pennell et al. 1997
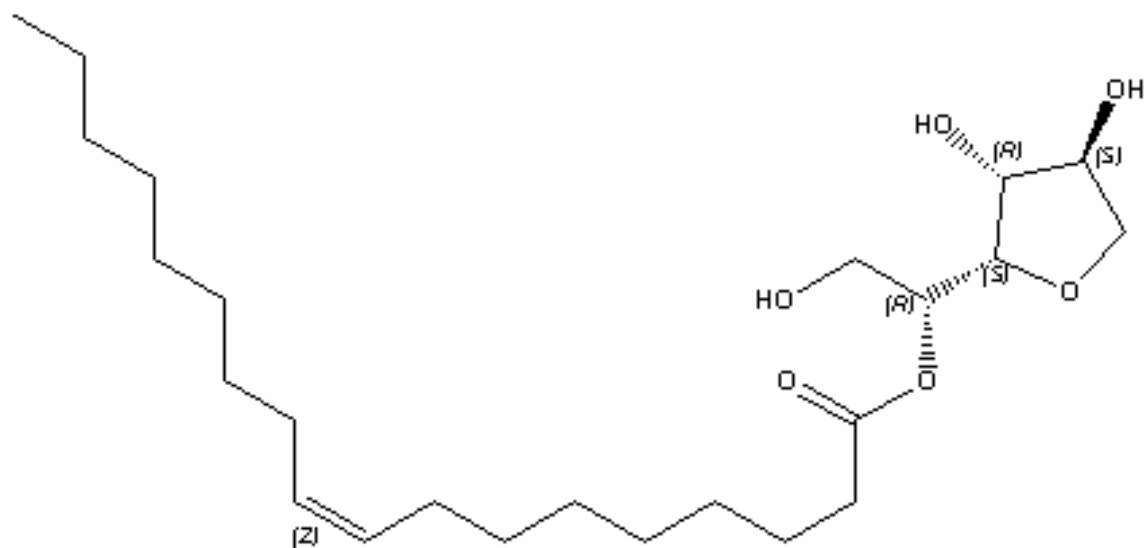
Average Molecular Weight (g/mol)	Hydrophile-Lipophile Balance	Aggregation Number	Critical Micelle Concentration (g/L)
428	4.3	Insoluble in Water	Insoluble in Water

Figure 3.1: Structures of polyoxyethylene (20) sorbitan monooleate (Tween 80, top) and sorbitan monooleate (Span 80, bottom).

Recent research has demonstrated the potential for using anionic surfactants to achieve significant solubilization and/or mobilization of a DNAPL during SEAR (e.g., Dwarakanath 1997, Ramsburg and Pennell 2001). The anionic surfactant sodium dihexyl sulfosuccinate (also referred to as sodium di(1,3-dimethylbutyl) sulfosuccinate or Aerosol MA) was selected for use during experiments requiring solubilization in conjunction with mobilization as well as the during the displacement phase of the DMD process. Aerosol MA was selected because it is a relatively nontoxic surfactant, and is often employed in the pharmaceutical industry (Ramsburg 2002). Figure 3.2 details the structure and physical properties of Aerosol MA, a non-toxic food-grade surfactant commonly used in the pharmaceutical industry (Dwarakanath et al. 1999). Sodium dihexyl sulfosuccinate was provided by Cytec Industries (West Paterson, NJ) as Aerosol MA80-I, a mixture composed of 80% active ingredient (sodium di(1,3-dimethylbutyl) sulfosuccinate) with the remaining 20% water and 2-propanol, and used without further purification.
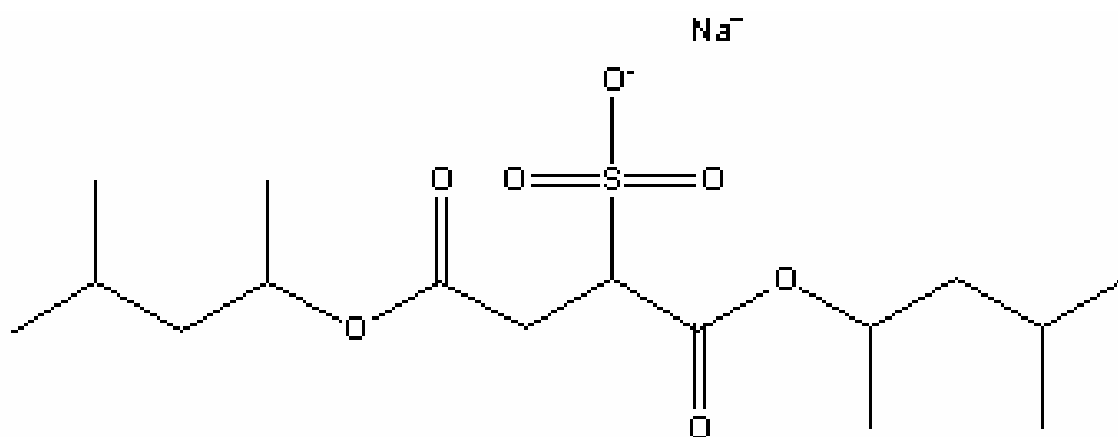
Molecular Weight (g/mol)	Hydrophile-Lipophile Balance	Aggregation Number	Critical Micelle Concentration (g/L)
388.46	Not Applicable	Not Available	Not Available

Data from Ramsburg, 2002

Figure 3.2: Structure of sodium di(1,3-dimethylbutyl) sulfosuccinate (Aerosol MA).

3.1.3 Porous Media

Four silica sands, 20-30 mesh Accusand, 40-50 mesh Accusand, F-70 (40-270 mesh) Ottawa sand, and Federal Fine (30-140 mesh) Ottawa sand, were selected as representative porous media for the 2-D aquifer cell and 1-D column experiments. The Accusand was purchased from Unimin Corporation (New Canaan, CT) and was used as received. Accusand was selected for use as the background porous media during selected aquifer cell experiments because it is a high purity, translucent to transparent sand, making it suitable for light transmission analysis. Both Ottawa sands were obtained from the U.S. Silica Company (Berkeley Springs, WV) and used as received. Federal Fine is classified as a medium sand and has a mean grain size (d_{50}) of 0.280 mm. Federal Fine was selected for use as the background porous media during the column and selected aquifer cell experiments due to its very low organic carbon (OC) content (not detected at detection limit of 0. 1 g_{oc}/kg_s) and light color, which allowed for easy observation of dyed aqueous and organic liquids within column and/or aquifer cell. F-70 Ottawa sand, a fine sand with a mean grain size of 0.174 mm, is lighter in color than Federal Fine, allowing for visual observation of system heterogeneity, while also providing an approximate one order-of-magnitude decrease in intrinsic permeability. F-70 was used during all aquifer cell experiments to simulate a lower confining layer along the bottom of the aquifer cell along with heterogeneous regions of low permeability lenses. Properties of the four sands are summarized in Table 3.2 and particle size distributions of the two Ottawa sands are presented in Figure 3.3.

Table 3.2: Properties of the sands used in column and aquifer cell experiments.

Property	20-30 Accusand	40-50 Accusand	F-70 Ottawa	Federal Fine
Organic Carbon (g/kg)	0.4[a]	0.3[a]	0.1[b]	0.1[b]
Intrinsic Permeability, k_i (m^2)	2.50×10^{-10} [a]	7.72×10^{-11} [a]	8.2×10^{-12} [d]	4.2×10^{-11} [c]
Mean Grain Size, d_{50} (mm)	0.500	0.300	0.174	0.280
Uniformity Index, U_i (d_{60}/d_{10})	1	1	1.65	1.66

a: Schroth et al. 1996
b: U.S. Silica Company
c: Ramsburg 2002
d: Kueper and Frind 1991
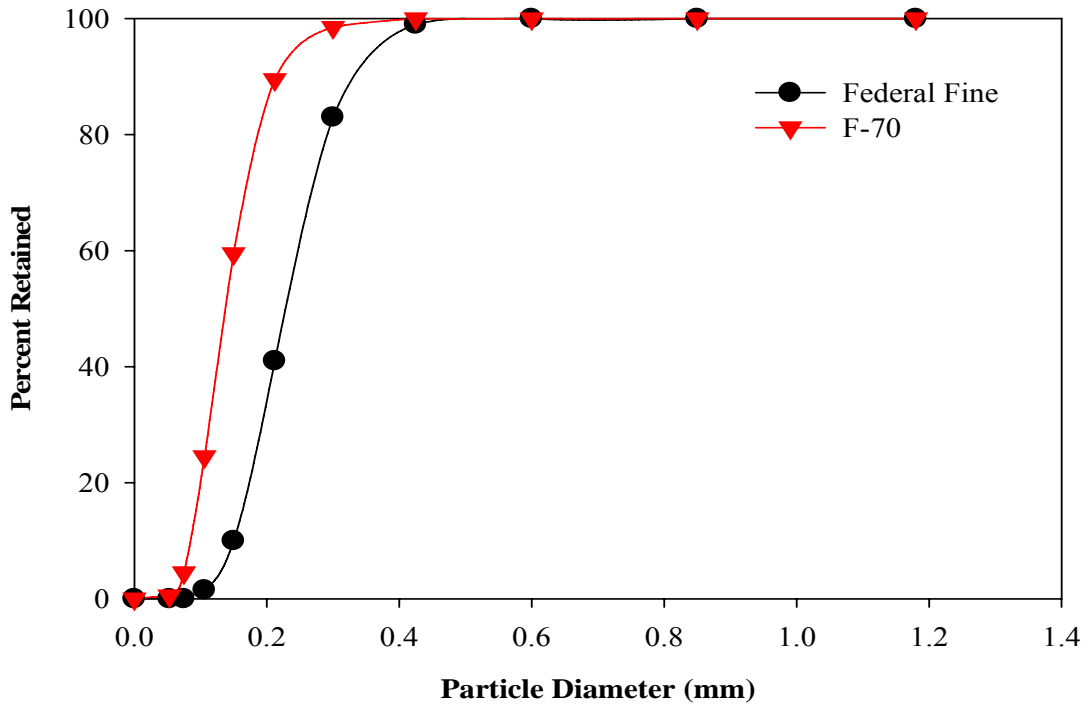
Figure 3.3: Particle size distributions for Ottawa F-70 and Federal Fine sand used in column and aquifer cell experiments (from U.S. Silica Company).

3.1.4 Column Microbial Inocula

Two distinct microbial inocula were employed during the reductive dechlorination column experiments. The first inoculum was a pure culture of *Sulfurospirillum multivorans*, a gram-negative, strictly anaerobic organism that is metabolically capable of dechlorinating PCE to *cis*-DCE (Neumann et al. 1994). The second was a mixed culture (Bio-Dechlor INOCULUM, BDI) capable of complete PCE dechlorination to ethene. The culture contains a number of relevant dechlorinating microorganisms, including *Dehalobacter, Geobacter,* and *Dehalococcoides* species. Both inocula were obtained from the laboratory of Dr. Frank Löffler at the Georgia Institute of Technology.

3.2 Experimental Protocols

3.2.1 Solution Preparation

Materials and techniques used to prepare the solutions employed in this research are described in individual sections below. Section 3.2.1.1 details preparation of aqueous surfactant solutions used in Chapters 4, 5, and 6. The formulation and preparation of the surfactant-stabilized 1-butanol emulsion used during the density modified displacement method (Chapter 6) is described in section 3.2.1.2. Finally, composition and preparation of the reduced mineral salts medium employed in the 1-D column experiments (Chapters 7 and 8) is briefly explained in section 3.2.1.3.

3.2.1.1 Aqueous Surfactant Solutions

All surfactant solutions were prepared in deionized water that was purified by passage through a Barnstead E-Pure system (Barnstead/Thermolyne Corporation,

Dubuque, IA). To achieve desired surfactant solution properties, or serve as non-reactive tracers, a number of salts were used in this research, including sodium chloride, calcium chloride, potassium iodide, and potassium bromide. All of the salts were purchased from Fisher Scientific, with calcium chloride obtained in the dihydrate form. Erioglaucin A, a dye used to color aqueous phase surfactant and tracer solutions blue for observational purposes was purchased from Fluka Chemical (Milwaukee, WI) and added to aqueous solutions at a concentration of 3×10^{-5} M. At the given concentration, the presence of Erioglaucin A has no observable effects on aqueous solution properties.

Surfactant solutions used in Chapters 4, 5, and 6 were prepared gravimetrically using a top loading Mettler PM4000 analytical balance (±0.0001 g). Chemicals were added in the following order: surfactants, salts, alcohols, water, and dye. After addition of all chemicals, solutions were mixed until all ingredients were completely dissolved using a Corning PC-420 magnetic stir plate at room temperature (22±3ºC). Once mixed, an aliquot of each solution was collected for subsequent compositional analysis.

3.2.1.2 Emulsions

Surfactant stabilized 1-butanol emulsions employed during DMD surfactant flushing experiments (Chapter 6) were prepared gravimetrically using a Mettler PM4000 analytical balance. Tween 80 was added first, followed by Span 80, 1-butanol, and water. Following addition of the chemicals, the mixture was emulsified using a commercial blender (Waring Commercial, model 36BL23) operating at 20,000 rpm, and allowed to rest for one hour. After resting, the mixture was emulsified again at 20,000 rpm and an aliquot of the solution was collected for analysis. Previous research has

shown that the presence of the aqueous dye Erioglaucin A, even at low concentrations, adversely affects emulsion stability (Ramsburg 2002). Therefore, the emulsions used in this research were not dyed.

3.2.1.3 Reduced Mineral Salts Media

The reduced mineral salts medium used in the microbial reductive dechlorination column experiments (Chapters 7 and 8) was prepared using the protocol described by Löffler et al. (1997). The following chemicals (obtained from Fisher Scientific) were added to distilled water and mixed until dissolved, producing the concentrations specified in Table 3.3: salts, trace elements, sodium sulfate, selenium/tungsten, TES, resazurin, and electron donor (pyruvate or acetate). The medium was then boiled under a nitrogen atmosphere for a period of 10-15 minutes and allowed to cool. Following cooling, l-cysteine, sodium sulfide, and sodium bicarbonate were added to the medium, yielding concentrations specified in Table 3.3. After addition of these chemicals the pH of the medium was adjusted to a stable value in the range of 7.2 to 7.3 using carbon dioxide gas and autoclaved. After being autoclaved, Wolin vitamin solution (Wolin et al. 1963) was added to the medium, resulting in chemical concentrations in the medium as shown in Table 3.3. After preparation, an aliquot of the medium was collected and reserved for subsequent chloride and organic acid analysis.

Table 3.3: Composition of reduced mineral salts medium.

Chemical	Concentration (mg/L)	Chemical	Concentration (mg/L)
Salts			
NaCl	1,000	NH$_4$Cl	300
MgCl$_2$ · 6 H$_2$O	500	KCl	300
KH$_2$PO$_4$	200	CaCl$_2$ · 2 H$_2$O	15
Trace Elements			
FeCl$_2$ · 4 H$_2$O	1,500	H$_3$BO$_3$	6
CoCl$_2$ · 6 H$_2$O	190	Na$_2$MoO$_4$ · 2 H$_2$O	36
MnCl$_2$ · 4 H$_2$O	100	NiCl$_2$ · 6 H$_2$O	24
ZnCl$_2$	70	CuCl$_2$ · 2 H$_2$O	2
Selenium/Tungsten			
Na$_2$SeO$_3$ · 5 H$_2$O	6	Na$_2$WO$_4$ · 2 H$_2$O	8
Wolin Vitamins			
Biotin	0.02	Nicotinic Acid	0.05
Folic Acid	0.02	Pantothenic Acid	0.05
Riboflavin	0.05	Vitamin B$_{12}$	0.001
Pyridoxine Hydrochloride	0.1	p-Aminobenzoic Acid	0.05
Thiamine	0.05	Thioctic Acid	0.05
Other Chemicals			
Na$_2$SO$_4$	710	l-Cysteine	35
TES	2,292	Na$_2$S	48
Resazurin	0.25 (mL/L)	NaHCO$_3$	2,520

3.2.2 Small Aquifer Cell

All experiments in Chapters 4 and 6 were conducted using a small two-dimensional (2-D) parallel plate aquifer cell apparatus designed to simulate the saturated zone of an unconfined aquifer. The aquifer cell was constructed from 6061 aluminum alloy with dimensions of 63.5 cm (length) by 38 cm (height) by 1.4 cm (thickness). A U-shaped frame was milled from a single block of aluminum in order to minimize potential leakage points. Non-tempered plate glass of 1.4 cm thickness served as the front and back of the experimental apparatus. Glass was selected in order to allow for visual observation of the experiments during their progression. The glass panels were secured

to the frame using two sets (front and rear, three pieces each) of aluminum clamps attached by screws to the frame along both the front and rear of the apparatus. Viton o-ring cord stock (nominal diameter of 0.318 cm) was purchased from McMaster-Carr and placed into o-ring groove tracks (two on each side, four total) milled into the aluminum frame. Vacuum grease was applied between the o-ring cord, frame, and glass panels in order to form a liquid-tight seal. End chambers were constructed by cutting small rectangular (0.203 mm thick) slits in square 6061 aluminum alloy tubing (1.27 cm x 1.27 cm). The end chambers were screened over the entire height of the aquifer cell.

The cell was packed with two sands of contrasting permeability under water saturated conditions. A layer of F-70 Ottawa sand (2 cm in depth) was emplaced over the entire lower boundary of the cell. In addition, two regions of low permeability lenses were created by placing F-70 Ottawa sand layers within the higher permeability background sand to simulate heterogeneous conditions. The first region of lenses (3 cm in depth) was placed directly above the lower F-70 Ottawa sand layer over the entire length of the cell. A second region of lenses was placed 19-22 cm above the confining layer and 19 cm from each end chamber. A representative image of the small 2-D aquifer cell following packing and prior to NAPL imbibition is presented in Figure 3.4.

A partially-screened injection well, constructed from 0.32 cm outside diameter 316 stainless steel tubing, was packed within the soil matrix approximately 3 cm from the left end chamber (Figure 3.4) and used during DMD experiments to introduce surfactant solution. The injection well was designed with partial screening (26 holes, 0.5 mm in diameter, drilled to face in one direction) over the bottom 5.2 cm in order to promote contact between the flushing solutions and organic phase. Similar schemes have been

employed in cosolvent flushing field trials (Jawitz et al. 2000) to minimize potential density override effects caused by flushing solutions that may be less dense than the resident solution (i.e., water). For solubilization experiments, where density override is not a concern, surfactant solutions were introduced via the fully-screen left end chamber of the aqueous cell.
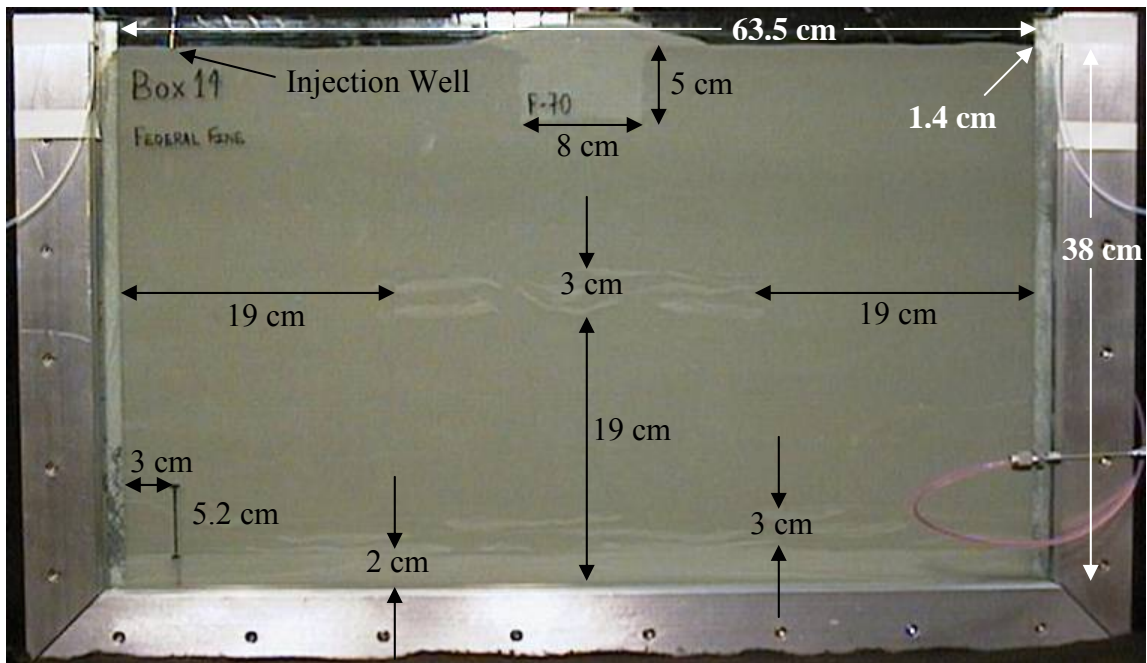
Figure 3.4: Representative packed small 2-D aquifer cell.

Flow of flushing solutions through the cell was established using either a 2 or 5 L Marriott bottle placed on a jack stand which allowed for height adjustments to maintain constant flow rate. Teflon® tubing (0.32 cm outside diameter, o. d.) was used to deliver fluids from the Marriott bottles to either the left end chamber of the cell or the partially screened injection well. Effluent samples were collected into 20 mL borosilicate scintillation vials using an Isco Retriever II (Lincoln, NE) fraction collector that was

connected to the aquifer cell at the midpoint of the effluent (right) end chamber via 0.32 cm o.d. Teflon® tubing. Hydraulic conductivity of the cell was determined using Darcy's law in conjunction with the head loss across the entire cell at three flow rates. During the hydraulic conductivity tests, deionized water was injected into the aquifer cell via the fully screened end chamber. Head loss was measured in triplicate at each flow rate using two piezometers constructed of 0.32 cm o. d. Teflon® tubing and installed in each end chamber. Figure 3.5 depicts the complete experimental setup for the small aquifer cell apparatus.
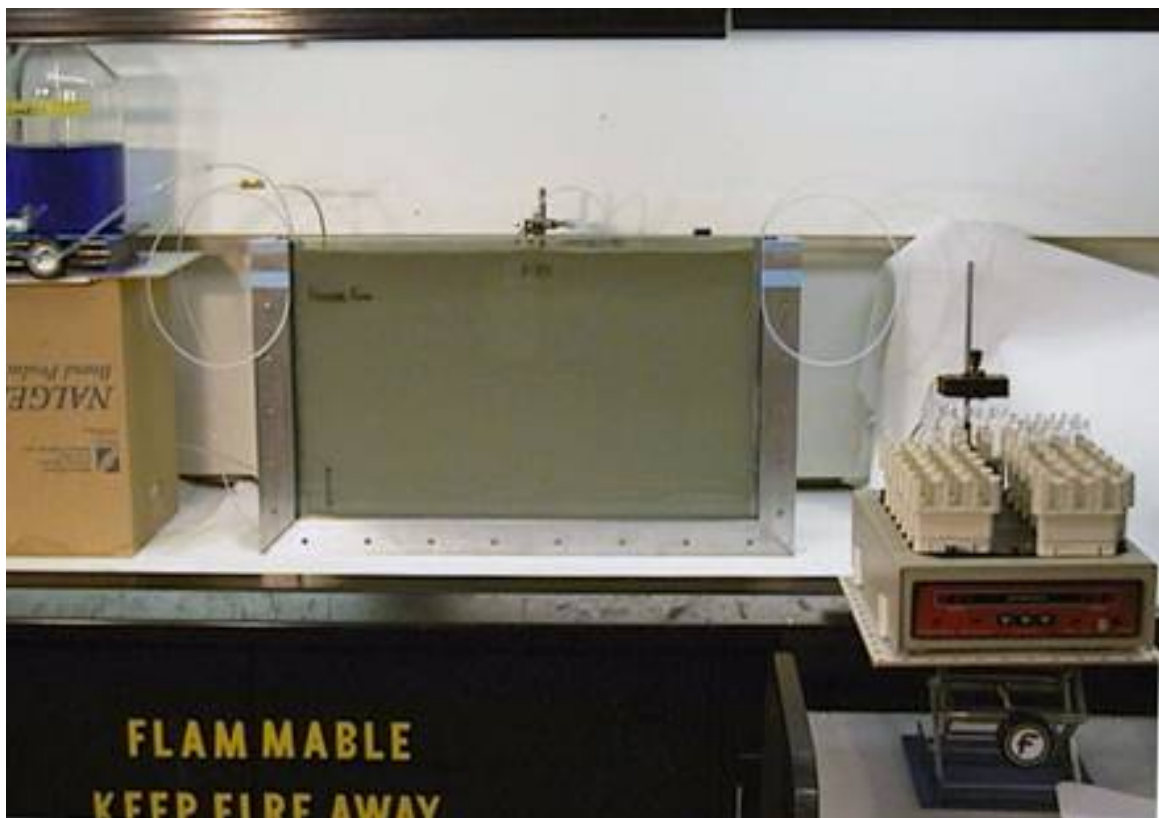
Figure 3.5: Small 2-D aquifer cell experimental setup (Ramsburg 2002).

All representative DNAPLs were injected into the aquifer cell using a 15.2 cm long, 18 gauge needle packed to a depth of approximately 7 cm below the sand surface. To minimize backflow of the DNAPL during the injection process, an 8 cm (length) by 5 cm (height) region of the low permeability F-70 Ottawa sand used as the lower layer was emplaced above the injection point. The injection needle was connected to a 50 mL glass syringe (Popper and Sons) using 0.32 cm o. d. Teflon® tubing. A Harvard Apparatus model 22 syringe pump was used to inject DNAPL into the aquifer cell at a constant flow rate of 1 mL/min. After injection of approximately 45 mL of DNAPL, the organic phase was allowed to redistribute within the cell for a period of at least 24 hours, after which time any free-phase organic liquid present in the end chambers was removed. Following DNAPL injection and redistribution, the overall hydraulic conductivity of the aquifer cell was again determined using Darcy's law and the head loss across the cell at three flow rates.

For experiments conducted in Chapter 6, water was injected into the aquifer cell via the left-hand end chamber at a constant nominal flow rate of 1 mL/min following DNAPL injection but prior to surfactant flushing. Water flushing was maintained for a period of approximately one week in order to monitor initial plume development and effluent mass flux down-gradient from the DNAPL source zone. During this time daily samples were taken from the aqueous effluent. Following initial plume development monitoring, surfactant solution was introduced into the aquifer cell either through the partially screened injection well (during DMD experiments) or the left fully screened end chamber (during all other surfactant floods) at constant nominal flow rates varying from 4 to 6 mL/min, depending on experimental objectives. The flow rate was maintained by

adjusting the heights of the influent bottle and the effluent collection point. The mass of flushing solution delivered was determined gravimetrically and converted to volume delivered based on measured solution density. Digital images of the aquifer cell were captured at regular time intervals (15 or 30 minutes) during surfactant flooding using a Nikon Coolpics 900 and water table height in the cell was measured using two piezometers located in the cell end chambers at 30 minute intervals. For Chapter 6 experiments, water flushing at a 1 mL/min nominal flow rate was resumed at the conclusion of the surfactant floods for a period of approximately one week, with daily effluent samples collected to evaluate plume development and mass flux following source zone treatment. It should be noted that pre- and post-treatment water flushing was not conducted for any of the experiments described in Chapter 5, and that surfactant flushing commenced immediately following DNAPL imbibition.

Following cessation of the surfactant and/or water flushing, the aquifer cell was drained through the either the partially screened injection well or the left-hand end chamber. To facilitate removal of residual fluids in the aquifer cell pore volume during draining, the cell was inclined approximately 6°, supported on a metal test tube rack. Following drainage, regions of the porous media that were observed to remain highly saturated with water, along with any regions of the porous media where entrapped DNAPL remained, were extracted for from the aquifer cell mass balance calculations. Extraction was accomplished by transferring solids and pore fluids into a container holding a known mass of 2-propanol. DNAPL and surfactant concentrations were then analyzed utilizing techniques described in section 3.3.2.

3.2.3 Large Aquifer Cell

A second, larger 2-D aquifer cell was employed during all experiments described in Chapter 5. Though design of the larger aquifer cell was similar to that of the small 2-D cell described in section 3.2.2 (i.e., glass panels separated by milled aluminum), the overall dimensions of the cell increased to 150 cm (length) by 48 cm (height). Cell thickness remained unchanged at 1.4 cm. In addition to the U-shaped frame and clamps described above, the large 2-D aquifer cell featured a separate milled aluminum brace running across the top of the entire cell and four vertical cross braces (2 each along the front and back of the cell) that were used to prevent bowing of the glass panels. End chamber design was identical to that used in the small box, and both the left- and right-hand chambers were screened over the entire height of the aquifer cell. The large 2-D aquifer cell contained two distinct regions: a "source area" designed to assess DNAPL mass recovery during treatment, and a "plume area" for monitoring post-treatment plume development and contaminant flux (see Figure 3.6). Twenty glass sampling ports were emplaced in the front glass panel within the plume area to monitor of post-treatment down-gradient plume development within the aquifer cell. The ports were constructed by attaching short lengths of 8 mm o. d. glass capillary tubing (i. d. 2 mm) to the tops of screw-cap HPLC vials; the ports were then emplaced within holes (pre-cut by water jet) in the front glass panel and attached to the panel using silicone. The ports possessed minimal internal dead volume (less than 0.5 mL), and could be easily replaced between experiments if necessary.
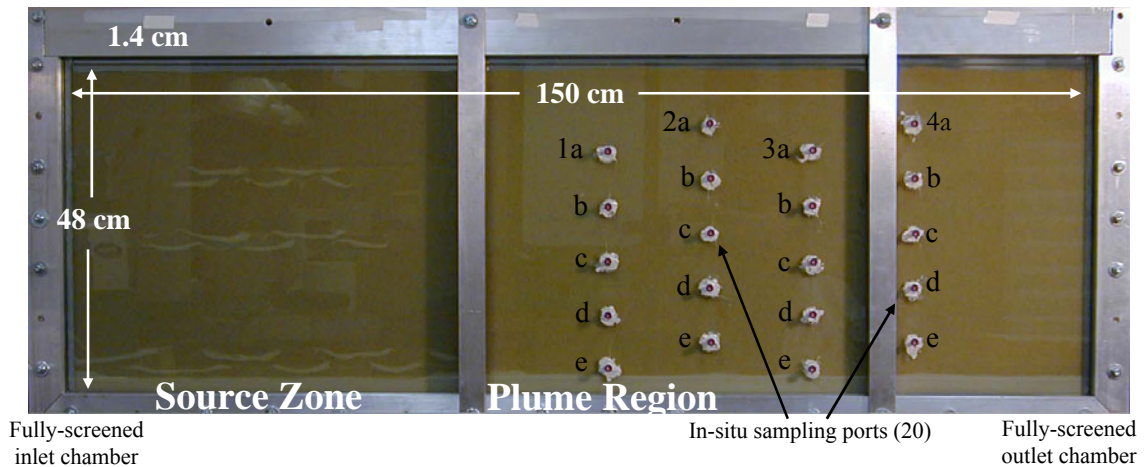
Figure 3.6: Schematic of large 2-D aquifer cell.

The aquifer cell was packed under water-saturated conditions in approximate 3 cm lifts. The plume region was comprised of a homogenous packing of the background porous media (either 20/30 mesh Accusand or a mixture of 50% 20/30 mesh Accusand and 50% 40/50 mesh Accusand), while the source area contained three regions of low permeability lenses that were created by emplacing F-70 Ottawa sand layers within the higher permeability background porous media. The first region of lenses (3 cm in height) was emplaced directly above the lower layer of F-70 Ottawa sand (2 cm in height) over the entire length of the source area of the cell. A second group of lenses, 37 cm in length, was located 19-22 cm above the lower F-70 Ottawa sand layer and 10 cm from the left-hand end chamber. The final set of lenses, located 29-32 cm above the lower F-70 layer and 15 cm from the left-hand end chamber, was 27 cm in length. A representative image of the source area region of the large 2-D aquifer cell following packing is presented in Figure 3.7.
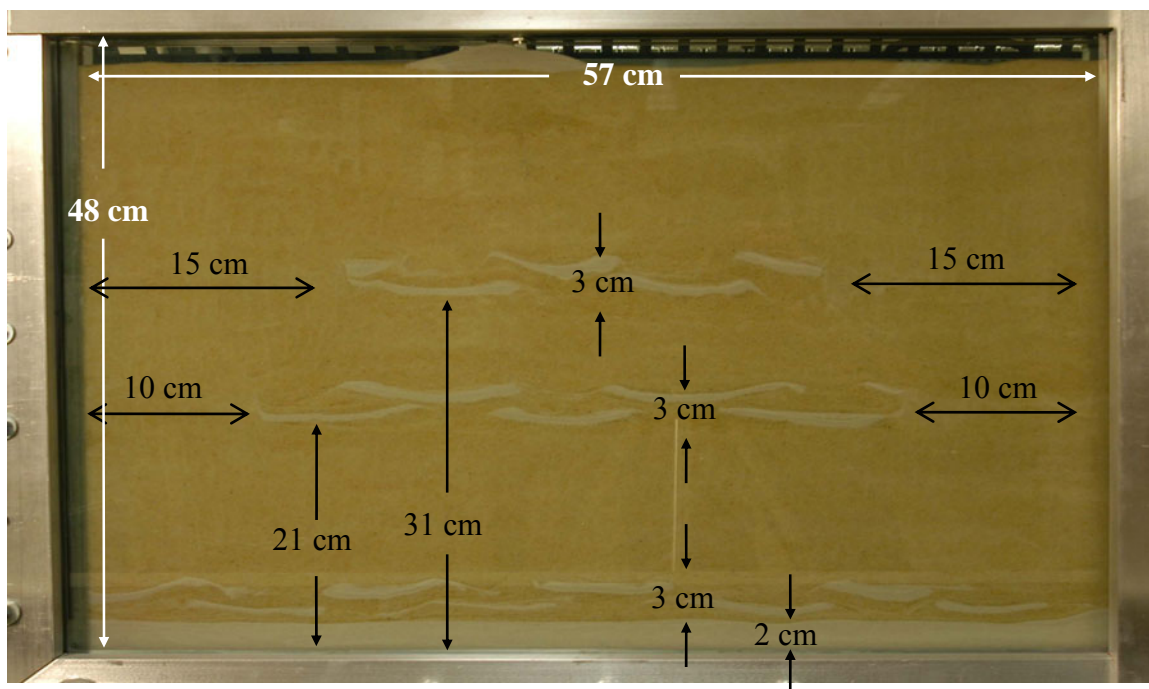
Figure 3.7: Representative image of the source area in the large 2-D aquifer cell.

Flushing solutions were introduced into the large 2-D aquifer cell using a system similar to that described in section 3.2.2. Effluent samples were collected into 20 mL borosilicate scintillation vials using either an Isco Retriever II fraction collector or by hand depending on the sampling frequency of the specific experiment. In either case, samples were taken via a 0.32 cm o. d. Teflon® tube that was connected to the aquifer cell at the midpoint of the effluent end chamber. Hydraulic conductivity of the aquifer cell was estimated using Darcy's law and the procedure outlined for the small aquifer cell. Head loss during the hydraulic conductivity tests was measured in triplicate using two piezometers, constructed of 0.32 cm o. d. Teflon® tubing, one installed in each end chamber. DNAPL was injected into the large aquifer cell using a procedure identical to that employed for the small aquifer cell. Following DNAPL injection, the organic phase was allowed to redistribute within the cell for a period of at least 24 hours and any free-

phase organic liquid present in the end chambers was removed. Overall hydraulic conductivity of the aquifer cell was then determined a second time using Darcy's law and the hydraulic head loss across the cell at three flow rates.

During the large aquifer cell experiments either two or three sequential surfactant floods, designed to recover increasing cumulative amounts of contaminant mass, were conducted. Prior to the initiation of each surfactant flood, the entire aquifer cell (source zone and plume region) was flushed with water at a nominal flow rate of 1mL/min for a period of several days in order to monitor dissolved-phase plume concentrations down-gradient from the DNAPL source zone. Aqueous effluent samples were collected daily into 20 mL scintillation vials and analyzed for contaminants. Following plume stabilization and measurement, surfactant solution was introduced into the larger aquifer cell through the left-hand end chamber at a constant nominal flow rate of 6 mL/min, which was maintained by adjusting the heights of the influent bottle and the effluent collection point. Duration of each sequential surfactant flood was estimated based on the DNAPL mass recovery goals for the specific experiment. The actual mass of flushing solution delivered was measured gravimetrically and converted to the volume delivered based on measured influent solution density. Sample collection during each sequential surfactant flood was identical to the methodology described for the small 2-D aquifer cell. At the conclusion of each surfactant flushing event, water flow through the entire cell was resumed at a nominal flow rate of 1 mL/min and down-gradient contaminant concentrations were monitored for a period of approximately 10 days. The above procedure was then repeated either one or two additional times to achieve additional DNAPL mass recovery.

At the conclusion of the final plume development period, water flushing through the aquifer cell was terminated and the cell drained through the fully screened end chamber. Unlike for the small aquifer cell, the large cell was not elevated during drainage. After draining, the porous media was extracted for mass balance calculations using the technique described in section 3.2.2. All contaminant concentrations were analyzed as described below.

3.2.4 Light Transmission Apparatus

In order to quantify DNAPL saturation and distribution (i.e., architecture) within the 2-D aquifer cell source zones, a light transmission (LT) system was developed for use with both the large and small aquifer cells. LT images of the aquifer cell source zones were captured immediately prior to and following each surfactant flushing event. A conceptual model of the LT system is shown in Figure 3.8, based on a design originally proposed by Tidwell and Glass (1994). For the LT system used in this research, a Kino Flo Flathead 80 system was selected as a light source. The Flathead 80 has dimensions of 130 cm (length) by 60 cm (height) and contains eight Kino Flo True Match 2900 Kelvin Tungsten fluorescent lamps. The Flathead 80 system was selected for its ability to provide nominally uniform transmission of light through the aquifer cell. In addition, the system employed external ballasts, limiting the amount of heat generated at the face of the aquifer cell. The light transmitted through the aquifer cell was captured using a Nikon Coolpics 900 digital camera capable of 1600x1200 pixel resolution. During LT analysis the camera was placed on a tripod approximately 1 meter from the front face of the aquifer cell. The resolution of the aquifer cell source zone LT images was

approximately 0.3 mm^2 per camera pixel. All images were then transferred to a personal computer as jpegs for subsequent processing and analysis.
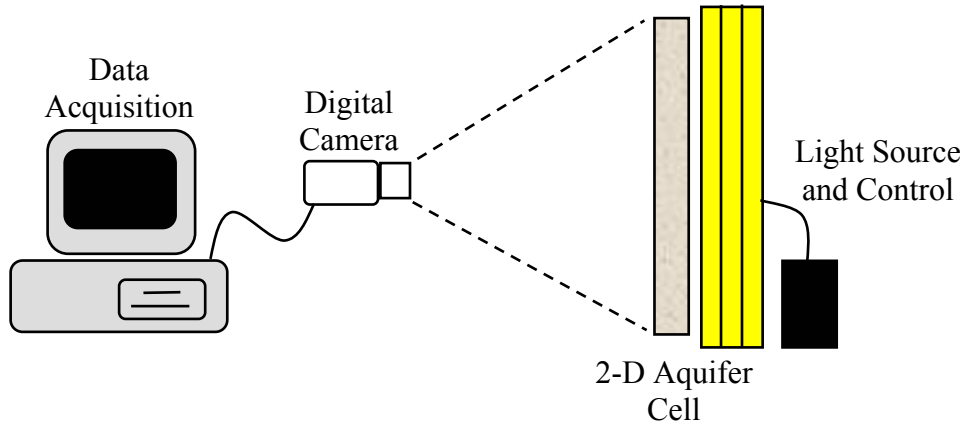
Figure 3.8: Conceptual model of light transmission system.

Following image acquisition and transfer, the digital images were processed using Adobe Photoshop 7.0.1 to crop the acquired image so that only pixels located within the aquifer cell source zone were considered during analysis. Image analysis was conducted using MATLAB 6.5, with each image initially imported into MATLAB as a three-dimensional array of size *m* x *n* x *3*. The values *m* and *n* represent the x and y dimensions of the image, expressed as pixel count, and the third dimension represents values for the red, green, and blue (RGB) vector of each pixel within the image. The RGB values for a given pixel may be converted to the hue using Equation 3.1 (Darnault et al. 1998).

$$H = 255 \left[\frac{1}{360} \left[T - \arctan \frac{2R - G - B}{\sqrt{3}(G - B)} \right] \right] \qquad (3.1)$$

In Equation 3.1, T is equal to 90 when G (the green value) is greater than or equal to B (the blue value) and 270 when G is less than B. Using Equation 3.1, the original three-

dimensional array describing the image is converted using MATLAB into a two-dimensional (*m* x *n* x *1*) array containing the hue values for the light transmission image. Using the method previously described by Darnault et al. (1998), a standard curve was developed correlating hue to Oil-Red-O dyed DNAPL saturation. The standard curve was used in MATLAB to convert the hue array into a two-dimensional saturation profile of the DNAPL source zone within the aquifer cell. It should be noted that the saturation profiles attained using the LT system were averaged over the 1.4 cm thick z-dimension of the aquifer cell.

After obtaining a saturation profile, the volume of DNAPL within each pixel was calculated based on the saturation, pixel volume, and estimated aquifer cell porosity. Porosity was estimated for individual aquifer cells using Equation 3.2, where ρ_s is the particle density (assumed to equal 2.65 g/cm^3) and the bulk density (ρ_b) was determined by dividing the mass of porous media added to the aquifer cell by the aquifer cell volume.

$$ n = 1 - \frac{\rho_b}{\rho_s} \qquad (3.2) $$

The DNAPL volumes were summed over the entire aquifer cell provide an LT-based estimate for the volume of mass present in the source zone. This was compared to the actual volume of DNAPL injected into the aquifer cell (measured during the injection process) to ensure that the saturation values determined via light transmission were reasonable. In general, the actual and LT-estimated DNAPL volumes did not differed by only 5-10%.

In addition, the DNAPL distribution within the aquifer cell source zone was quantified using a metric known as the ganglia-to-pool ratio (GTP). As described by Lemke et al. (2004), GTP is the ratio of DNAPL volume present in the cell at saturations

less than the residual saturation of the porous media (i.e., DNAPL ganglia) to the volume of DNAPL present in the cell at saturations greater than residual (i.e., pooled DNAPL). A low GTP (less than 1) indicates a large volume of pooled DNAPL is present in the aquifer cell, relative to the ganglia volume, while a high GTP implies the opposite. When DNAPL volumes are being summed during LT analysis, any pixels with DNAPL present at values lower than (or equal to) residual saturation have their DNAPL volumes summed to determine a cumulative DNAPL ganglia volume. Pixels having DNAPL present at values greater than residual saturation are similarly summed to determine a cumulative DNAPL pool volume. After summation, the ganglia volume is divided by the pool volume to provide an estimate of the GTP value. Residual saturation values were calculated for individual porous media using the grain size-saturation correlation developed by Powers (1992). For the two porous media employed during LT, 20/30 mesh Accusand and a mixture of 50% 20/30 mesh and 50% 40/50 mesh Accusand, the residual saturations were estimated to be 0.11 and 0.13, respectively. These values are comparable to those reported by Pennell et al. (1996), where residual saturation for 20/30 mesh Ottawa sand was determined to be approximately 0.11.

Saturation field (and as a result, GTP) was calculated on a per-pixel basis, with each pixel encompassing 0.3 mm^2 of the source zone. GTP will generally decrease as pixel area increases, due to incorporation of source zone regions containing little (or no) DNAPL into (generally much smaller) regions having higher DNAPL saturations. The impact of pixel size on GTP was investigated by recalculating GTP values for a source zone distribution using average DNAPL saturation values over a pixel of increased size. Two larger pixels were analyzed, one using a *10* x *10* square of individual pixels (new

93

pixel area of 30 mm^2) and one using a *20* x *20* square of individual pixels (new pixel area of 120 mm^2). GTP increased from 0.12 for an area 0.3 mm^2 to values of 0.13 (30 mm^2) and 0.15 (120 mm^2), indicating that for the source zone distributions typical in the aquifer cell, varying pixel size did not greatly impact GTP estimates.

3.2.5 Column Studies

A one-dimensional glass column, designed to evaluate microbial reductive dechlorination in the immediate vicinity of a PCE-DNAPL source zone, was constructed for use during experiments conducted in Chapters 7 and 8. Two experiments were conducted using an inoculum of *S. multivorans* (Chapter 7). Previous research (Powers et al. 1992) has demonstrated that for columns containing residual DNAPL, effluent concentrations will be near aqueous solubility. As a result, two different PCE-NAPLs were imbibed into the *S. multivorans* columns, a pure PCE-DNAPL (solubility of 1,200 µM or 200 mg/L) and a mixed NAPL comprised of 0.25 mol/mol PCE in hexadecane (solubility of 300 µM or 50 mg/L). A third experiment (Chapter 8) was conducted in a column imbibed with the mixed PCE/hexadecane NAPL and inoculated with BDI.

The borosilicate glass column (Kontes Glass Company, Vineland, NJ) included Teflon end plates, with overall dimensions of 60 cm in length by 4.8 cm inside diameter. The column was designed to incorporate two regions: a 10 cm long "source area" designed to assess biological activity in the presence of PCE-DNAPL, and a 50 cm long "plume region" for monitoring plume development, contaminant transformation, and electron donor consumption. Following purchase, the column was modified to incorporate sampling ports located every 5 cm along the entire length of the column, allowing for spatial determination of contaminant degradation and electron donor usage.

The sampling port design was similar to that used for the large aquifer cell, with the ports constructed by attaching glass 8 mm o. d. capillary tubing (2 mm i. d.) to the upper portion of glass screw-cap HPLC vials. The ports were then permanently attached to the glass column by melting them into place. A representative schematic of the 1-D column experimental setup is shown in Figure 3.9.
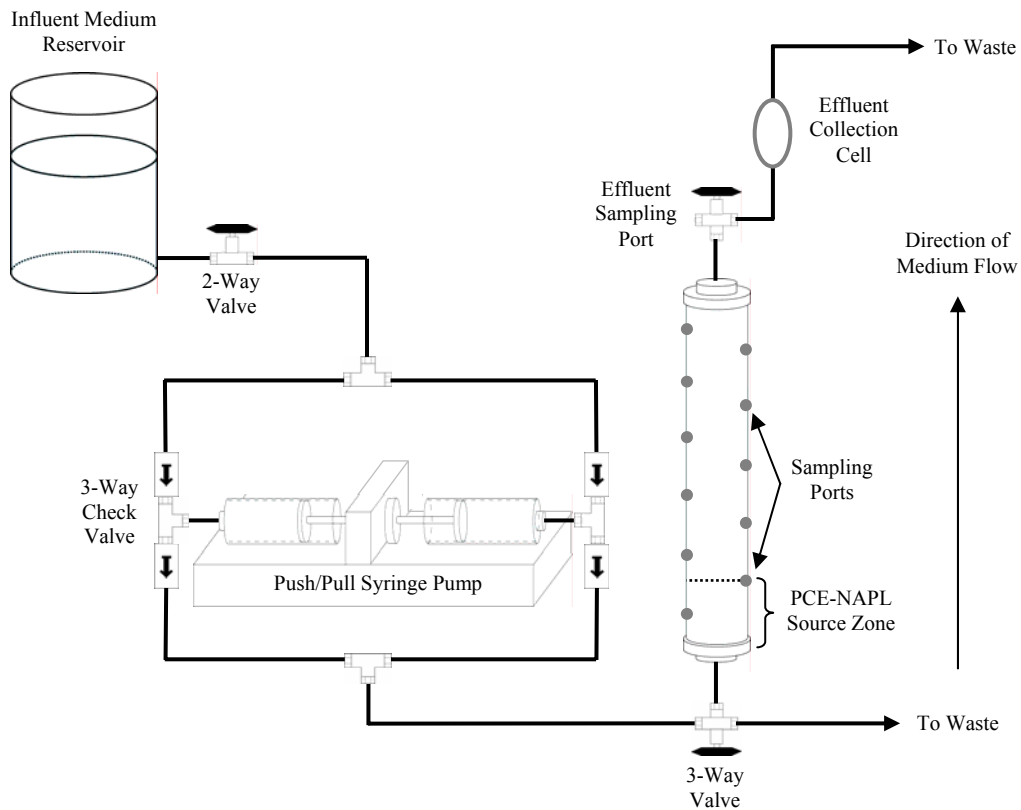
Figure 3.9: Schematic diagram of 1-D column experimental setup.

An influent system was constructed to operate at low flow rates of less than 1 mL/min during column operation. The influent medium reservoir was consisted of a 2 L Erlenmeyer flask with the mouth modified so that the flask could be sealed using a butyl rubber stopper. During column operation, the reservoir was maintained at an

overpressure of 15 psig to prevent intrusion of air into the sealed flask. Medium was delivered to the column via two 25 mL gas-tight Hamilton syringes using a Harvard Apparatus model PHD 2000 syringe pump. The pump selected was a push/pull model capable of both infusion and withdrawal, allowing for continuous operation of the column (i.e., one syringe injects medium into the column while the other syringe is refilled from the medium reservoir). The 25 mL syringes were connected to the medium reservoir and the column using 0.316 cm o. d. stainless steel tubing. During flushing, the column was operated in an upflow manner (i.e., medium entered through the bottom of the column and exited through the top). A schematic of the 1-D column influent system is shown in Figure 3.9. A column effluent collection bulb was also designed to allow for collection of relatively large sample volumes (approximately 20 mL) to allow analysis of chlorinated ethenes as well as biomass (analytical procedures described in section 4.3). The cell was constructed from glass tubing and was connected to the column using 0.32 cm (o. d.) Teflon® tubing. Samples from the effluent bulb were collected from a port located at a Hamilton four-way 90° valve using a 20 mL syringe (see Figure 3.10).

The column was packed under water-saturated conditions (2 cm lifts) using a reduced mineral salts medium containing a dense microbial inoculum as the aqueous phase and autoclaved Federal Fine Ottawa sand as the porous media. This packing strategy was selected so that a nominally uniform initial distribution of microorganisms within the column could be obtained. In order to maintain anoxic conditions within the column during packing, the column was placed within a system of glove bags that were continually flushed with nitrogen. Following packing, the column was kept in the glove bag system for approximately 24 hours to maintain anoxic conditions and promote

microbial attachment to the porous media. Reduced mineral salts medium was then flushed through the column at a nominal flow rate of 0.25 mL/min for approximately 5 pore volumes (PV) to remove unattached biomass. Because the medium did not contain a carbon source, electron donor, or electron acceptor, minimal growth and/or decay of microbial species within the column was assumed. Deoxyribonucleic acid (DNA) was extracted from effluent samples taken periodically during column washout and analyzed to quantify biomass.
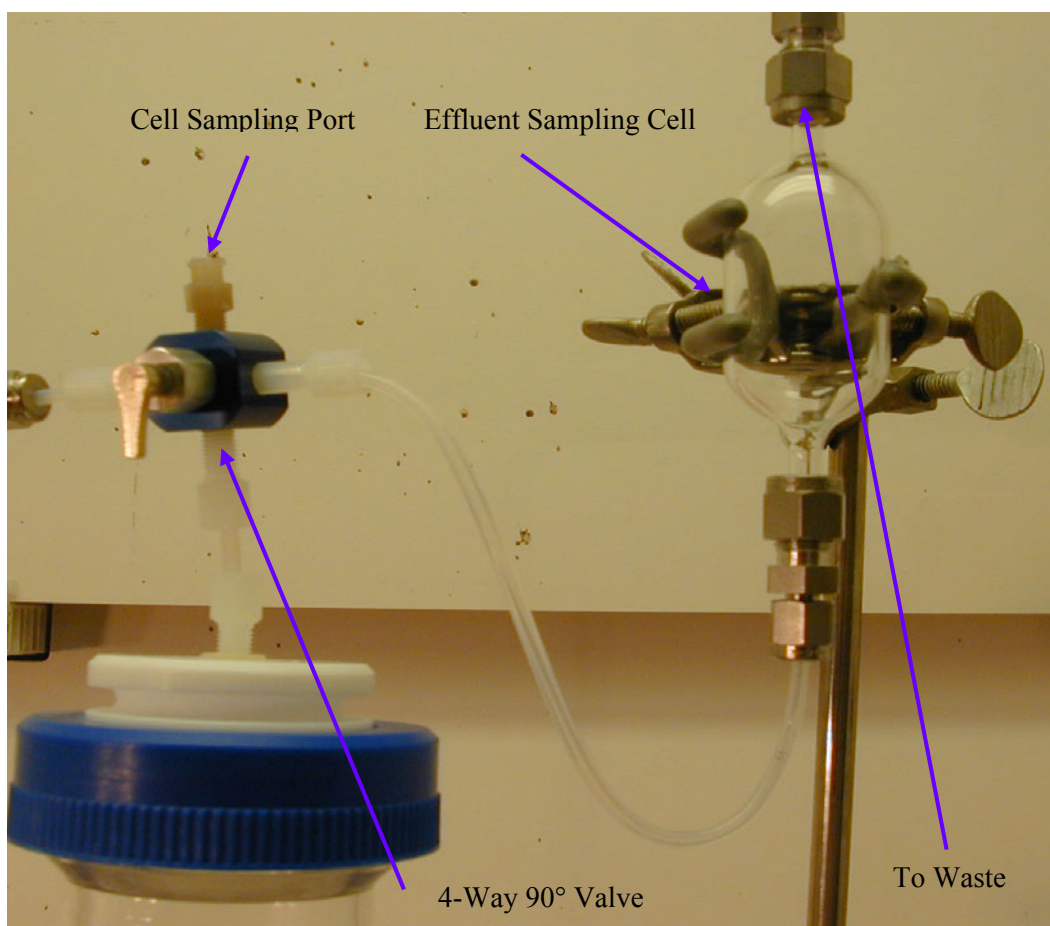
Figure 3.10: 1-D column effluent sampling cell.

Following removal of unattached biomass from the column, the column was imbibed with anoxic, dyed NAPL in order to establish a source zone. The NAPL contained either pure PCE or a mixture of 0.25 mol/mol PCE in hexadecane, depending on the experiment. The column was imbibed through a Hamilton three-way valve located at the bottom of the column. The valve was connected to a 100 mL gas-tight glass syringe (Hamilton) using 0.32 cm (o. d.) Teflon$^{®}$ tubing. A syringe pump (Harvard Apparatus model 22) was used to inject NAPL into the column at a constant flow rate of 1 mL/min until the NAPL source zone saturated the first 10 cm of the column. NAPL injection was then terminated and downward flushing of the column with reduced mineral salts medium was initiated at a rate of 1 mL/min for a period of approximately 60 minutes in order to establish a source zone containing residual DNAPL. At the conclusion of downward flushing, approximately 15 mL of residual DNAPL were entrapped within the first 10 cm of the column, corresponding to an organic phase saturation of approximately 0.13.

After establishment of a residual DNAPL source zone, the column was operated for a period of up to several weeks in order to monitor microbial dechlorination activity. During this phase of the experiment, the influent medium contained either pyruvate or lactate as a carbon source and electron donor. Medium was injected into the aquifer cell at a flow rate of 0.25 mL/min, yielding an approximate hydraulic retention time of 1.1 days. Daily samples were taken from the effluent sampling cell, and analyzed for pH, organic acids, chlorinated ethenes, and biomass (see section 3.3 for descriptions of analytical techniques). In addition, the ports along the length of the column were sampled weekly using a Hamilton 2.5 mL gas-tight glass syringe and analyzed for

chlorinated ethenes, organic acids, and in some cases biomass. In order to minimize disruption of aqueous flow within the column during sampling, samples were taken at a constant rate of 0.1 mL/min using the withdrawal function of a Harvard Apparatus model 22 syringe pump.

At the conclusion of each column experiment, the column was returned to the anoxic glove bag system used during packing and sectioned into six 10 cm long soil cores. Cores were recovered by driving an aluminum cylinder (3.8 cm o. d.) into the uppermost exposed 10 cm of column containing porous media. The top of the cylinder was sealed and the core removed from the column and frozen to prevent additional microbial activity and redistribution of the liquid phases. Each soil core was further sub-sectioned into 2 cm lengths, homogenized. DNA was extracted from representative sections and analyzed to estimate the final distribution of dechlorinating microorganisms within the column (see section 3.3).

3.3 Analytical Methods

In describing the analytical techniques used in this research it should be noted that a variety of techniques (e.g., real-time PCR, etc.) were employed to analyze the 1-D microbial reductive dechlorination columns. This work was carried out by Ben Amos under the supervision of Dr. Frank Löffler. Key findings from the microbial analysis are presented in Chapters 7 and 8; however, the details of the analytical techniques employed and a detailed description of the microbial analysis will be presented Ben Amos's PhD dissertation (expected in May 2007).

3.3.1 Density

During all surfactant flushing aquifer cell experiments (i.e., Chapters 4-6), liquid densities of both the influent surfactant solutions and aqueous effluent samples were determined using 2 mL pycnometers purchased from Ace Glass. Prior to use, the pycnometers were calibrated gravimetrically using a Mettler-Toledo AG245 analytical balance based on the mass of purified water required to fill the vessel at room temperature (22 ± 3°C). Purified water mass measurements were performed in quintuplet and the average mass added was used in conjunction with the density of water at room temperature to determine the pycnometer volume. For all aquifer cell experiments, aqueous phase effluent densities at all DNAPL loadings were calculated from the mass of the fluid required to fill the pycnometer and the calibrated volume. Densities of influent surfactant solutions were measured in triplicate and reported as average values with one standard deviation. Standard deviations were calculated using Equation 3.3 where n is the total number of samples, x_i is the value of sample i, and $\bar{x}$ is the arithmetic mean of n samples.

$$s = \sqrt{\frac{\sum_{i=1}^{n}(x_i - \bar{x})^2}{n-1}} \qquad (3.3)$$

3.3.2 Chlorinated Ethene Analysis

For the surfactant flushing experiments, aqueous phase chlorinated ethene (CE) concentrations were determined using a Hewlett-Packard model 6890 gas chromatograph (GC) equipped with a flame ionization detector (FID). The GC inlet was equipped with a surfactant trap consisting of a packed borosilicate glass split liner, purchased from

Agilent Technologies (Palo Alto, CA, model number 5181-3382). Approximately 0.5 cm of glass wool was placed in the bottom of the liner to support a packed bed of 1.5 cm height. The bed pack was composed of Porapack P 80/100 mesh purchased from Supelco, and an additional 0.5 cm glass wool placed on top of the Porapack to prevent spillage. Separation of chlorinated ethenes was attained using a 0.32 mm inside diameter, 30 m long DB-5 column purchased from J&W Scientific, with a sample retention time of approximately 2.4 minutes (TCE) and 4.4 minutes (PCE). Oven temperature, along with other GC method information including quantification limit, inlet and detector temperatures, and split ratios are summarized in Table 3.4. Prior to analysis, samples were diluted by a factor of approximately five with 2-propanol in order to fall within calibration curves. A six-point calibration curve over a concentration range of $0 - 24,000$ mg/L (PCE) or $0 - 65,000$ mg/L (TCE) was obtained prior to each sequence run and confirmed with a single calibration sample every 10 effluent samples for quality assurance. Samples were rerun if calibration checks deviated from the calibration value by more than 10%. PCE and TCE detection limits for the FID were approximately 10 mg/L. For all samples collected during the aquifer cell experiments, single injection analysis was performed.

Table 3.4: Aquifer cell experiment gas chromatography method information.

Parameter	Value
Column, Column Length (m), Column Diameter (mm)	DB-5, 30, 0.32
Injected Volume (μL)	1
Inlet Temperature (°C)	210
Split Ratio	20:1
Column Pressure (psi)	14.5
Oven Temperature (°C)	35
Detector Temperature (°C)	250
Approximate TCE Retention Time (min)	2.4
Approximate PCE Retention Time (min)	4.4
PCE and TCE Detection Limit (mg/L)	10

Chorinated ethene (PCE, TCE, *cis*-DCE, *trans*-DCE, VC, and ethene) concentrations during the microbial reductive dechlorination column experiments were quantified using a Hewlett-Packard model 7694 headspace autosampler and model 6890 GC equipped with a FID. Aqueous samples were prepared by injecting 1 mL of sample into a 20 mL headspace vial sealed with a Teflon[®]-lined butyl-rubber septum. Chlorinated ethene separation was achieved using an HP-624 column having dimensions of 60 m in length by 0.32 mm in diameter and a nominal film thickness of 1.8 μm. Operational parameters for both the autosampler and GC, along with other GC method information are summarized in Table 3.5. Six point standard curves for each chlorinated ethene species were prepared using the method developed by Gossett (1987). Briefly, a known quantity of chlorinated ethene was dissolved in methanol and added to bottles containing medium. PCE standards contained only PCE; TCE, *cis*-DCE, and *trans*-DCE standards contained all three chlorinated ethenes. Mixed VC and ethene standards were prepared from the respective gases. Aqueous phase concentrations were determined using Henry's constants specific for each chlorinated ethene (Gossett 1987). Detection

limits for CE analysis were less than 70 µg/L. Single injection analysis was performed

for all aqueous samples obtained during column operation.

Table 3.5: Column experiment gas chromatography method information.

Parameter	Value
Autosampler Parameters	
Oven Temperature (°C)	70
Vial Equilibration Time (min)	15
Sample Loop Volume (mL)	1
Sample Loop Temperature (°C)	125
Transfer Line Temperature (°C)	125
Pressurization Time (min)	0.5
Loop Fill Time (min)	0.03
Loop Equilibration Time (min)	0.05
Inject Time (min)	0.5
Carrier Gas Pressure (psig)	2
Vial Pressure (psig)	10
GC Parameters	
Column, Column Length (m), Column Diameter (mm)	HP-624, 60, 0.32
Inlet Temperature (°C)	200
Inlet Pressure (psig)	23.11
Inlet Flow Rate (mL/min)	5.7
Split Ratio	0.1:1
Initial Oven Temperature (°C)	60 (2 minutes)
Temperature Ramp (°C/min)	25
Final Oven Temperature (°C)	200
Column Flow Rate (mL/min)	3.0
Column Pressure (psi)	23.11
Detector Temperature (°C)	280
Detection Limit (µg/L)	70

CHAPTER 4

EFFICIENT RECOVERY OF TRICHLOROETHENE USING A

BIODEGRADABLE NONIONIC SURFACTANT

4.1 Introduction

Numerous *in situ* treatment technologies, including surfactant and cosolvent flushing, thermal treatment, air sparging, and chemical oxidation have been developed to overcome limitations associated with conventional pump-and-treat remediation of aquifer formations contaminated with dense non-aqueous phase liquids (DNAPLs) (NRC 1997, NRC 2004). Over the past decade, several field-scale tests have demonstrated the ability of these technologies to recover and/or destroy substantial quantities of contaminant mass in DNAPL source zones (AATDF 1997, Falta et al. 1999, Gierke et al. 1999, Jackson 2003, Jawitz et al. 2000, Londergan et al. 2001). While DNAPL mass recoveries exceeding 90% have been reported, it is now acknowledged that a substantial fraction of the initial DNAPL mass is likely to persist after aggressive source zone treatment (NRC 2004, Stroo et al. 2003). For example, up to 10% of DNAPL mass initially present was not recovered from lower-permeability zones (intrinsic permeability of 9.1×10^{-10} cm^2) following surfactant flushing at Camp Lejeune, North Carolina (Holzmer et al. 2000), and 35% to 38% of the initially present tetrachloroethene (PCE) mass remained after co-solvent flushing of a former dry cleaning facility in Jacksonville, Florida (Jawitz et al. 2000). While PCE groundwater concentrations at the Jacksonville site were reduced by 92% in spite of the relatively low mass recovery (approximately 60%), dissolved-phase contaminant concentrations within, and immediately down gradient from, treated source zones may nonetheless exceed drinking water standards for prolonged periods of time

(Sale and McWhorter 2001, Soga et al. 2004). While aggressive source zone treatment may be unable to achieve complete removal of DNAPL from a source zone (or reduce concentrations to regulatory endpoints), they still serve an important function by reducing the life cycle over which contaminant dissolution may occur.

Source zone life cycle was evaluated using a numerical model by Dekker and Abriola (2000b) for both natural gradient dissolution (i.e., no source zone treatment) and surfactant flushing. They found that use of surfactant flushing was able to significantly decrease source zone longevity, but regions of incomplete recovery were observed and post-treatment plume concentrations were not evaluated. These results, along with the previously discussed field data, indicate that while it may be possible to realize the potential advantages of *in situ* treatment technologies (namely shortened life cycles), it will be necessary to utilize more holistic remediation strategies combining aggressive mass removal with effective residual contaminant treatment to fully leverage aggressive source zone treatment. An emerging strategy to accomplish this is the combination physicochemical source zone treatments and tertiary (or polishing) treatment of residual contamination using bioaugmentation or biostimulation. A simplified mathematical assessment of NAPL dissolution was conducted by Christ et al. (2005a) to estimate source zone longevity for several DNAPL distributions, ranging from uniform throughout the source zone to one comprised of a limited number of idealized pools, when surfactant flushing with tertiary biostimulation was employed as a remedial technique. Results from the assessment indicated that, by combining remedies such as surfactant flushing with post-treatment biostimulation, it may be possible to decrease source longevity from decades (or centuries) to only a few years (or less), particularly for source zones not

105

characterized by extensive pooling. While promising, coupling of biological treatment of residual NAPL source zones with physicochemical source treatment is dependent on numerous factors, including the remedial strategy employed.

One promising technology that may be coupled with tertiary biological reductive dechlorination is surfactant enhanced aquifer remediation (SEAR). Laboratory studies have demonstrated efficient mass recovery via low interfacial tension mobilization using anionic surfactant formulations, both with (Ramsburg et al. 2004a) and without (Dwarakanath et al. 1999, Ramsburg and Pennell 2001) density modification. The effect of the presence of anionic surfactants on microbial reductive dechlorination was evaluated by McGuire and Hughes (2003). For Steol CS-330, a surfactant similar to those employed in low interfacial tension surfactant formulations (e.g., Aerosol MA), dechlorination activity beyond *cis*-DCE was not observed at surfactant concentrations exceeding 25 mg/L.

Additional SEAR studies have reported greater than 80% mass recovery in both one- (Pennell et al. 1993) and two-dimensional (Taylor et al. 2001) domains using nonionic surfactant formulations designed to recover contaminants via enhanced dissolution. Unlike with CS-330, McGuire and Hughes (2003) observed complete reductive dechlorination of PCE to ethene, albeit at a decreased rate, in the presence of polyoxyethylene (20) sorbitan monooleate (Tween 80), the nonionic food grade surfactant used in the studies conducted by Taylor et al. (2001). In addition, at the Bachman Road field site in Oscoda, Michigan, a 6% (wt.) solution of Tween 80 was flushed through a shallow aquifer formation containing a PCE-DNAPL (Ramsburg et al. 2005). Following the surfactant flood the down-gradient concentrations of volatile fatty

acid increased, indicating the potential for post-treatment stimulation of biotic reductive dechlorination of residual contaminants (Ramsburg et al., 2004b). In addition, Tween 80 costs are relatively low (e.g., $1.35 per pound), making it an attractive option for use in remedial strategies.

The above discussion indicates that non-ionic surfactants, in particular Tween 80, may be suitable for coupled SEAR and post-treatment microbial reductive dechlorination. However, few studies have directly compared the recovery efficiency of surfactant-enhanced solubilization using non-ionic surfactants to other SEAR-based remedial strategies. The primary objectives of this research were to directly compare surfactant-based TCE-DNAPL solubilization and mobilization mass recovery efficiencies and evaluate the effects of TCE-DNAPL source zone saturation distribution on the effectiveness of solubilization-based surfactant flushing.

4.2 Results and Discussion

Laboratory experiments were conducted to evaluate TCE-DNAPL recovery efficiency as a function of surfactant solution formulation, aqueous phase flow rate, and TCE-DNAPL distribution. Batch experiments were conducted to characterize the relevant physicochemical properties of the surfactant formulations; a 4% (wt.) Tween 80 + 500 mg/L $CaCl_2$ solution designed to achieve efficient DNAPL solubilization without mobilization, and a 3.2% (wt.) Aerosol MA + 8% (wt.) 2-propanol + 6 g/L NaCl solution capable of achieving rapid solubilization with accompanying DNAPL mobilization. TCE mass recovery for the Tween 80 and Aerosol MA formulations were evaluated using a 2-D aquifer cell (the smaller aquifer cell described in Chapter 3), allowing for comparisons under controlled experimental conditions. Three aquifer cell experiments were

conducted using the Tween 80 formulation, evaluating miscible displacement efficiency for TCE-DNAPL source zone distributions ranging from ganglia-dominated (GTP = 1.8, 36.0% of TCE present as pools) to pool-dominated (GTP = 0.2, 83.7% of TCE present as pools). Two Aerosol MA experiments were conducted at different flow rates to assess the effect of aqueous-phase velocity on the displacement and recovery of TCE-DNAPL. Experimental results are presented visually to illustrate differences between the recovery mechanisms evaluated (solubilization and mobilization), and the effects of DNAPL saturation distribution and aqueous phase flow rate on mass recovery. Effluent contaminant concentrations were monitored and analyzed to evaluate overall mass recovery. In addition, mass recovery results from the Tween 80 and Aerosol MA aquifer cell experiments, along with previously published results for density modified displacement of TCE (Ramsburg and Pennell 2002b, Ramsburg 2002), are directly compared to assess the relative effectiveness of the various SEAR-based treatment strategies.

4.2.1 Surfactant Solution Properties

A series of batch measurements were conducted to characterize the physicochemical properties (density, viscosity, IFT, TCE solubility, and solubility parameter) of the surfactant flushing solutions employed during the aquifer cell experiments; results are summarized in Table 4.1. The measured densities for the surfactant solutions prior to introduction into the aquifer cell were 1.002 ± 0.001 g/cm^3 and 0.994 ± 0.001 g/cm^3 for the Tween 80 (4% (wt.) Tween 80 + 500 mg/L CaCl$_2$, designated T80) and Aerosol MA (3.2% (wt.) Aerosol MA + 8% (wt.) 2-Propanol + 6 g/L NaCl, designated AMA) formulations, respectively. Both formulations had densities

comparable to water, which was desired in order to minimize the potential for density override of the surfactant solution during aquifer cell flushing. Viscosity of the 4% Tween 80 solution was 1.29±0.04 centipoise (cP) at 22ºC, while the viscosity of the Aerosol MA formulation was 1.64±0.02 cP, both representing minimal increases over the viscosity of water (1.00 cP). While it is often desirable to employ a high-viscosity solution during surfactant flushing in order to obtain a uniform flow front, an increase in viscosity may lead to excessive head loss and limit flow rate through porous media in unconfined systems. Given the moderate viscosity increases observed for both the 4% Tween 80 and 3.2% Aerosol MA surfactant formulations, viscous head loss during the 2-D aquifer cell experiments was not expected to be significant. Head loss per unit length of travel distance ($\Delta H/\Delta L$) was calculated using Darcy's law (Equation 4.1), where q is the Darcy velocity through the aquifer cell, k is the intrinsic permeability of the porous media, ρ and μ are the density and viscosity of the aqueous phase, and g is the gravitational constant.

$$q = \frac{k\rho g}{\mu}\frac{\Delta H}{\Delta L} \qquad (4.1)$$

Assuming an overall intrinsic permeability of 5×10^{-7} cm^2 and a Darcy velocity of 1.2 m/day, values typical for previous aquifer cell experiments (see e.g., Ramsburg and Pennell 2001, Taylor et al. 2001), head loss per unit length of travel distance through the aquifer cell was calculated to be 0.037 cm/cm and 0.045 cm/cm for the Tween 80 and Aerosol MA formulations, respectively. For two-dimensional aquifer cell experimental apparatus used for the experiments described below (63.5 cm in length), moderately low theoretical head losses of 2.37 cm and 2.88 cm were estimated for the Tween 80 and Aerosol MA surfactant solutions.

Table 4.1: Properties of flushing solutions used in aquifer cell experiments at 22°C.

Surfactant Solution Parameter	Water	4% (wt.) Tween 80 + 500 mg/L CaCl$_2$	3.2% (wt.) Aerosol MA + 8% (wt.) 2-Propanol + 6 g/L NaCl
Density (g/cm^3)	0.997[b]	1.002±0.001[a]	0.994±0.001
Dynamic Viscosity (cP)	1.00[b]	1.29±0.04	1.64±0.02
Interfacial Tension with TCE (dyne/cm)	35.2[b]	10.4±0.8	0.19[c]
TCE Solubility (mg/L)	1,100[b]	63,500±900	39,100±200
Weight Solubilization Ratio (g$_{TCE}$/g$_{surf}$)	n/a	1.735±0.005	1.206±0.006
Solubility Parameter (mL$_{TCE}$/mL$_{surf}$)	n/a	1.263±0.004	0.705±0.004

a: Standard deviation
b: Riddick and Bunger 1970
c: Dwarakanath et al. 1999

The interfacial tension (IFT) between TCE and the aqueous phase decreased from 35.2 dyne/cm to 10.4 dyne/cm in the presence of the 4% Tween 80 surfactant formulation and to 0.19 dyne/cm in the presence of the Aerosol MA solution (see Table 4.1). IFT reduction accompanying the Tween 80 solution was moderate, and a total trapping number (N_T) of 2.1×10^{-5} for the aquifer cell was estimated based on surfactant solution properties and the intrinsic permeability and Darcy's velocity previously assumed for the viscous head loss calculations. Because this value comparable to the critical trapping number for immiscible PCE displacement (2×10^{-5}, Pennell et al. 1996), minimal displacement of residual or entrapped TCE-DNAPL within the aquifer cell during flushing with the Tween 80 solution was anticipated. Using the same assumptions, a total trapping number of 1.1×10^{-3} was calculated for the aquifer cell during flushing with the Aerosol MA formulation. This value is larger than the critical N_T value necessary for complete NAPL displacement (1×10^{-4}) reported by Pennell et al. (1996), indicating that

immiscible displacement of residual TCE-DNAPL was likely to occur during flushing with the Aerosol MA solution.

The equilibrium solubility values for TCE in the Tween 80 and Aerosol MA surfactant formulations were measured in triplicate and determined to be 63,500±900 mg/L and 39,100±200 mg/L, respectively. TCE solubilities in micellar solutions of Tween 80 at 22±3ºC over a Tween 80 concentration range of 6,000 mg/L to 60,000 mg/L are shown in Figure 4.1 (95% confidence interval curves included), along with the TCE solubility in the Aerosol MA surfactant formulation used in this research. Aqueous solubility of TCE increased linearly as Tween 80 concentrations increased
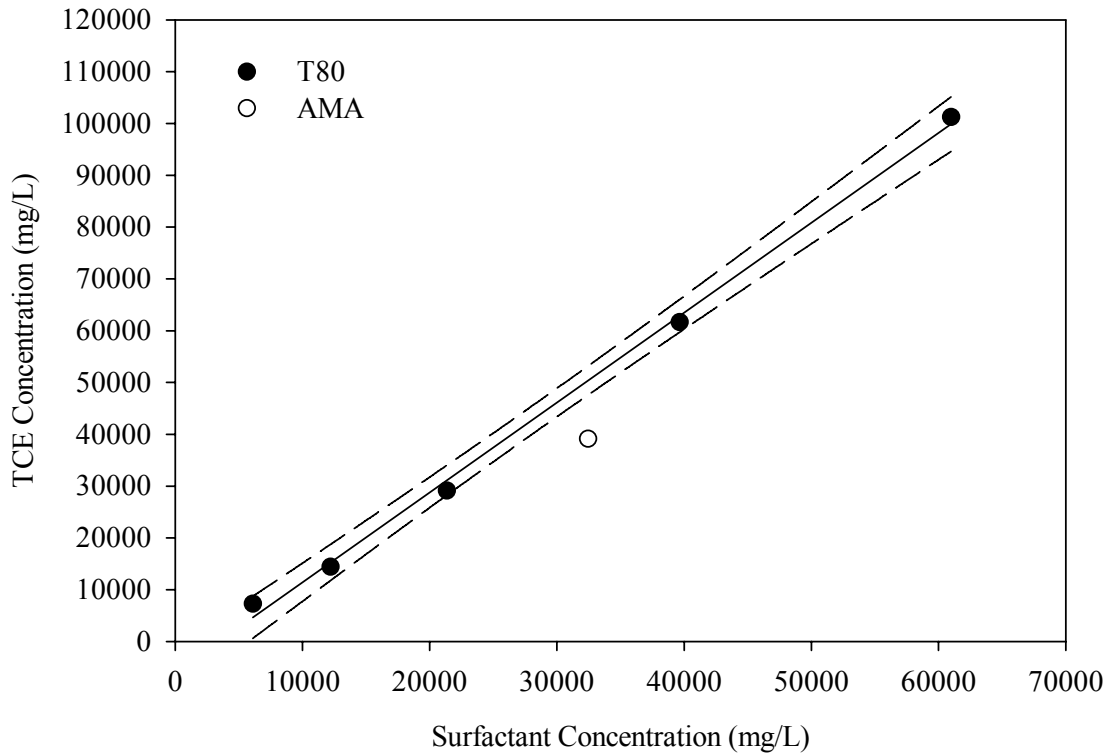
Figure 4.1: TCE solubility as a function of Tween 80 and Aerosol MA concentration at 22ºC. Error bars present but too small to see.

($R^2 = 0.997$), consistent with the expected behavior of a Winsor Type I system (Winsor 1954, Pennell et al. 1993). A weight solubilization ratio (WSR) of 1.735±0.005 g TCE/g Tween 80 was determined by performing linear regression analysis on the equilibrium solubility curve at Tween 80 concentrations above the critical micelle concentration, with the best fit regression line shown in Figure 4.1. The TCE-Tween 80 WSR may be expressed as:

$$WSR = \frac{C_C - C_{C,sat}}{C_S - C_{S,CMC}} \qquad (4.2)$$

where C_C is the TCE concentration in a Tween 80 solution of concentration C_S, $C_{C,sat}$ is the TCE aqueous solubility (1,100 mg/L), and $C_{S,CMC}$ is the critical micelle concentration of Tween 80 (13 mg/L). The molar solubilization ratio (MSR) of TCE in Tween 80 was calculated to be 17.3±0.05 mol TCE/mol Tween 80, based on the average molecular weight of Tween 80 (1310 g/mol) and the molecular weight of TCE (131.4 g/mol). For the Aerosol MA formulation employed in this research, a WSR of 1.206±0.006 g TCE/g Aerosol MA was obtained, with a corresponding MSR of 2.90±0.02 mol TCE/mol Aerosol MA.

The MSR value of TCE in Tween 80 (17.3 mol/mol) was significantly larger than previously measured molar solubilization ratios for TCE in other surfactants, which generally ranged from 1 to 3 mole/mole (Table 4.2), indicating the sizable capacity of Tween 80 to solubilize TCE. West (1992) measured MSR values for TCE in several nonionic surfactant solutions at concentrations up to 1% (wt.) and observed MSR values ranging from 1.23 mol/mol for Triton X-100 to 15.18 mol/mol for Tergitol NP-10. It is unclear why the Tergitol value was so large, although the system may have been unstable given that West was unable to measure the MSR of *trans*-DCE in a similar system due to

Table 4.2: Comparison of surfactant-TCE molar solubilization ratios (MSR).

Reference	Surfactant Formulation	HLB[a]	MSR[b] (mole/mole)	WSR[c] (g/g)	S[d] (mL/mL)
	4% (wt.) Tween 80 + 500 mg/L CaCl$_2$	13	17.3	1.74	1.26
	3.2% (wt.) Aerosol MA + 8% (wt.) 2-Propanol + 6 g/L NaCl	n/a	2.90	1.21	0.75
Dwarakanath et al. 1999	4% (wt.) Aerosol MA + 8% (wt.) 2-Propanol + 4 g/L NaCl	n/a	2.89	1.20	0.67
Diallo et al. 1994	0.4% – 1.5% (wt.) Dodecyl Alcohol Ethoxylates	13	0.1	0.023	0.017
Diallo et al. 1994	0.4% – 1.5% (wt.) Dodecyl Alcohol Ethoxylates	15	0.3	0.054	0.041
Diallo et al. 1994	0.4% – 1.5% (wt.) Dodecyl Alcohol Ethoxylates	16	1.1	0.160	0.120
Diallo et al. 1994	0.4% – 1.5% (wt.) Dodecyl Alcohol Ethoxylates	18	1.0	0.084	0.063
West 1992	1% (wt.) Brij 30	n/a	1.39	0.47	0.35
West 1992	1% (wt.) Triton X-100	n/a	1.23	0.40	0.30
West 1992	1% (wt.) Tergitol NP-10	n/a	15.18	0.47	0.35

a: Hydrophile-lipophile balance
b: Molar solubilization ratio
c: Weight solubilization ratio
d: Solubility parameter

instabilities. The effect of the hydrophile-lipophile balance (HLB) on the MSR was investigated by Diallo et al. (1994), with the TCE MSR ranging from 0.5 mol/mol to 1.5 mol/mol in the presence of dodecyl alcohol ethoxylates of varying HLB, with the maximum MSR occurring at a surfactant HLB of 17. In addition, the MSR of TCE in Tween 80 was much larger than that of PCE in similar surfactant solutions as measured by Taylor et al. (2001) (5.41 mol/mol in Tween 80) and Pennell et al. (1993) (6.39 mol/mol in Witconol 2722, a structural analog of Tween 80), indicating that Tween 80

solubilization capacity is considerably greater for TCE than for PCE. TCE solubility in an Aerosol MA surfactant solution similar to the one employed in this research was investigated by Dwarakanath et al. (1999), and comparable values for both equilibrium TCE solubility and the TCE-Aerosol MA molar solubilization ratio (39,000 mg/L and 2.89 mol/mol, respectively) were observed.

The solubilization efficiency of an organic (i.e., TCE) by a surfactant can be alternately described on the basis of the solubilization parameter (S), which has units of mL organic/mL surfactant. Based on the previously determined WSR values and the densities of Tween 80 and Aerosol MA, solubilization parameters of 1.263 and 0.705 mL TCE/mL surfactant were calculated for Tween 80 and Aerosol MA, respectively. The TCE solubilization parameter for Tween 80 is three times greater than solubilization parameters previously reported for PCE (e.g., Pennell et al. 1993, Taylor et al. 2001), again demonstrating the extremely large TCE solubilization capacity of Tween 80. The interfacial tension between the aqueous (i.e., surfactant solution) and organic phase may be related to the solubilization parameter by the Chun-Huh equation (Huh 1979):

$$\gamma = C/S^2 \qquad (4.3)$$

where γ is the interfacial tension (dyne/cm), S is the solubilization parameter (mL organic/mL surfactant), and C is an empirical constant that has been correlated to a value approximately equal to 0.3 when the organic phase is comprised of chlorinated solvents such as PCE and TCE (Pope and Wade 1995). It can be inferred from the Chun-Huh equation that an increase in the aqueous solubility of a contaminant (expressed in terms of the solubility parameter) will be accompanied by a corresponding reduction in the interfacial tension (IFT) between the aqueous and organic phases. The Chun-Huh

114

behavior arises from the accumulation of surfactant monomers at the interface between two immiscible liquids, which acts to render the interface more diffuse, thereby both decreasing the interfacial tension between the two phases and increasing the miscibility of the phases (Pennell and Abriola 1997). Based on Equation 4.3 (with C assumed to equal 0.3) and the estimated solubility parameters for Tween 80 and Aerosol MA (see Table 4.1), respective theoretical TCE/surfactant solution IFT values of 0.19 and 0.61 dyne/cm were predicted for the Tween 80 and Aerosol MA solutions employed in this research. The IFT predicted by the Chun-Huh equation for the Aerosol MA formulation compares favorably to the experimentally determined value (0.19 dyne/cm); however, Equation 4.3 under-predicts the IFT associated with the 4% Tween 80 solution by nearly two orders-of-magnitude (an estimated value of 0.16 dyne/cm versus a measured value of 10.4±0.8 dyne/cm). Experimental IFT values for the Tween 80 and Aerosol MA solutions are plotted as a function of the solubility parameter in Figure 4.2, along with previously reported experimental results and the expected IFT/solubility parameter behavior based on the Chun-Huh equation. From Figure 4.2, it can be inferred that while the Chun-Huh equation works reasonably well for predicting interfacial tension reductions with anionic surfactants (e.g., SDS and AMA), it may not accurately predict observed IFT reductions when nonionic surfactants or mixtures of nonionic and anionic surfactants are employed. Reliance on the Chun-Huh equation for predicting interfacial tension reductions (and NAPL mobilization resulting from these reductions) can therefore be problematic, especially for nonionic surfactants that exhibit large solubilization capacities (e.g., TCE in Tween 80).
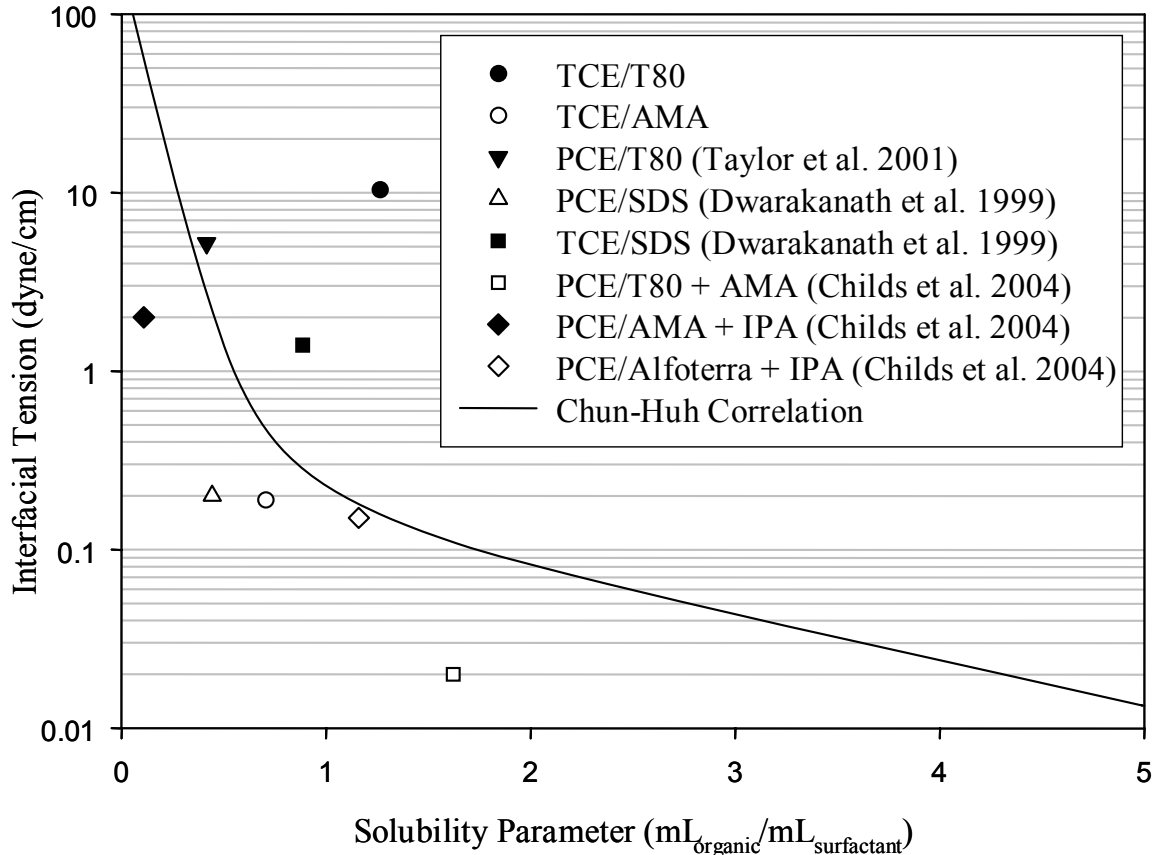
Figure 4.2: Chlorinated solvent-surfactant solution interfacial tension as a function of solubility parameter.

4.2.2 Tween 80 Aquifer Cell Experiments

Based on the promising batch results observed for TCE/Tween 80 systems (i.e., high TCE solubility with moderate interfacial tension reduction), a series of three two-dimensional aquifer cell experiments was conducted using a 4% Tween 80 solution to assess the ability of the formulation to recover TCE from a source zone, and to evaluate the effects of TCE-DNAPL saturation distribution on recovery efficiency. Relevant aquifer cell conditions during each of the three experiments are summarized in Table 4.3. Federal Fine Ottawa sand was used as the background porous media during the first experiment (T80-HI), where a TCE-DNAPL distribution characterized by extensive

formation of residual NAPL ganglia (i.e., high source zone GTP) was desired. The pore volume of the aquifer cell was 1,370 mL and the overall intrinsic permeability 4.85×10^{-11} m^2 prior to TCE injection. The second aquifer cell experiment (T80-MID), which was characterized by more moderate ganglia formation, used a mixture of 50% 20/30 mesh Accusand and 50% 40/50 mesh Accusand as the background porous media and had a pore volume of 1,180 mL and an intrinsic permeability of 1.45×10^{-10} m^2. For the final experiment (T80-LO, characterized by increased pooling of TCE-DNAPL at saturations greater than residual or a low GTP), 20/30 mesh Accusand was used as the background media. The aquifer cell pore volume for T80-LO was 1,280 mL and the intrinsic permeability 6.01×10^{-10} m^2. Differences in aquifer cell pore volume and permeability resulted from a combination of the differences in the porous media employed in the experiments and aquifer cell packing height.

Table 4.3: Summary of two-dimensional aquifer cell conditions for Tween 80 experiments.

Aquifer Cell Parameter	T80-HI	T80-MID	T80-LO
Background Porous Media	Federal Fine	Mixed Accusand[b]	20/30 Mesh Accusand
Overall Pore Volume (mL)	1,370	1,180	1,280
Intrinsic Permeability (m^2)	4.85×10^{-11}	1.45×10^{-10}	6.01×10^{-10}
NAPL Injection Volume (mL)	32.7	29.5	26.1
Overall NAPL Saturation (%)	2.4	2.7	2.0
Initial TCE GTP[a]	1.8	1.5	0.2
Flow Rate (mL/min)	4.29 ± 0.18^c	3.84 ± 0.34	4.47 ± 0.88
Darcy Velocity (mm/min)	0.802 ± 0.030	0.721 ± 0.064	0.840 ± 0.165
Volume of Surfactant Flood (mL)	9,600	2,520	2,800

a: Ganglia-to-pool ratio
b: 50% 20/30 mesh Accusand + 50% 40/50 mesh Accusand
c: Standard deviation

For experiment T80-HI, a total of 32.7 mL of TCE-DNAPL were present in the aquifer cell following injection and redistribution, resulting in an overall NAPL saturation of 2.4% (see Table 4.3). A representative photograph of the initial distribution of the TCE-DNAPL within the aquifer cell during T80-HI is shown in Figure 4.3a. The background porous media employed during T80-HI (Federal Fine Ottawa sand) is too fine to allow for light transmission analysis; however, a ganglia-to-pool (GTP) ratio was estimated based on observation of DNAPL distribution at the face of the aquifer cell. Using the image shown in Figure 4.3a, an initial GTP value of 1.8 was estimated for experiment T80-HI. Of the 32.7 mL of TCE-DNAPL initially present in the aquifer cell, 64.3% (21.0 mL) existed as residual NAPL ganglia entrapped within the pore space and the remaining 33.7% (11.7 mL) existed as NAPL pools having locally high saturation (i.e., NAPL saturations greater than 0.15).
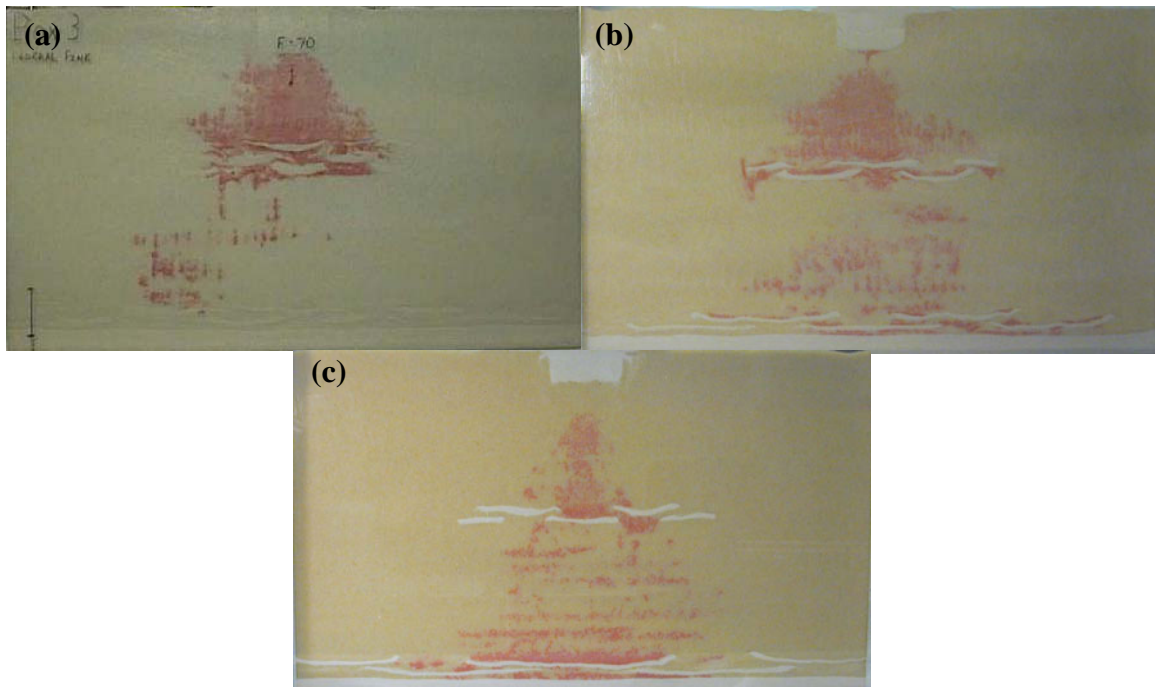
Figure 4.3: Representative photographs of initial TCE-DNAPL source zone distributions for (a) T80-HI, (b) T80-MID, and (c) T80-LO aquifer cells.

The overall NAPL saturation for experiment T80-MID was 2.7%, with a total of 29.5 mL of TCE-DNAPL initially present in the aquifer cell following injection and redistribution. A photograph of the initial TCE-DNAPL source zone distribution for experiment T80-MID is shown in Figure 4.3b, and the resulting NAPL saturation profile determined via light transmission (LT) is shown in Figure 4.4a. Based on the LT analysis, the GTP value for the initial TCE-DNAPL distribution of experiment T80-MID was estimate to be approximately 1.5, corresponding to 60% (17.7 mL) of TCE being present as NAPL ganglia and 40% (11.8 mL) as high saturation pools. The GTP value determined for experiment T80-MID was comparable to that estimated for T80-HI, indicating the experiments had similar initial TCE-DNAPL distributions, which is apparent from the similar saturation distributions shown in Figure 4.3. For experiment T80-LO, a photograph of the initial TCE-DNAPL distribution is shown in Figure 4.3c. At total of 26.1 mL of TCE were initially present in the aquifer cell during experiment T80-LO, resulting in an overall NAPL saturation of 2.0%. A very low GTP value of 0.2 was estimated for T80-LO based on light transmission analysis (Figure 4.4b), indicating the occurrence of substantial TCE-DNAPL pools within the source zone. Of the 26.1 mL of TCE initially present in the aquifer cell, 16.7% (4.4 mL) were present as NAPL ganglia with the remaining 83.3% (21.7 mL) existing as high saturation NAPL pools.

During each of the Tween 80 surfactant flushing experiments, the nominal flow rate of the surfactant solution was 4 mL/min, with actual flow rates of 4.29±0.18 mL/min for T80-HI, 3.84±0.34 mL/min for T80-MID, and 4.47±0.88 mL/min for T80-LO. Corresponding Darcy velocities for the experiments were 0.802±0.030, 0.721±0.064, and 0.840±0.165 mm/min, respectively. A total of 9,600 mL (7 pore volumes) of the 4%

Tween 80 solution were injected over the course of experiment T80-HI, whereas approximately 2,400 mL (2 pore volumes) of surfactant solution were injected during experiments T80-MID and T80-LO. The flushing parameters (flow rate and solution volume) for each of the three aquifer cell experiments are summarized in Table 4.3.
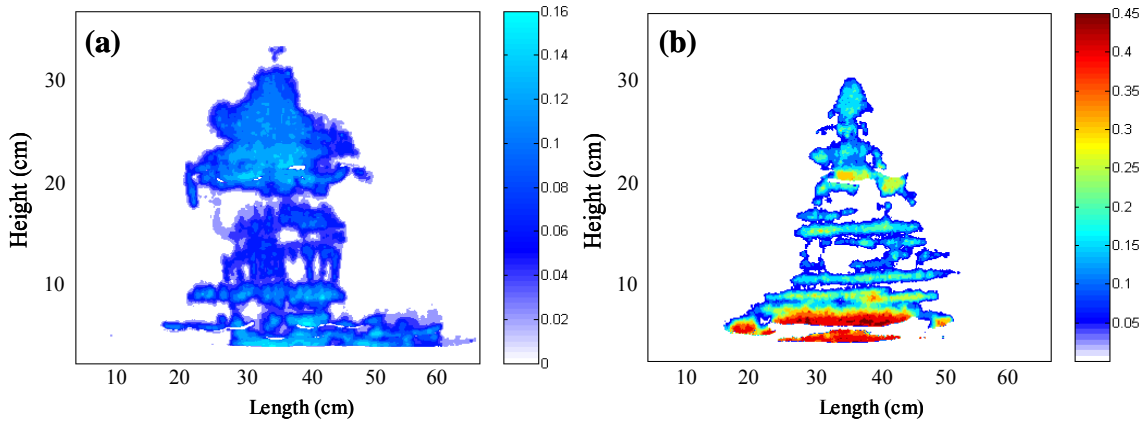
Figure 4.4: Light transmission images of initial TCE-DNAPL saturation distributions in (a) T80-MID (1.5) and (b) T80-LO (0.2).

The measured aqueous phase effluent concentrations of TCE during experiment T80-HI are shown in Figure 4.5a. Effluent TCE concentrations rapidly increased to values significantly greater than the TCE solubility following introduction of 1 pore volume (approximately 1,200 mL) of surfactant solution, eventually reaching a maximum concentration of 25,000 mg/L after just over 1.25 pore volumes (1730 mL) of flushing. While the maximum effluent concentration observed was much lower than the equilibrium solubility of excess TCE in the 4% Tween 80 solution (63,500 mg/L), it still represents a 23-fold increase in contaminant solubility when compared to the equilibrium solubility of TCE in water (1,100 mg/L). Upon reaching the maximum value, effluent TCE concentrations during T80-HI declined with additional surfactant flushing, dropping

120

to concentrations below the GC-FID detection limit (10 mg/L) after approximately 3.2 pore volumes (4,400 mL) of flushing.
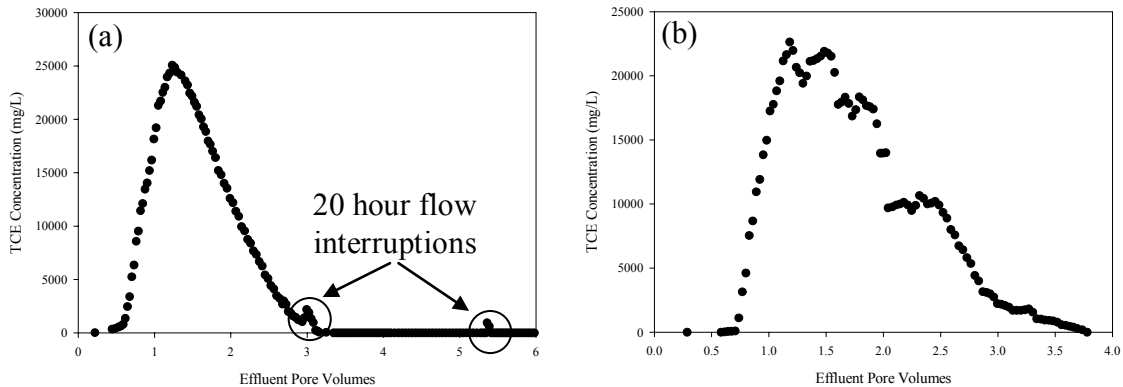
Figure 4.5: Effluent TCE concentrations during experiments (a) T80-HI and (b) T80-MID.

During experiment T80-HI, two small peaks in TCE effluent concentrations were observed (see Figure 4.5a), corresponding to flow interruptions of approximately 20 hours each. The first occurred following 3.1 pore volumes (4200 mL) of flushing, with TCE concentrations increasing to 2,200 mg/L, and the second, with TCE concentrations reaching 1,000 mg/L, occurred following 5.5 pore volume (7,500 mL) of surfactant flushing. Both increases were attributed to rate-limited TCE solubilization by Tween 80, a phenomenon that has been observed for the solubilization of PCE during surfactant flushing (see e.g., Pennell et al. 1993, Rathfelder et al. 2001). In this experiment the concentration increases due to flow interruption were small due to the fact that little TCE mass remained present in the aquifer cell, and the effect did not play a major role in overall TCE mass recovery.

Effluent TCE concentrations for experiments T80-MID and T80-LO are shown in Figures 4.5b and 4.6, respectively. As with T80-HI, effluent TCE concentrations for both experiments rapidly increased following flushing with approximately 1 pore volume (1,200 mL) of surfactant solution. The maximum effluent concentration during T80-MID was just less than 25,000 mg/L after approximately 1.5 pore volumes (1,800 mL) of flushing, which was comparable to that observed during the T80-HI experiment. In contrast, T80-LO had a much lower maximum effluent concentration, reaching approximately 11,000 mg/L after similar levels of surfactant flushing. The similarity between the effluent TCE concentrations observed for experiments T80-HI and T80-MID (apparent when comparing Figures 4.5a and 4.5b) was expected due to the similar initial source zone saturation distributions as expressed by GTP values (1.8 and 1.5). In contrast, the lower effluent concentrations observed in experiment T80-LO were attributed to the presence of large volumes of pooled DNAPL that were not readily available for solubilization, as described by the low GTP value of the initial TCE-DNAPL distribution (i.e., 0.2).

Based on visual observation of the progression of the dyed surfactant solution fronts, relatively little preferential flow of surfactant solution along the bottom of the aquifer cell occurred during any of the Tween 80 experiments, despite the surfactant solution having a density greater than that of water (1.002 g/mL versus 0.997 g/mL). The relative lack of increased flow along the cell bottom when compared to previous experiments by Taylor et al. (2001, 2003) was attributed to the relatively high surfactant solution flow rates within the cell (nominally 4 mL/min). The surfactant fronts therefore exhibited a nominal "piston displacement", as described by Taylor et al. (2001), which

may be advantageous for NAPL distributions characterized by high GTP values (i.e., limited volumes of pooled DNAPL), such as those observed in experiments T80-HI and T80-MID.
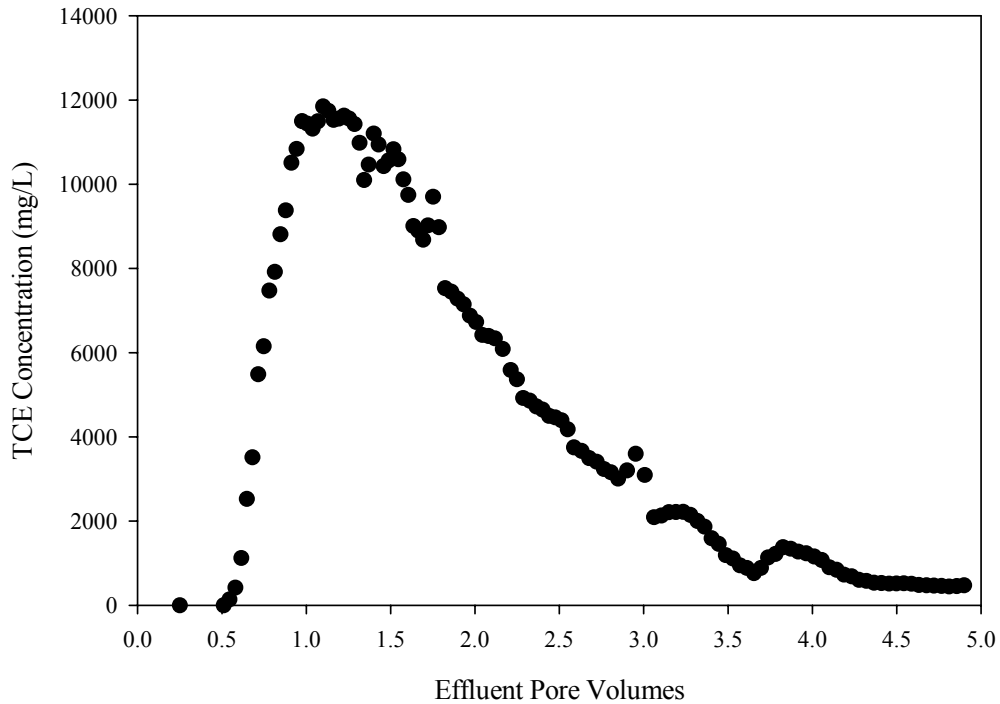
Figure 4.6: Effluent TCE concentrations during experiment T80-LO.

During all three experiments, TCE, and therefore Tween 80, breakthrough occurred after approximately 1 pore volume of surfactant flushing, as was expected since the relatively high flow rate of the surfactant fronts minimized early breakthrough of Tween 80. To validate this observation, a retardation factor (R_F) for Tween 80 was calculated to quantify the effect of sorption processes on surfactant transport. Previously conducted experiments (e.g., Taylor et al. 2001, Adeel and Luthy 1995) have demonstrated that nonionic surfactants exhibit Langmuir behavior when sorbed to porous media of low organic carbon content such as that used in all three Tween 80 experiments.

As a result, the magnitude of surfactant retardation in the aquifer cell may be estimated using the Langmuir retardation factor ($R_{F,Lang}$):

$$R_{F,Lang} = 1 + \frac{\rho_b S_{m,max}^{s} b}{ns_a \left(1 + bC_a^{s}\right)^2} \qquad (4.4)$$

where ρ_b is the bulk density of the porous media, $S_{m,max}^{S}$ is the maximum amount of surfactant sorbed, b is the ratio of the adsorption and desorption rates, n is the aquifer cell porosity, s_a is the aqueous phase saturation, and C_a^{S} is the aqueous phase concentration of the surfactant. Based on sorption experiments conducted by Taylor et al. (2001) using porous media similar to the two-dimensional aquifer cell packing, $S_{m,max}^{S}$ and b values of 0.16 mg/g and 0.02 L/mg, respectively, were used to calculate R_F. Experiment T80-HI had a bulk density of 1.54g/cm^3 and a porosity of 0.42, yielding in a Tween 80 Langmuir retardation factor of 1.00002 and indicating that sorption would not significantly impact surfactant transport through the porous media. Maximum theoretical surfactant losses to the solid phase in the aquifer cell were calculated for experiment T80-HI, with the sorbed-phase Tween 80 concentration set to $S_{m,max}^{S}$. At $S_{m,max}^{S}$, surfactant losses to the porous media were calculated to be 0.83 g, which represents only 0.23% of the total amount of Tween 80 injected during T80-HI (approximately 350 g). Respective Langmuir retardation factors of 1.00003 and 1.00002 were estimated for T80-MID and T80-LO, assuming that $S_{m,max}^{S}$ and b for the Accusand are comparable to those reported by Taylor et al. (2001) due to the similarities between the porous media. Therefore, it can be inferred that surfactant sorption was not significant during the Tween 80 experiments, regardless of the background porous media employed.

Effluent TCE concentrations for all three experiments are consistent with results describing transient NAPL dissolution as reported by Rathfelder et al. (2001), where

unobstructed NAPL globules are preferentially solubilized early during surfactant flushing, leading to a rapid rise in effluent contaminant concentration as the high specific surface area globules are solubilized. Following dissolution of the NAPL globules, contaminant removal is controlled by the volume and distribution of remaining areas of high-saturation pooled NAPL, which are characterized by relatively low interfacial area and may act as long-term, rate-limited sources of TCE mass transfer throughout the course of a solubilization flood. In addition, visual observation of the aquifer cells indicated that early TCE mass removal was most pronounced in up-gradient areas of the aquifer cell (i.e., the left side), where the difference between the aqueous-phase TCE concentration in the bulk surfactant solution and the equilibrium TCE concentration was greatest. Taylor et al. (2001) described the rate of TCE-DNAPL dissolution using a linear driving force expression (Equation 4.5), where k is the mass transfer coefficient, a_o is the specific surface area of the NAPL, C is the bulk aqueous phase TCE concentration and $C^{a, eq}$ is the equilibrium TCE concentration in the aqueous phase.

$$\frac{dC}{dt} = ka_o\left(C^{a, eq} - C\right) \qquad (4.5)$$

Equation 4.5 indicates that maximum contaminant dissolution will occur when the difference between the equilibrium and bulk TCE concentrations is the greatest, a scenario which occurs in the up-gradient regions of the aquifer cell where TCE-free surfactant solution is being continuously introduced.

Visual observation during each of the Tween 80 flushing experiments confirmed that dissolution of TCE-DNAPL ganglia occurred readily, with TCE located in regions of heavy DNAPL pooling was much more difficult to remove. Representative photographs of the three TCE-DNAPL source zones at the conclusion of surfactant flushing are shown

in Figure 4.7, and TCE-DNAPL saturation distributions determined via light transmission analysis are shown in Figure 4.8 for experiments T80-MID and T80-LO. For both experiment T80-HI (Figure 4.7a) and T80-MID (Figures 4.7b and 4.8a), TCE remaining in the aquifer cell at the conclusion of surfactant flushing was limited to a few regions of pooled (i.e., high-saturation) DNAPL. However, for experiment T80-LO (Figures 4.7c and 4.8b) large regions along the bottom of the aquifer cell that were characterized by extensive TCE-DNAPL pooling remained at the cessation of surfactant flushing, a result of incomplete dissolution of the large TCE pools initially present in the source zone.

TCE-DNAPL remained relatively stationary over the course of experiments T80-HI and T80-MID, with little to no significant downward migration of free product. In contrast, some slight redistribution of the TCE-DNAPL was observed during experiment T80-LO, consistent with results expected based on the total trapping number concept. Capillary (N_{Ca}), Bond (N_B), and total trapping numbers (N_T) for each of the three Tween 80 surfactant flushing experiments are summarized in Table 4.4. Total trapping number values for T80-HI and T80-MID were calculated to be 1.97×10^{-5} and 3.15×10^{-5}, respectively. Both values are near the critical value of 2×10^{-5} required to initiate PCE-NAPL displacement in 1-D soil columns (Pennell et al. 1996), indicating minimal risk of DNAPL displacement. Conversely, a total trapping number of 1.30×10^{-4} was calculated for experiment T80-LO, indicating TCE displacement could be expected since this value falls within the transition zone for immiscible displacement of residual PCE-DNAPL as described by Pennell et al. (1996). The larger trapping number calculated for T80-LO was attributed to the comparatively high intrinsic permeability of the 20/30 mesh Accusand (6.01×10^{-10} m^2, see Table 4.3) acting to reduce the Bond number.
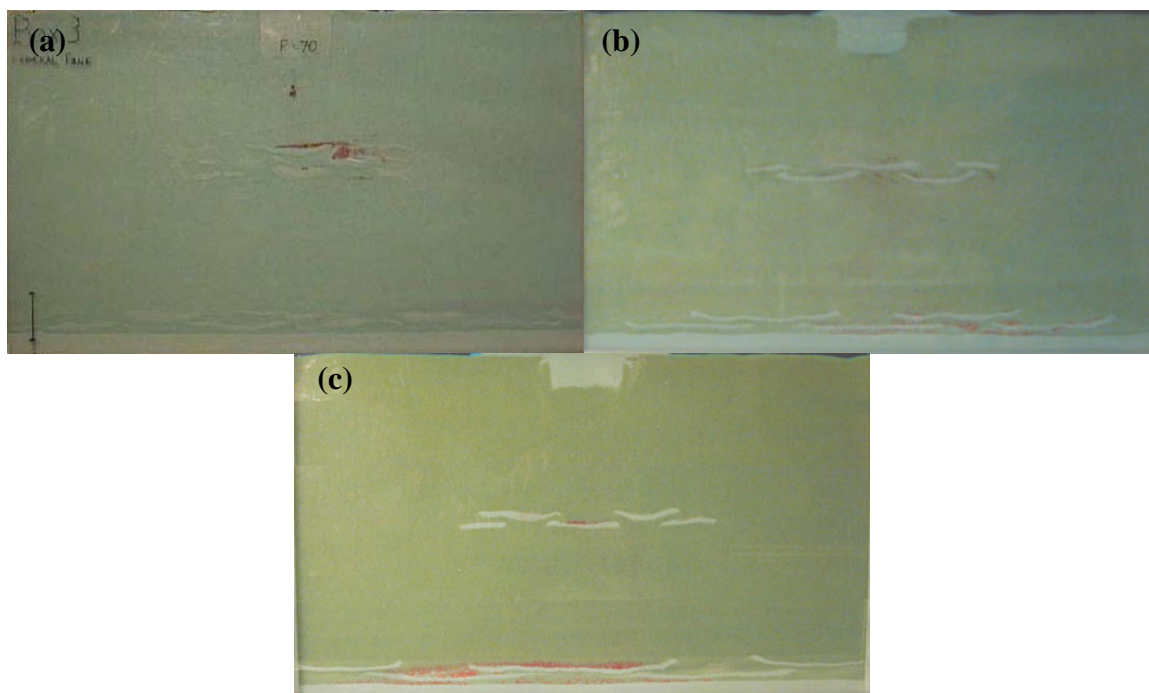
Figure 4.7: Representative photographs of final TCE-DNAPL source zone distributions for (a) T80-HI, (b) T80-MID, and (c) T80-LO aquifer cells.

TCE mass recoveries for the Tween 80 surfactant flushing experiments are summarized in Table 4.4 (recovery curves for the experiments are presented and discussed in greater detail in section 4.2.4 below). Because the TCE remained relatively stationary over the course of all three experiments, all TCE recovered was dissolved in the aqueous phase rather than as free-phase organic liquid. The total volume of TCE recovered in the effluent during experiment T80-HI was 28.6 mL, a percentage recovery of 87.4%. Overall TCE mass recovery was comparable for experiment T80-MID (26.1 mL, 83.1%), which was again expected due to the similarities between the initial TCE-DNAPL source zone distributions of experiments T80-HI and T80-MID. TCE mass recovery during experiment T80-LO was somewhat lower than observed in the other experiments (17.3 mL, 66.2%) due to incomplete dissolution of high-saturation TCE pools present within the aquifer cell; however, it is possible that TCE-DNAPL mass

127

recovery could have been improved with additional surfactant flushing. The generally high overall TCE recoveries achieved during all three experiments was primarily attributed to the large increases in apparent TCE solubility during flushing with Tween 80, in spite of the fact that the equilibrium solubility value was not attained.
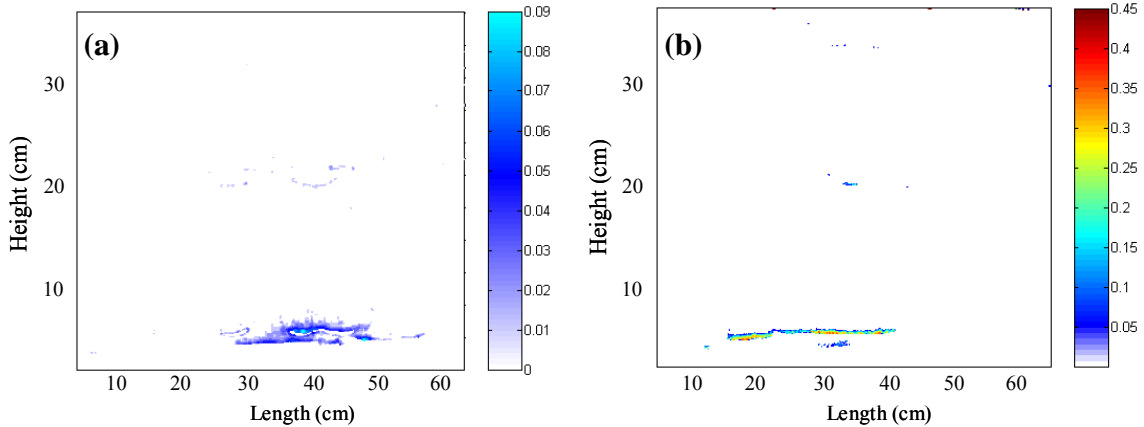
Figure 4.8: Light transmission images of final TCE-DNAPL saturation distributions in (a) T80-MID and (b) T80-LO.

Table 4.4: TCE mass recovery and trapping number analysis for Tween 80 aquifer cell experiments.

Aquifer Cell Parameter	T80-HI	T80-MID	T80-LO
Tween 80 Pore Volumes	7.01	2.14	2.19
TCE Volume Recovered (mL)	28.6	26.1	17.3
TCE Recovery (%)	87.4	83.1 [2]	66.2
Capillary Number (N_{Ca})	1.65×10^{-6}	1.49×10^{-6}	1.74×10^{-6}
Bond Number (N_B)	2.00×10^{-5}	3.15×10^{-5}	1.30×10^{-4}
Total Trapping Number (N_T)	1.97×10^{-5}	3.15×10^{-5}	1.30×10^{-4}

4.2.3 Aerosol MA Aquifer Cell Experiments

Two additional 2-D aquifer cell experiments were conducted to assess TCE recovery efficiency as a function of the rate of surfactant solution injection into the aquifer cell. The surfactant solution used in these experiments was comprised of 3.2%

(wt.) Aerosol MA + 8% (wt.) 2-propanol + 6 g/L NaCl. Results from these experiments are compared to the TCE mass recoveries obtained during surfactant flushing with a 4% (wt.) Tween 80 solution. The Aerosol MA formulation was selected because experiments employing similar surfactant formulations have shown the ability to achieve extremely efficient DNAPL recovery, although with the potential for mobilization of free-phase organic liquid (see e.g., Dwarakanath et al. 1999). Both Aerosol MA experiments used Federal Fine Ottawa sand as background porous media. The first aquifer cell experiment, AMA-HI 1, had an overall pore volume of 1,340 mL and an intrinsic permeability of 4.53×10^{-11} m^2. Approximately 1,500 mL (1.1 pore volumes) of surfactant solution were injected into the aquifer cell at a flow rate of 4.24±0.22 mL/min (reported with one standard deviation), corresponding to a Darcy velocity of 0.797±0.041 mm/min. Overall aquifer cell pore volume was 1,330 mL for experiment AMA-HI 2, with an intrinsic permeability of 7.91×10^{-11} m^2. During AMA-HI 2, 1,600 mL (1.2 pore volumes) of surfactant solution were injected at a flow rate of 9.89±0.85 mL/min, corresponding to a Darcy velocity of 1.86±0.16 mm/min. Experimental conditions of the aquifer cells are summarized in Table 4.5.

Photographs of the initial TCE-DNAPL distributions within the aquifer cell during experiments AMA-HI 1 and AMA-HI 2 are shown in Figures 4.9a and 4.9b, respectively. During experiment AMA-HI 1, 28.7 mL of TCE were initially present following injection and redistribution, yielding an overall aquifer cell NAPL saturation of 2.2%. The initial overall NAPL saturation during experiment AMA-HI 2 was 2.9%, with a total of 39.3 mL of TCE present in the aquifer cell. Comparing Figures 4.9a and 4.9b, it is apparent that the initial TCE-DNAPL saturation distributions in the two experiments

are comparable. However, use of Federal Fine Ottawa sand as the background porous media in these experiments precluded the use of light transmission analysis to directly estimate the TCE-DNAPL distributions. Based on light transmission results from experiment T80-MID, which had an initial GTP value of 1.5, it is likely that the GTP values for the Aerosol MA aquifer cells are greater than 1.5 since Federal Fine sand has a lower average grain size than the Accusand mixture used in T80-MID and GTP generally increases with decreasing grain size. A GTP value of 1.5 corresponds to 60% of the TCE-DNAPL being present in the aquifer cells as residual ganglia, with the remainder located within regions of high-saturation pools. As such, it is likely that 60% (or more) of the TCE injected into the Aerosol MA cells was entrapped as residual NAPL ganglia.

Table 4.5: Summary of two-dimensional aquifer cell conditions for Aerosol MA experiments.

Aquifer Cell Parameter	AMA-HI 1	AMA-HI 2
Background Porous Media	Federal Fine	Federal Fine
Overall Pore Volume (mL)	1,340	1,330
Intrinsic Permeability (m^2)	4.53x10^{-11}	7.91x10^{-11}
NAPL Injection Volume (mL)	28.7	39.3
Overall NAPL Saturation (%)	2.2	2.9
Estimated Initial TCE GTP[a]	1.5+	1.5+
Flow Rate (mL/min)	4.24±0.22[b]	9.89±0.85
Darcy Velocity (mm/min)	0.797±0.041	1.86±0.16
Volume of Surfactant Flood (mL)	1,520	1,590

a: Ganglia-to-pool ratio
b: Standard deviation

Effluent TCE concentrations observed during experiments AMA-HI 1 and AMA-HI 2 are shown in Figure 4.10a and 4.10b, respectively. Effluent concentrations for both experiments increased rapidly following flushing with approximately one pore volume of surfactant solution, similar to the behavior observed in the aquifer cells flushed with the

Tween 80 surfactant formulation. A maximum TCE concentration during AMA-HI 1 of

23,000 mg/L was reached following 1.1 pore volumes (1,400 mL) of flushing. A

somewhat larger maximum TCE concentration (31,600 mg/L) was attained after 1.05

pore volumes (1,300 mL) of surfactant solution flushing during AMA-HI 2. Mayer et al.

(1999) investigated TCE mass transfer in the presence of Aerosol MA surfactant

formulations, observing that mass transfer rates were relatively insensitive to flow rate

but depended heavily on NAPL saturation. As such, the greater TCE concentrations

observed during AMA-HI 2 were primarily due to the larger volume of NAPL present

(39.3 mL versus 28.7 mL for AMA-HI 1) and hence greater saturation. In both cases,

while the maximum observed concentrations were significantly less than the equilibrium

solubility of TCE in the Aerosol MA solution (approximately 39,100 mg/L), they

nonetheless represented greater than 20-fold increases over the aqueous solubility of

TCE. In addition, effluent concentration behavior for the AMA experiments was

comparable to those observed with Tween 80 assuming similar initial TCE-DNAPL

distributions, indicating that TCE recovery efficiencies for these two surfactant

formulations may be comparable.
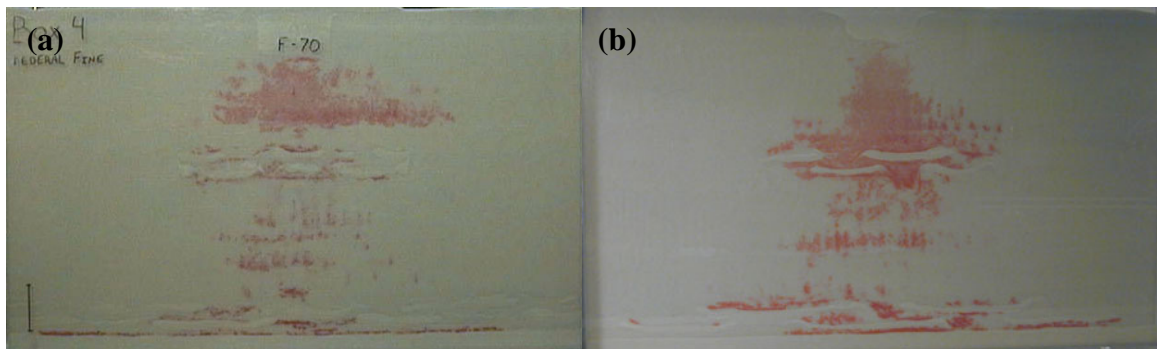
Figure 4.9: Representative photographs of initial TCE-DNAPL source zone distributions
for (a) AMA-HI 1 and (b) AMA-HI 2 aquifer cells.
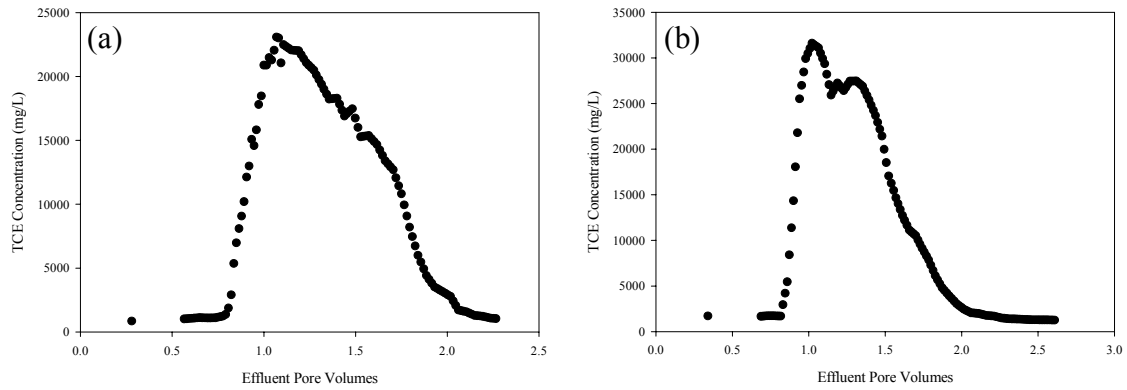
Figure 4.10: Effluent TCE concentrations during experiments (a) AMA-HI 1 and (b) AMA-HI 2.

Based on Figure 4.10 (panels a and b), effluent TCE concentrations during both AMA experiments rapidly increased following approximately one pore volume of surfactant flushing, implying that surfactant solution breakthrough also occurred after one pore volume of flushing. This was expected due to the fact that the surfactant solution traveled through the aquifer cell in a nominal "piston displacement" (i.e., no preferential flow along the bottom of the cell) and because sorption of anionic surfactants to silica material such as Federal Fine sand is not significant (Dwarakanath et al. 1999) because of anion-anion interactions between silica groups and the hydrophilic head of the surfactant. A general estimate of the magnitude of Aerosol MA retardation in the two aquifer cells was obtained using a Langmuir retardation factor (Equation 4.6), assuming a bulk density of 1.6 g/cm^3, aquifer cell porosity of 0.40, and aqueous phase saturation of 0.978.

$$R_{F,Lang} = 1 + \frac{\rho_b S_{m,max}^s b}{n s_a \left(1 + b C_a^s\right)^2} \qquad (4.6)$$

No estimates for Aerosol MA sorption parameters were available for use with Equation 5.6; however Dwarakanath et al. (1999) estimated respective $S_{m,max}^s$ and b values of 0.16

mg/g and 0.0017 L/mg for sodium dihexyl sulfosuccinate, a similar anionic surfactant. Based on the above parameters, a Langmuir retardation factor for Aerosol MA in the aquifer cell of 1.000003 was estimated, implying that sorption does not significantly impact surfactant transport through the aquifer cell. Surfactant losses to the solid phase in the aquifer cell were also estimated, assuming the sorbed-phase Aerosol MA concentration was equal to $S^S_{m,max}$. At this sorbed-phase concentration (0.16 mg/g), surfactant losses to the porous media were estimated at less than one gram, which is not significant when compared to the mass of Aerosol MA injected during the either of the two surfactant floods (in excess of 50 g for both experiments).

Over the course of experiment AMA-HI 1, significant downward migration of the TCE-DNAPL was observed. Figure 4.11a demonstrates this behavior, with TCE entering into the lower confining layer of F-70 sand along the left-hand side of the aquifer cell where TCE-DNAPL and the Aerosol MA surfactant formulation were in direct contact for the longest period of time. TCE penetration into the lower confining layer continued through the remainder of AMA-HI 1, with increasing amounts of DNAPL mobilized in a primarily downward trajectory. TCE penetration into the lower confining layer was expected based on theoretical entry pressure calculations for pooled NAPL over F70 sand. Using Equation 4.7, developed by McWhorter and Nelson (1979), and assuming an interfacial tension of 0.19 dyne/cm, hydraulic conductivity of 0.079 cm/s, and porosity of 0.39 (experimental values from AMA-HI 2), the entry pressure was estimated to be 0.11 cm, much lower than the observed TCE-DNAPL pool height above the lower confining layer of the aquifer cell.

$$Z_n = 9.6 \left(\frac{\rho_w}{\rho_n - \rho_w} \right) \left(\frac{\gamma}{\gamma_{aw}} \right) \left(\frac{K}{n} \right)^{-0.403} \qquad (4.7)$$

The occurrence of significant downward TCE migration during AMA-HI 1 was anticipated based on a total trapping number (N_T) analysis, with a N_T number of 3.61×10^{-3} calculated (see Table 4.6) assuming horizontal aqueous phase flow. This value is substantially larger than 2×10^{-5}, the critical N_T value at which NAPL displacement (i.e., mobilization) begins to occur (Pennell et al. 1996). In addition, the dimensionless bank number (see Willson et al. 1999) and angle of NAPL displacement relative to the x-axis (τ) were determined. For AMA-HI 1, a bank number of 0.03 was calculated and an angle of displacement of 88.2° determined using Equation 4.8:

$$\tau = \arctan\left(\frac{N_B}{N_{Ca}}\right) \qquad (4.8)$$

where N_{Ca} is the capillary number, N_B is the Bond number, and an angle of 0° would imply perfectly horizontal DNAPL displacement. Both results imply extreme downward and relatively little horizontal free-phase organic migration, consistent with behavior observed during AMA-HI 1. Downward TCE-DNAPL migration was also apparent during experiment AMA-HI 2; however this experiment was also characterized by the formation and horizontal displacement of a shallow bank of free-phase TCE (see Figure 4.11b). A total trapping number of 9.91×10^{-4} was calculated for AMA-HI 2, significantly greater than the critical value for the onset of DNAPL displacement. The bank number for experiment AMA-HI 2 was determined to be 0.28, within the range where NAPL migration perpendicular to aqueous phase flow rather than parallel is predicted to be dominant (Willson et al. 1999). In addition, the angle of NAPL displacement relative to the x-axis for experiment AMA-HI 2 was estimated to be 73.4°, comparable to the angle of the NAPL bank observed in Figure 4.11b and implying that, although some horizontal

DNAPL displacement may be expected, downward DNAPL mobilization will be more significant. The total trapping number, bank number, and angle of displacement values for the Aerosol MA surfactant flushing experiments are summarized in Table 4.6.
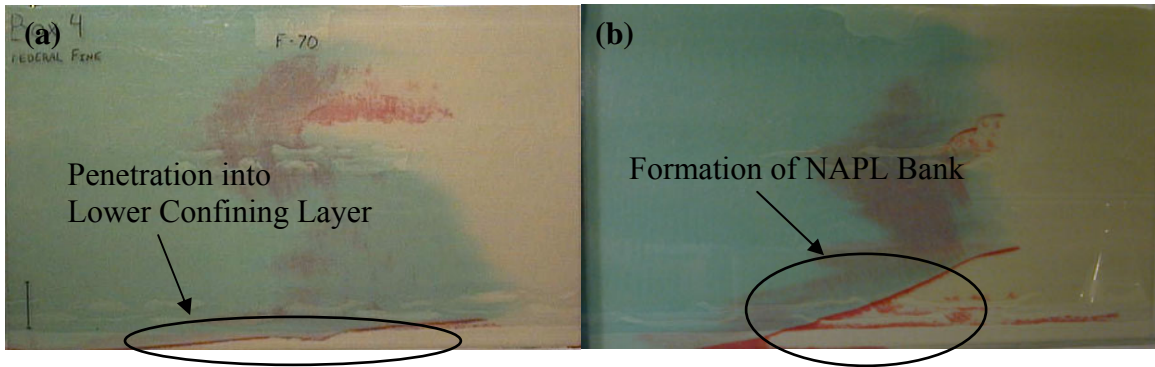
Figure 4.11: Representative photographs demonstrating TCE-DNAPL mobilization behavior during experiments (a) AMA-HI 1 and (b) AMA-HI 2.

Based on visual observations of Figures 4.11a and 4.11b, along with comparison of bank number and angle of DNAPL displacement results for AMA-HI 1 and AMA-HI 2, it is clear that TCE migration behavior is impacted by aqueous-phase flow field considerations to some extent, since the two experiments nominally differed only by surfactant solution flow rate. In order to quantify the effects of the aqueous flow field on organic-phase displacement, the viscous-to-gravity ratio (R_{vg}) was developed by Ruith and Meiburg (2002):

$$R_{vg} = \frac{U\mu_o}{gk(\rho_o - \rho_w)}\frac{H}{L} \qquad (4.9)$$

where U is the pore water velocity within the aquifer cell, which was equal to 0.199 cm/min for AMA-HI 1 and 0.465 cm/min for AMA-HI 2. Additionally, in Equation 4.9, μ_o is the viscosity of the organic phase, g is the gravitational constant, k is the intrinsic

permeability of the porous media, ρ_o is the organic phase (i.e., NAPL) density, ρ_w is the aqueous phase density, H is the maximum height in the aquifer cell where TCE-DNAPL was located (assumed to be 32 cm), and L is the distance between the TCE-DNAPL center of mass and the effluent end chamber (assumed to be 31.75 cm). These terms were identical for the two experiments, indicating that differences between the viscous-to-gravity ratios of the two aquifer cells were solely due to difference in the surfactant solution injection rate. Based on Equation 4.8, R_{vg} was calculated to be 0.077 for AMA-HI 1 and 0.180 for AMA-HI 2. R_{vg} has been equated to the ratio of time scales for horizontal and vertical organic-phase displacement (see e.g., Tchelepi 1994) using Equation 4.10, where t_v is the time scale for vertical NAPL displacement and t_h is the time scale for horizontal NAPL displacement.

$$R_{vg} = \frac{t_v}{t_h} \qquad (4.10)$$

The residence time for perfectly horizontal flow from the vertical centerline of the aquifer cell to the extraction end chamber (i.e., t_h) was calculated to be approximately 160 min for AMA-HI 1 and 70 minutes for AMA-HI 2, based on the pore water velocity for the respective experiments. Using these values for t_h along with Equation 4.10, the respective time scales for vertical DNAPL migration (t_v) during experiments AMA-HI 1 and AMA-HI 2 were both calculated to be approximately 12 minutes. TCE displacement during both experiments occurred over much longer periods of time (several hours), indicating that NAPL displacement was incomplete and some re-entrapment of the mobilized TCE was ongoing. In addition, the maximum DNAPL densities that could be expected to be recovered through the effluent end chamber (i.e., the density at which t_h is equal to t_v, resulting in a R_{vg} value of unity) were calculated to be 1.03 g/cm^3 for AMA-

HI 1 and 1.07 g/cm^3 for AMA-HI 2. Both of these values are significantly lower than the

density of TCE (1.46 g/cm^3), indicating that downward DNAPL migration was not

significantly affected by the aqueous-phase flow regime, although the effect was more

significant for AMA-HI 2. Given the rapid rate expected for TCE-DNAPL, increasing

the flow rate is unlikely to increase organic-phase recovery and may not be feasible in

unconfined systems, depending on system permeability. Instead, extraction path length

should be shortened by emplacing extraction wells as near the NAPL as possible.

Table 4.6: TCE mass recovery and trapping number analysis for Aerosol MA aquifer cell
experiments.

Aquifer Cell Paramter	AMA-HI 1	AMA-HI 2
TCE Volume Recovered (mL)	17.3	32.0^a
TCE Recovery (%)	62.9	81.3
Capillary Number (N_{Ca})	1.14x10^{-4}	2.67x10^{-4}
Bond Number (N_B)	3.61x10^{-3}	9.55x10^{-4}
Total Trapping Number (N_T)	3.61x10^{-3}	9.91x10^{-4}
Bank Number (N_{Ba})	0.03	0.28
Angle of NAPL Mobilization (τ)	88.2	73.4

a: 10 mL recovered in right-hand end chamber as free-phase organic TCE

TCE mass recoveries for experiments AMA-HI 1 and AMA-HI 2 are summarized

in Table 4.6. No free-phase organic product was recovered during AMA-HI 1 despite the

occurrence of TCE-DNAPL mobilization because the DNAPL remained at the bottom of

the aquifer cell during surfactant flushing rather than moving toward the effluent end

chamber, precluding recovery of free-phase TCE. However, a total of 18.1 mL (62.9%)

of the TCE initially present in the aquifer cell was recovered from the aqueous effluent

during AMA-HI 1. Overall TCE mass recovery was much higher for experiment AMA-

HI 2 (81.3%), with a total of 32.0 mL of TCE recovered. Approximately 10 mL of the

total TCE removed from the aquifer cell was recovered as free organic-phase TCE, implying that the increased aqueous phase Darcy velocity during AMA-HI 2 (1.86±0.16 mm/min versus 0.797±0.041 mm/min for AMA-HI 1) was sufficient to attain significant (although incomplete) recovery of the displaced organic phase. Based on the results from AMA-HI 2, a further increase in Darcy velocity may potentially allow for additional free product recovery and limit (or eliminate) DNAPL migration into the lower confining layer. However, this could prove difficult to implement in the field, particularly for unconfined aquifer systems, due to viscous head losses. For both AMA-HI 1 and 2, the mass of dissolved-phase TCE recovered was high (18.1 mL and 22.0 mL, respectively), a result that was attributed to the high solubilization capacity of the Aerosol MA surfactant formulation employed.

4.2.4 TCE Mass Recovery Comparison

Cumulative TCE mass recovery curves as a function of total aqueous phase pore volumes flushed through the aquifer cell were generated for each of the three Tween 80 and two Aerosol MA experiments. Mass recovery curves from the Tween 80 and Aerosol MA experiments were compared to TCE recovery results from two previously conducted density modified displacement (DMD) experiments, one using an aqueous preflood (DMD-AQ) and one using an emulsion preflood (DMD-EM). During DMD-AQ (Ramsburg and Pennell 2002b), a preflood of 6% 1-butanol was employed to achieve density conversion, followed by a displacement flood comprised of 4% (4:1) Aerosol MA/OT + 20% 1-butanol + 500 mg/L CaCl$_2$. A preflood of 4.7% Tween 80 + 1.3% Span 80 + 15% 1-butanol was used in experiment DMD-EM (Ramsburg 2002), followed by a displacement flood of 10% Aerosol MA + 5% 1-butanol + 15 g/L NaCl + 1 g/L CaCl$_2$.

Surfactant formulations employed for each of the aquifer cell experiments compared in this research are summarized in Table 4.7.

Cumulative TCE mass recovery curves following treatment by the surfactant-based flushing schemes are shown in Figure 4.12. Cumulative mass recovery was high for both T80-HI and T80-MID, reaching respective values of 83% and 87% following approximately 2.5 pore volumes of surfactant flushing. The efficient TCE recovery observed during these experiments was attributed to the high TCE solubilization capacity of the 4% Tween 80 surfactant formulation and the lack of significant TCE-DNAPL pooling in the source zone. Cumulative mass recovery was lower for experiment T80-LO, 66% following 2.5 pore volumes of surfactant flushing, due to the higher degree of TCE-DNAPL pooling (i.e., lower GTP value) in the source zone. The rate of contaminant recovery was also lower for T80-LO compared to T80-HI and T80-MID, a result that is apparent when comparing the slopes of the mass recovery curves for the experiments (see Figure 4.12).

TCE mass recovery during AMA-HI 1 was comparable to that of T80-LO, reaching approximately 63% at the conclusion of the experiment. No free-phase TCE was recovered during AMA-HI 1, however, and significant downward DNAPL migration was observed, culminating in TCE entry into previously uncontaminated regions of the aquifer cell and hence limiting overall contaminant recovery. TCE recovery was significantly higher during AMA-HI 2, reaching a total value of 81%. Of the TCE recovered during AMA-HI 2, 56% was recovered in the aqueous phase, a value that is comparable to the TCE recovery during AMA-HI 1. This is not unexpected due to the similarities in the TCE-DNAPL distributions initially present in the two experiments.

Table 4.7: Comparison of TCE recoveries following surfactant flushing in 2-D aquifer cell.

Experiment	Preflood Formulation	Surfactant Flood Formulation	Initial Saturation (%)	Pore Volumes Flushed	Mass Recovered (%)	Percent Solubilized	Percent Mobilized
T80-HI	n/a	4% (wt.) Tween 80 + 500 mg/L CaCl$_2$	2.4	7.0	87.4	100	0
T80-MID	n/a	4% (wt.) Tween 80 + 500 mg/L CaCl$_2$	2.7	1.7	83.1	100	0
T80-LO	n/a	4% (wt.) Tween 80 + 500 mg/L CaCl$_2$	2.0	2.0	66.2	100	0
AMA-HI 1	n/a	4% (wt.) Aerosol MA + 8% (wt.) 2-Propanol + 6 g/L NaCl	2.2	1.2	63.0	100	0
AMA-HI 2	n/a	4% (wt.) Aerosol MA + 8% (wt.) 2-Propanol + 6 g/L NaCl	2.9	1.2	81.3	55.9	25.4
DMD-AQ (Ramsburg and Pennell 2002b)	6% (wt.) 1-butanol	4% (4:1) Aerosol MA/OT + 20% (wt.) 1-butanol + 500 mg/L CaCl$_2$	2.4	4.9 (Preflood) 1.2 (Surfactant)	85.2	22.4	62.8
DMD-EM (Ramsburg 2002)	4.7% (vol.) Tween 80 + 1.3% (vol.) Span 80 + 15% (vol.) 1-butanol	10% (wt.) Aerosol MA + 5% (wt.) 1-butanol + 15 g/L NaCl + 1 g/L CaCl$_2$	2.2	1.2 (Preflood) 1.2 (Surfactant)	86.0	72.6	13.4

The remaining 25% (10 mL) of TCE mass removed over the course of AMA-HI 2 was recovered as free-phase TCE. Recovery of the free-phase product was a result of the increase in surfactant solution injection rate during AMA-HI 2 being sufficient for partial horizontal displacement of the TCE-DNAPL to occur. Although limited horizontal DNAPL displacement was observed, TCE migration remained in a primarily downward direction, with penetration in to the lower confining layer of the 2-D aquifer cell.

Cumulative TCE recovery during density modified displacement was high (over 85%), when either the aqueous and emulsion preflood was employed. In addition, successful density conversion of the TCE-DNAPL was attained during both DMD-AQ and DMD-EM, with little downward migration of free product observed. Contaminant recovery when using an aqueous preflood was relatively slow, requiring approximately 7 pore volumes of flooding to attain 85% mass recovery (22% in aqueous phase, 63% recovered as free-phase TCE). The lengthy flushing time required was due primarily to the prolonged preflood (approximately 5.5 pore volumes) necessary to achieve density conversion when an aqueous 1-butanol solution is utilized. As a result, TCE recovery efficiency when using the DMD approach with an aqueous preflood is lower than that observed for less aggressive strategies such as Tween 80 flushing. In contrast, TCE recovery was much more rapid when an emulsion preflood was employed, with 85% recovery (72% in aqueous phase, 13% as free-phase TCE) following 2.5 pore volumes of flushing, with significant contaminant recovery (62%) during the preflood. Recovery efficiency during DMD-EM was comparable that that achieved during T80-HI and T80-MID, and may become a more attractive strategy as TCE-DNAPL pooling within a source zone increases.
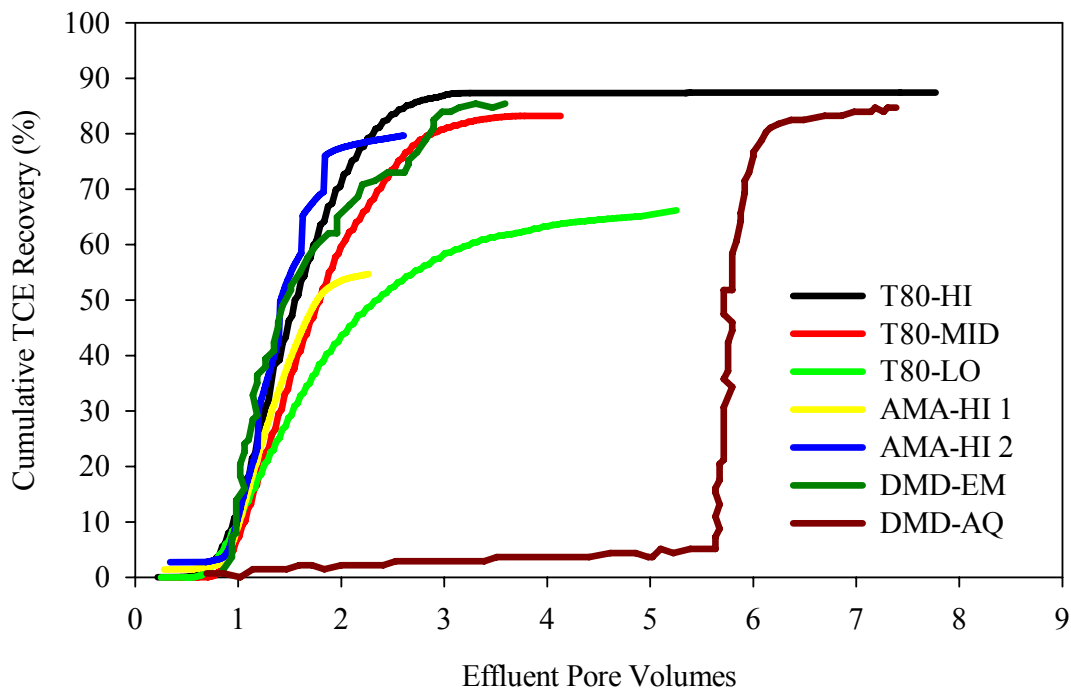
Figure 4.12: Cumulative TCE mass recovery as a function of total pore volumes flushed through 2-D aquifer cell.

4.3 Summary and Conclusions

A series of experiments were conducted to assess factors impacting TCE recovery efficiency under controlled experimental conditions, using Tween 80 and Aerosol MA based surfactant formulations. Above the critical micelle concentration (CMC), Tween 80 addition resulted in a weight solubilization ratio (WSR) of 1.74 g TCE/g surfactant, with limited reduction in interfacial tension (from 35.2 to 10.4 dynes/cm). Flushing of aquifer cells with less than 2.5 pore volumes of 4% Tween 80 achieved TCE recoveries ranging from 66% for pool-dominated source zones to 85% for ganglia-dominated source zones, with no visible evidence of TCE mobilization. TCE recoveries using an Aerosol MA surfactant formulation were comparable, with a WSR of 1.21 g/g and mass

142

recoveries of up to 81%, provided that the aqueous-phase flow rates were sufficient for horizontal displacement and capture of mobilized TCE, an outcome which may be difficult to achieve at the field scale. In addition, TCE mass recovery using a 4% Tween 80 surfactant formulation was comparable to previously published recoveries when the density modified displacement approach was employed using either an aqueous or emulsion preflood. Taken together, these results support the consideration of Tween 80 (or similar surfactants) for remediation of TCE source zones, particularly in situations where aggressive mass removal is combined with enhanced in situ bioremediation of residual contamination. However, it should be noted that DNAPL saturation distribution in the subsurface will effect SEAR-based treatment selection, with an increase in the extent of DNAPL pooling (relative to the volume of DNAPL ganglia) making dissolution-based flushing strategies (such as flushing with Tween 80) less favorable due to a decrease in the interfacial area available for mass transfer. Under these conditions, immiscible displacement strategies such as DMD become more efficient for mass recovery.

CHAPTER 5

REDUCTIONS IN CONTAMINANT MASS FLUX FOLLOWING

PARITAL MASS REMOVAL FROM DNAPL SOURCE ZONES

5.1 Introduction

A number of *in situ* remediation technologies, including surfactant and/or cosolvent flushing, thermal treatment, air sparging, and chemical oxidation have been developed to aggressively treat DNAPL source zones (see e.g., AATDF 1997, Stroo et al. 2003). Some pilot scale studies, including surfactant floods conducted at the Bachman Road (Abriola et al. 2001, Abriola et. 2003), Alameda Point (Hasegawa et al. 2000), and Hill Air Force Base OU2 (Londergan et al. 2001) sites have reported estimated DNAPL mass recoveries of greater than 90%. It should be noted, however, that mass recovery estimates often do not incorporate uncertainties in the initial estimations of DNAPL mass present in the source zone and that source zone treatments can alter both the distribution and physicochemical properties of DNAPL that is not removed (Stroo et al. 2003). Generally speaking, it is now widely accepted that some (potentially significant) fraction of initial DNAPL mass present within a source zone will persist following treatment (see e.g., Stroo et al. 2003, NRC 2004). In fact, several recent, well-controlled field-scale tests of both surfactant and cosolvent flushing suggest that DNAPL recoveries in the range of 60-70% are more typical (e.g., Brooks et al. 2004, Holmzer et al. 2000, Jawitz et al. 2000, Rao et al. 1997, Soga et al. 2004). Postulated reasons for the limited mass recoveries include aqueous-phase flow bypassing of contaminated regions and contaminant mass transfer limitations. Consequently, dissolved-phase contaminant concentrations within, and emanating from, DNAPL source zones are likely to exceed

drinking water standards for considerable periods of time, even with aggressive treatment (Sale and McWhorter 2001, Soga et al. 2004). It is therefore reasonable to question the benefits of incomplete or partial mass removal with respect protection of human health and the environment (Cherry et al. 1997, Freeze 2000, U.S. EPA 2003).

To date, critical assessments of the benefits and limitations of partial mass removal from DNAPL source zones have been based almost exclusively on mathematical predictions of dissolution, often leading to conflicting interpretations (e.g., Rao and Jawitz 2003, McWhorter and Sale 2003). Using an analytical solution for DNAPL ganglia and pool dissolution in a uniform aqueous flow field, and limited experimental data, Sale and McWhorter (2001) concluded that almost complete mass removal is required to approach regulatory drinking water standards, and that partial mass reduction will provide only minimal improvements in groundwater quality in the short term. Conversely, Rao and Jawitz (2003) investigated source zone mass discharge as a function of contaminant recovery using an analytical model consisting of "stream tubes" containing a uniform DNAPL distribution subjected to non-uniform flow, reporting that an 80% reduction in dissolved-phase contaminant mass flux could be achieved after only 50% DNAPL mass removal. However, neither non-uniform DNAPL distributions nor partial (as opposed to complete) stream tube mass removal was considered as part of this approach, leading to underestimates of mass reductions accompanying a specified flux reduction.

Jawitz et al. (2005) later extended the work of Rao and Jawitz (2003) by expanding the stream tube analytical framework to include both DNAPL distribution non-uniformity and partial mass removal from stream tubes. By combining both DNAPL

distribution and the porous media permeability field variability into a single variable describing the overall spatial variability of the source zone, Jawitz et al. (2005) determined that as the source zone spatial variability decreases, the amount of mass removal required to achieve a given reduction in contaminant mass flux is increased. In addition, Wood et al. (2005), using a comparable stream tube modeling approach, evaluated the pilot-scale cosolvent flushing of a mixed NAPL test cell at Hill Air Force Base, predicting that 60% source zone mass removal would result in an 80% reduction in contaminant mass flux.

In addition to the analytical models described above, limited numerical simulations have been performed to evaluate mass flux reductions as a function of source zone DNAPL mass removal. Parker and Park (2004) evaluated dissolution of non-uniform DNAPL distributions in a homogenous porous medium and observed dissolution rate to be strongly dependent on DNAPL distribution. Mass recovery was most limited when the source zone contained regions of extensive DNAPL pooling. Lemke et al. (2004) performed a series of numerical simulations of dissolution of a non-uniform PCE-DNAPL distribution in a statistically homogeneous, non-uniform sandy aquifer. Results from the model realizations predicted mass removals ranging from 60 to 99% and two orders-of-magnitude reductions in dissolved-phase concentration and mass flux. These results demonstrate the potential variability in mass removal versus mass flux relationships, even for relatively homogeneous systems, prompting Lemke et al. (2004) to caution that predictions based on simplified conceptual models of DNAPL source zone architecture and flow may not accurately capture reductions in contaminant flux resulting from partial mass removal.

While a great deal of mathematical modeling (either analytical or numerical) has been conducted in an effort to understand the impacts of partial source zone mass removal, correspondingly few experiments, at either laboratory- or field-scale, have been conducted to evaluate the accuracy of these numerical approaches. As such, the objective of this study was to perform laboratory-scale experiments to quantify, as a function of the initial DNAPL saturation distribution, the effects of partial source zone mass removal on dissolved-phase contaminant mass flux. Experimental results are presented visually to illustrate the differing initial saturation distributions within the aquifer cell, and to demonstrate how the distributions vary with increasing contaminant mass removal. Effluent contaminant concentrations were monitored throughout the experiments and analyzed to evaluate both overall mass recovery and post-treatment effluent contaminant concentration and mass flux as a function of mass removal. Finally, experimental results were compared to estimates from several upscaled mass transfer correlations, a tool used by modelers to estimate source zone longevity and effluent contaminant concentrations.

5.2 Results and Discussion

A series of four experiments were conducted in a two-dimensional (2-D) aquifer cell (the large aquifer cell described in Chapter 3) containing a PCE-DNAPL source zone and a down-gradient plume region. Sequential pulses of 4% (wt.) Tween 80 were injected into the cell to achieve incremental PCE mass removals ranging from 45 to 80%; each pulse was then followed by water floods to re-establish steady-state plume concentrations. Tween 80 was selected for use because it possesses a large PCE solubilization capacity (weight solubilization ratio ~0.67 g/g) and a relatively high interfacial tension with PCE (~5.0 dyne/cm), allowing for accelerated mass removal with

minimal risk of PCE mobilization (Taylor et al. 2001). Changes in the source zone PCE-DNAPL saturation distribution were measured after each surfactant flood using a light transmission system, while the down-gradient plume and flux-averaged effluent concentrations were monitored daily.

5.2.1 Initial Saturation Distribution

For each of the four aquifer cell experiments, different saturation distributions were created within the source zone region by varying the background porous medium used and the liquid PCE injection volume and rate. The resulting PCE saturation distributions were subsequently analyzed by light transmission and described in terms of the ganglia-to-pool (GTP) ratio. The first experiment (designated HI-GTP) was designed to simulate a ganglia-dominated PCE-DNAPL source zone and employed a background porous media comprised of a mixture of 50% 20/30 mesh Accusand and 50% 40/50 mesh Accusand. The total pore volume within the aquifer cell was 3,630 mL, with a source zone pore volume of 1,380 mL and an overall intrinsic permeability of 4.18×10^{-11} m^2. A total of 40.9 mL of PCE were initially present in the aquifer cell source zone following redistribution, resulting in an overall DNAPL saturation of 1.1% and a source zone DNAPL saturation of 3.0%. An initial GTP value of 1.60 for experiment HI-GTP was determined via light transmission, indicating that 62% (25.2 mL) of the PCE existed as discrete DNAPL ganglia or droplets, while the remaining 38% (15.7 mL) was present in higher-saturation ($S_{PCE} > 13\%$) pools. A photograph (taken during light transmission) of the initial PCE-DNAPL distribution for experiment HI-GTP is shown in Figure 5.1a; the resulting DNAPL saturation profile determined via light transmission is shown in Figure 5.2a.
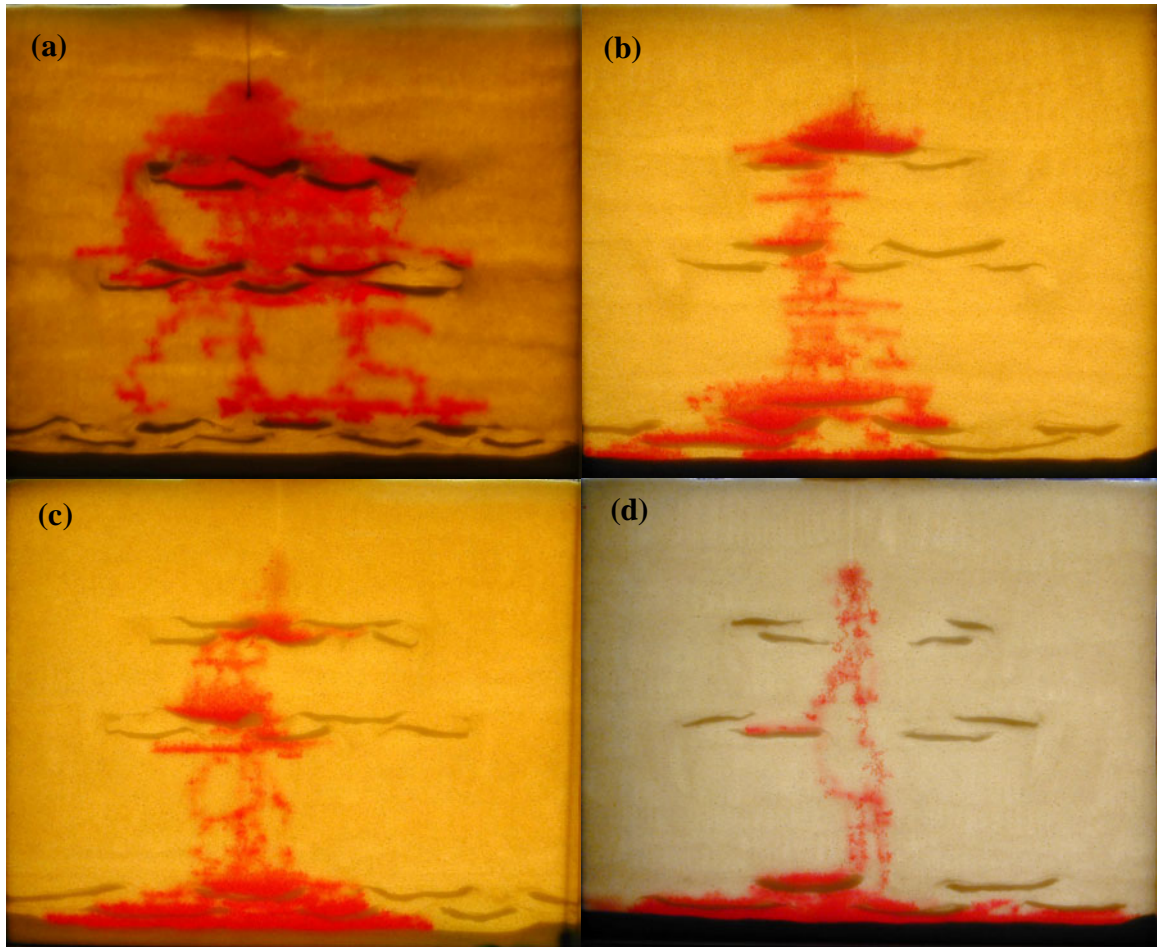
Figure 5.1: Photographs taken during light transmission analysis of initial PCE-DNAPL source zones for (a) HI-GTP, (b) MID-GTP, (c) MID/LO-GTP, and (d) LO-GTP aquifer cells.

Following completion of HI-GTP, two experiments characterized by intermediate levels of PCE-DNAPL pooling (MID-GTP and MID/LO-GTP) were conducted. For the intermediate GTP cells, 20-30 mesh Accusand was used as the background porous media to reduce the amount of PCE entrapped as residual ganglia. Both experiments were characterized by total and source zone pore volumes of 3,950 mL and 1,500 mL, respectively. Intrinsic permeability of the aquifer cell was 8.85×10^{-11} m^2 for MID-GTP and 1.83×10^{-10} m^2 for MID/LO-GTP. Approximately 15 mL of PCE was introduced into the MID-GTP aquifer cell, resulting in an overall PCE-DNAPL saturation of 0.4%, a

source zone PCE-DNAPL saturation of 1.0%, and a GTP value of 0.4, a value at which 28.6% (4.4 mL) of the PCE was present as ganglia and 71.4% (10.9 mL) present at saturations greater than residual ($S_{PCE} > 11\%$). The initial PCE-DNAPL distribution and NAPL saturation profile determined via light transmission for experiment MID-GTP are shown in Figures 5.1b and 5.2b. In the MID/LO-GTP aquifer cell, the PCE volume released was increased to 25.5 mL, corresponding to increases in the overall and source zone DNAPL saturations to respective values of 0.6% and 1.7%. The increase in PCE volume released also served to further reduce the relative amount of residual PCE present in the aquifer cell, decreasing the initial GTP to 0.26, or 20.6% (5.3 mL) of the PCE present as ganglia and 79.4% (20.2 mL) above residual saturation (Figure 5.1c and 5.2c).
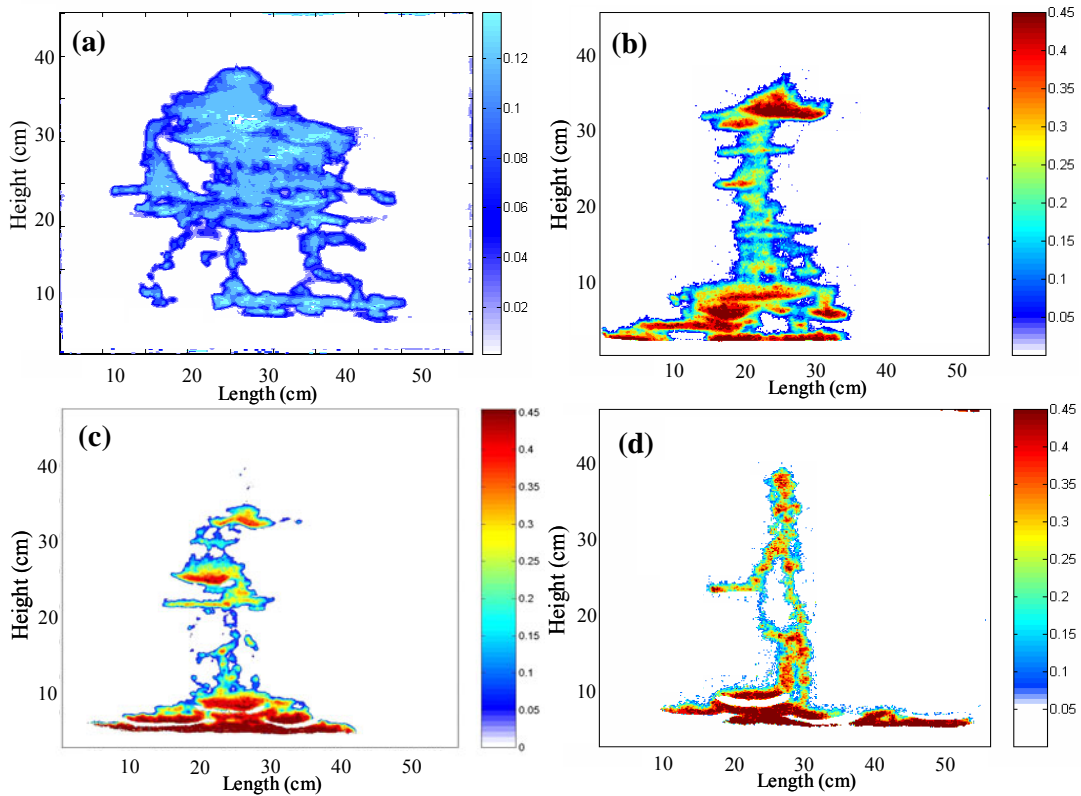
Figure 5.2: Light transmission images of initial PCE-DNAPL saturation distributions in (a) HI-GTP (1.6), (b) MID-GTP (0.4), (c) MID/LO-GTP (0.26), and (d) LO-GTP (0.16) aquifer cells.

In order to simulate a DNAPL source zone characterized by nearly complete organic-phase pooling, a final experiment (LO-GTP) was conducted. The LO-GTP cell was again packed with 20/30 mesh Accusand; however, the NAPL imbibition rate was lowered from the 1.0 mL/min value used for all the previous experiments to 0.1 mL/min in order to promote minimal ganglia formation. Total and source zone pore volumes for the experiment were 3,820 mL and 1,450 mL, and the intrinsic permeability of the cell was 5.06×10^{-10} m^2. Of the 25.1 mL of PCE introduced into the LO-GTP aquifer cell, 86% (21.6 mL) existed in high saturation pools primarily located immediately above the lower confining layer of the cell (Figures 5.1d, 5.2d), with the remaining 14% (3.5 mL) present as ganglia, resulting in an initial GTP value of 0.16. Overall and source zone PCE-DNAPL saturations for LO-GTP were 0.6% and 1.7%, respectively. The initial conditions for each of the four aquifer cell experiments are summarized in Table 5.1.

Table 5.1: Summary of initial 2-D aquifer cell experimental conditions.

Aquifer Cell Parameter	HI-GTP	MID-GTP	MID/LO-GTP	LO-GTP
Background Porous Media	Mixed Accusand[b]	20/30 Mesh Accusand	20/30 Mesh Accusand	20/30 Mesh Accusand
Overall Pore Volume (mL)	3630	3950	3950	3820
Source Zone Pore Volume (mL)	1380	1500	1500	1450
Intrinsic Permeability (m^2)	4.18×10^{-11}	8.85×10^{-11}	1.83×10^{-10}	5.06×10^{-10}
NAPL Injection Rate (mL/min)	1.0	1.0	1.0	0.1
NAPL Injection Volume (mL)	40.9	15.3	25.5	25.1
Overall NAPL Saturation (%)	1.1	0.4	0.6	0.6
Source Zone NAPL Saturation (%)	3.0	1.0	1.7	1.7
Initial PCE GTP[a]	1.60	0.40	0.26	0.16

a: Ganglia-to-pool ratio
b: 50% 20/30 mesh Accusand + 50% 40/50 mesh Accusand

5.2.2 Mass Recovery

Two sequential 4% Tween 80 surfactant floods, separated by a water flood and designed to recover approximately 75% of PCE mass initially present, were conducted in the HI-GTP (GTP = 1.60) aquifer cell. During the first flood, 4,500 mL (1.23 pore volumes) of surfactant solution were introduced into the aquifer cell. Effluent aqueous-phase PCE concentrations recorded during this flood are shown in Figure 5.3a. PCE concentrations began to exceed aqueous solubility (200 mg/L) following approximately 1 pore volume (3,600 mL) of flushing, consistent with previous experimental results (see Chapter 4 of this work) and indicating that Tween 80 sorption to the porous media used in the aquifer cell was not significant. PCE concentrations reached a maximum value of 6,500 mg/L after approximately 1.25 pore volumes of flushing and remained at this elevated level for an addition 0.5 pore volumes of flooding, when water was being introduced into the aquifer cell at an elevated flow rate for surfactant recovery. While lower than the equilibrium solubility of PCE in a 4% Tween 80 solution measured by Taylor et al. (2001) (27,000 mg/L), this value nonetheless represents an approximate 30-fold increase over the solubility of PCE in water. The sustained occurrence of these relatively high PCE effluent concentrations is believed to be a result of the large relative volume of NAPL ganglia initially available for dissolution in the aquifer cell.
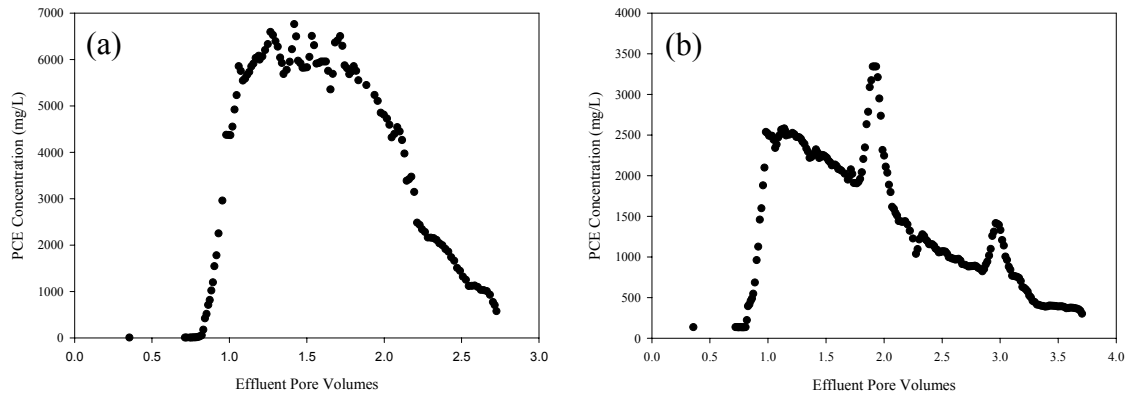
Figure 5.3: Effluent PCE concentrations observed during experiment HI-GTP following the (a) first and (b) second surfactant floods.

During the second Tween 80 flood for experiment HI-GTP, effluent PCE concentrations again increased rapidly following approximately 1 pore volume of flushing (Figure 5.3b). The maximum observed concentration during the second flood (excluding flow interruptions) was approximately 2,500 mg/L following 1.25 pore volumes of flushing, less than half of the maximum value observed during the first flood. The lower maximum value observed during this flood can be attributed to the occurrence of preferential dissolution of PCE-DNAPL ganglia during the first flood. As a result, the interfacial area of the remaining PCE available for dissolution during the second flood was lower, reducing the amount of mass transfer that could occur. Two flow interruptions, each approximately 12 hours in duration, occurred during the second surfactant flood following 1.75 and 3 pore volumes of flushing, respectively. The interruptions were marked by significant increases in PCE effluent concentration, indicating rate-limited solubilization of the PCE-DNAPL similar to that observed by Pennell et al. (1993) and Taylor et al. (2001). After reaching a maximum concentration, PCE concentrations decreased over the remainder of the flood (with the exception of two

flow interruptions) due to a continued decrease in the amount of PCE-DNAPL available for dissolution.

During HI-GTP, a total 21 mL of PCE were recovered over the course of the first (1.23 pore volume) surfactant flood, while the second 2.25 pore volume surfactant flood yielded an additional 10 mL of PCE. Total mass recovery at the conclusion of the experiment was approximately 75% (31 mL). Surfactant flushing conditions (volume flushed and nominal flow rate) and mass recovery data for experiment HI-GTP are summarized in Table 5.2, and cumulative PCE recovery over the course of the entire experiment HI-GTP is shown in Figure 5.4a. Both the rate and extent of PCE recovery were greater during the first surfactant flood compared to the second flood, as indicated by the PCE to surfactant recovery efficiency, which declined from 0.12 g/g (i.e., g PCE recovered/g Tween 80 injected) during the first flood to 0.06 g/g during the second. This behavior was attributed to preferential dissolution of high-interfacial area PCE ganglia, which accounted for 62% of the initial PCE volume, followed by less favorable dissolution of PCE from low-interfacial area pools. In addition, little redistribution of PCE-DNAPL was observed during HI-GTP. This is consistent with total trapping number calculations, where N_T for the aquifer cell (2.72×10^{-5}) was within or slightly larger than the critical region where DNAPL mobilization begins to occur.
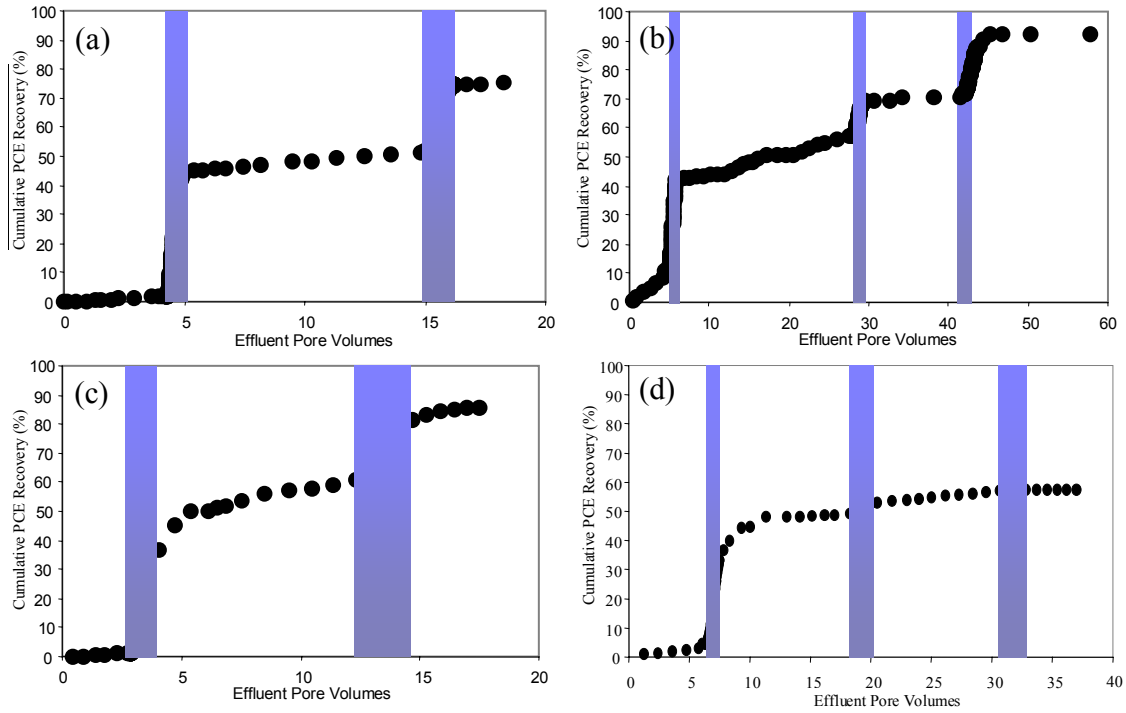
Figure 5.4: Cumulative PCE mass recovery for (a) HI-GTP, (b) MID-GTP, (c) MID/LO-GTP, and (d) LO-GTP. Shaded areas represent the volume of 4% Tween 80 injected.

In the MID-GTP (GTP = 0.4) experiment, three surfactant floods, separated by two natural-gradient water floods, were conducted. During the first flood, 3,210 mL of 4% Tween 80 solution were injected into the aquifer cell (see Table 5.2). The initial flood was followed by two subsequent floods having pore volumes of 3,130 mL and 4,480 mL. Effluent PCE concentrations for the first, second and third surfactant floods conducted during MID-GTP are shown in Figure 5.5a, 5.5b, and 5.5c, respectively. As expected, PCE concentrations began to exceed aqueous solubility following approximately one pore volume of flushing during all three surfactant floods, consistent with previous experimental results. During the first surfactant flood, PCE concentrations reached a maximum value of slightly more than 3,000 mg/L after approximately 1.25 pore volumes of surfactant flushing. This value, while lower than the equilibrium

solubility of PCE in a 4% Tween 80 solution by a factor of 10, represents a 15-fold increase over the solubility of PCE in water. However, it should also be noted that this value is less than half of the maximum PCE concentration observed during the first surfactant flood conducted for experiment HI-GTP. The difference is likely due to the PCE-DNAPL pooling in the MID-GTP source zone resulting in a lower interfacial area initially available for PCE dissolution. After reaching the maximum value, effluent PCE concentrations steadily decreased over the remaining 1.5 pore volumes of flushing when water was flushed through the aquifer cell to recover surfactant solution.

Table 5.2: Mass recovery and trapping number analysis for 2-D aquifer cell experiments.

| Aquifer Cell Parameter	HI-GTP	MID-GTP	MID/LO-GTP	LO-GTP
Total PCE Recovered (mL) [%]	30.7 [75.2]	14.1 [92.2]	21.7 [85.1]	14.4 [57.4]
Surfactant Flood 1				
Flood Volume (mL)	4500	3210	5360	3370
Flood Flow Rate (mL/min)	5.72 ± 0.50^a	5.71 ± 1.84	6.05 ± 0.35	8.59 ± 2.27
PCE Recovered (mL) [cumulative %]	20.9 [51.3]	7.8 [51.0]	13.2 [51.8]	12.0 [47.9]
PCE Recovery Efficiency (g/g)	0.12	0.10	0.10	0.14
Surfactant Flood 2				
Flood Volume (mL)	8180	3130	8290	3500
Flood Flow Rate (mL/min)	5.47 ± 0.21	8.12 ± 1.81	5.52 ± 0.46	7.12 ± 2.50
PCE Recovered (mL) [cumulative %]	9.8 [75.2]	3.0 [70.6]	8.5 [85.1]	1.2 [55.7]
PCE Recovery Efficiency (g/g)	0.06	0.04	0.04	0.014
Surfactant Flood 3				
Flood Volume (mL)	n/a	4480	n/a	3630
Flood Flow Rate (mL/min)	n/a	8.00 ± 2.47	n/a	7.38 ± 2.26
PCE Recovered (mL) [cumulative %]	n/a	3.3 [92.2]	n/a	0.3 [57.4]
PCE Recovery Efficiency (g/g)	n/a	0.03	n/a	0.004
Trapping Number Analysis				
Capillary Number (N_{Ca})	3.71×10^{-6}	4.83×10^{-6}	3.84×10^{-6}	5.11×10^{-6}
Bond Number (N_B)	2.69×10^{-5}	5.70×10^{-5}	1.18×10^{-4}	3.26×10^{-4}
Total Trapping Number (N_T)	2.72×10^{-5}	5.72×10^{-5}	1.18×10^{-4}	3.26×10^{-4}

a: Standard deviation

Figure 5.5: Effluent PCE concentrations observed during experiment MID-GTP following the (a) first, (b) second, and (c) third surfactant floods.

During the second and third 4% Tween 80 floods for experiment MID-GTP, effluent PCE concentrations again rapidly increased following approximately 1 pore volume of flushing. In both cases, maximum effluent PCE concentrations of just below 1,000 mg/L were observed after 1.25 pore volumes of flushing. These values were significantly lower than the maximum value observed during the first flood, which may be attributed to preferential dissolution of PCE-DNAPL ganglia during the first surfactant flushing event and the long-term persistence of a large PCE pool having a relatively low interfacial area along the bottom of the aquifer cell. After attaining maximum concentrations, effluent PCE concentrations tended to decrease over the remainder of the

second and third surfactant floods as the volume (and interfacial area) of PCE-DNAPL available for dissolution decreased.

PCE mass recoveries for the three surfactant floods conducted during MID-GTP are summarized in Table 5.2, and the corresponding cumulative PCE mass recovery curve for the experiment is shown in Figure 5.4b, with shaded areas corresponding to the volume of 4% Tween 80 solution injected. Over the course of MID-GTP, 14.1 mL of PCE was recovered, yielding an overall mass recovery of 92.2%. Of the total PCE recovered, 51.0% (7.8 mL) was removed during the first 0.81 pore volume surfactant flood. An additional 3.0 mL and 3.3 mL of PCE were recovered during the second (0.8 pore volume) and third (1.13 pore volume) surfactant floods, corresponding to 19.6% and 21.6% of the initial PCE present in the source zone. As with experiment HI-GTP, mass removal was most pronounced during the first surfactant flood due to rapid and preferential dissolution of any PCE-DNAPL ganglia initially present in the source zone, and the three sequential surfactant floods yielded PCE to surfactant recovery efficiencies of 0.10, 0.04 and 0.03 g PCE/g Tween 80, respectively. The PCE-DNAPL remained relatively stationary over the course of the surfactant floods, consistent with expectations based on the total trapping number concept. A total trapping number of 5.72×10^{-5} was calculated for experiment MID-GTP, significantly greater than the critical value for PCE-DNAPL displacement and indicating little chance of organic-phase displacement.

Two surfactant floods separated by a natural-gradient water flood, were conducted during the MID/LO-GTP (GTP = 0.26) experiment, an initial 5,360 mL (1.36 pore volume) flood followed by a second flood of 8,290 mL (2.10 pore volumes). Surfactant flushing volumes and flow rates for MID/LO-GTP are summarized in Table

158

5.2. Effluent PCE concentrations for experiment MID/LO-GTP are shown in Figure 5.6. PCE concentrations during the first surfactant flood (Figure 5.6a) began to exceed aqueous solubility following approximately 0.75 pore volumes of flushing, slightly sooner than previously discussed results. A maximum effluent concentration of approximately 2,100 mg/L was observed during the first surfactant flood, comparable to the maximum concentration observed during the first surfactant flood of experiment MID-GTP. The behavior of the PCE effluent concentrations during these experiments were expected to be relatively comparable due to the superficial similarities between the initial PCE-DNAPL source zone architectures. During MID/LO-GTP, however, a significantly slower rate of increase in effluent PCE concentrations prior to reaching the maximum concentration was observed. This phenomenon was attributed to a combination of incomplete capture of the surfactant flushing solution by the extraction well along with dilution with water from down-gradient regions of the aquifer cell (i.e., the plume region). Upon reaching the maximum value, effluent PCE concentrations steadily decreased over an approximate 0.75 pore volumes of additional flooding.
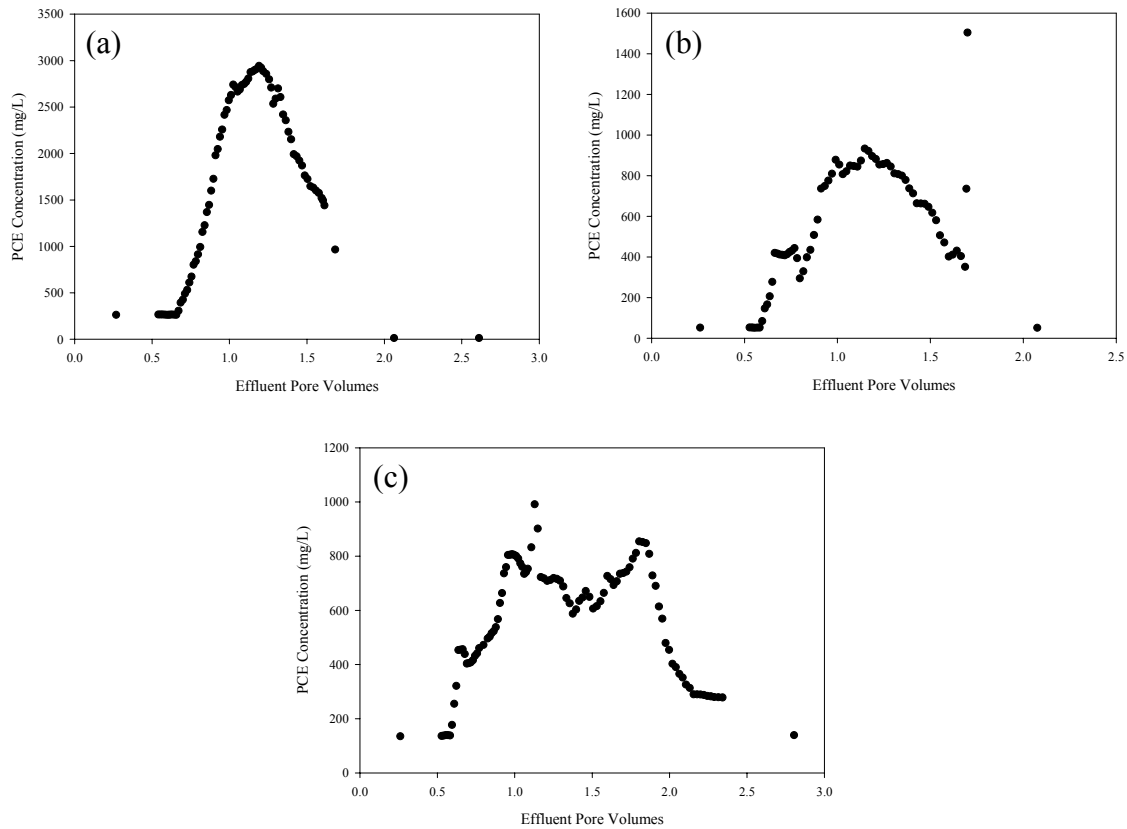

Figure 5.6: Effluent PCE concentrations observed during experiment MID/LO-GTP following the (a) first and (b) second surfactant floods.

Effluent PCE concentrations rapidly increased following approximately 0.5 pore volume of flushing during the second MID/LO-GTP 4% Tween 80 flood (Figure 5.6b). A maximum effluent concentration of approximately 250 mg/L was observed following approximately 0.8 pore volumes of flushing. This was significantly lower than the maximum concentration observed during the first flood, due to preferential dissolution of PCE-DNAPL ganglia during the first surfactant flushing event and the persistence of large PCE pools along the bottom of the aquifer cell. In addition, this value was significantly lower than the maximum effluent PCE concentrations observed during the second and third surfactant floods of experiment MID-GTP. As with the first MID/LO-GTP surfactant flood, this discrepancy can be attributed to incomplete capture of the 4% Tween 80 solution by the source zone extraction well and dilution with water from the plume development region of the aquifer cell. PCE concentrations steadily decreased over the remainder of the second surfactant flood, reaching a minimum value of less than 10 mg/L following approximately 2.5 total pore volumes of flushing (including surfactant solution and recovery water).

PCE mass recovery for experiment MID/LO-GTP is shown in Figure 5.4c and summarized in Table 5.2. At total of 21.7 mL of PCE were recovered during the course of the experiment, corresponding to a cumulative mass recovery of 85.1%. Of the total PCE recovered, 13.2 mL, or 51.8% of PCE mass initially present in the source zone, was recovered during the first (1.36 pore volume) surfactant flood. During the second flood (2.10 pore volumes), an additional 8.5 mL PCE were recovered, corresponding to 33.3% of PCE initially present in the aquifer cell. Recovery efficiency for the first and second surfactant floods were determined to be 0.10 and 0.4 g PCE/g Tween 80, respectively.

The similarity in recovery efficiencies obtained for the MID- and MID/LO-GTP experiments, despite differences in the initial PCE volume present (15.3 mL versus 25.5 mL) and surfactant flushing sequence (3 floods versus 2 floods), indicates that the fraction of PCE mass existing as ganglia, as expressed by the GTP ratio, strongly governs partial mass recovery resulting from enhanced dissolution. A total trapping number of 1.18×10^{-4}, significantly greater than the critical value for PCE mobilization, was calculated for experiment MID/LO-GTP. This value implies potential for significant DNAPL redistribution, an outcome that was not observed during the experiment. It is therefore likely that the intrinsic permeability of the aquifer cell was overestimated, resulting in overestimation of the total trapping number.

For the final aquifer cell experiment (LO-GTP, GTP = 0.16), characterized by a source zone dominated by a single DNAPL pool above the lower confining layer, three sequential surfactant floods, separated by two natural-gradient water floods, were conducted. The respective volumes of the three floods were 3,370 mL (0.88 pore volume), 3,500 mL (0.92 pore volume) and 3,630 mL (0.95 pore volume). Surfactant flushing volumes and flow rates for LO-GTP are summarized in Table 5.2. Figure 5.7 shows effluent PCE concentrations for each of the three surfactant floods conducted during experiment LO-GTP. PCE concentrations observed during the first surfactant flood (Figure 5.7a) began to exceed the aqueous solubility of PCE (approximately 200 mg/L) following 0.6 pore volumes of surfactant flushing, somewhat lower than observed in previous experiments. This phenomenon was attributed to development of a banked surfactant flow front, with the lower regions of the aquifer cell experiencing early breakthrough. The maximum PCE concentration observed during the first surfactant

flood was 3,600 mg/L following 1.25 total pore volumes of flushing (surfactant solution and recovery water), representing a 23-fold increase over the aqueous solubility of PCE. The maximum observed concentration is comparable to maximum values observed during the first surfactant floods of experiments MID-GTP and MID/LO-GTP. This can likely be attributed to the fact that the three experiments had comparable initial volumes of PCE-DNAPL ganglia readily available for dissolution (due to differences in injected PCE volume), despite the fact that experiment LO-GTP was characterized primarily by a single large pool of DNAPL.
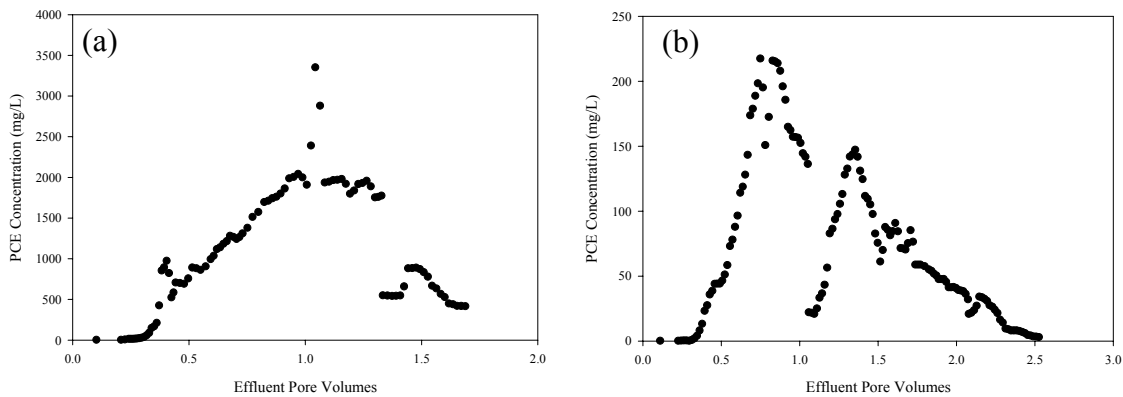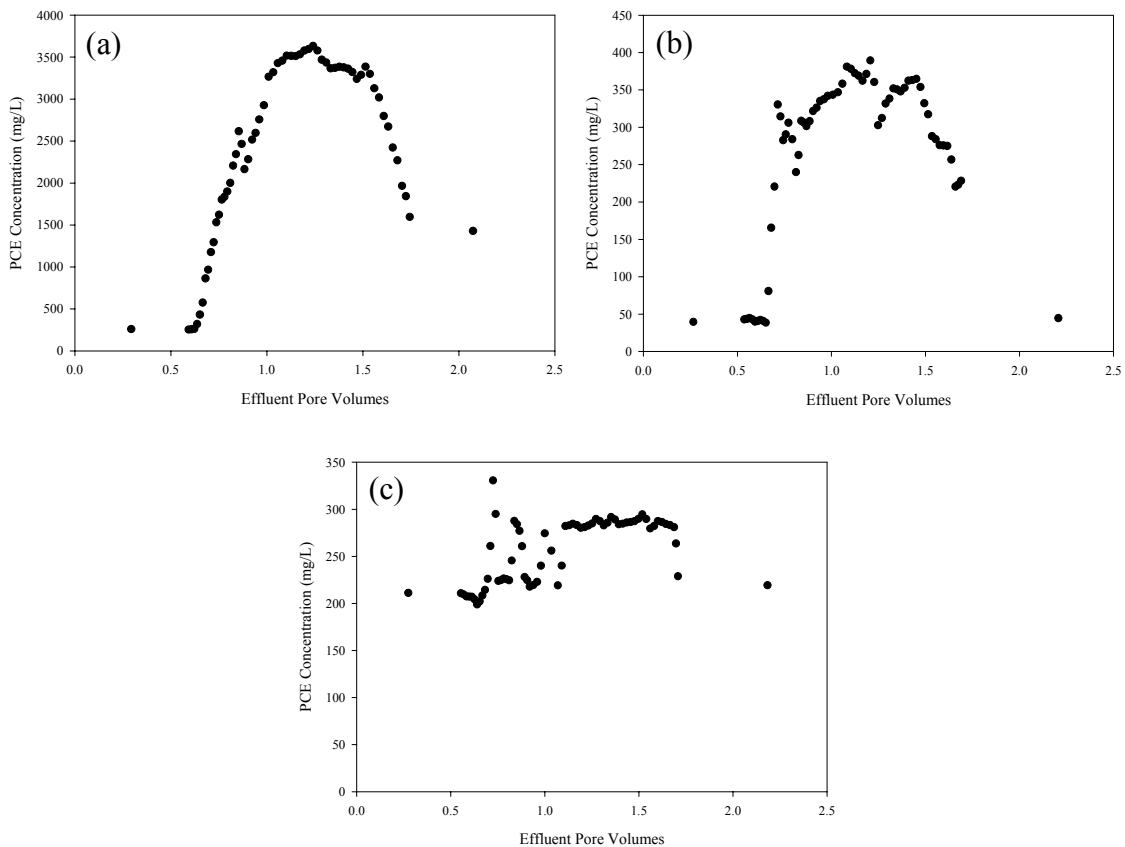

Figure 5.7: Effluent PCE concentrations observed during experiment LO-GTP following the (a) first, (b) second, and (c) third surfactant floods.

Effluent PCE concentrations during the second (Figure 5.7b) and third (Figure 5.7c) surfactant floods of experiment LO-GTP also increased rapidly following approximately 0.6 pore volumes of flushing, again attributed to development of a banked surfactant solution flow front. For the second surfactant flood a maximum PCE effluent concentration of 400 mg/L was observed. This value is significantly lower than the maximum value observed during the first surfactant flood, due to a combination of the preferential dissolution of PCE-DNAPL ganglia that occurred early in the experiment (i.e., during the first flood) and the extremely low interfacial area available for mass transfer of the remaining pools within the source zone. In addition, the maximum observed PCE concentration was also lower those observed during comparable surfactant floods for experiments MID-GTP and MID/LO-GTP, which was also attributed to mass transfer limitations arising from the remaining PCE-DNAPL available for the second LO-GTP surfactant flood being characterized primarily by low interfacial areas (i.e., pools). For the third surfactant flood, only an approximate 100 mg/L increase in PCE effluent concentrations was observed (from 200 mg/L to 300 mg/L). This extremely slight increase due to the source zone during the third surfactant flood containing a PCE-DNAPL distribution with only a single PCE pool that was characterized by an extremely low interfacial area, thereby limiting PCE dissolution,.

The PCE mass recoveries achieved during LO-GTP are summarized in Table 5.2, with the corresponding cumulative PCE mass recovery curve shown in Figure 5.4d. A total of 14.4 mL of PCE were recovered during the three sequential surfactant floods, yielding an overall mass recovery of only 57.4%, up to 35% less than overall recoveries observed in less pool-dominated source zones. Of the total volume of PCE recovered

from the aquifer cell, 12.0 mL were removed during first (0.9 pore volume) surfactant flood, corresponding to 47.9% of the PCE initially present. The PCE to surfactant recovery efficiency during the first flood was 0.14 g/g, which is similar to the values obtained for the initial 4% Tween 80 floods of the other aquifer cell experiments (see Table 5.2). The observed consistency in initial mass recovery efficiencies regardless of the GTP ratio is attributed to the dissolution of PCE ganglia, which accounted for a minimum of 14% of the initial PCE mass in all experiments. However, PCE recovery was much lower during the second and third surfactant floods, as PCE ganglia were depleted in the source zone. An additional 1.2 mL of PCE was recovered during the second surfactant flood (7.8% of PCE initially present in the source zone) and a final 0.3 mL (1.7%) recovered during the third. Mass recovery efficiencies during these floods also declined substantially; to 0.014 g/g in the second flood and 0.004 g/g in the third flood. Taken together, these data suggest that pool-dominated source zones, in which ganglia represent a relatively small fraction (e.g., < 25%) of the total DNAPL mass, remediation strategies based on, or dependent upon, enhanced dissolution will achieve diminishing returns over time. Finally, some redistribution of PCE-DNAPL in the LO-GTP source zone was observed during surfactant flushing. This was consistent with expectations based on the calculated total trapping number of 3.62×10^{-4} for the aquifer cell, a value nearly an order-of-magnitude greater than the reported critical value for DNAPL displacement (2×10^{-5}).

5.2.3 Change in Saturation Distribution

In an effort to quantify the effects of partial source zone mass removal on PCE saturation distributions, light transmission analysis was conducted after each sequential

164

surfactant flood to estimate changes to the PCE-DNAPL ganglia-to-pool ratio (GTP). Figure 5.8 shows an example of a light transmission (LT) analysis following an intermediate surfactant flood. A representative photograph taken during LT of the PCE-DNAPL source zone for experiment MID/LO-GTP following the first surfactant flood is shown (Figure 5.8a) along with the corresponding light transmission image (Figure 5.8b). In comparing the two panels of Figure 5.8, it is clear that LT can accurately describe source zone conditions between sequential surfactant floods. Light transmission images of the PCE saturation distributions present in the aquifer cell source zone at the conclusion of each experiment are also shown in Figure 5.9. With the exception of experiment HI-GTP (Figure 5.9a), the PCE saturation distributions at the conclusion of surfactant flushing are characterized by extensive regions of relatively high saturation PCE-DNAPL pools immediately above the lower confining layer of the aquifer cell source zone.
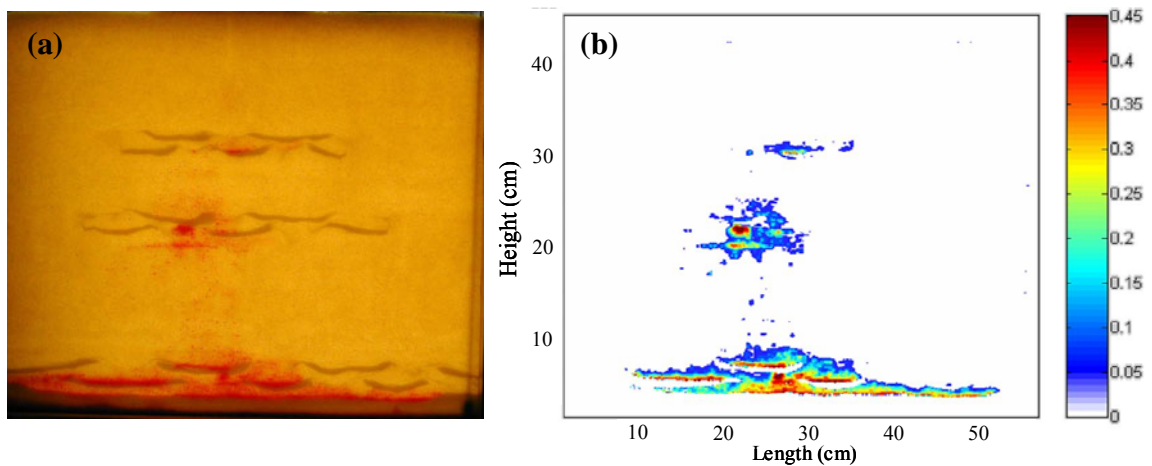
Figure 5.8: Representative example of (a) photograph taken during light transmission and (b) light transmission image of PCE saturation distribution during intermediate surfactant flood. Experiment is MID/LO-GTP immediately prior to second surfactant flood.
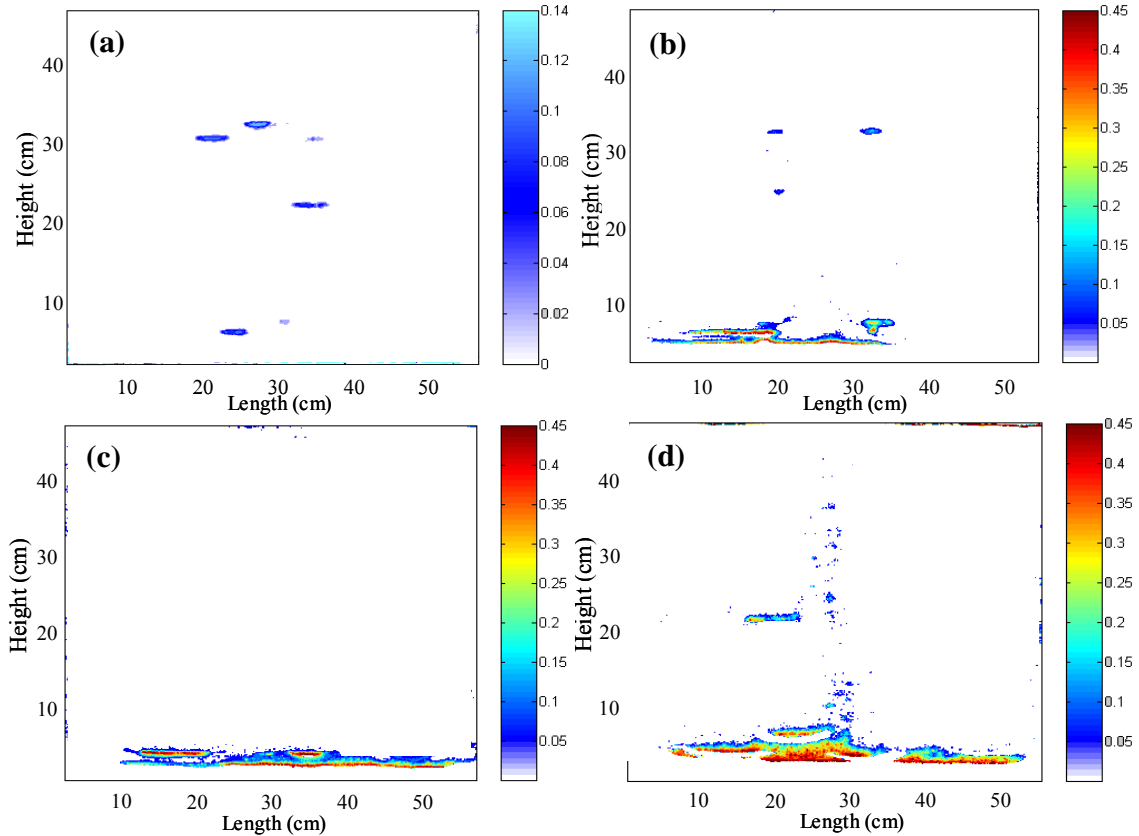
Figure 5.9: Light transmission images of final PCE saturation distributions in (a) HI-GTP (1.6), (b) MID-GTP (0.4), (c) MID/LO GTP (0.26) and (d) LO-GTP (0.16) aquifer cells.

The GTP values for all four aquifer cell experiment following sequential surfactant flushing are summarized in Table 5.3, along with the corresponding percentage of PCE-DNAPL remaining in each aquifer cell as residual ganglia (i.e., $S_{PCE} \leq 11\%$ or 13%) and the corresponding DNAPL ganglia and pool volumes (in mL) for each aquifer cell. As anticipated, GTP values were observed to decrease with increasing PCE mass recovery in all four experiments (along with a decrease in the percentage of PCE-DNAPL remaining as residual ganglia), providing further evidence that high interfacial area ganglia are readily removed during enhanced dissolution floods, compared to lower interfacial area pools. Reductions in the PCE-DNAPL ganglia volume and GTP were most pronounced for the HI-GTP experiment, in which the GTP decreased from an initial

value of 1.60 (25.1 mL) to a final value of 0.60 (3.8 mL). In contrast, for the LO-GTP experiment the GTP decrease was much more moderate, from an initial value of 0.16 (3.46 mL as ganglia) to a final value of 0.05 (0.55 mL as ganglia). The large GTP decrease during HI-GTP may be attributed to the large volume of PCE-DNAPL ganglia initially available for dissolution. Preferential removal of these ganglia resulted in a large decrease in GTP relative to the other experiments which were characterized by much lower initial volumes of PCE-DNAPL ganglia.

Table 5.3: Effect of surfactant flushing on PCE-DNAPL source zone ganglia-to-pool (GTP) ratio in 2-D aquifer cells.

Aquifer Cell Parameter	HI-GTP	MID-GTP	MID/LO-GTP	LO-GTP
Initial GTP[a] [% Ganglia]	1.60 [61.5]	0.40 [28.6]	0.26 [20.6]	0.16 [13.8]
Ganglia Volume (mL)	15.7	10.9	20.2	21.6
Pool Volume (mL)	25.2	4.4	5.3	3.5
Surfactant Flood 1				
PCE Recovered (mL) [cumulative %]	20.9 [51.3]	7.8 [51.0]	13.2 [51.8]	12.0 [47.9]
GTP [% Ganglia]	0.90 [47.4]	0.30 [23.1]	0.19 [16.0]	0.12 [10.7]
Pool Volume (mL)	10.5	5.8	10.3	11.7
Ganglia Volume (mL)	9.4	1.7	2.0	1.4
Surfactant Flood 2				
PCE Recovered (mL) [cumulative %]	9.8 [75.2]	3.0 [70.6]	8.5 [85.1]	1.2 [55.7]
GTP [% Ganglia]	0.60 [37.5]	0.25 [20.0]	0.16 [13.8]	0.06 [5.7]
Pool Volume (mL)	6.3	4.8	3.3	10.5
Ganglia Volume (mL)	3.8	1.2	0.5	0.6
Surfactant Flood 3				
PCE Recovered (mL) [cumulative %]	n/a	3.3 [92.2]	n/a	0.3 [57.4]
GTP [% Ganglia]	n/a	0.15 [13.0]	n/a	0.05 [4.7]
Pool Volume (mL)	n/a	1.0	n/a	10.2
Ganglia Volume (mL)	n/a	0.2	n/a	0.5

a: Ganglia-to-pool ratio

The changes in saturation distribution behavior for each of the aquifer cell experiments are summarized in Figure 5.10, with the black bars representing the volume of PCE ganglia, the white bars representing the PCE pool volume, and the stack the total PCE volume present in the aquifer cell following a given surfactant flood. For example, the volume of PCE present during experiment HI-GTP decreased from an initial value of 40.9 mL, of which 25.1 mL (61.5%) was present as ganglia, to a final value of 10.1 mL, of which only 3.8 mL (37.5%) was ganglia. By comparison, only 13.8% (3.46 mL) of the 25.1 mL of PCE initially present during experiment LO-GTP was ganglia decreasing to 4.7% (0.55 mL out of 11.7 mL) at the conclusion of the final surfactant flood.
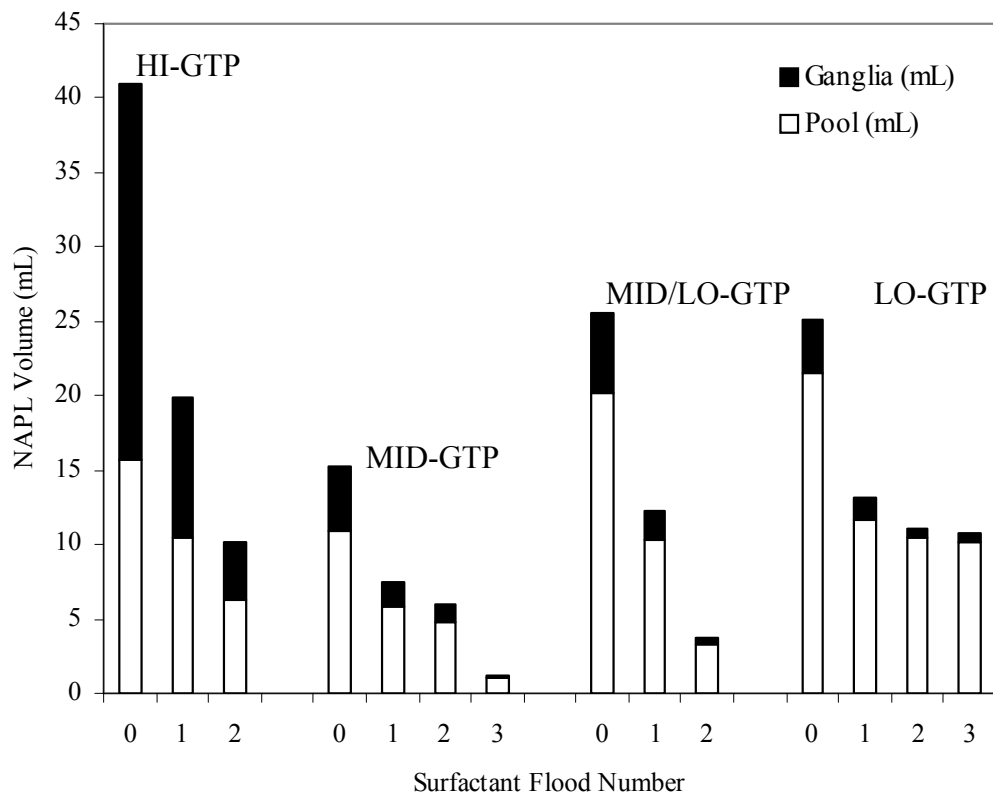
Figure 5.10: Volume of PCE existing as ganglia and pools in the source zone of the 2-D aquifer cells after each surfactant flood.

5.2.4 Effluent Concentration and Mass Flux

For each of the four aquifer cell experiments, effluent PCE concentrations were monitored following each surfactant flood to evaluate the impact of source zone mass removal on down-gradient contaminant concentrations and mass flux. Effluent PCE concentration and mass flux, normalized by dividing by initial (i.e., prior to surfactant flushing) values, are summarized in Table 5.4 and plotted as a function of cumulative PCE mass recovery for concentration (panel a) and mass flux (panel b) in Figure 5.11. Substantial reductions in effluent PCE concentration (and mass flux), ranging from 25% to 65%, were observed after the first surfactant flood conducted during the MID-GTP, MID/LO-GTP, and LO-GTP experiments. The magnitude of decrease following the first surfactant flood generally increased with decreasing PCE-DNAPL GTP (i.e., increased PCE pooling), which was attributed to enhanced (preferential) dissolution of PCE ganglia mass and relatively small pools located above low permeability lenses in the center of the source zone. During the HI-GTP experiment, relative PCE mass flux and effluent concentrations remained essentially constant, even with removal of greater than 50% of the PCE mass initially present in the aquifer cell. However, a 60% reduction in relative mass flux was observed at the conclusion of the second surfactant flood, when 85% of PCE mass initially present as ganglia had been removed. In the MID-GTP and MID/LO-GTP experiments, further decreases in the relative PCE effluent concentration and mass flux followed subsequent surfactant flushing due to continued enhanced dissolution of PCE ganglia and pools. In the pool-dominated experiment LO-GTP, the initial reduction in mass flux was the greatest (65% after 55% PCE mass removal), but decreased only slightly following the second and third surfactant floods. At the conclusion of this

169

experiment, the remaining PCE mass existed in high saturation pools (GTP = 0.05), located immediately above the lower confining layer of the aquifer cell, that could not be effectively treated by enhanced dissolution.

Based on results from all four experiments, mass flux and effluent concentrations can be expected to decrease substantially (up to 96%) following partial (50%-70%) source zone mass removal employing miscible displacement (i.e., enhanced dissolution) as the contaminant recovery mechanism. Observed changes in concentration and mass flux were clearly dependent on the initial PCE saturation distribution within the aquifer cell. For example, a 75% reduction in mass flux was obtained in the pool-dominated system (LO-GTP) after only 52% mass removal, compared to a slight increase in mass flux for the ganglia-dominated scenario (HI-GTP) after 51% mass removal.

Table 5.4: Effect of surfactant flushing on relative effluent concentration (C/C_o) and relative mass flux (MF/MF_o) in 2-D aquifer cells.

Aquifer Cell Parameter	HI-GTP	MID-GTP	MID/LO-GTP	LO-GTP
Surfactant Flood 1				
PCE Recovered (mL) [cumulative %]	20.9 [51.3]	7.8 [51.0]	13.2 [51.8]	12.0 [47.9]
C/C_o	1.00±0.12[a]	0.68±0.06	0.48±0.10	0.35±0.10
MF/MF_o	1.07±0.17	0.77±0.07	0.50±0.12	0.35±0.10
Surfactant Flood 2				
PCE Recovered (mL) [cumulative %]	9.8 [75.2]	3.0 [70.6]	8.5 [85.1]	1.2 [55.7]
C/C_o	0.36±0.04	0.59±0.17	0.04±0.04	0.26±0.13
MF/MF_o	0.31±0.02	0.74±0.17	0.04±0.04	0.26±0.13
Surfactant Flood 3				
PCE Recovered (mL) [cumulative %]	n/a	3.3 [92.2]	n/a	0.3 [57.4]
C/C_o	n/a	0.27±0.11	n/a	0.23±0.15
MF/MF_o	n/a	0.35±0.11	n/a	0.23±0.15

a: Standard deviation

Relative effluent concentration and mass flux values were nearly identical within each experiment, as is evident when comparing Figures 5.11a and 5.11b. This outcome was anticipated due to the relatively uniform aqueous flow field in the aquifer cell. The differences between effluent concentration and mass flux that did arise (most notably during experiment MID-GTP) were due to variations in the aqueous flow rate during the natural-gradient water flushing phases of the experiments. The variations in flow rate affect mass flux, since it is the product of the aqueous phase contaminant concentration and Darcy velocity (Equation 5.1), which is the aqueous flow rate divided by the cross-sectional area of the aquifer cell.

$$MF = C \times q_w \qquad (5.1)$$

For example, during MID-GTP, the natural-gradient water flow rate increased from 1.14 mL/min prior to surfactant flushing to 1.36 mL/min following the first surfactant flood, accounting for the difference between normalized effluent concentration and mass flux (0.68±0.06 and 0.77±0.07, respectively).
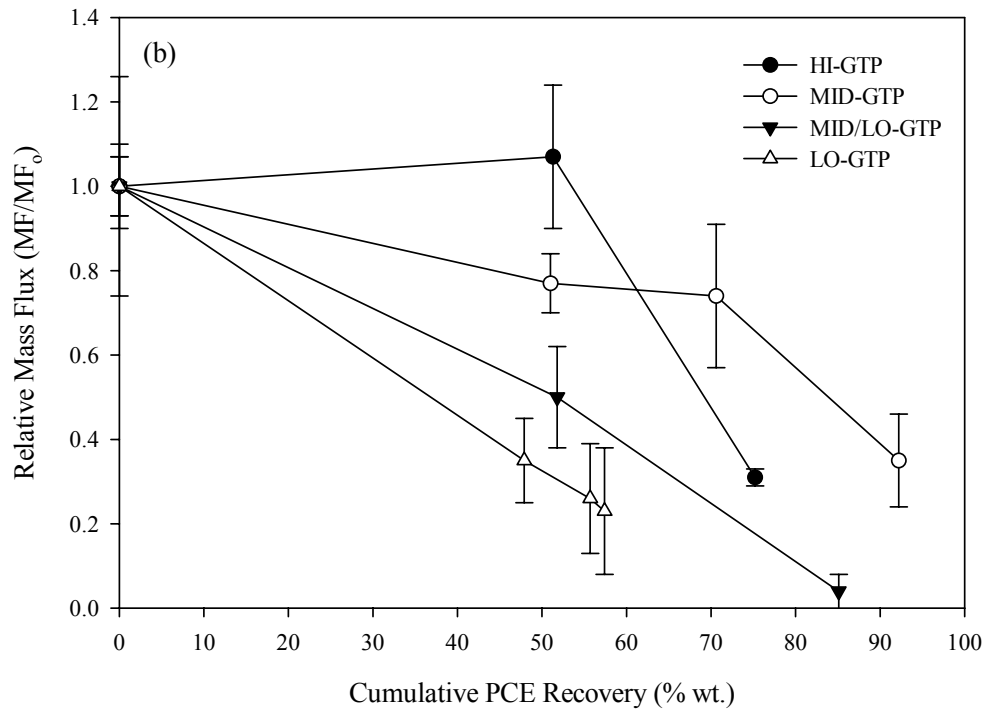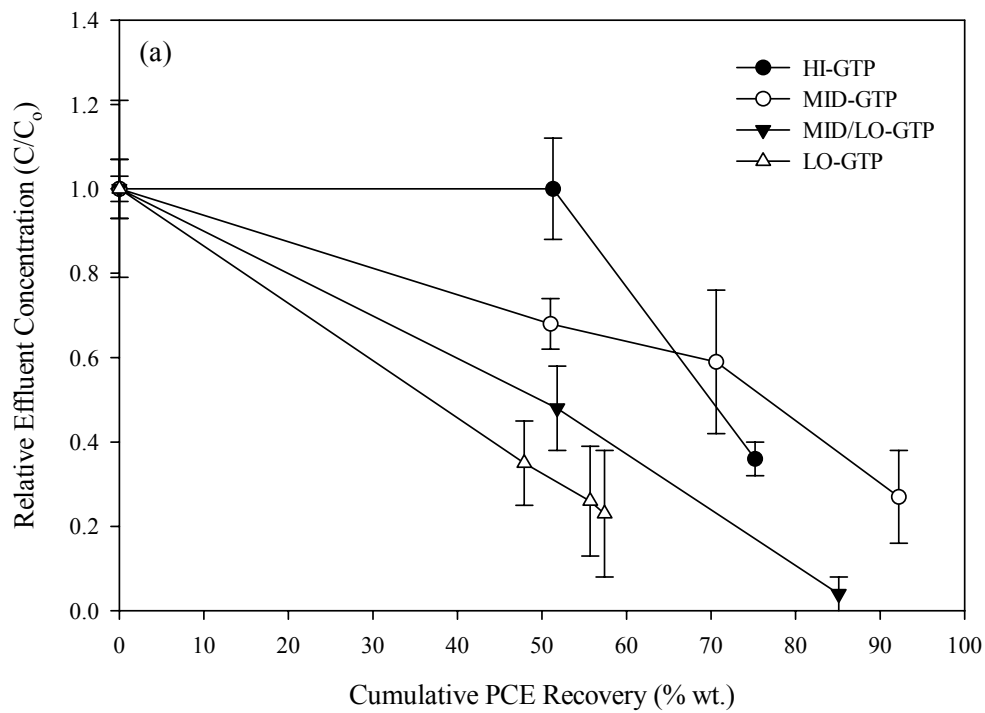
Figure 5.11: Normalized effluent PCE concentrations (a) and (b) mass flux as a function of source zone architecture and cumulative PCE mass recovery. Error bars represent one standard deviation.

5.2.5 Mass Removal Correlations

A number of mass transfer correlations have been developed and utilized to estimate DNAPL source zone longevity and effluent contaminant concentrations as a function of mass removal (e.g., Parker and Park 2004, Zhu and Sykes 2005, Falta et al. 2005). However, these models do not typically include information on source zone saturation distribution, and therefore tend to under-predict source zone longevity, especially for systems dominated by DNAPL pools (Christ et al. 2005b). In an effort to address this issue, Christ et al. (2006) developed an upscaled mass transfer correlation incorporating DNAPL saturation distribution via the ganglia-to-pool ratio:

$$C^a \Big/ C^{a,eq} = 1 - \left(1 - C^{a,t=0} \Big/ C^{a,eq}\right)^{\left(M \big/ M^0\right)^{A \times GTP^B}} \qquad (5.2)$$

In Equation 5.2, C^a is the effluent contaminant concentration, $C^{a,\,eq}$ is the equilibrium contaminant concentration, $C^{a,\,t=0}$ is the effluent contaminant concentration prior to dissolution, M/M^0 is the fraction of the initial contaminant mass remaining in the source zone, GTP is the ganglia-to-pool ratio, and A and B are fitting parameters. Christ et al. (2006) estimated A and B fitting parameters of 1.54 and -0.27, respectively, for simulated PCE-DNAPL source zones with GTP ratios ranging from 1.5 to 24.0. Using these fitting parameters, effluent PCE concentrations predicted using the upscaled mass transfer correlation were compared to effluent concentrations measured in the 2-D aquifer cells as a function of cumulative mass removal (Figure 5.12a). Results shown in Figure 5.12a demonstrate that, although the unmodified correlation captured the general dependence of the effluent concentration curves on the initial GTP ratio, the measured decrease in effluent PCE concentrations was consistently over-predicted in all four experiments. Root mean-square error (RMSE) values were also generally poor for the unmodified

correlation (Table 5.5), particularly for experiments HI-GTP and MID-GTP, with an overall RMSE for all four experiments of 0.239.

In an effort to improve the accuracy of Equation 5.2, parameters *A* and *B* were fit to the aquifer cell experimental data following the same procedure employed by Christ et al. (2006). Using this procedure, the estimated *A* and *B* parameters for the adjusted correlation were 0.87 and -0.35, respectively. Figure 6.12b shows the comparison between the adjusted mass transfer correlation predictions and measured effluent PCE concentrations as a function of cumulative mass removal. Once adjusted, the upscaled mass transfer correlation of Chirst et al. (2006) was able to capture the dependence of effluent PCE concentrations on the initial GTP ratio, and closely matched measured values obtained in the MID/LO-GTP and LO-GTP experiments. In addition, RMSE values for these experiments were very low (0.064 and 0.032, respectively) and the overall RMSE was significantly better than that of the unmodified correlation (0.144 versus 0.239). However, the correlation was still unable to completely represent the trend observed in the HI-GTP experiment, in which no change in relative effluent concentration was observed until more than 50% of the initial PCE was removed.

Figure 5.12: Comparisons between measured PCE effluent concentrations and predictions based on the mass transfer correlation of Christ et al. (2006), using (a) literature and (b) experimentally-derived fitting parameters. Error bars represent one standard deviation.

Table 5.5: Root mean-square error (RMSE) analysis for mass removal correlations evaluated in this research.

Correlation	RMSE[a]				
	HI-GTP	MID-GTP	MID/LO-GTP	LO-GTP	Overall
Christ et al. (2006) – Literature (A = 1.54, B = -0.27)	0.323	0.326	0.084	0.099	0.239
Christ et al. (2006) – Experimental (A = 0.87, B = -0.35)	0.195	0.200	0.064	0.032	0.144
Parker and Park (2004) (Γ = 1.40)	0.332	0.242	0.063	0.086	0.208
Falta et al. (2005) + GTP[b] (A = 2.30, B = 0.63)	0.149	0.150	0.062	0.075	0.117

a: Root mean-square error
b: Ganglia-to-pool ratio

To demonstrate the benefits of incorporating the source zone DNAPL distribution (i.e., the GTP ratio) into mass transfer correlations, the predictive utility of the correlation developed by Parker and Park (2004) (Equation 5.3) was evaluated.

$$ C^a / C^{a,eq} = 1 - \left(1 - C^{a,t=0} / C^{a,eq} \right)^{\left(M/M^0 \right)^{\Gamma}} \qquad (5.3) $$

Equation 5.3 is similar to the correlation developed by Christ et al. (2006); however, it does not account for DNAPL distribution in the source. Instead, a single fitting parameter (Γ) is employed; a value of 1.40 was suggested by Parker and Park (2004) based on results from numerically simulated mass recovery from PCE-DNAPL source zones. Figure 5.13a shows the comparison of this model to the experimental PCE effluent concentrations as a function of cumulative PCE mass recovery from the source zone. Figure 5.13a demonstrates that estimates based on Equation 5.3 are similar regardless of source zone DNAPL distribution, as was expected since the correlation developed by Parker and Park (2004) does not incorporate this information. In addition,

it is apparent that Equation 5.3 will tend to over-predict effluent concentration reductions for ganglia-dominated DNAPL distributions and under-predict reductions source zones characterized by extensive DNAPL pooling. The relatively poor fit of the Parker and Park correlation was confirmed by RMSE analysis, with RMSE values ranging up to 0.332 (for experiment HI-GTP) and an overall RMSE for all four experiments of 0.208.

Finally, the power-law function employed by Falta et al. (2005) was modified to incorporate the GTP in the exponent term (see Equation 5.4) in order to further evaluate the predictive utility of the GTP ratio.

$$1 - C/C_o = \left(1 - M/M^0\right)^{A \times GTP^B} \qquad (5.4)$$

In this case, the fitting parameters A and B were estimated by fitting the experimental data to Equation 5.4. Using this approach, the respective values for A and B were determined to be 2.30 and 0.63, and the r^2 value for the fit was relatively high (greater than 0.75). Once modified to incorporate GTP, the correlation of Falta et al. (2005) provided reasonable predictions of the measured effluent concentrations as a function of source zone mass reduction, with the predictions most closely matching results from the LO-GTP and MID/LO-GTP experiments (see Figure 5.13b). As with each of the other correlations, however, the predictions were less accurate for the MID- and HI-GTP experiments. Results from RMSE analysis of the modified Falta et al. (2005) correlation were comparable to those observed for the adjusted Christ et al. (2006) correlation (see Table 5.5). This analysis indicates that additional experimental and mathematical modeling work will be required to accurately represent mass flux versus mass removal relationships in ganglia-dominated source zones.
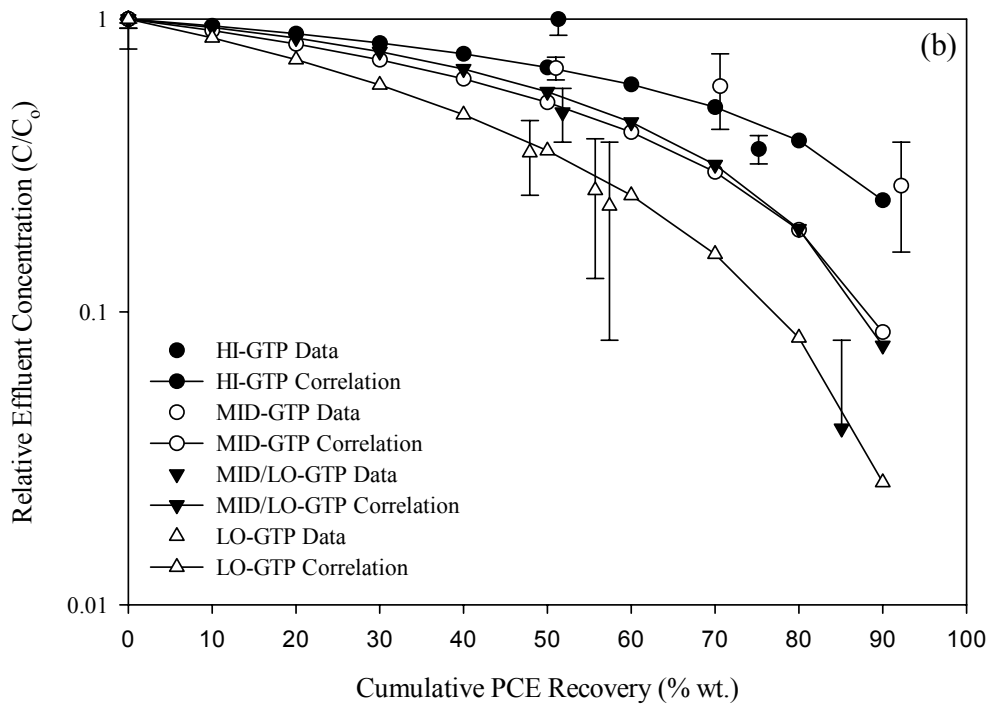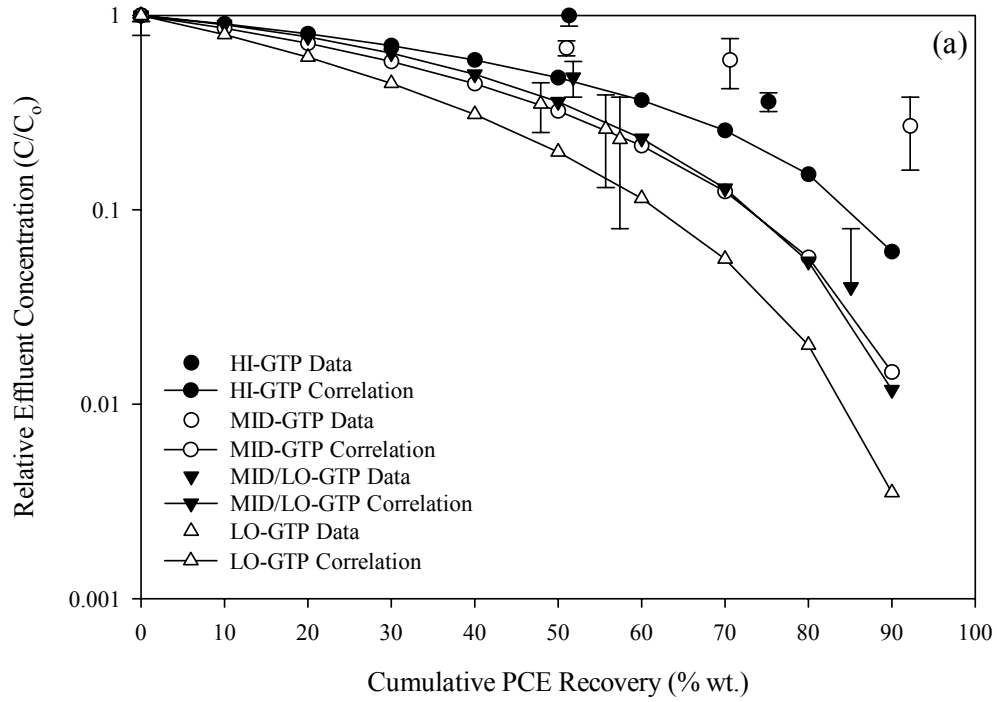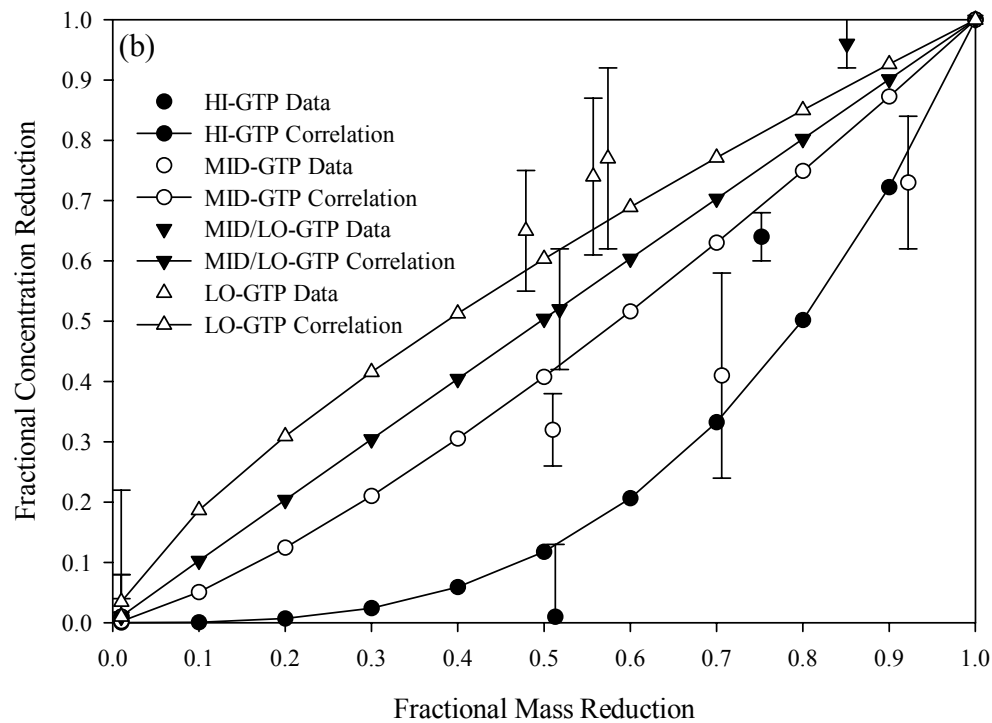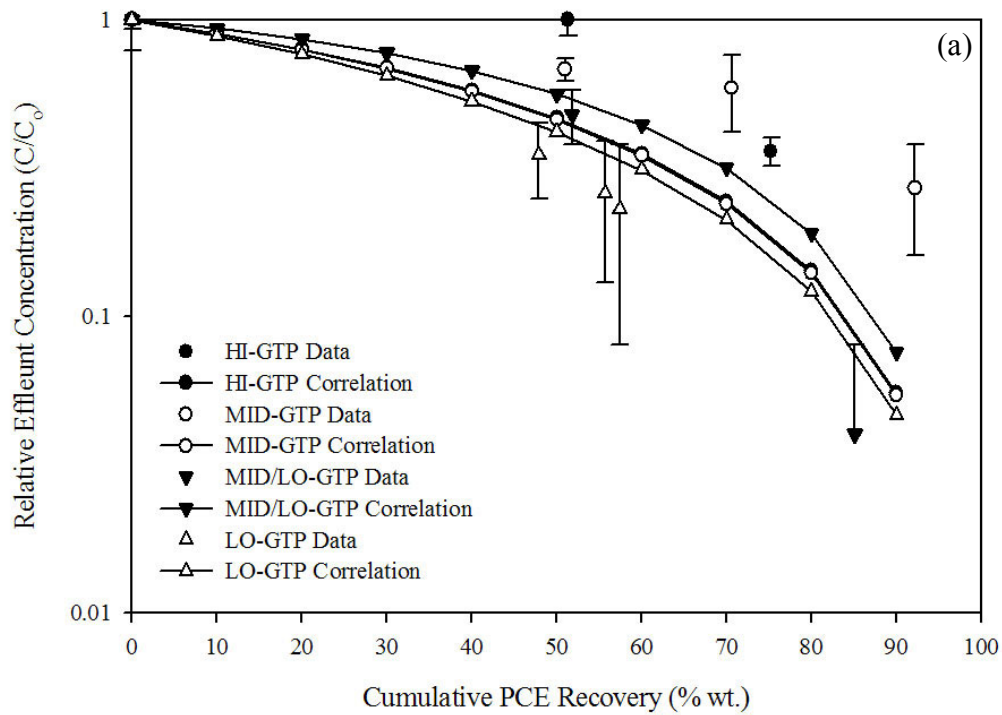
Figure 5.13: Comparisons between measured PCE effluent concentrations and predictions based on the mass transfer correlations of (a) Parker and Park (2004) and (b) Falta et al. (2005), modified to incorporate GTP. Error bars represent one standard deviation.

5.3 Summary and Conclusions

The experimental results presented here represent one of the only comprehensive data sets documenting the effects of partial DNAPL source zone mass removal on down-gradient plume concentrations and mass flux. Light transmission analysis of the PCE-DNAPL source zones allowed for direct quantification of changes in PCE saturation distributions as a function of mass removal. Results from the analysis clearly demonstrate that the initial PCE-DNAPL saturation distribution plays a central role in mass recovery and corresponding reductions in effluent concentration and mass flux. For ganglia-dominated source zones such as experiment HI-GTP, where the ganglia-to-pool ratio (GTP) was greater than 1.0 and over 50% of the initial PCE mass was present as residual DNAPL ganglia, substantial mass removal (greater than 70%) was required prior to observation of reductions in effluent concentration and mass flux. In contrast, for source zones characterized by a large fraction of high-saturation PCE-DNAPL pools (i.e., GTP less than 0.3, or 75% of initial mass present in pools), such as experiment LO-GTP, less mass removal (50%) was necessary to achieve substantial (50-65%) reductions in PCE concentrations and mass flux. Hence, partial DNAPL mass removal from a source zone may be an effective remediation strategy, particularly in situations where there is significant DNAPL pooling within the source. In addition, partial mass removal may be especially attractive in situations where tertiary treatment approaches (e.g., bioaugmentation or biostimulation to achieve reductive dechlorination) or combined remedies can be employed to effectively control subsequent plume development.

CHAPTER 6

CONTAMINANT MASS FLUX FOLLOWING PARTIAL MASS REMOVAL FROM DNAPL SOURCE ZONES: IMPLICATIONS OF RECOVERY MECHANISM

6.1 Introduction

Surfactant enhanced aquifer remediation (SEAR) relies on two primary recovery mechanisms for DNAPL recovery. The first, miscible displacement (i.e., solubilization), is based on an increase in the aqueous solubility of a contaminant in the presence of surfactants resulting from partitioning of the contaminant into surfactant micelles. The DNAPL generally remains relatively stationary within the subsurface during miscible displacement surfactant flushing. The second recovery mechanism, immiscible displacement (i.e., mobilization), relies on a reduction in the interfacial tension (IFT) between the organic (DNAPL) and aqueous phases resulting from accumulation of surfactant molecules at the interface between the two phases. Decreasing the IFT allows entrapped and pooled DNAPL to be released (mobilized) from the subsurface porous media matrix, forming a bank of organic phase contaminant that can be recovered as free product. A potential side effect of this process can be significant DNAPL redistribution within the subsurface. In addition, it should be noted that miscible and immiscible displacement are not mutually exclusive, with many surfactant solutions designed to achieve immiscible displacement resulting in significant DNAPL solubilization.

Numerous laboratory studies have investigated miscible displacement surfactant flushing. Early one-dimensional column experiments (Fountain et al. 1991) investigating

recovery of residual PCE-DNAPL yielded promising results. However, issues such as spontaneous emulsion formation and low overall recovery (approximately 45%) were encountered. Refinements of surfactant formulations have increased contaminant recoveries associated with surfactant-based miscible displacement, with recoveries greater than 80% reported for both one-dimensional column (Pennell et al. 1993) and two-dimensional aquifer cell (Taylor et al. 2001) studies. Recovery efficiencies were somewhat limited, however, due to factors such as rate-limited solubilization (Abriola et al. 1993, 2000), with up to 8 pore volumes of surfactant solution required. Modified flushing strategies such as electrolyte concentration gradients (Sabatini et al. 2000) and addition of alcohols to surfactant formulations (Martel et al. 1998a, 1998b) have further increased DNAPL recovery via solubilization.

One-dimensional column experiments conducted by Dwarakanath et al. (1999) demonstrated that very high (greater than 90%) DNAPL recovery was possible using low-IFT surfactant solutions capable of immiscible contaminant displacement and coupled with high solubilization capacities. Recovery was very efficient in terms of surfactant flushing requirements, with approximately 1.5 pore volumes of the immiscible displacement solutions required to achieve contaminant mass recovery. Significant free product was mobilized, however, indicating potential for uncontrolled DNPAL migration. PCE ass recovery during a subsequent aquifer cell experiment (Ramsburg and Pennell 2001) using a comparable surfactant formulation was approximately 80%, although PCE-DNAPL entry into a previously uncontaminated low permeability confining layer was observed. A number of techniques for mitigating downward DNAPL mobilization have been investigated, including vertical flushing (Longino and Kueper 1995), increasing

density of the aqueous phase through introduction of highly concentrated electrolyte solutions (Miller et al. 2000), and DNAPL density modification through use of a partitioning alcohol (i.e., density modified displacement).

Density modified displacement (DMD) is a subset of immiscible displacement surfactant flushing, where an alcohol cosolvent preflood is first used as a chemical means for reducing NAPL density *in situ* without organic phase mobilization. After conversion from a dense NAPL to a neutrally buoyant or light NAPL, a low interfacial tension surfactant flood is subsequently employed to mobilize the organic phase. Ramsburg and coworkers (2004a) evaluated PCE recovery via DMD using an aqueous 1-butanol preflood formulation in a two-dimensional aquifer cell. Recovery was high (greater than 90%), with successful DNAPL to LNAPL conversion. Significant volumes of alcohol flushing were required for PCE density conversion (6.5 pre volumes of 6% 1-butanol preflood solution), however, limiting the attractiveness of DMD when compared to other flushing technologies. To lower the preflood solution requirements, Ramsburg et al. (2004a) evaluated a surfactant-stabilized emulsion for 1-butanol delivery to PCE-DNAPL. A macroemulsion of 4.7% (vol.) Tween 80 + 1.3% (vol.) Span 80 + 15% (vol.) 1-butanol was able to successfully convert PCE from DNAPL to LNAPL. PCE recovery was high, with a large fraction of contaminant removal occurring via solubilization during the emulsion preflood. The required preflood volume was also greatly reduced, with 1.2 pore volumes of the emulsion required to convert PCE to an LNAPL.

All of the surfactant-based recovery mechanisms described above, if properly designed and implemented, are capable of removing significant fractions of DNAPL mass from a contaminated source zone. However, questions remain regarding post-

treatment plume development and contaminant mass flux following surfactant flushing. Previous research efforts have focused on the impacts of partial source zone mass removal on subsequent down-gradient plume development; however, contaminant recovery has been achieved either through water flushing or miscible displacement (solubilization) surfactant flushing. These cases are characterized by DNAPL distributions that remain relatively stationary within the source zone, and correspondingly few experiments evaluating post-treatment contaminant concentrations have been conducted using other DNAPL recovery mechanisms (e.g., mobilization or density modified displacement). The objective of this study was to conduct laboratory-scale experiments to evaluate the impact of contaminant recovery mechanism on post-treatment dissolved-phase contaminant concentrations and mass flux. Experimental results are presented visually to demonstrate the differing recovery mechanisms during surfactant flushing. Contaminant concentrations in the aquifer cell effluent were monitored throughout the experiments, with the results used to estimate overall mass recovery and post-treatment effluent concentrations. Experimental results were compared, both in terms of contaminant recovery efficiency and effluent concentration reductions, to results from solubilization-based DNAPL recovery (i.e., Chapter 5 results).

6.2 Results and Discussion

Following investigation of PCE mass flux following partial source zone mass removal via miscible displacement (i.e., solubilization; see Chapter 5 of this work), a series of three two-dimensional aquifer cell experiments were conducted to evaluate mass flux of PCE following source zone treatment via either immiscible displacement (i.e., mobilization) or density modified displacement (DMD). Experiments were conducted in

the small aquifer cell described in Chapter 3, with each cell using Federal Fine Ottawa sand as the background porous media to produce ganglia-dominated (HI-GTP) DNAPL distributions. Following water flushing to establish initial steady-state PCE effluent concentrations, cells AMA4-HI and AMA8-HI assessed contaminant mass flux from a PCE-DNAPL source zone following flushing with a surfactant formulation containing either 4% (wt.) or 8% (wt.) Aerosol MA and designed to mobilize the organic phase. Mass flux following density modified displacement of a PCE-DNAPL was evaluated during experiment DMD-HI.

6.2.1 Surfactant Solution Properties

The surfactant solution used for the immiscible displacement experiment AMA4-HI was comprised of 4% (wt.) Aerosol MA + 8% (wt.) 2-Propanol + 6 g/L NaCl. The surfactant solution used in AMA4-HI was similar to the Aerosol MA formulation used in Chapter 4 that demonstrated significant (greater than 80%) mass recovery from a TCE-DNAPL when the aqueous flow rate of the solution was maintained at a nominal value of 10 mL/min. Relevant parameters of the solution are summarized in Table 6.1. Density and viscosity of the 4% Aerosol MA solution were 0.994 ± 0.001 g/ cm^3 and 1.64 ± 0.02 cP respectively, representing limited deviations from the properties of water. As such, density override of the surfactant solution was not expected and the theoretical head loss across the aquifer cell at operating conditions was relatively low (2.88 cm). Equilibrium PCE solubility in the 4% Aerosol MA surfactant formulation was $15,300\pm100$ mg/L, which is significantly greater than aqueous PCE solubility (200 mg/L) but a relatively moderate increase compared to many surfactant formulations. Based on the equilibrium PCE solubility, the solubilization parameter (S) of the 4% Aerosol MA formulation was

184

estimated to be 0.377 mL PCE/mL Aerosol MA. The interfacial tension (IFT) between

PCE and the 4% Aerosol MA solutions was estimated using the Chun-Huh equation (Huh

1979, Equation 6.1) to be 2.1 dyne/cm, a moderately high value.

$$\gamma = 0.3/S^2 \qquad (6.1)$$

The relatively large IFT suggests that the total trapping number (N_T) within the aquifer

cell during flushing with 4% Aerosol MA formulation may not be reduced to the below

the critical value for complete NAPL displacement ($1x10^{-4}$) as reported by Pennell et al.

(1996), but may instead reside within the transition region where partial displacement

may be expected.

Table 6.1: Properties of flushing solutions used in aquifer cell experiments at 22ºC.

Surfactant Solution	Density (g/cm^3)	Viscosity (cP)	Interfacial Tension with PCE (dyne/cm)
Water	0.997	1.00	47.0
4% (wt.) Aerosol MA + 8% (wt.) 2-Propanol + 6 g/L NaCl	0.994±0.001[a]	1.64±0.02	2.1 (Est.)
8% (wt.) Aerosol MA + 8% (wt.) 2-Propanol + 15 g/L NaCl + 1 g/L CaCl$_2$	1.009±0.001[b]	2.47[b]	0.160±0.004[b]
4.7% (wt.) Tween 80 + 1.3% (wt.) Span 80 + 15% 1-Butanol	0.979±0.001[c]	2.52±0.05[c]	n/a
10% (wt.) Aerosol MA + 6% (wt.) 1-Butanol + 15 g/L NaCl + 1 g/L CaCl$_2$	1.015±0.001[c]	2.99±0.06[c]	0.13±0.01[d]

a: Standard deviation
b: Ramsburg and Pennell 2001
c: Ramsburg et al. 2003
d: Ramsburg 2002

A second Aerosol MA surfactant solution, designed to more completely displace

the PCE-DNAPL, was used during experiment AMA8-HI. The solution was developed

by Ramsburg and Pennell (2001) and was comprised of 8% (wt.) Aerosol MA + 8% (wt.)

2-Propanol + 15 g/L NaCl + 1 g/L CaCl$_2$. Density and viscosity of the 8% AMA solution were both somewhat higher than the values reported for the 4% solution (see Table 6.1), but not so large as to cause excessive head drop across the aquifer cell at the 10 mL/min flow rate employed. The IFT between the 8% surfactant solution and PCE was very low, approximately 0.16 dyne/cm, sufficient to reduce the total trapping number (N_T) of the aquifer cell to below the critical value for displacement of 1×10^{-4} reported by Pennell et al. (1996), and indicating that immiscible DNAPL displacement during flushing with the 8% Aerosol MA solution was likely. In addition, equilibrium PCE solubility in the 8% Aerosol MA surfactant formulation was reported by Ramsburg and Pennell (2001) to be high, 76,400±2400 mg/L. Such a large increase in equilibrium solubility indicates that in addition to DNAPL mass recovery via immiscible displacement, significant solubilization of contaminant the PCE-DNAPL during surfactant flushing may be expected.

The relatively low aqueous solubility (74,500 mg/L) of 1-butanol, the partitioning alcohol selected for use in the preflood phase of DMD, necessitates that the volume of preflood solution injected into the source zone be large. For example, Ramsburg et al. (2004a) reported that 6.4 pore volumes of a 6% (wt.) aqueous solution of 1-butanol was required to convert TCE from DNAPL to LNAPL, and even larger volumes would be required for PCE conversion. As such, the density modified displacement approach has been refined in an effort to increase the volume of 1-butanol that can be delivered to the subsurface while retaining favorable conditions for alcohol partitioning into the NAPL. Kibbey and collaborators (2002) investigated the use of micellar surfactant solutions to increase the mass of 1-butanol delivery. This approach reduced 1-butanol partitioning into the NAPL, requiring an increase in the aqueous 1-butanol concentration to achieved

desired 1-butanol concentrations in TCE- and PCE-DNAPL. Since this behavior limits the usefulness of micellar solutions (i.e., microemulsions), it was hypothesized that a properly designed macroemulsion could be used to deliver 1-butanol to the subsurface.

Based on this hypothesis, Ramsburg (2002) and Ramsburg et al. (2003) developed a surfactant-stabilized macroemulsion comprised of 4.7% (wt.) Tween 80 + 1.3% (wt.) Span 80 + 15% 1-butanol. Tween 80 and Span 80 were selected based on preliminary data indicating synergistic effects resulting in macroemulsion stability on the order of hours. The emulsion density was comparable to water 0.979 ± 0.001 g/cm^3 (Ramsburg 2002, see Table 6.1). More importantly, the viscosity of the emulsion at 22ºC was not significantly greater than that of water and the IFT reduction between the organic phase (in this case PCE) and the emulsion was moderate. Due to the moderate IFT reductions, total trapping number analysis conducted by Ramsburg et al. (2003) indicated that significant DNAPL mobilization during the emulsion preflood was not expected.

Following the emulsion preflood, the density-converted LNAPL was recovered using a low-IFT displacement solution that was developed by Ramsburg et al. (2003) and comprised of 10% (wt.) Aerosol MA + 6% (wt.) 1-butanol + 15 g/L NaCl + 1 g/L CaCl$_2$. Aerosol MA selected for use in the displacement solution based on previous experimental results demonstrating its ability to immiscibly displace NAPL (see e.g., Pennell et al. 1996, Loverde et al. 1997, Dwarakanath et al. 1999, Ramsburg and Pennell 2001). Salts were added to the displacement solution in order to destabilize the emulsion preflood to prevent NAPL occlusion from bulk flow (Fountain et al. 1991), increase the density of the displacement solution, and further decrease the IFT between the NAPL and the aqueous phase. Alcohol addition (in the form of 1-butanol) to the solution promoted

system transition from Winsor Type I (oil in water microemulsion) to Winsor Type II (water in oil microemulsion) (Winsor 1954), resulting in surfactant (along with water and alcohol) partitioning into the NAPL and facilitating density conversion (Ramsburg et al. 2002a). Physical properties of the displacement solution are summarized in Table 6.1.

6.2.2 Aquifer Cell Experimental Conditions

The three aquifer cells were packed with Federal Fine Ottawa sand, a relatively fine sand having a d_{50} value of 0.280 mm. The grain size Federal Fine is small enough to preclude the light transmission analysis conducted in Chapters 4 and 5. Based on visual observation of the DNAPL distributions at the face of the aquifer cell (see Figure 6.1) it is clear that the majority of organic liquid was entrapped as DNAPL ganglia within the Federal Fine sand, implying that the ganglia-to-pool (GTP) ratio of the aquifer cells was relatively large (i.e., greater than 1.5). The first experiment, AMA4-HI, was designed to assess post-treatment contaminant mass flux following treatment of a PCE-DNAPL by mobilization with a surfactant formulation containing 4% Aerosol MA. The aquifer cell pore volume during AMA4-HI was 1,350 mL, with an overall intrinsic permeability of 5.37×10^{-11} m^2. Following NAPL injection and redistribution, a total of 28.4 mL of PCE, corresponding to an overall DNAPL saturation of 2.1%, were initially present in the aquifer cell. A representative photograph of the initial PCE-DNAPL distribution for experiment AMA4-HI is shown in Figure 6.1a. A second, similar experiment (AMA8-HI) was conducted to evaluate contaminant mass flux following treatment with an Aerosol MA formulation containing a higher surfactant loading, in this case 8%. The experiment was characterized by an aquifer cell pore volume of 1,290 mL and an intrinsic permeability of 7.89×10^{-11} m^2. Approximately 39.9 mL of PCE were injected

into the aquifer cell, yielding an overall DNAPL saturation of 3.1%, and initial the PCE-DNAPL distribution shown in Figure 6.1b. Relevant experimental conditions during aquifer cell experiments AMA4-HI and AMA8-HI are summarized in Table 6.2.
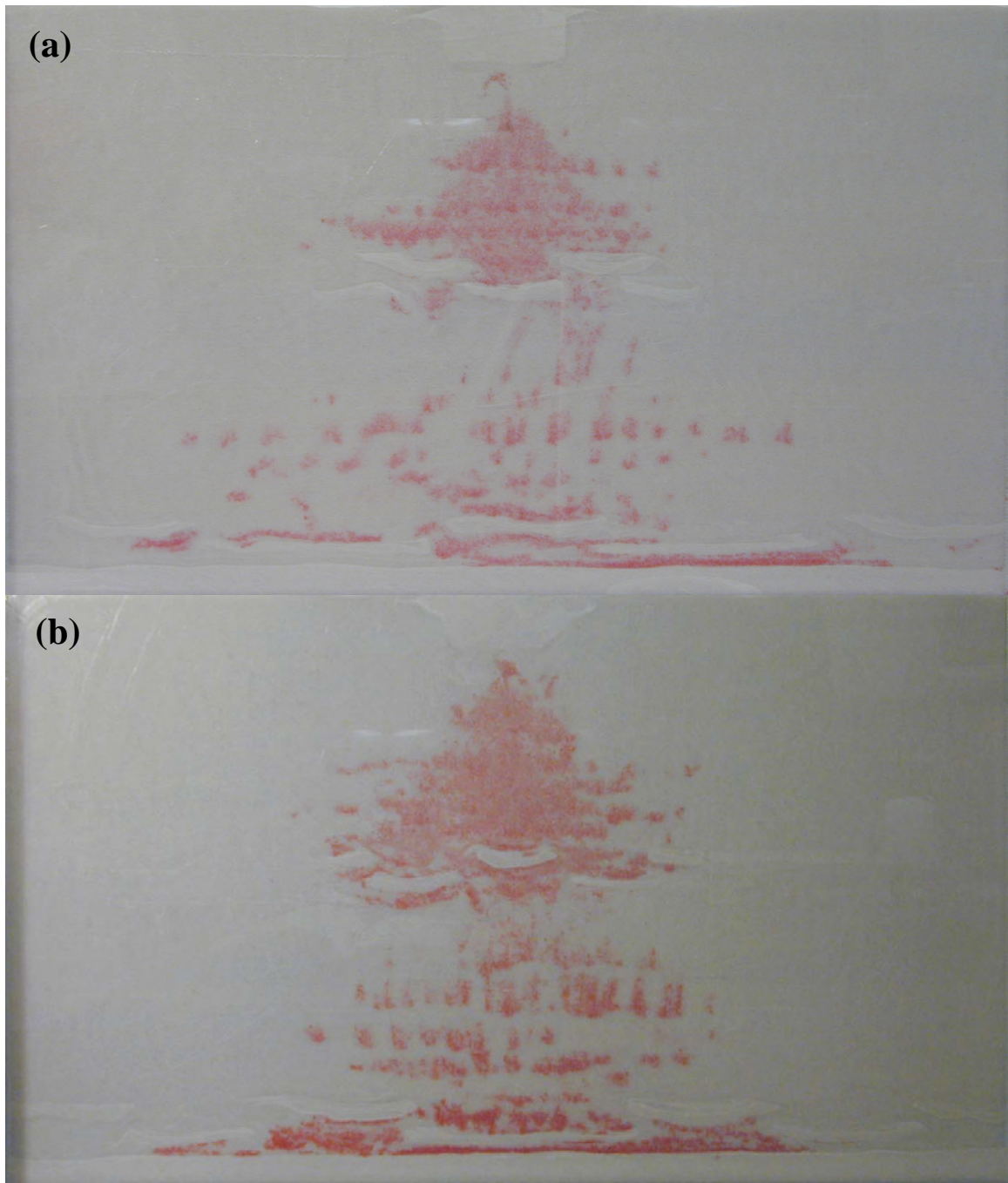
Figure 6.1: Photographs of initial PCE-DNAPL saturation distributions in (a) AMA4-HI and (b) AMA8-HI aquifer cells.

Table 6.2: Summary of initial 2-D aquifer cell experimental conditions.

Aquifer Cell Parameter	AMA4-HI	AMA8-HI	DMD-HI
Overall Pore Volume (mL)	1,350	1,290	1,280
Intrinsic Permeability (m^2)	5.37x10^{-11}	7.89x10^{-11}	1.32x10^{-10}
NAPL Injection Volume (mL)	28.4	39.9	31.2
Overall DNAPL Saturation (%)	2.1	3.1	2.4
Density Modification Flood			
Flow Rate (mL/min)	n/a	n/a	3.65±0.25[a]
Darcy Velocity (mm/min)	n/a	n/a	0.69±0.05
Flood Volume (mL)	n/a	n/a	1,510
Displacement Flood			
Flow Rate (mL/min)	9.86±0.48	9.38±0.57	3.74±0.20
Darcy Velocity (mm/min)	1.85±0.09	1.76±0.11	0.70±0.04
Flood Volume (mL)	1,600	1,540	1,370

a: Standard deviation

In addition to the experiments evaluating post-treatment mass flux from a PCE-DNAPL source zone following treatment via immiscible displacement, a third experiment (DMD-HI) was conducted to evaluate mass flux at the conclusion of density modified displacement. The pore volume of the aquifer cell during DMD-HI was 1,280 mL and the intrinsic permeability 1.32x10^{-10} m^2 (see Table 6.2). A total of 31.2 mL of PCE-DNAPL (2.4% overall DNAPL saturation) were initially present in the cell, with the initial PCE-DNAPL distribution shown in Figure 6.2.

Figure 6.2: Photograph of initial PCE-DNAPL saturation distribution in DMD-HI aquifer cell.

Operational conditions during both immiscible displacement experiments (i.e., AMA4-HI and AMA8-HI) were comparable. During each Aerosol MA experiment, approximately 1.2 pore volumes of either the 4% (wt.) or 8% (wt.) Aerosol MA surfactant solution were flushed through the aquifer cells at a nominal flow rate of 10 mL/min. The actual respective values are summarized in Table 6.2 and were 1,600 mL (1.19 pore volumes) at 9.86±0.48 mL/min for AMA4-HI and 1,540 mL (1.19 pore volumes) at 9.38±0.57 mL/min for AMA8-HI. The density modified displacement experiment (DMD-HI) was comprised of an approximate 1.2 pore volume flood of emulsion preflood (4.7% (wt.) Tween 80 + 1.3% (wt.) Span 80 + 15% 1-butanol) followed by 1.2 pore volumes of a low-IFT displacement flood (10% (wt.) Aerosol MA + 6% (wt.) 1-butanol + 15 g/L NaCl + 1 g/L CaCl$_2$). Both floods were conducted at a nominal flow rate of 4 mL/min. For DMD-HI, the actual flood volumes and flow rates

were 1,510 mL (1.18 pore volumes) at 3.65±0.25 mL/min and 1,370 mL (1.07 pore volumes) at 3.70±0.20 mL/min for the emulsion and displacement floods, respectively.

6.2.3 Contaminant Mass Recovery

Following PCE-DNAPL imbibition and water flushing through the aquifer cell to establish initial steady-state plume conditions, the cells were flushed with surfactant solution to achieve contaminant recovery via either immiscible displacement without density modification or density modified displacement. During surfactant flushing, PCE-NAPL displacement behavior within the aquifer cells was observed and the effluent PCE concentration was measured, along with (in the case of experiment DMD-HI) 1-butanol concentration and effluent density. Effluent PCE concentrations were used to construct contaminant mass recovery curves. Surfactant flushing results for each of the three aquifer cell experiments are presented in individual subsections below.

6.2.3.1 Immiscible Displacement with 4% Aerosol MA Surfactant Formulation

A total of 1,600 mL (1.2 pore volumes) of 4% Aerosol MA + 8% 2-propanol + 6 g/L NaCl were flushed through aquifer cell AMA4-HI at a nominal flow rate of 10 mL/min. The PCE-DNAPL source zone is shown in Figure 6.3 following (a) 740 mL (0.55 pore volumes) and (b) 1,330 mL (0.99 pore volumes) of surfactant flushing, respectively. During flushing, the low-IFT displacement solution was dyed blue-green in color to allow for visualization of the aqueous-phase flow front. Some migration of PCE-DNAPL was observed during AMA4-HI, particularly within the lower regions of the aquifer cell where a bank of free organic product was present directly above the lower confining layer and migrated horizontally through the box. However, when comparing

Figures 6.1a and 6.3b, it is clear that a majority of the PCE-DNAPL ganglia with the source zone, representing a significant fraction of the organic mass, were not mobilized by the 4% Aerosol MA surfactant formulation.

In an effort to better understand this result, a total trapping number analysis was conducted on experiment AMA4-HI (see Table 6.3). The capillary and Bond numbers for AMA4-HI were calculated to be 2.40×10^{-5} and 1.47×10^{-4} respectively. Assuming horizontal aqueous flow, the resulting total trapping number (N_T) was determined to be 1.49×10^{-4}, above the critical N_T value described by Pennell et al. (1996) at which NAPL displacement begins to occur, but within the region where partial displacement may be expected. Given that the trapping number for AMA4-HI falls within this region, it could be expected that actual NAPL displacement within the aquifer cell would be controlled by factors such as local PCE-DNAPL saturation, with regions with locally high saturation (i.e., NAPL pools) being displaced and NAPL ganglia at residual saturation remaining stationary. This was in fact observed during AMA4-HI, as is clear when examining the PCE-DNAPL distributions in Figures 6.3a and 6.3b. The entry pressure (in units of NAPL height) for pooled NAPL over F70 sand was estimated using the empirical correlation developed by McWhorter and Nelson (1979, Equation 6.2) to be 15.9 cm, significantly greater than the actually pooled NAPL height observed during the experiment.

$$Z_n = 9.6 \left(\frac{\rho_w}{\rho_n - \rho_w} \right) \left(\frac{\gamma}{\gamma_{aw}} \right) \left(\frac{K}{n} \right)^{-0.403} \qquad (6.2)$$

Based on Equation 6.2, a PCE-surfactant solution IFT of 0.72 dyne/cm (much less than that estimated for the 4% Aerosol MA solution) would be required to reduce the entry pressure to less than 1 cm, or approximately the PCE-DNAPL pool height observed in

AMA4-HI just above the lower confining layer. The dimensionless bank number (Willson et al. 1999) and angle of NAPL displacement relative to the x-axis (τ) during AMA4-HI were determined to be 0.16 and 80.8° respectively, both implying that NAPL migration was dominated by vertical rather than horizontal flow. This was consistent with observed experimental results, where little horizontal PCE-DNAPL movement was seen prior to its reaching the lower confining layer of the aquifer cell.

Effluent PCE concentrations during AMA4-HI as a function of the total pore volumes flushed through the aquifer cell are shown in Figure 6.4. PCE concentrations rapidly increased following approximately 1 pore volume of flushing, coinciding with breakthrough of the dyed surfactant solution, as was expected due to the fact that the surfactant solution did not significantly sorb to the aquifer cell porous media (see Chapter 4). After 1.1 pore volumes of flushing the effluent PCE concentration reached a value of approximately 7,500 mg/L, where it remained for an addition 0.7 pore volumes of flushing before decreasing over the remainder of the surfactant flood as water was flushed through the aquifer cell to recovery the resident Aerosol MA formulation. The observed concentration of 7,500 mg/L is much lower than the equilibrium PCE solubility in the 4% Aerosol MA formulation (15,300±100), but remains significantly larger than PCE solubility in water (200 mg/L). A slight increase in effluent PCE concentration (to 8,500 mg/L) was observed following 1.4 pore volumes of flushing and was attributed to solubilization of free-phase PCE-DNAPL that had accumulated within the aquifer cell end chamber.
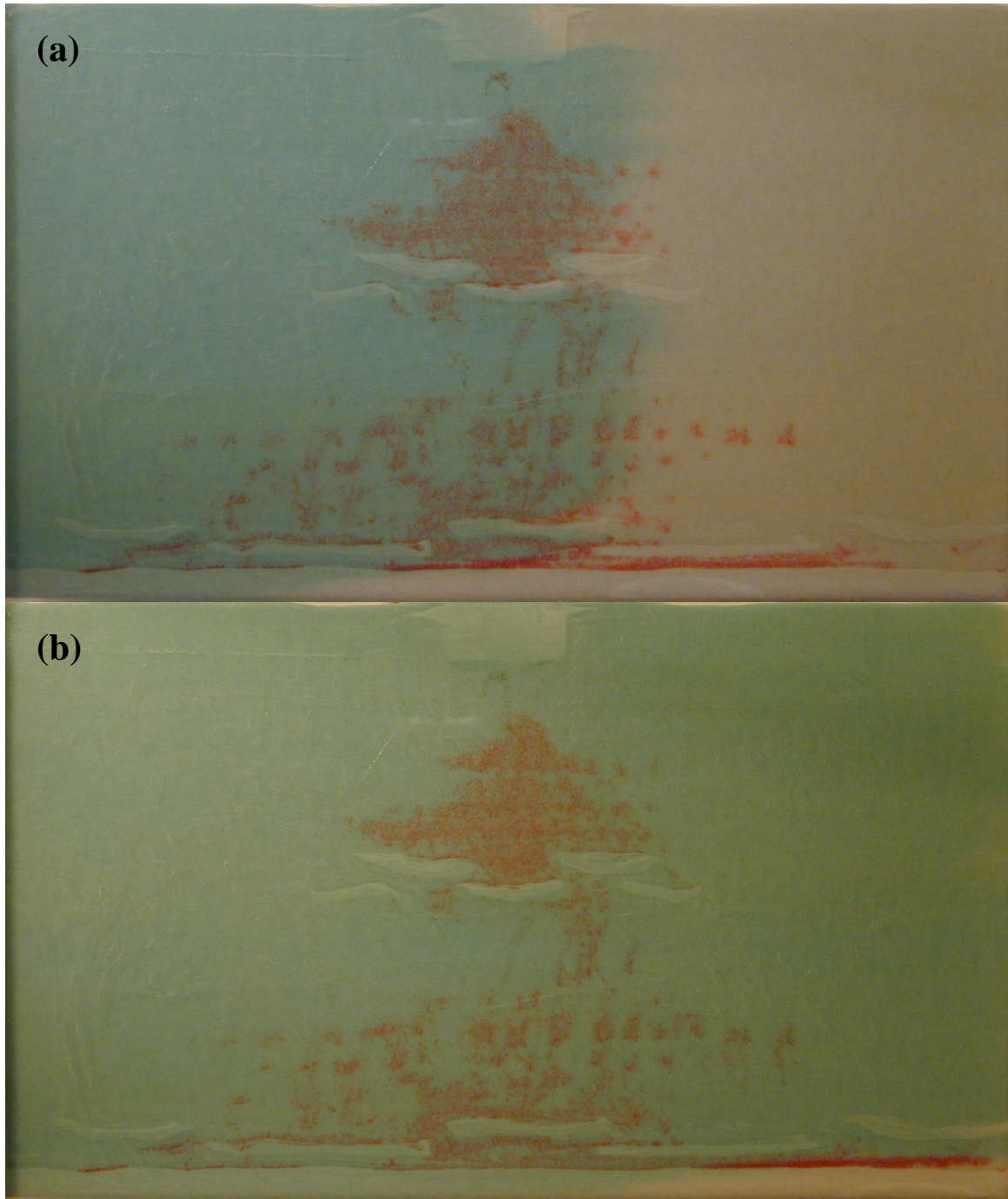
Figure 6.3: Photographs of AMA4-HI source zone following (a) 740 mL (0.55 pore volumes) and (b) 1,330 mL (0.99 pore volumes) of flushing with the 4% Aerosol MA surfactant formulation.
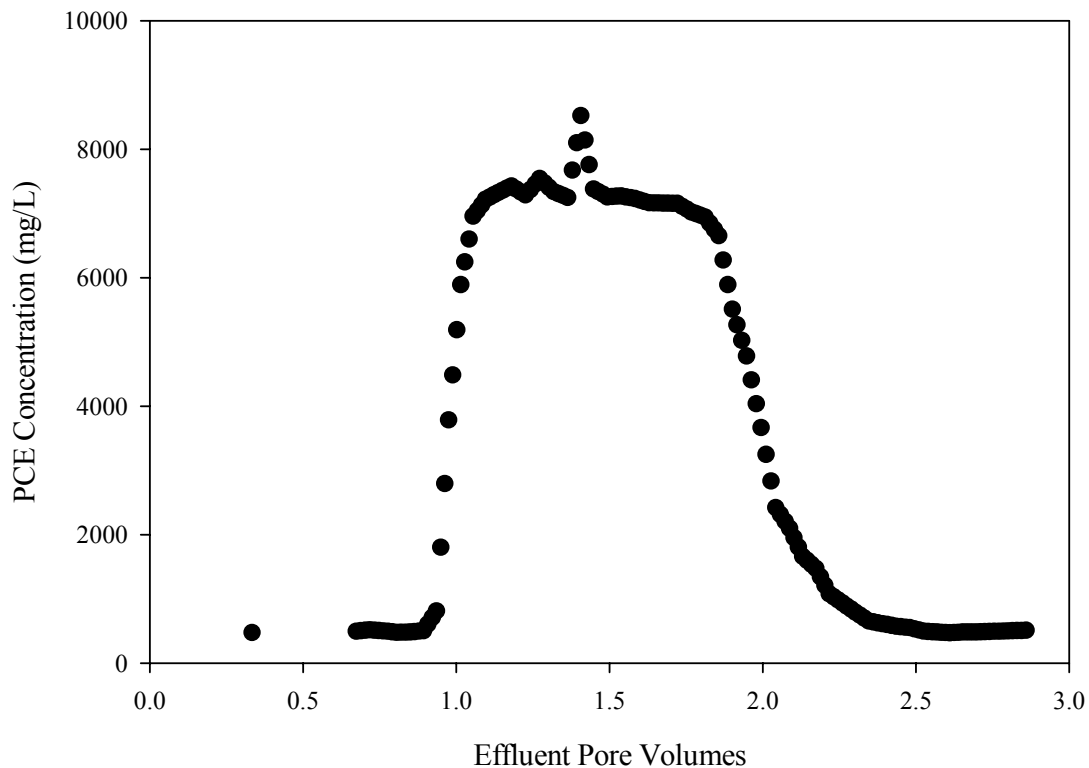
Figure 6.4: Effluent aqueous phase PCE concentrations measured during AMA4-HI.

Cumulative PCE mass recovery as a function of the pore volume of solution flushed through the aquifer cell during AMA4-HI is shown in Figure 6.5. Overall PCE recovery during this experiment was relatively low, 49.0%, as summarized in Table 6.3. The low mass recovery was attributed to a combination of two factors: the relatively low equilibrium solubility of PCE in the 4% Aerosol MA surfactant formulation (15,300±100) and incomplete mobilization of the PCE-DNAPL by the surfactant solution. Two large gaps can be seen in the PCE mass recovery curve of AMA4-HI, corresponding to recovery of PCE-DNAPL from the end chamber of the aquifer cell following 1.26 and 1.38 pore volumes of flushing, respectively. Approximately 6.9 mL (24.4%) of the PCE initially present in the aquifer cell was recovered in the aqueous

efflent.   PCE-DNAPL recovery during AMA4-HI was significant, accounting for remaining 7.0 mL (24.6%) of PCE removed from the source zone and implying that by modifying Aerosol MA formulation to achieve more complete DNAPL mobilization higher mass recoveries may be attainable.
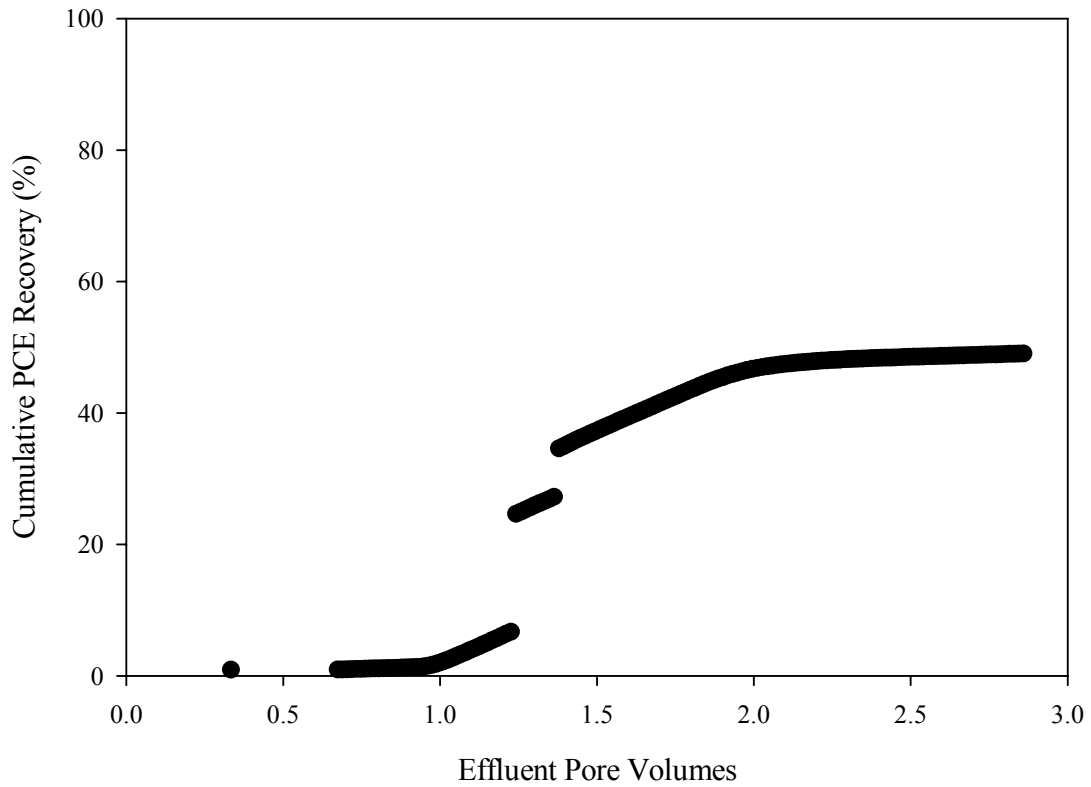
Figure 6.5: Cumulative PCE mass recovery curve for experiment AMA4-HI.

Table 6.3: Mass recovery and trapping number analysis for 2-D aquifer cell experiments.

Aquifer Cell Parameter	AMA4-HI	AMA8-HI	DMD-HI
PCE Mass Recovery			
PCE Injection Volume (mL)	28.4	39.9	31.2
Total PCE Recovered (mL) [%]	13.9 [49.0]	31.8 [79.7]	27.0 [86.4]
PCE Recovered as NAPL (mL) [%]	7.0 [24.6]	10.0 [25.0]	4.0 [12.8]
PCE Recovered in Emulsion Preflood (mL) [%]	n/a	n/a	18.8 [60.1]
PCE Recovered in Displacement Solution (mL) [%]	6.9 [24.4]	21.8 [54.7]	4.2 [13.6]
PCE Recovery Efficiency (g/g)	0.35	0.41	0.19
Post-Flushing C/C_0	0.73 ± 0.07^a	0.15 ± 0.07	0.22 ± 0.06
Trapping Number Analysis			
Capillary Number (N_{Ca})	2.40×10^{-5}	4.53×10^{-4}	n/a
Bond Number (N_B)	2.70×10^{-5}	2.79×10^{-3}	n/a
Total Trapping Number (N_T)	2.74×10^{-5}	2.83×10^{-3}	n/a
Bank Number (N_{Ba})	0.16	0.16	n/a
Angle of Displacmenet (τ)	80.8°	80.8°	n/a

a: Standard deviation

6.2.3.2 Immiscible Displacement with 8% Aerosol MA Surfactant Formulation

During experiment AMA8-HI, 1,540 mL (approximately 1.2 pore volumes) of an 8% Aerosol MA + 8% 2-propanol + 16 g/L NaCl + 1 g/L CaCl₂ surfactant formulation were introduced into the aquifer cell at a nominal flow rate of 10 mL/min. IFT between PCE and the surfactant formulation was low (0.16 dyne/cm), facilitating efficient immiscible displacement of the PCE-DNAPL. Representative photographs of the PCE-DNAPL source zone following (a) 560 mL (0.43 pore volumes) and (b) 1130 mL (0.87 pore volumes) of flushing with the 8% Aerosol MA surfactant formulation (dyed blue-green for visualization purposes) are shown in Figure 6.6. Nearly complete PCE-DNAPL mobilization was observed during AMA8-HI, especially in the lower regions of the cell that were characterized by higher organic saturations. Mobilization in the upper regions of the cell where PCE saturation was near residual was less pronounced, although by the

conclusion of surfactant flushing PCE had been completely removed from the upper regions of the cell. It is unclear how much of this removal was due to solubilization by the surfactant formulation, rather than low-IFT displacement into the lower regions of the cell. In general, PCE-DNAPL mobilization was much more efficient and complete when the 8% Aerosol MA formulation was employed, compared to the 4% formulation.

The total trapping number for experiment AMA8-HI was calculated using the method described by Pennell et al. (1996) (Table 6.3). The respective Bond and capillary numbers for AMA8-HI were 2.79×10^{-3} and 4.53×10^{-4}, resulting in a total trapping number (N_T) of 2.83×10^{-3} for horizontal aqueous phase flow. This value falls within N_T range describing complete organic phase mobilization, the outcome observed during AMA8-HI, where PCE-DNAPL formed of a bank of free organic along the bottom of the aquifer cell, traveling horizontally through the aquifer cell. The dimensionless bank number (Willson et al. 1999) and angle of NAPL displacement relative to the x-axis (τ) were estimated to quantify bank formation during AMA8-HI. The respective values were 0.16 and 80.8°, indicating that NAPL migration occurred primarily in the vertical direction, excepting horizontal displacement along the bottom of the aquifer cell. In addition, the bank number and τ for AMA4-HI and AMA8-HI were nearly identical (Table 6.3), implying that, although reducing the interfacial tension of a surfactant formulation may result in more complete DNAPL displacement, it will not alter the directionality of displacement. Changing the direction of NAPL migration will require altering of other surfactant flushing design parameters, including aqueous-phase flow rate and viscosity. Experiment AMA8-HI was also characterized by extensive PCE-DNAPL penetration into the lower confining layer of F-70 sand (Figure 6.6), consistent with entry pressure

calculations for pooled NAPL over F-70 Ottawa sand. Using the empirical correlation developed by McWhorter and Nelson (1979, see Equation 6.2), an entry pressure of 0.22 cm was estimated, lower than the height of pooled NAPL observed during AMA8-HI. NAPL penetration into previously unconfined aquifer regions can therefore be expected during flushing with surfactant formulations characterized by ultra-low IFT values, and care must be taken during remedial design to account for this possibility.

Effluent PCE concentrations during experiment AMA8-HI are shown in Figure 6.7 as a function of total pore volumes flushed through the aquifer cell. As with AMA4-HI (see Figure 6.4), a rapid increase in PCE concentration was observed to coincide with approximately 1 pore volume of flushing, attributed to the absence of significant surfactant sorption within the aquifer cell. PCE reached a maximum effluent concentration of just over 41,000 mg/L at pore volume 1.18. While this value is lower than equilibrium solubility of PCE in the 8% Aerosol MA surfactant formulation (76,400±2400 mg/L), it is nonetheless several orders-of-magnitude greater than aqueous PCE solubility. The large observed PCE concentrations were consistent with the observed PCE-DNAPL solubilization occurring in the AMA8-HI aquifer cell, particularly within the upper regions of the cell. In addition, effluent PCE concentrations were much greater during AMA8-HI compared to AMA4-HI, a difference due almost entirely to differences in surfactant formulations, highlighting the importance of careful flushing solution optimization. PCE behavior during AMA8-HI differed somewhat from that of AMA4-HI, with concentrations maintained near maximum values for a shorter period of flushing and a longer tail observation during flushing with water to recover the Aerosol MA solution (pore volumes 1.2-2.8). These were attributed to differences in PCE-
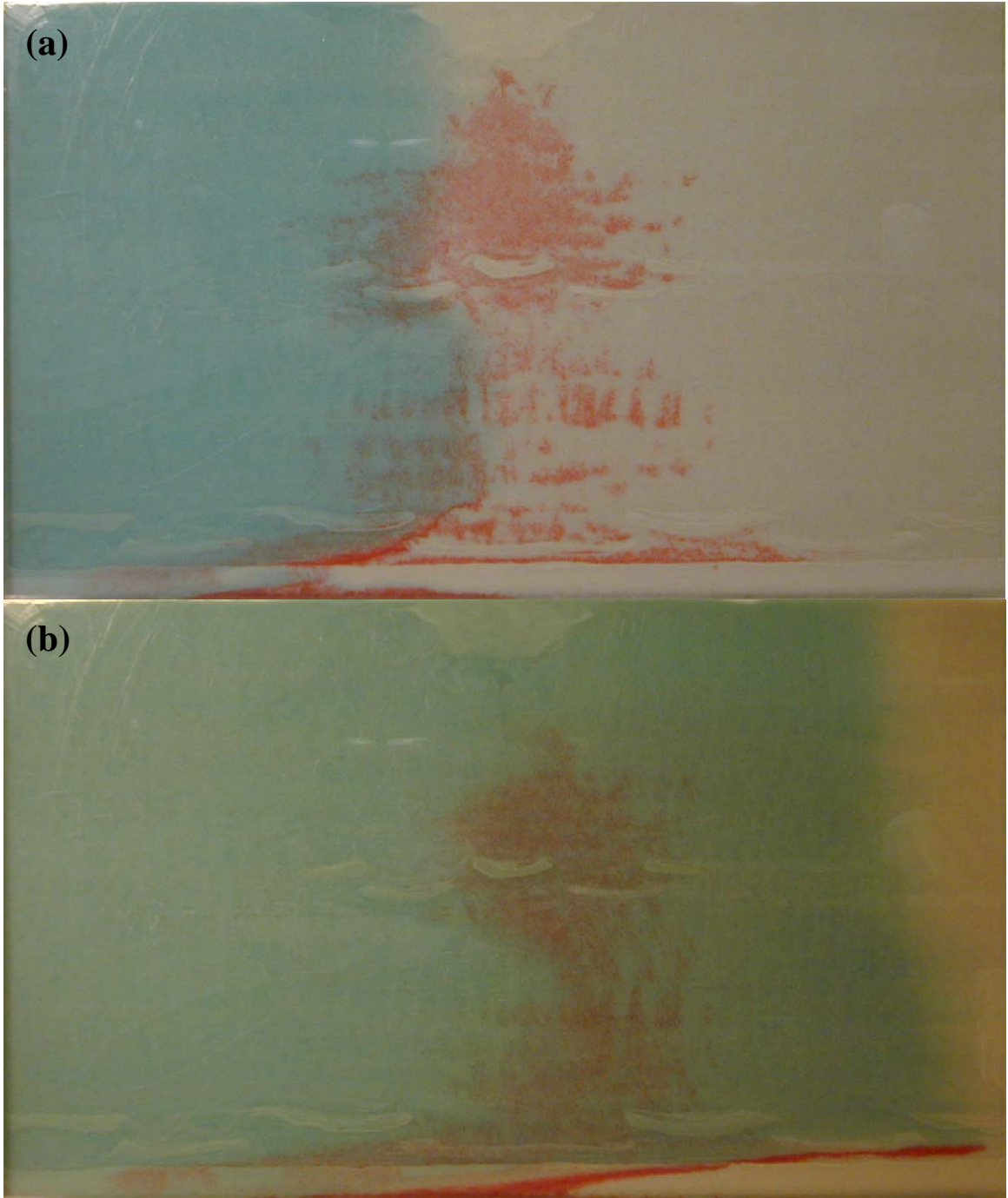
Figure 6.6: Photographs of AMA8-HI source zone following (a) 560 mL (0.43 pore volumes) and (b) 1130 mL (0.87 pore volumes) of flushing with the 8% Aerosol MA surfactant formulation.

DNAPL mobilization observed during the two experiments. For AMA4-HI, regions of residual DNAPL ganglia remained present due to incomplete mobilization; the ganglia were characterized by high specific surface areas, allowing for efficient mass transfer from the organic to aqueous phase, maintaining effluent concentrations near the maximum value. Conversely, the more complete mobilization that occurred during AMA8-HI resulted in loss of DNAPL ganglia and formation of a single large pool located at the bottom of the aquifer cell. The resulting loss in specific surface area resulted in a loss in solubilization efficiency, lowering the observed effluent PCE concentrations. PCE concentration rebounded to approximately 10,000 mg/L at pore volume 2.5 due to presence of small amounts of DNAPL in the aqueous samples and solubilization of PCE-DNAPL that had accumulated within the aquifer cell end chamber.
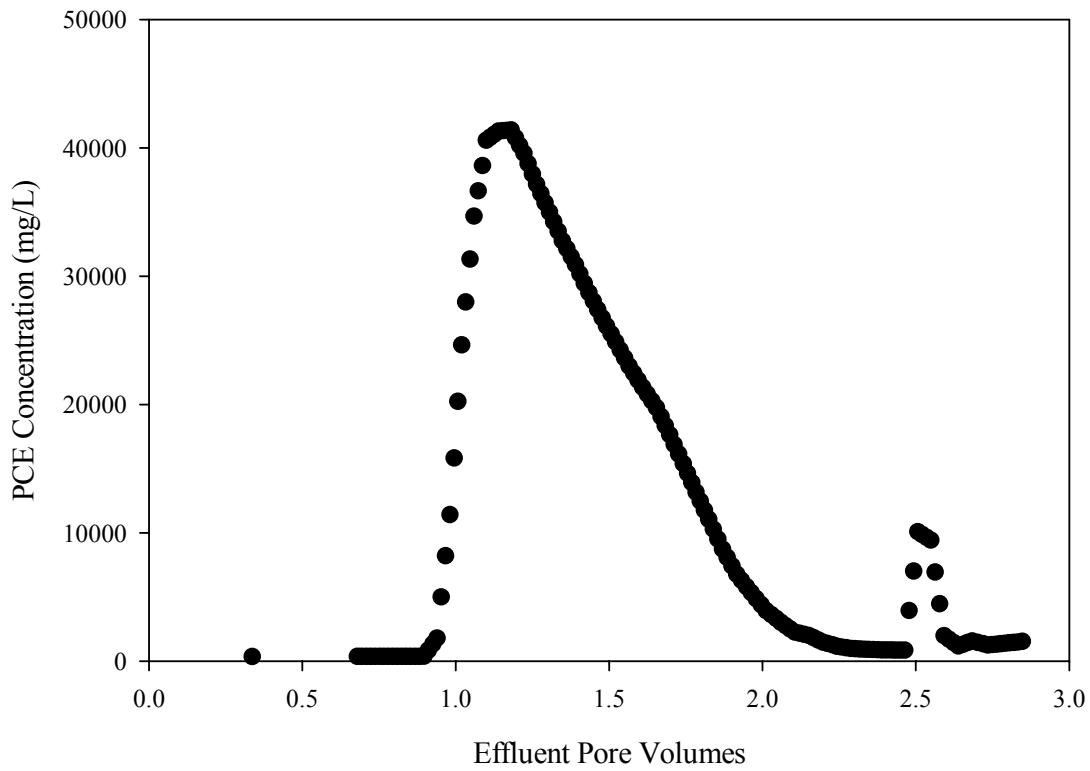
Figure 7.6: Effluent aqueous phase PCE concentrations measured during AMA8-HI.

Cumulative PCE recovery for experiment AMA8-HI is shown in Figure 6.8 and summarized in Table 6.3. The observed discontinuities in the PCE mass recovery curve correspond to removal of mobilized PCE-DNAPL from the aquifer cell end chamber. Overall recovery during AMA8-HI was 79.7%, considerably higher than that observed for AMA4-HI. Organic liquid recovery was comparable for the two experiments, with 10.0 mL of PCE-DNAPL removed from the end chamber during AMA8-HI, representing 25.0% of the PCE initially present in the aquifer cell, compared to 7.0 mL (24.6%) for AMA4-HI. The similarity in organic phase recovery was not unexpected given that the flow regimes in the two aquifer cells were comparable. The increased recovery observed during AMA8-HI was almost entirely due to the high solubilization capacity of the 8% Aerosol MA formulation, with 21.8 mL of PCE (54.7% of PCE initially present) recovered in the aquifer cell effluent.
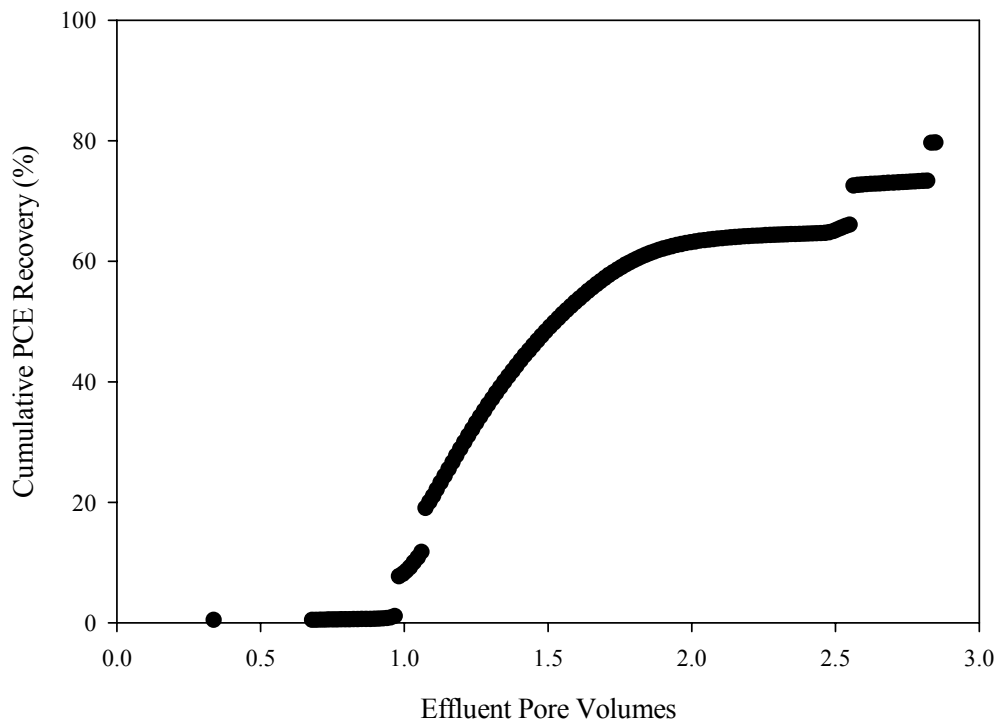
Figure 6.8: Cumulative PCE mass recovery curve for experiment AMA8-HI.

6.2.3.3 Density Modified Displacement

Following PCE-DNAPL injection and redistribution, approximately 1,500 mL (1.2 pore volumes) of the 4.7% (wt.) Tween 80 + 1.3% (wt.) Span 80 + 15% 1-butanol emulsion preflood were flushed through aquifer cell DMD-HI at a flow rate of 3.65±0.25 mL/min. Photographs of the PCE-DNAPL source zone following 670 mL (0.52 pore volumes) and 1,460 mL (1.14 pore volumes) of flushing with the emulsion preflood are shown in Figures 6.9a and 6.9b, respectively. Presence of the dye Erioglaucine A was observed to negatively impact emulsion stability, so neither the emulsion nor the resident water initially present in the aquifer cell were dyed. It is clear from Figure 6.9a that at early time the PCE-NAPL did not significantly migrate over much of the source zone, although some penetration of PCE into the lower confining layer did occur at the lower left of the aquifer cell. In addition, the emulsion became milky white when contacting regions of high PCE saturation near the center of the aquifer cell, indicating significant partitioning of PCE into the emulsion. At later times (Figure 6.9b), more pronounced displacement of the PCE-NAPL was observed due to IFT reductions associated with 1-butanol partitioning into the NAPL. The majority of the displacement occurred horizontally, indicating the PCE-NAPL was near neutral buoyancy.

At the conclusion of the emulsion preflood, 1.1 pore volumes (1,400 mL) of the low-IFT surfactant formulation (10% (wt.) Aerosol MA + 6% (wt.) 1-butanol + 15 g/L NaCl + 1 g/L CaCl$_2$) were flushed through DMD-HI at a rate of 3.70±0.20 mL/min to recover the density-converted PCE-NAPL. The low-IFT displacement solution was dyed blue-green for visualization purposes and representative photographs following flushing with (a) 340 mL (0.26 pore volumes) and (b) 900 mL (0.70 pore volumes) of the solution

are shown in Figure 6.10. The PCE-NAPL displaced from the upper two-thirds of the aquifer cell traveled in an approximately horizontal direction, indicating successful density conversion. However, PCE-NAPL penetration into the lower confining layer of the aquifer cell was also observed, indicating that density conversion, particularly for the PCE initially located near the lower confining layer, was incomplete. This result indicates that the DMD approach with an emulsion preflood can successfully convert PCE from a DNAPL to LNAPL; however, the duration of the emulsion preflood was not sufficient for PCE-NAPL density conversion in this particular case. Trapping number analysis was not conducted on DMD-HI since organic phase composition (and hence density and IFT) changed throughout the experiment. However, it is clear from Figure 6.10 that, at least in the case of the low-IFT displacement solution, the trapping number was below 2×10^{-5}, the critical region for NAPL displacement (Pennell et al. 1994).

Aqueous-phase effluent concentrations of PCE and 1-butanol measured during DMD-HI are shown in Figure 6.11. The vertical lines in Figure 6.11 represent the phases of experiment DMD-HI during which emulsion preflood, displacement solution, and post-displacement water were flushed through the aquifer cell. Effluent PCE concentrations were observed to rapidly increase following approximately 1 pore volume of flushing, reaching a maximum value of 47,000 mg/L after nearly 1.3 pore volumes of operation. The increase in PCE concentration was coincident with breakthrough of the emulsion preflood, based on the observed increase in 1-butanol concentration. This is indicative of emulsification of PCE by the preflood, which is consistent with the visual observation of the emulsion preflood becoming milky white upon contact with source zone regions of high PCE saturation (see Figure 6.9a). Following breakthrough, effluent
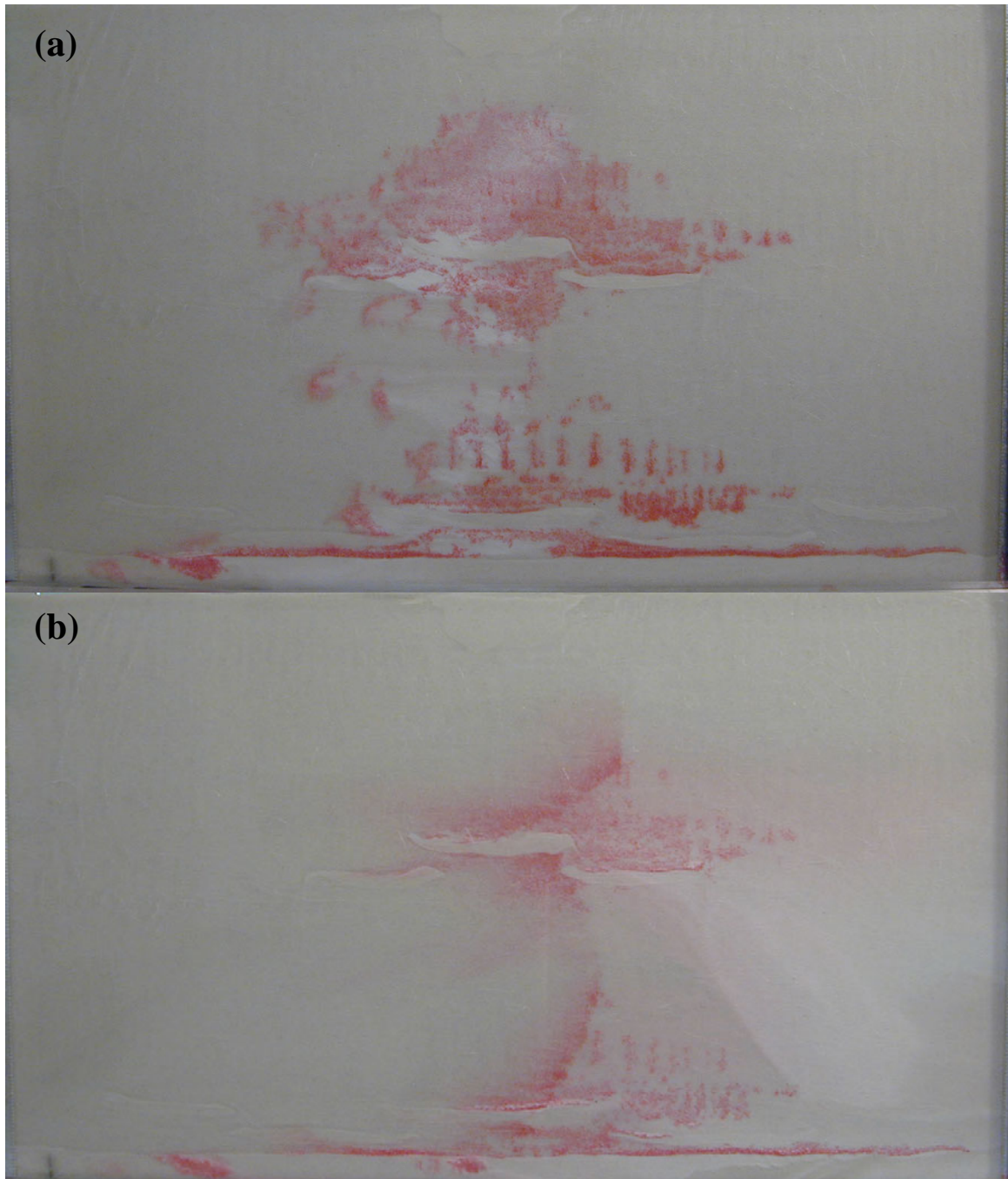
Figure 6.9: Photographs of DMD-HI source zone following (a) 670 mL (0.52 pore volumes) and (b) 1,460 mL (1.14 pore volumes) of flushing with the emulsion preflood.
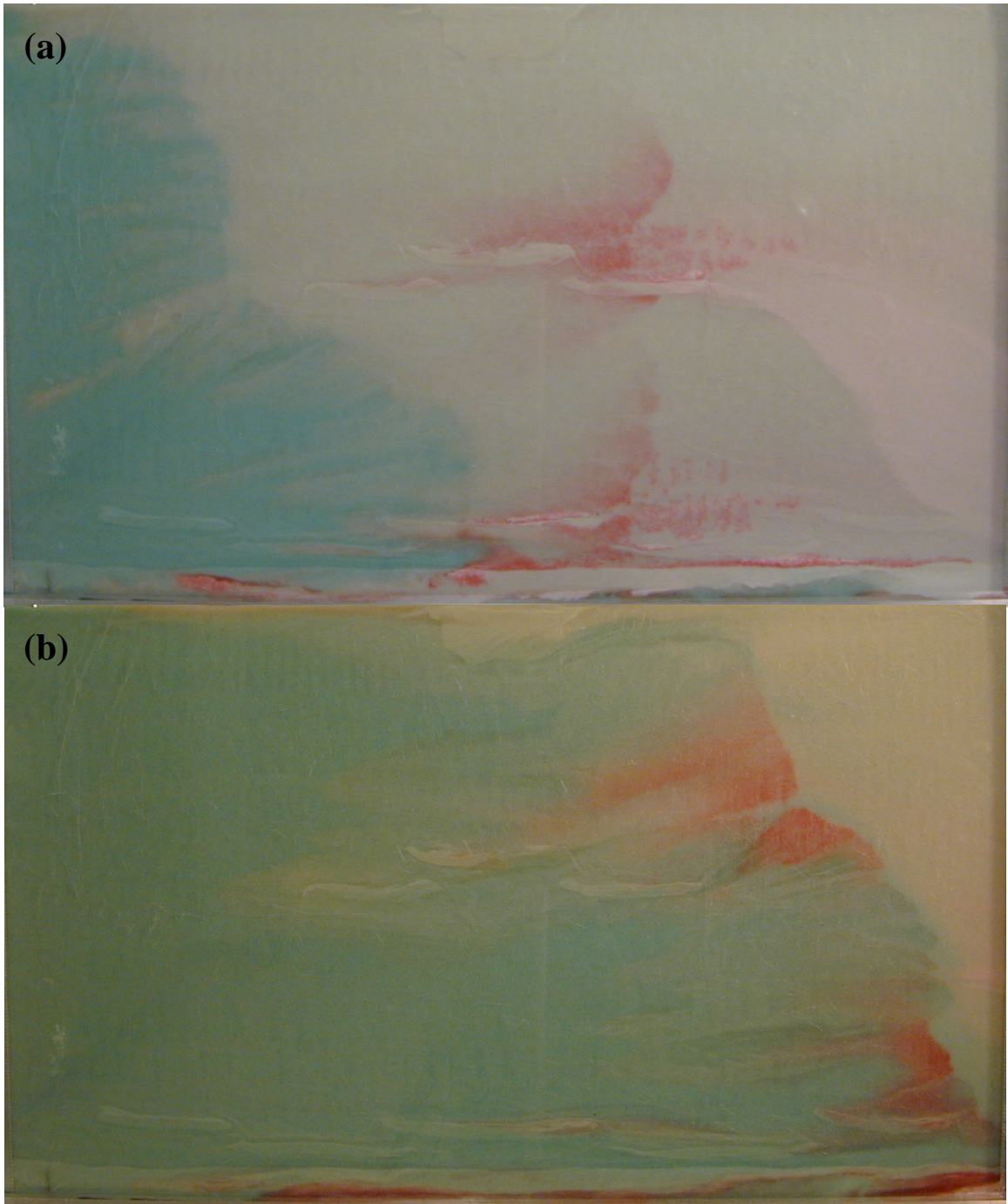
Figure 6.10: Photographs of DMD-HI source zone following (a) 340 mL (0.26 pore volumes) and (b) 900 mL (0.70 pore volumes) of flushing with the displacement solution.

1-butanol concentrations during the emulsion preflood reached a value of approximately 90,000 mg/L, significantly less than the influent 1-butanol concentration (150,000 mg/L) and indicative of partitioning of the alcohol into the PCE-NAPL. Upon reaching maximum values, both PCE and 1-butanol concentrations decreased over the remainder of the emulsion flood. At the onset of breakthrough of the low-IFT displacement solution (2 pore volumes of total flushing), effluent PCE and 1-butanol concentrations rebounded to maximum values of 14,000 mg/L and 140,000 mg/L, respectively. This is due to destabilization and mixing of the emulsion and displacement solutions as well as the phenomenon described by Ramsburg (2002) wherein solubilization of the 1-butanol-rich PCE-NAPL by the displacement solution results in an increase in effluent concentration of both the PCE as well as the partitioning alcohol.
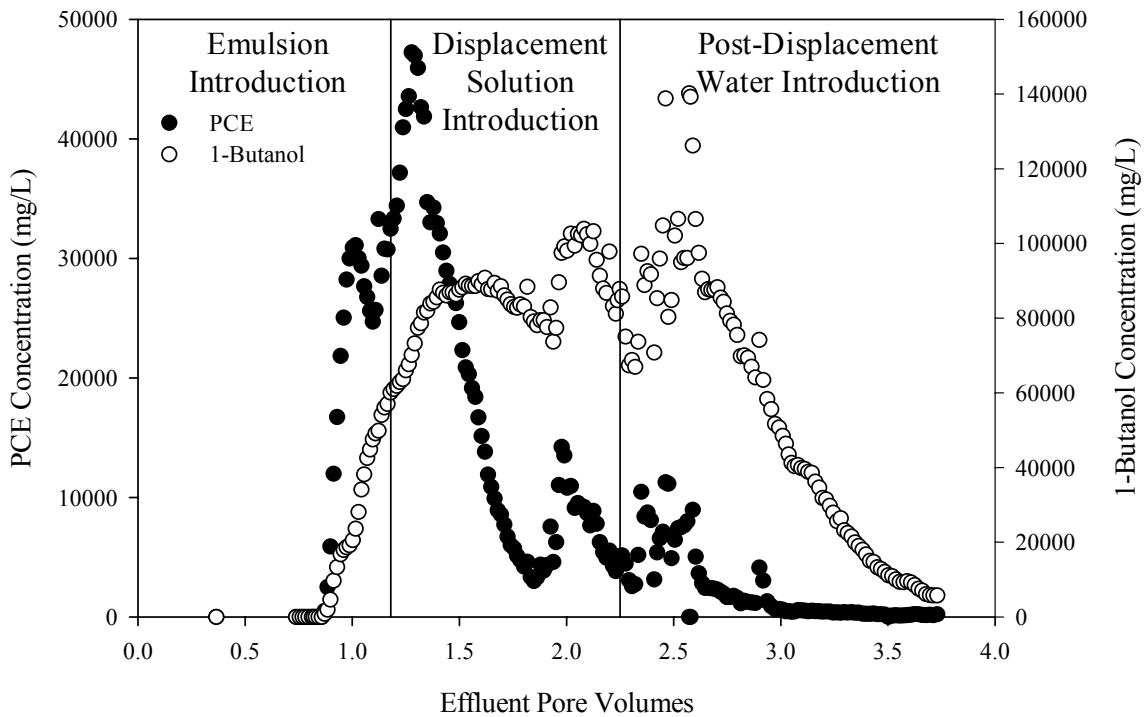
Figure 6.11: Effluent aqueous phase PCE and 1-butanol concentrations measured during DMD-HI. Vertical lines delineate influent flushing solution.

The densities of the aqueous phase effluent samples, as well as any free PCE-NAPL recovered, are shown in Figure 6.12. The vertical lines again delineate introduction of the emulsion preflood, displacement solution, and post-displacement water into the aquifer cell, and the horizontal lines represent the respective densities of the influent solutions. Aqueous-phase density (circle markers in Figure 6.12) increased following breakthrough of the emulsion preflood, a result attributed to the high PCE concentration in the aqueous phase. Introduction of the low-IFT displacement solution saw the aqueous density rise to values approximately equal to the density of the influent solution (1.015 g/cm^3). Incorporation of 1-butanol into the PCE-NAPL during the emulsion preflood resulted in a decrease of the free-phase effluent NAPL density to a minimum value of 0.96 g/cm^3, much lower than the density of aqueous flushing solutions. However, successful density modification was limited to only three of the nine PCE-NAPL samples recovered from the aquifer cell effluent, with organic-phase effluent densities of up to 1.125 g/cm^3 observed. The superficial velocity for downward migration of the NAPL was estimating using the equation developed by Tchelepi et al. (1994):

$$v_g = \frac{kg(\rho_o - \rho_w)}{\mu_o} \qquad (6.3)$$

For the NAPL with a density of 1.125 g/cm^3, the superficial downward velocity was 1.07×10^{-1} cm/min, with the time scale for downward migration over the entire aquifer cell height (38 cm) approximately 570 minutes. The residence time in the aquifer cell was 910 minutes (assuming a Darcy velocity of 0.70 mm/min, see Table 7.2), implying that the NAPL with a 1.125 g/cm^3 density would migrate at an approximate 32° downward angle and would not be captured in domains with small aspect ratios (i.e., small ratio of

height to length). Results from the density analysis suggest that the 1.2 pore volume emulsion preflood employed during DMD-HI was insufficient for complete density conversion and a longer duration preflood will be necessary for successful application of the DMD method.
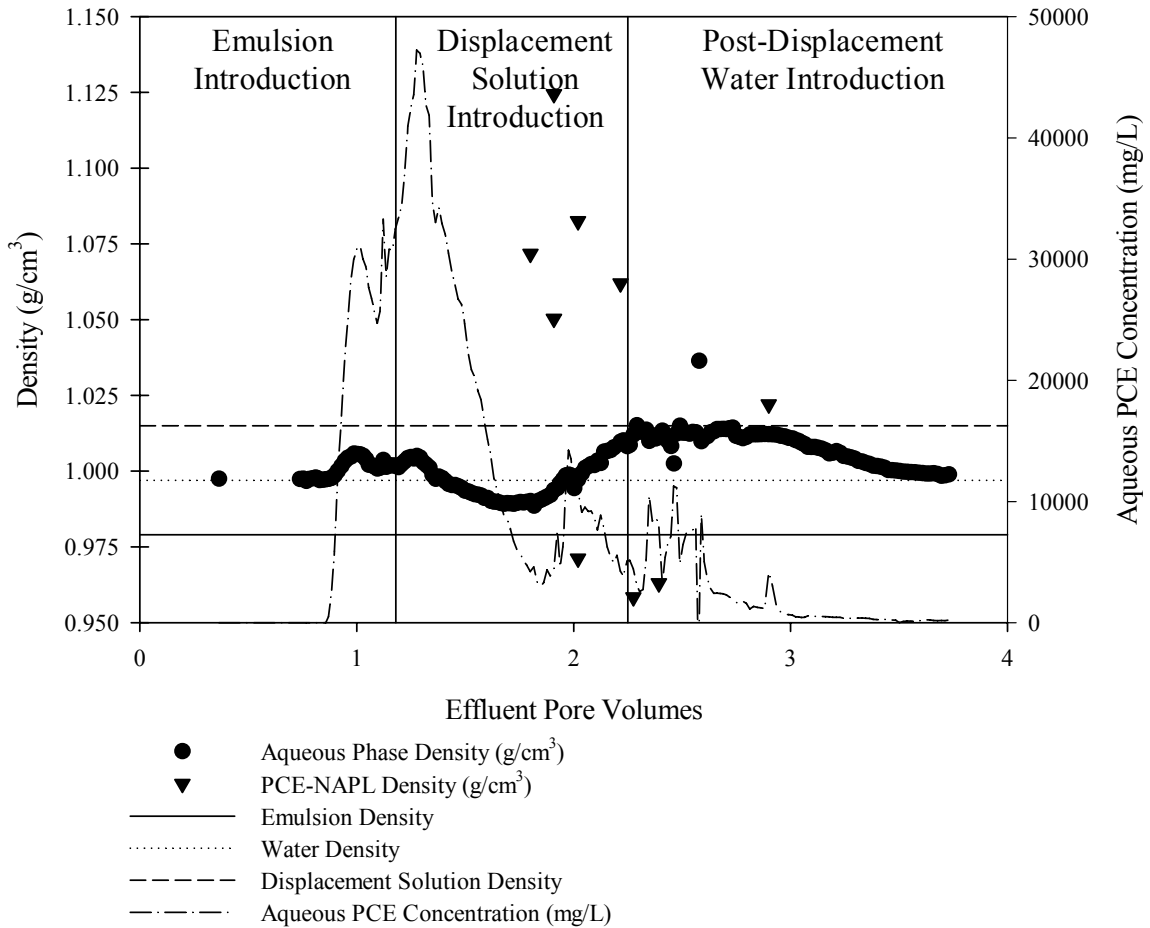
Figure 6.12: Effluent aqueous phase and PCE-NAPL densities during DMD-HI. Vertical lines delineate influent flushing solution, horizontal lines influent solution density, and dashed line aqueous phase PCE concentration.

The cumulative PCE mass recovery curve during experiment DMD-HI is shown in Figure 6.13. Overall recovery was 86.4% (27.0 mL, see Table 6.3) following flushing

with less than 2.4 pore volumes of surfactant solution, a relatively high value that was comparable to those previously reported for DMD flushing strategies (see e.g., Ramsburg and Pennell 2002b, Ramsburg et al. 2003, Ramsburg et al. 2004a). Only a small fraction of the total PCE recovered, 4.0 mL or 12.8%, was recovered as PCE-NAPL, with the remaining 23.0 mL (73.7%) recovered from the aqueous phase. Of the PCE recovered in the aqueous phase, 18.8 mL (60.1%) were recovered in the emulsion preflood and 4.2 mL (13.6%) in the low-IFT displacement solution, respectively.
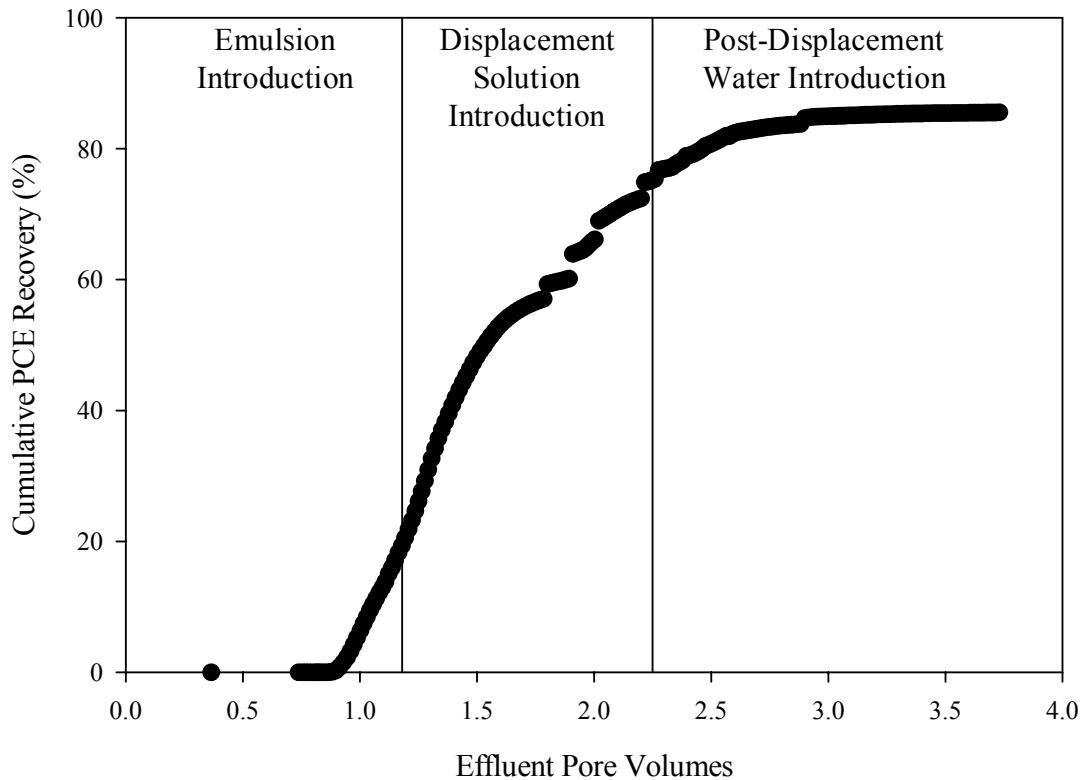
Figure 6.13: Cumulative PCE mass recovery curve for experiment DMD-HI.

6.2.4 Effluent PCE Concentrations

Effluent PCE concentrations for the three aquifer cell experiments were monitored at the conclusion of surfactant flushing to evaluate the impact of recovery

mechanism on down-gradient contaminant concentrations. Table 6.3 summarizes the post-treatment effluent PCE concentrations, normalized by dividing by concentrations prior to surfactant flushing, and the results are plotted in Figure 6.14. Results from Chapter 5 (i.e., effluent concentrations following partial mass recovery by surfactant-enhanced solubilization) are included in Figure 6.14 as a reference. Experiment AMA4-HI was characterized by a limited reduction in effluent concentration, reaching a value of 0.73±0.07 at 49.0% mass removal. This was comparable to results following the first surfactant flushing events during the MID-GTP, MID/LO-GTP, and LO-GTP experiments. The similarity was likely a result of preferential dissolution of PCE ganglia mass (similar to that observed for the solubilization experiments), along with downward mobilization of the small pools located above low permeability lenses in the center of the source zone that acted to reduce the contaminant mass present in the upper regions of the aquifer cell. Conversely, reductions in effluent concentration for both AMA8-HI as well as DMD-HI were significant. For AMA8-HI, normalized post-treatment concentration was 0.15±0.07 at 79.7% recovery; the respective values for DMD-HI were 0.22±0.06 and 86.4%. Results (mass recovery and effluent concentration) were comparable to those observed near the conclusion of experiments HI-GTP, MID-GTP, and MID/LO-GTP. The final PCE-DNAPL source zone distributions (i.e., at the conclusion of surfactant flushing) for all of these experiments were characterized by nearly complete PCE recovery in the upper regions of the aquifer cell and the presence of high saturation pools located just above, or within, the aquifer cell lower confining layer. Given the similarities in the final DNAPL distributions, it is therefore unsurprising that the resulting down-gradient effluent PCE concentrations would be similar.
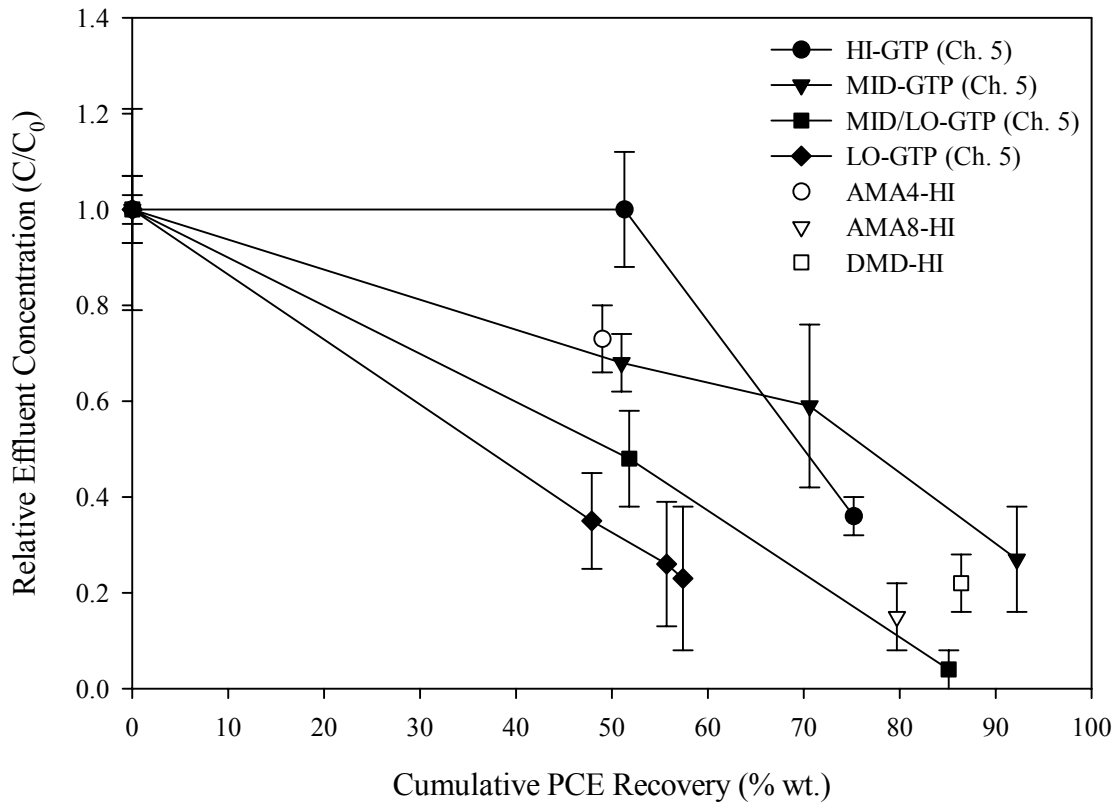
Figure 6.14: Normalized effluent PCE concentration as a function of cumulative PCE-DNAPL mass recovery and recovery mechanism. Error bars represent one standard deviation.

In addition to effluent concentration reductions, it is illustrative to consider the PCE recovery efficiency (in terms of g PCE/g surfactant) for each of the flushing strategies employed. The respective recovery efficiencies were 0.35 g PCE/g Aerosol MA for AMA4-HI, 0.41 g PCE/g Aerosol MA for AMA8-HI, and 0.19 g PCE/g surfactant (all surfactants) for DMD-HI (see Table 6.3). The efficiency for DMD-HI was somewhat lower due to the surfactant requirements in the emulsion preflood; using an aqueous 1-butanol flood would reduce the surfactants needed and increase efficiency (at the cost of a longer preflood flushing duration). For all three cases, however, efficiency

was much greater than those observed during the solubilization floods conducted in Chapter 5 (see Table 5.2). As such, surfactant-based immiscible displacement strategies may be very attractive in that they require much lower volumes of flushing solution to achieve comparable (or even greater) post-treatment contaminant mass recovery and effluent concentration reductions. This is particularly true for scenarios where downward DNAPL mobilization into pristine aquifer regions can be mitigated, either through geological formation, proper design of the aqueous flow field to recovery mobilized DNAPL, use of the DMD method, or tailoring the surfactant formulation to prevent DNAPL penetration into aquifer confining layers (similar to experiment AMA4-HI).

6.3 Summary and Conclusions

The experimental results presented here are an important advancement in the understanding of the effect of DNAPL recovery mechanism on post-treatment down-gradient plume concentrations and mass flux. Visual observation of DNAPL migration within the source zone was coupled with direct quantification of effluent PCE concentrations. Analysis of these results demonstrates that immiscible displacement can be an efficient mechanism for PCE-DNAPL recovery. All three experiments were characterized by PCE recovery efficiencies much greater than those observed with miscible displacement (0.35 g PCE/g Aerosol MA for AMA4-HI, 0.41 g PCE/g Aerosol MA for AMA8-HI, and 0.19 g PCE/g surfactant (all surfactants) for DMD-HI). Normalized effluent PCE concentration following flushing with the 4% Aerosol MA surfactant formulation (50% mass recovery) decreased by approximately 25% due to a combination of preferential solubilization of DNAPL ganglia and mobilization of small high saturation DNAPL pools in the upper region of the aquifer cell. Mass recovery and

214

effluent concentration reductions (both approximately 80%) were significantly higher with the 8% Aerosol MA and density modified displacement surfactant formulations. The remaining contaminant mass was present as high saturation pools located either just above or within the aquifer cell lower confining layer, similar to distributions observed at the conclusion of surfactant-enhanced solubilization. Immiscible displacement may be a highly efficient mechanism for remediation of DNAPL source zones, with reduced volumes of surfactant required to achieve significant contaminant recovery. However, care must be exercised when designing immiscible displacement flushing strategies to limit mobilization of DNAPL into previously uncontaminated aquifer regions.

CHAPTER 7

QUANTITATIVE PCR CORRELATES MICROBIAL ACTIVITY AND DISTRIBUTION WITH ENAHNCED CONTAMINANT DISSOLUTION FROM A PCE-NAPL SOURCE ZONE PART 1: *SULFUROSPIRILLUM MULTIVORANS*

7.1 Introduction

Although aggressive physicochemical treatment of DNAPL source zones can be highly effective, with mass recoveries in excess of 90% occasionally reported (Hasegawa et al. 2000), it is generally recognized that contaminant mass recoveries on the order of 60-70% are a more likely remedial result (see e.g., Brooks et al. 2004, Holmzer et al. 2000, Jawitz et al. 2000, NRC 2004, Rao et al. 1997, Soga et al. 2004, Stroo et al. 2003). Removal of the contaminant mass remaining post-treatment may require significant additional treatment time, particularly in cases where dissolution of the DNAPL is limited due to contaminant distribution within the source zone porous media (Christ et al. 2005b). A promising strategy for the efficient detoxification and recovery of post-treatment contaminant mass is the use of microbial reductive dechlorination as a tertiary treatment (or polishing step).

During reductive dechlorination, PCE and TCE are sequentially reduced, either metabolically or cometabolically, to the chlorinated ethenes *cis*-DCE, vinyl chloride, and ethene, as well as hydrochloric acid. Anaerobic cometabolic reductive dechlorination of PCE has been widely observed (see e.g., Fathepure and Boyd 1988, Cole et al. 1995) but is of limited use as a source zone treatment due to slow rates and incomplete

216

detoxification. More promising is metabolic reductive dechlorination (also known as chlororespiration), a strictly anaerobic process that while requiring introduction of an electron donor into the source zone is also a possible efficient mechanism for bioremediation of PCE- and TCE-contaminated sites (He et al. 2003a). A number of phylogenetic groups are capable of metabolic reductive dechlorination, including *Dehalobacter* spp. (Holliger et al. 1998), *Sulfurospirillum* spp. (Neumann et al. 1994), *Desulfuromonas* spp. (Sung et al. 2003), *Desulfitobacterium* spp. (Gerritse et al. 1996), *Clostridium bifermentans* strain DPH-1 (Chang et al. 2000), *Geobacter* spp. (Sung et al. 2006) and *Dehalococcoides* spp. (Löffler and Edwards 2006), however most of the isolated organisms are incapable of complete dechlorination to ethene (Löffler et al. 2003) and may produce toxic intermediates (particularly vinyl chloride) within the subsurface. However, recent breakthroughs have linked the presence of *Dehalococcoides* species with the complete conversion of parent chlorinated compounds to ethene (Ritalahti et al. 2001), with *Dehalococcoides* species BAV1 capable of metabolic conversion of all DCE isomers and vinyl chloride to ethene (He et al. 2003a, 2003b).

Originally it was thought that toxic effects would preclude reductive dechlorination at aqueous PCE concentrations near saturation or within PCE-DNAPL source zones (Robertson and Alexander 1996). However, PCE dechlorination has been demonstrated in batch systems at both high aqueous PCE concentrations (Nielson and Keasling 1999, Yang and McCarty 2000) and in the presence of PCE-DNAPL (Carr et al. 2000). Based on these promising results, a number of column studies have been conducted to evaluate the plausibility of microbial reductive dechlorination activity at high aqueous PCE concentrations or within a DNAPL source zone. Both Cope and

Hughes (2001) and Yang and McCarty (2002) observed dechlorination activity, however activity stalled at vinyl chloride for the former and *cis*-DCE for the latter. While complete dechlorination of chlorinated ethenes to ethene is a primary goal of tertiary treatment via microbial reductive dechlorination, partial dechlorination may still act to enhance DNAPL dissolution rate and decrease source zone longevity, with reported dissolution enhancement factors in column experiments ranging from 3-fold (Yang and McCarty 2002) to 6-fold (Cope and Hughes 2001). These results imply that significant decreases in post-treatment source zone longevity may be possible through microbial activity, although technical obstacles such as column bio-clogging (Yang and McCarty 2002), partitioning of dechlorination products into the DNAPL (Adamson et al. 2004), and pH toxicity effects (Cope and Hughes 2001) were apparent.

The objectives of this study were to evaluate microbial reductive dechlorination performance and distribution of *Sulfurospirillum multivorans*, an organism capable of PCE to *cis*-DCE dechlorination, in the vicinity of a PCE-NAPL source zone. The experiments were designed in such a manner as to overcome the limitations associated with previous biologically-enhanced NAPL dissolution experiments, featuring uniform (and known) initial NAPL and biomass distributions and use of molecular tools to quantify and track genes of interest (i.e., *pceA* gene) within the biocolumn. As designed, dechlorination and microbial activity may be potentially linked within the biocolumn, and the biocolumn results may be effectively compared to results from future modeling studies. Abiotic experimental results characterizing the physicochemical parameters of the biocolumn are presented and effluent concentrations (chlorinated ethenes and biomass) were monitored over the entire course of both experiments to evaluate reductive

dechlorination performance down-gradient from a biologically-active NAPL source zone. In addition, periodic samples were taken from side ports located along the length of the biocolumn to monitor chlorinated ethene and biomass concentration profiles within the biocolumn. Finally, the cumulative chlorinated ethene recoveries for the experiments were determined and compared to expected abiotic recoveries in order to estimate enhancement to contaminant mass transfer arising from biological activity.

7.2 Results and Discussion

Two experiments were conducted using the one-dimensional (1-D) biocolumn described in Chapter 3. Following packing, inoculation, and a period of flow through the column designed to establish an active microbial community, the biocolumn was imbibed with either a mixed NAPL comprised of 0.25 mol/mol PCE in hexadecane (experiment SM-Mixed) or a pure PCE-DNAPL (experiment SM-Pure). At this point, reduced mineral salts medium amended with 20 mM pyruvate was flushed through the biocolumn and effluent chlorinated ethene and biomass concentrations monitored daily. In addition, weekly samples were taken from the biocolumn side ports and analyzed for chlorinated ethene (and in some cases biomass) concentrations. At the conclusion of the experiments, the columns were destructively sampled to estimate biomass concentrations associated with the porous media.

7.2.1 Column Physicochemical Characterization

Prior to the beginning of the microbial enhanced dissolution experiments (e.g., biocolumns), a series of two non-reactive tracer experiments were performed in the 1-D column to assess the hydrodynamic dispersion following packing but prior to imbibition

of the NAPL. Both columns were packed with Ottawa Federal Fine sand, and a nominal

intrinsic permeability in the columns of $4.2x10x10^{-11}$ m^2 was assumed. The first tracer

was flushed through the column at a relatively high flow rate of 1.99±0.01 mL/min and

had with a hydraulic retention time of approximately 200 minutes, while the second test

was conducted at the operational flow rate of the biocolumns (0.24±0.01 mL/min) with a

retention time of 1.1 days. The tracer solution employed in both experiments was

comprised of 0.01 M potassium iodide that was analyzed via HPLC and 0.25 g/L

Erioglaucine A, a blue-green dye that was used to visualize the position of the tracer

front. Potassium iodide breakthrough curves for the 2 mL/min and 0.25 mL/min tracer

tests are shown in Figures 7.1a and 7.1b, respectively, with the black circles representing

experimental results. Both tracer experiments were characterized by nominally

symmetric breakthrough curves, indicating that aqueous flow through the column was

uniform and an absence of physical non-equilibrium. In order to estimate the Peclet

number and dispersivity of the tracer studies, the experimental results were fit to the one-

dimensional (1-D) advective-dispersive-reactive (ADR) transport equation using the BTC

program (version 4.2), which simulates solute breakthrough using 1st or 3rd Type

boundary conditions. Potassium iodide breakthrough curves simulated by BTC (solid
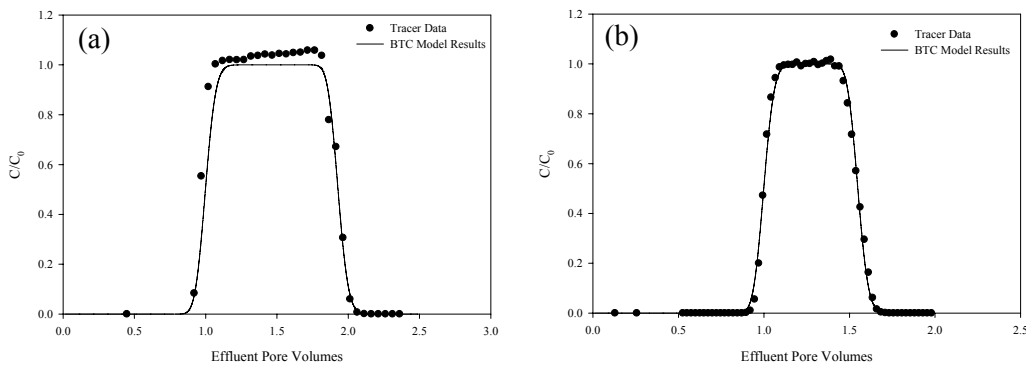
Figure 7.1: Potassium iodide breakthrough curves for non-reactive tracer experiments
conducted in 1-D column at aqueous flow rates of (a) 2 mL/min and (b) 0.25 mL/min.

lines in Figures 7.1a and 7.2b) were comparable to experimental results, with respective

minimized sum of square values of 0.161 and 0.040 at 2 mL/min and 0.25 mL/min. In

addition, the Peclet number and dispersivity for the 2 mL/min tracer study were estimated

to be 590±150 and 0.07±0.02 cm, while these values were estimated at 850±120 and

0.07±0.01 cm for the 0.25 mL/min experiment. Results from both tracer experiments are

summarized in Table 7.1.

Table 7.1: Summary of potassium iodide tracer experiments in 1-D biocolumn prior to
NAPL imbibition.

Aquifer Cell Parameter	Tracer Experiment 1	Tracer Experiment 2
Overall Pore Volume (mL)	400	390
Tracer Flow Rate (mL/min)	1.99±0.01[b]	0.24±0.01
Darcy Velocity (mm/min)	1.11±0.01	0.138±0.01
Volume of Tracer Flood (mL)	960	770
SSQ[a] for BTC Breakthrough Curve	0.161	0.040
BTC Estimated Peclet Number	590±150	850±120
BTC Estimated Dispersivity (cm)	0.10±0.02	0.07±0.01

a: Minimized sum of square value
b: Standard deviation

At the conclusion of the second non-reactive tracer study, a mixed NAPL

comprised of 0.25 mol/mol PCE in hexadecane was imbibed into the column to evaluate

abiotic dissolution of PCE from the NAPL at the operational flow rate of the biocolumns

(0.25 mL/min). At this flow rate, aqueous phase PCE concentrations throughout the

entire column length increased to values comparable to the aqueous PCE solubility of the

mixed NAPL (50 mg/L) following 1.5 pore volumes of flushing (see Figure 7.2 where

Port 1 is at the bottom of the column), indicating the absence of abiotic mass transfer

limitations. This result is comparable to those observed by Powers et al. (1992), where

mass transfer limitations in 1-D column systems were not observed unless the column

length was very short (3-5 cm) and the aqueous flow rate high. In addition, a mass transfer coefficient (K_L) of 7.7×10^{-4} min^{-1} was calculated using the correlation developed by Powers et al. (1992) (Equation 7.1) where d_{50} is the mean grain diameter of the porous media, D_L is the free liquid diffusivity of PCE, Re is the Reynolds number, and U_i is the coefficient of uniformity of the porous media.

$$\frac{K_L (d_{50})^2}{D_L} = 57.7 \, \text{Re}^{0.61} \, d_{50}^{0.64} \, U_i^{0.41} \qquad (7.1)$$

Given the long column length and low aqueous flow rate employed in the biocolumn experiments, the mass transfer coefficient calculated using Equation 7.1 is sufficient for PCE solubility to reach equilibrium throughout the column, a result that is apparent based on the measured concentrations in Figure 7.2.
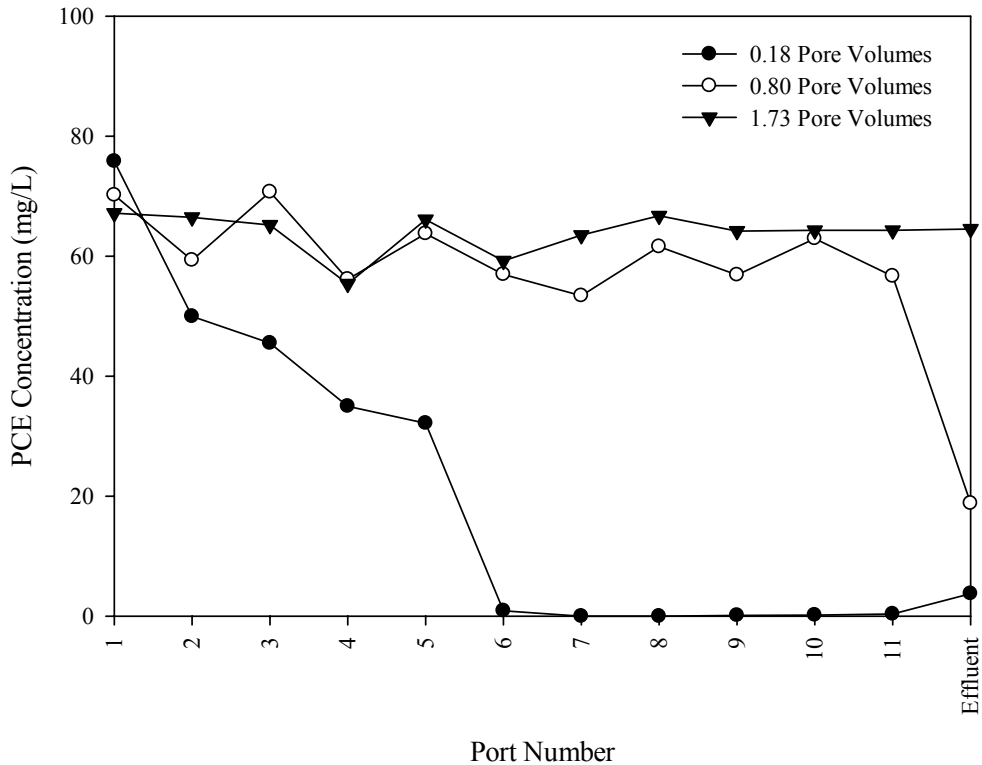
Figure 7.2: Abiotic dissolution of PCE from mixed PCE/hexadecane NAPL (0.25 mol/mol PCE) in 1-D biocolumn at operational flow rate of 0.25 mL/min.

7.2.2 Microbial Community Establishment and NAPL Imbibition

Following packing, both biocolumns (SM-Mixed and SM-Pure) were kept in the anoxic glove bag system used for packing for a period of 24 hours in the absence of aqueous-phase flow to promote establishment of an active microbial community within the column. At the conclusion of this 24 hour period, reduced mineral salts medium was flushed through the columns at a nominal flow rate of 0.25 mL/min in order to remove (or elute) unattached biomass. The mineral salts medium employed during this period was not amended with a carbon source, electron donor, or electron acceptor; thus it was assumed that minimal growth and/or decay of the microbial species present in the columns was occurring. DNA was extracted from samples taken periodically during the elution phase of the column experiments and RTmPCR subsequently performed on the extracted DNA to enumerate the number of organisms eluted.

A total of 4.3 pore volumes of reduced mineral salts medium were flushed through the biocolumn during the elution phase of experiment SM-Mixed, with the effluent *pceA* gene copies/mL as a function of total pore volumes flushed shown in Figure 7.3a. The measured *pceA* genes copies/mL in the effluent samples, which represents the number of unattached *S. multivorans* cells that eluted from the column, were low (less than 5.0×10^6) for the first 1.5 pore volumes of flushing. At that point, a large increase in *pceA* gene copies/mL was observed, reaching a maximum value of 1.0×10^7, before decreasing to a relatively constant value of approximately 5.0×10^6 for the remaining 2.3 pore volumes of flushing. While this maximum value may represent the peak of *S. multivorans* elution from the column, it is difficult to say with certainty given the limited number of data points available. Regardless, *pceA* gene copies/mL for all

samples taken were significantly lower than the *pceA* genes copies/mL in the inoculum (8.0×10^7), indicating relatively little elution of biomass from the column. The cumulative recovery of *pceA* gene copies in the effluent during the microbial elution phase is shown in Figure 7.3b, along with the percent recovery of *pceA* genes, assuming no growth or decay. Under these assumptions, significant attachment and/or retention of *S. multivorans* in the column was apparent, with only 26% of the biomass initially present during packing removed during the elution phase.

S. *multivorans* retention within the column was also analyzed during the experiment where a pure PCE-DNAPL was imbibed (SM-Pure). The measured effluent *pceA* gene copies/mL during the elution phase of this experiment were somewhat higher than during SM-Mixed, ranging from 2.0×10^7 to 5.0×10^7 (see Figure 7.4a). There was, however, a corresponding increase in the number of *pceA* gene copies/mL in the inoculum used in this experiment (approximately 1×10^9) as compared to the one used during SM-Mixed. The cumulative percentage of *pceA* genes recovered in the effluent, as shown in Figure 7.4b, was relatively low (approximately 30%), again demonstrating that a significant fraction of the biomass present in the column during packing was retained. The large fraction of *S. multivorans* retained within the columns was somewhat surprising, given that microbial transport is typically enhanced in the presence of ionic species such as those present in the reduced mineral salts medium flushed through the column during the elution phase (see e.g., Rogers and Logan 2000). However, a systematic evaluation of *S. multivorans* transport through porous media will be required before any conclusions may be drawn regarding mechanistic reasons for the significant attachment and/or retention of the organisms within the biocolumn.
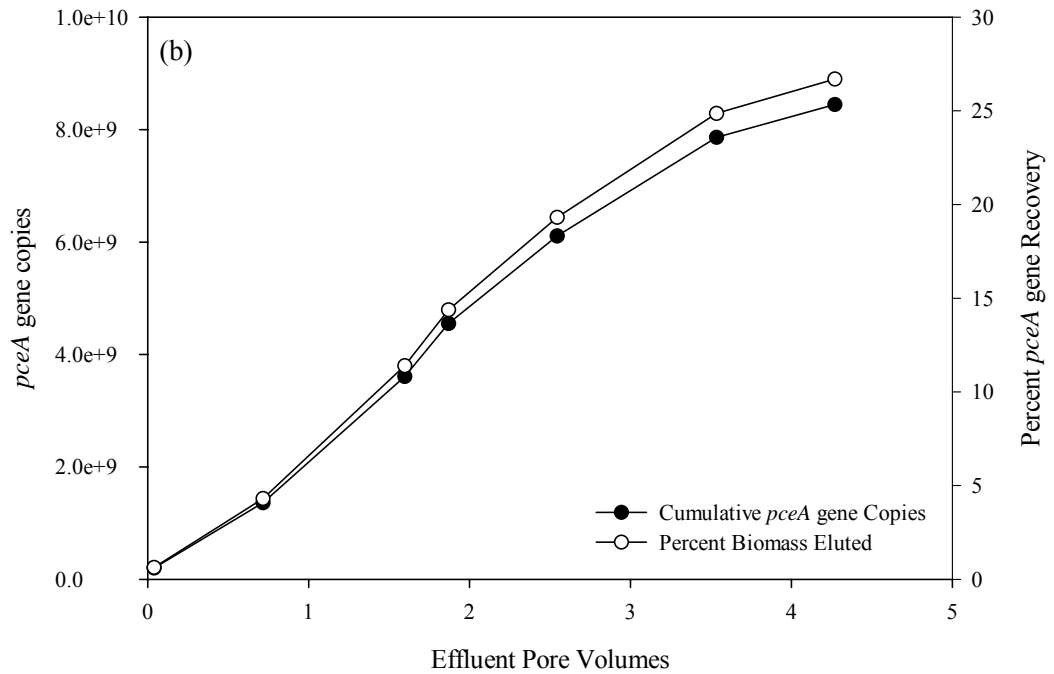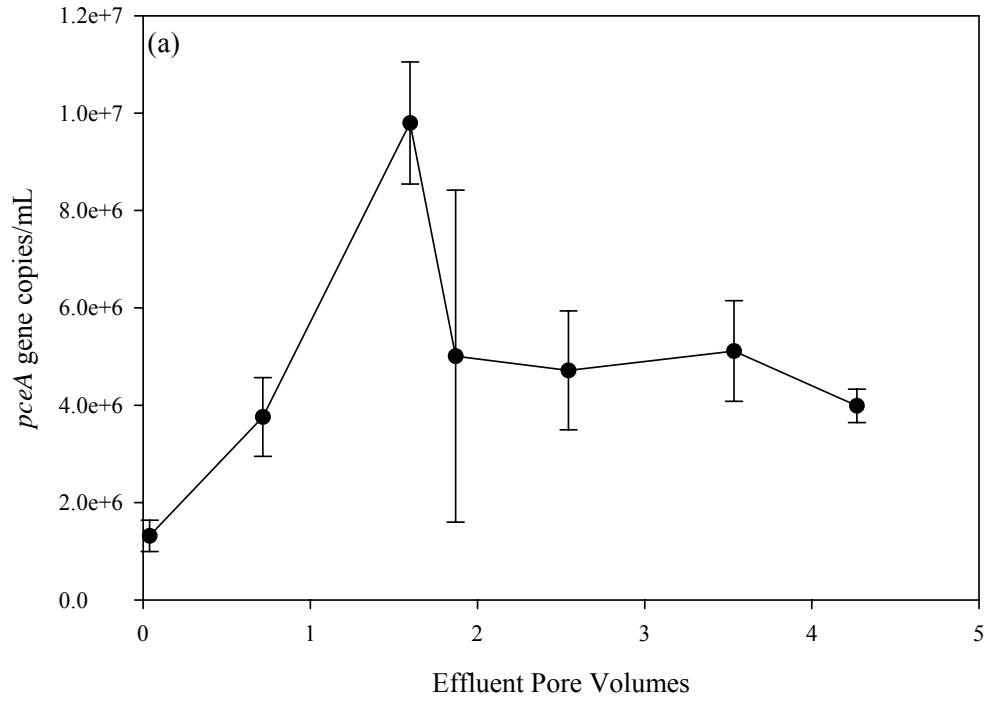
Figure 7.3: Effluent *pceA* gene copies/mL (a) and cumulative *pceA* gene copies (b) as a function of pore volumes flushed during microbial elution phase of experiment SM-Mixed.
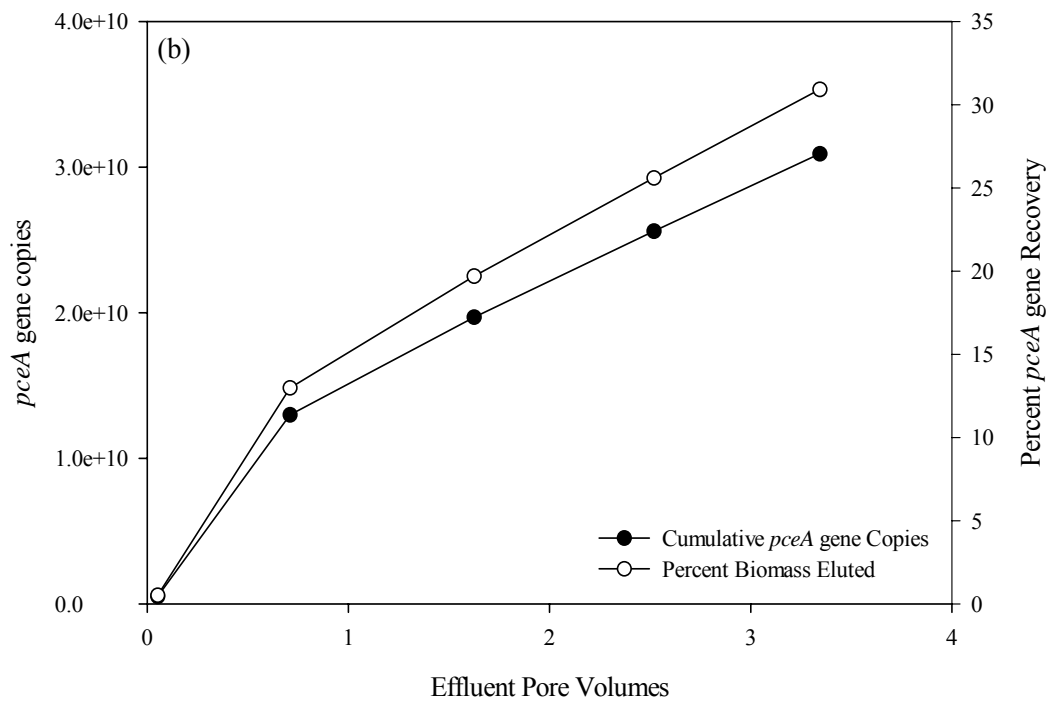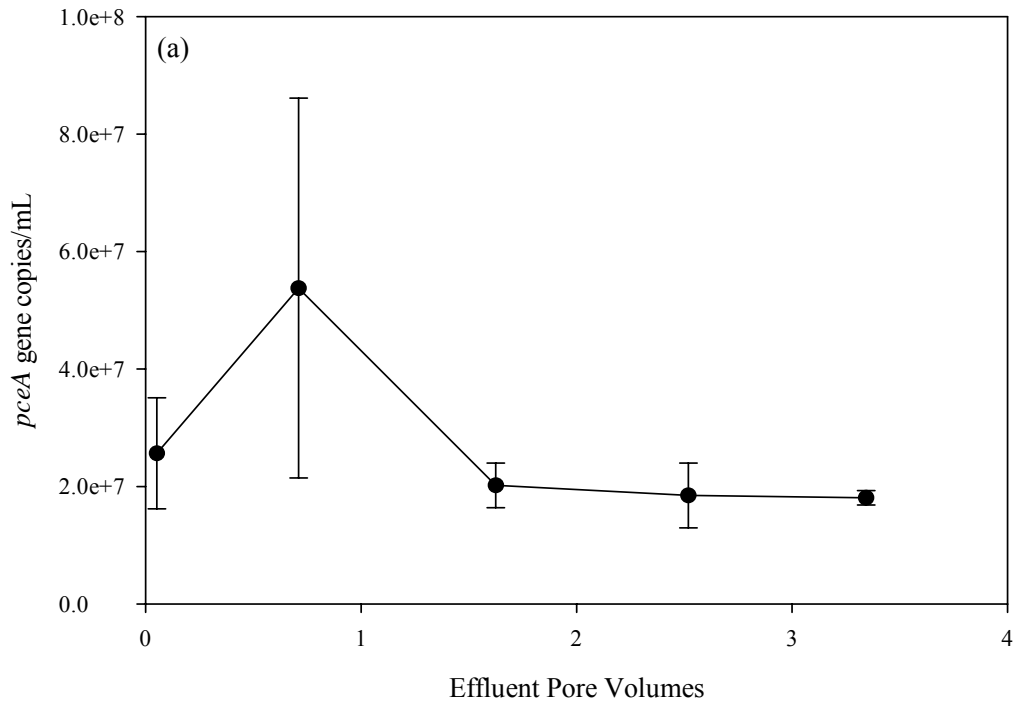
Figure 7.4: Effluent *pceA* gene copies/mL (a) and cumulative *pceA* gene copies (b) as a function of pore volumes flushed during microbial elution phase of experiment SM-Pure.

At the conclusion of the elution phase of the two *S. multivorans* biocolumn experiments, NAPL was imbibed and a residual source zone established over the bottom 10 cm of each column. Column SM-Mixed was imbibed with a mixed NAPL comprised of 0.25 mol/mol PCE in hexadecane and having an equilibrium PCE solubility of approximately 300 μM (50 mg/L). This NAPL formulation was selected to ensure that aqueous PCE concentrations in the column would remain below values inhibitory to *S. multivorans*, or approximately 540 μM (90 mg/L) (Nambi et al. 2003). The density of the mixed NAPL was 0.86 g/cm^3, and approximately 14 mL (1.45 mL PCE) were imbibed over the bottom 10 cm of the column. The total pore volume of the column during SM-Mixed was 390 mL, and the residual NAPL saturation in the column source zone was 21%. Although the NAPL distribution within the source zone was relatively uniform, some fingering of the NAPL was apparent following imbibition. This fingering was not factored in to determination of residual saturation, which may have resulted in an erroneously high estimate of source zone NAPL saturation. Pure PCE-DNAPL, having a density of 1.62 g/cm^3 and an equilibrium solubility of 1,200 μM (200 mg/L), was imbibed into the biocolumn during experiment SM-Pure. Approximately 9 mL of PCE were imbibed over the bottom 10 cm of the column; residual organic-phase saturation in the column source zone (i.e., bottom 10 cm) was 11%, given that the overall pore volume of the column during this experiment was 400 mL. Compared to SM-Mixed, less NAPL fingering was observed during SM-Pure, with imbibition resulting in a relatively uniform DNAPL distribution within the column source zone. Relevant experimental conditions for both experiment SM-Mixed and SM-Pure are summarized in Table 7.2.

Table 7.2: Summary of one-dimensional biocolumn conditions for *S. multivorans* experiments.

Biocolumn Parameter	SM-Mixed	SM-Pure
Column Pore Volume (mL)	390	400
NAPL Composition	Mixed[a]	Pure PCE
NAPL Density (g/cm^3)	0.86	1.62
Equilibrium PCE Solubility (μM) [mg/L]	300 [50]	1200 [200]
NAPL Injection Volume (mL)	14	9
Source Zone NAPL Saturation (%)	21	11

a: 0.25 mol/mol PCE in hexadecane

7.2.3 NAPL Dissolution: Effluent and Side Port Samples

Following NAPL imbibition, the reduced mineral salts medium flushed through the biocolumn was amended with 20 mM pyruvate to act as a carbon source and electron donor, and the NAPL dissolution phase of the experiments begun. During this phase of the experiments, daily effluent samples were collected and analyzed for chlorinated ethenes, pH, and biomass. In addition, weekly samples were taken from the side ports located along the column length. The side port samples were analyzed for chlorinated ethenes and in some cases, biomass. Effluent and side port results from the two *S. multivorans* biocolumn experiments are presented below, with the two experiments separated into individual subsections.

7.2.3.1 Experiment SM-Mixed

Following establishment of a PCE/hexadecane mixed-NAPL residual source zone over the first 10 cm of the biocolumn, experiment SM-Mixed was operated for 18.6 pore volumes during the NAPL dissolution phase to monitor reductive dechlorination activity. The side ports located along the length of the column were sampled for chlorinated ethenes following 5, 11, and 17.5 pore volumes of flushing with the pyruvate-amended

mineral salts medium. In addition, biomass samples were taken during the 17.5 pore volume sampling event.

Effluent chlorinated ethene concentrations and pH measured during experiment SM-Mixed are shown in Figure 7.5, with the arrows indicating times at which side port samples were taken. The dashed line in Figure 7.5 shows the expected total chlorinated ethene concentration, including PCE, TCE, *cis*-DCE, and *trans*-DCE, assuming that no biological enhancement of mass transfer from the NAPL was occurring. Given the results from the NAPL dissolution experiment in the abiotic column (see section 7.2.1), this value was expected to be equal to the equilibrium solubility of PCE, or 301.5 µM (50 mg/L) in the case of the mixed NAPL. Dechlorination activity was minimal for the first two pore volumes of column operation. Following this initial period, however, PCE was completely dechlorinated to primarily *cis*-DCE (trace amounts of *trans*-DCE were detected), with PCE no longer detected in the effluent samples following 3 pore volumes of flushing. Effluent *cis*-DCE concentrations began to increase rapidly following 3 pore volumes of flushing, reaching a maximum value of approximately 3,500 µM at 8 pore volumes of flushing. This represents a maximum biological enhancement factor of 13.6 for experiment SM-Mixed at this point, or a 13.6-fold increase in total effluent chlorinated ethene concentration over the expected total chlorinated ethene concentration (i.e., 300 µM). Effluent *cis*-DCE concentrations decreased over much of the remaining 10 pore volumes of operation during the NAPL dissolution phase of experiment SM-Mixed, reaching a pseudo-steady state value of approximately 700 µM at the conclusion of flushing. While this value is significantly lower than the maximum *cis*-DCE concentration observed, it is nonetheless greater then twice the expected total chlorinated

229

ethene concentration and indicates that biologically-enhanced dissolution of PCE from the NAPL was ongoing even at the termination of SM-Mixed.
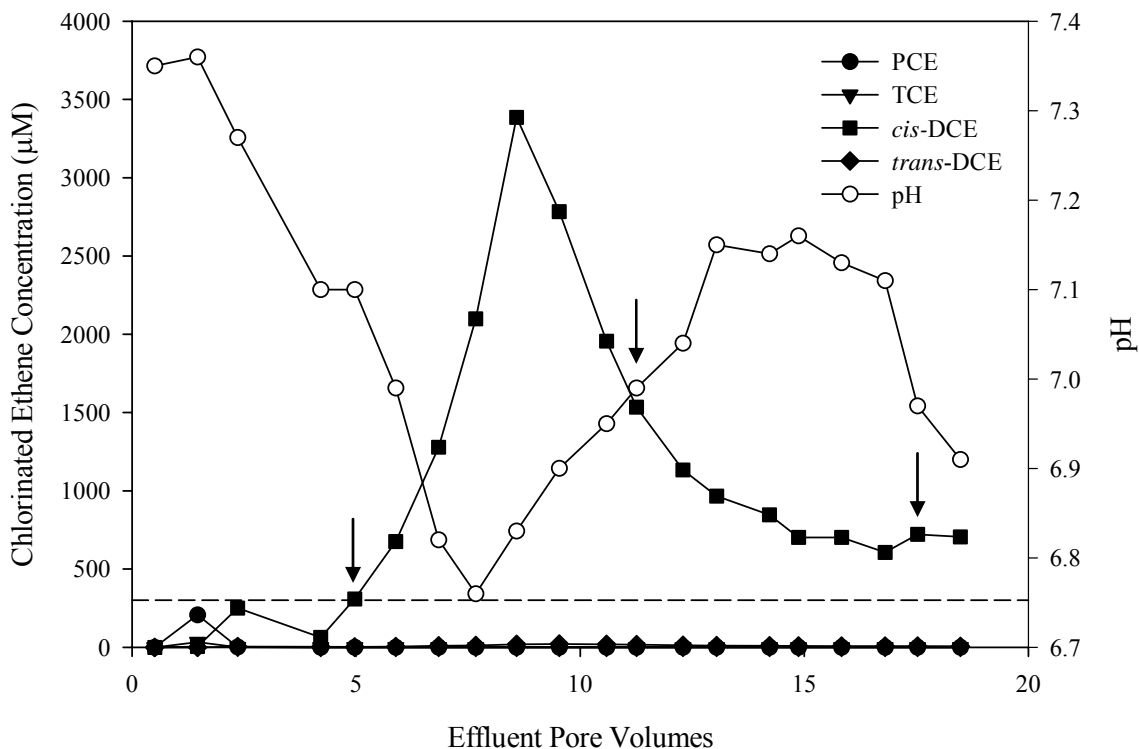
Figure 7.5: Effluent chlorinated ethene concentrations and pH measured during NAPL dissolution phase of experiment SM-Mixed. Arrows indicate side port sampling events.

From Figure 7.5 it is clear that pH decreased with increasing dechlorination activity (i.e., increasing *cis*-DCE concentrations). This was expected since the microbial reductive dechlorination process converts chlorinated ethenes in a stepwise fashion (i.e., PCE is converted to TCE, which is converted to DCE, etc.), with each step producing one mole of hydrochloric acid (HCl) as a side product per mole of chlorinated ethene converted. Therefore, transformation of one mole of *cis*- (or *trans*-) DCE results in the formation of two moles of hydrochloric acid, implying that reductive dechlorination may produce acid in sufficient quantities to subsequently decrease system pH. This was true

during experiment SM-Mixed, where the maximum effluent *cis*-DCE concentration observed (3,500 μM) represented the release of approximate 7,000 μM HCl. Despite the fact that the mineral salts medium flushed through the column was buffered with 60 mM bicarbonate, the HCl generation was sufficient to decrease the effluent pH from an initial value of 7.35 to a minimum of 6.76 when effluent *cis*-DCE concentrations approached 3,500 μM, an approximate change of 0.6 pH units. Reductive dechlorination by *S. multivorans* occurs optimally only within a narrow pH range (7.0-7.5), although dechlorination activity has been observed at pH values as low as 6.0 (Neumann et al. 1994). The decrease in effluent pH to levels below 7.0 that was observed during SM-Mixed may have therefore contributed to a decline in the dechlorination performance of *S. multivorans*, a possible explanation for the decrease in *cis*-DCE concentrations that followed exposure to low pH levels. In general, pH decreases in biologically-active DNAPL source zone may be expected unless the system is well buffered, and NAPL dissolution enhancement and subsequent microbial reductive dechlorination could lead to decreased performance of such biological systems due to low pH levels. This outcome is true for *S. multivorans* and may also occur in situations where other microorganisms that are important to the microbial reductive dechlorination process (e.g., *Dehalococcoides* species) exhibit narrow optimal pH ranges.

In addition to chlorinated ethene concentrations and pH, effluent biomass concentrations were monitored during experiment SM-Mixed. Figure 7.6 shows the measured effluent biomass concentrations (measured by *pceA* gene copies/mL), with the filled circles and open circles representing concentrations during the elution and NAPL dissolution phases of the experiment, respectively. Biomass concentrations were not
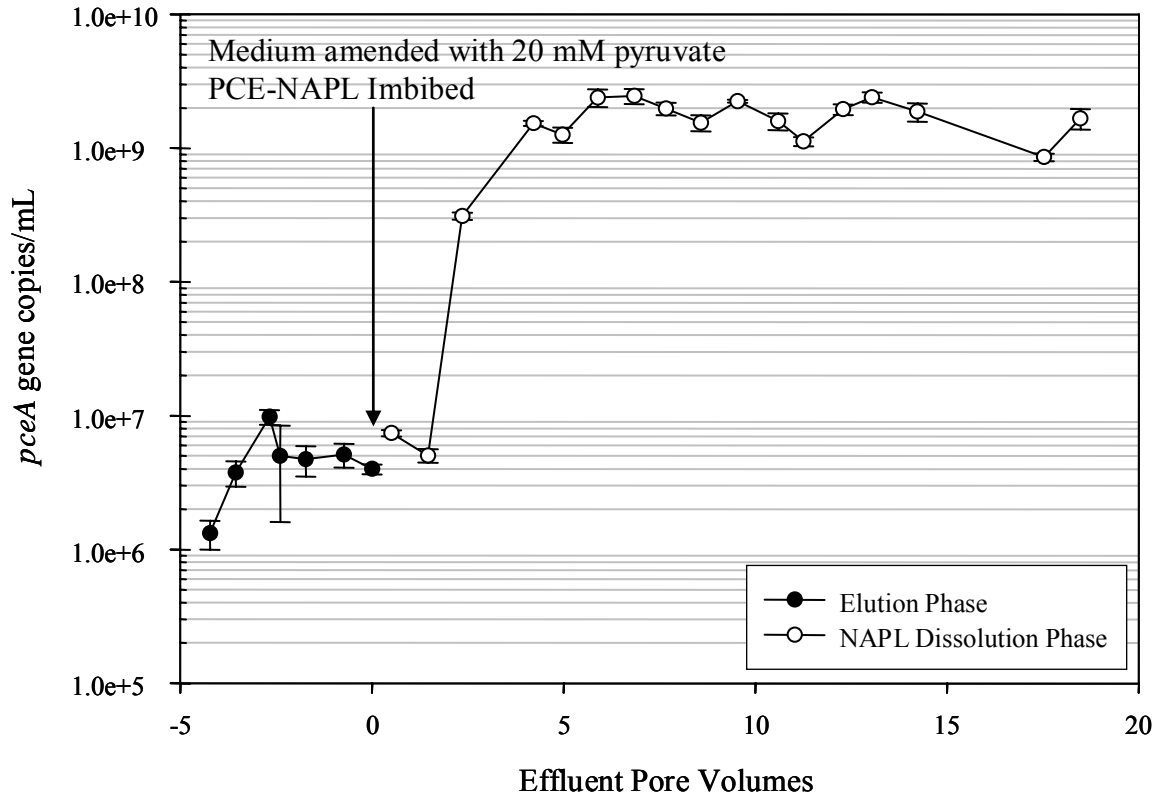
Figure 7.6: Effluent biomass concentrations measured during NAPL dissolution phase of experiment SM-Mixed. The arrow indicates NAPL imbibition and start of flushing with pyruvate-amended medium.

observed to increase significantly over those observed during the elution phase during the first two pore volumes of flushing with the pyruvate-amended mineral salts medium. However, following two pore volumes of flushing, a nearly 3 order-of-magnitude increase in effluent biomass concentrations was observed, with biomass increasing from approximately 6.0×10^6 *pceA* gene copies/mL to 2.0×10^9 *pceA* gene copies/mL (note that the y-axis of Figure 8.6 is on a logarithmic scale). Biomass concentrations remained relatively constant at this elevated level for the remainder of the NAPL dissolution phase of experiment SM-Mixed. At total of 1.0×10^{13} *pceA* gene copies were recovered over the course of the NAPL dissolution. This value is significantly greater than the number of *pceA* gene copies that were present in the column at the beginning of the NAPL

dissolution phase (2.4×10^{10} *pceA* gene copies), indicating that significant *S. multivorans* growth was ongoing in the biocolumn.

The first set of side port samples during SM-Mixed were taken following 5 pore volumes of flushing with the pyruvate-amended medium. The side port chlorinated ethene concentration profiles for the samples taken at 5 pore volumes are shown in Figure 7.7, with Port 1 located at the bottom of the column (i.e., nearest the influent medium). PCE concentrations within the mixed NAPL source zone (Ports 1 and 2), were comparable to the total chlorinated ethene concentration expected assuming no mass transfer enhancement (dashed line in Figure 7.7, 300 µM). In addition, *cis*-DCE concentrations in the source zone were relatively low (less than 100 µM), implying that any biological enhancement to mass transfer at this time was limited. Complete conversion of PCE to *cis*-DCE (as well as limited amounts of *trans*-DCE) was observed, however, by Port 4 of the column, and differences in *cis*-DCE concentrations over the remainder of the column may be due to differences in the source zone NAPL architecture along the right side and left side of the biocolumn, where the odd and even numbered ports were respectively located. Finally, effluent ethene concentrations corresponding to the 5 pore volume sampling event (see Figure 7.5) were not significantly greater than the expected total chlorinated ethene concentration (300 µM) further evidence of the absence of significant mass transfer enhancement within the NAPL source zone.

Figure 7.7: Side port chlorinated ethene concentrations for experiment SM-Mixed following 5 pore volumes of flushing. Port 1 is nearest the influent while port 11 is nearest the effluent.

A second series of side port samples were taken following 11 pore volumes of flushing during the NAPL dissolution phase, and the chlorinated ethene concentration profiles measured during this sampling event are shown in Figure 7.8. Corresponding effluent samples taken at this time (see Figure 7.5) demonstrated significant enhancement of contaminant dissolution, with measured *cis*-DCE concentrations (1,500 μM) that were significantly greater than the expected total chlorinated ethene concentration (300 μM). A similar conclusion can be reached by examining Figure 7.8, where the NAPL source zone (Ports 1 and 2) was not only characterized by high PCE concentrations, but by

elevated levels of TCE and, in particular, *cis*-DCE. The presence of TCE and *cis*-DCE within Ports 1 and 2 indicate that dechlorination was ongoing within the NAPL source zone; more importantly, the total chlorinated ethene concentrations within the source zone greatly exceed the value expected in the absence of mass transfer enhancement (300 μM). In addition, PCE and TCE were complete converted to DCE by Port 4 and *cis*-DCE concentrations over the remaining seven ports and effluent remained nominally stable at the elevated level of 1,300 to 1,500 μM.
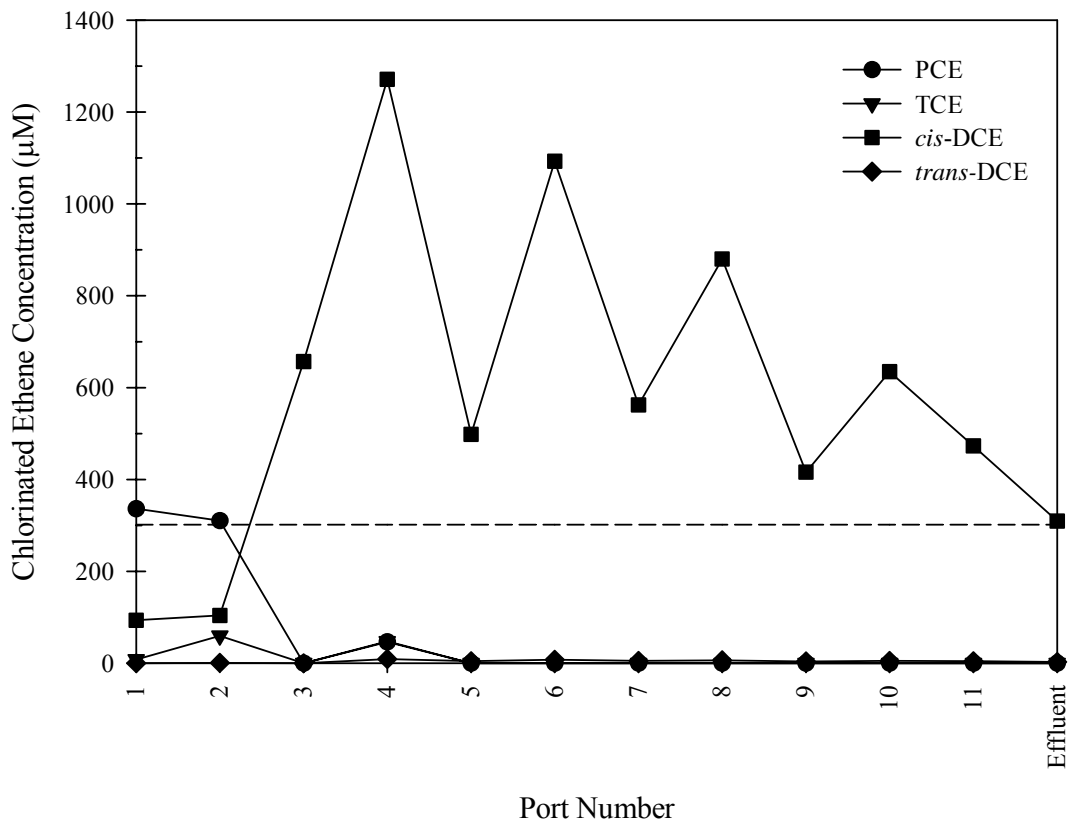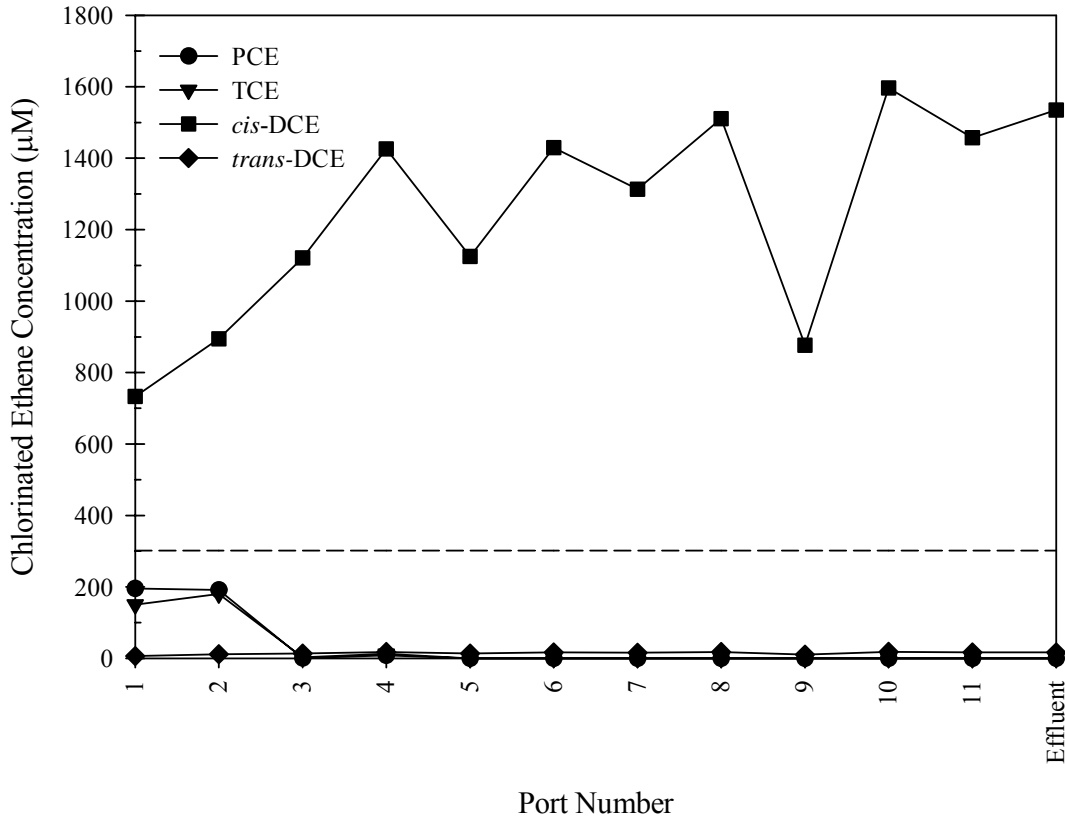

Figure 7.8: Side port chlorinated ethene concentrations for experiment SM-Mixed following 11 pore volumes of flushing. Port 1 is nearest the influent while port 11 is nearest the effluent.

A final set of side port samples were taken during experiment SM-Mixed following 17.5 pore volumes of flushing with pyruvate-amended mineral salts medium. In addition to chlorinated ethene concentrations, the samples were also analyzed for biomass, with both the chlorinated ethene and biomass concentration profiles shown in Figure 7.9. The chlorinated ethene profiles measured following 17.5 and 11 (Figure 7.8) pore volumes of flushing were comparable, with both profiles exhibiting elevated TCE and *cis*-DCE concentrations within the NAPL source zone (Ports 1 and 2) as well as complete conversion of PCE to DCE by Port 4. Chlorinated ethene concentrations were somewhat lower in the 17.5 pore volumes samples, however, a result consistent with effluent data showing that *cis*-DCE concentrations decreased from 1,500 µM at 11 pore volumes to 700 µM following 17.5 pore volumes. The difference in chlorinated ethene concentration could be due to a number of factors, including depletion of PCE from the mixed NAPL or a decrease in *S. multivorans* dechlorination performance arising from increased *cis*-DCE levels or decreased system pH. Biomass concentrations within the column (measured as *pceA* gene copies/mL) increased from 4.5×10^8 to 1.4×10^9 between Ports 1 and 4, after which the concentrations decreased to a nominally stable value of 6.0×10^8 to 8.0×10^8 over the remaining sampling ports. Biomass concentrations closely coincided with the measured *cis*-DCE concentrations, particularly over the first four sampling ports, implying that the majority of biological activity within the column was occurring within the mixed NAPL source zone.
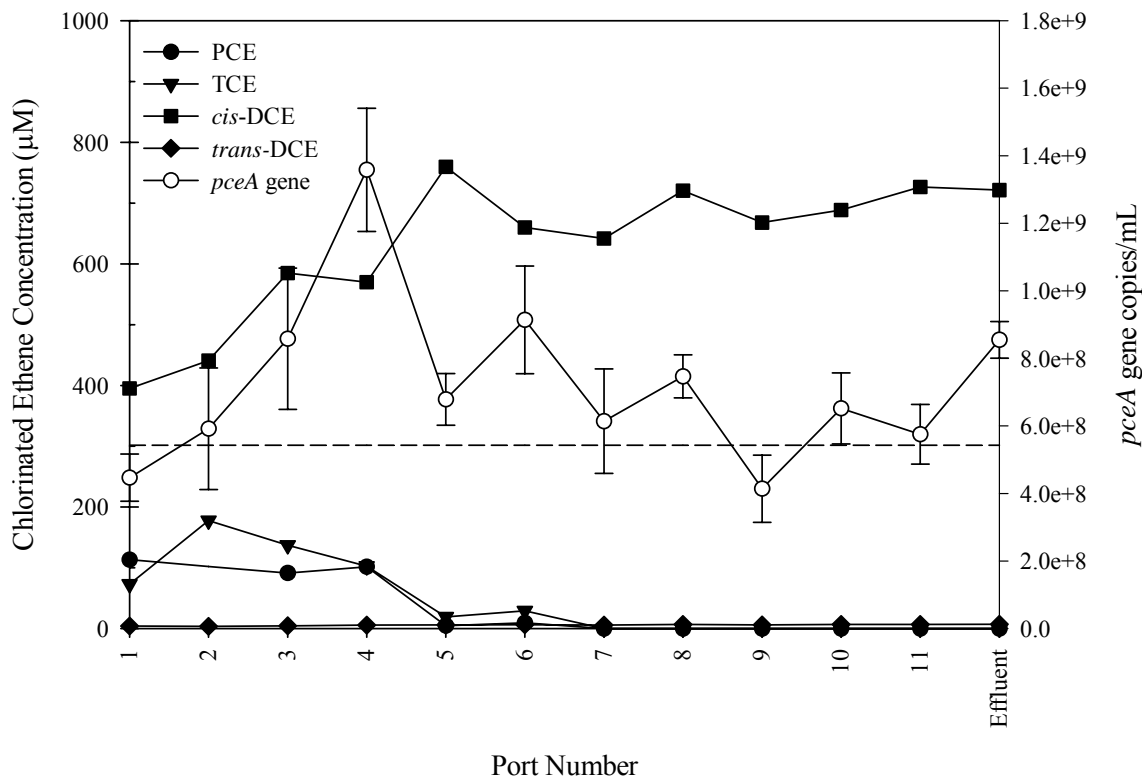
Figure 7.9: Side port chlorinated ethene and biomass concentrations for experiment SM-Mixed following 17.5 pore volumes of flushing. Port 1 is nearest the influent while port 11 is nearest the effluent.

Biomass was extracted from the biocolumn porous media, which was excavated from the column following cessation of flushing with pyruvate-amended mineral salts medium (18.6 pore volumes of operation), and the porous media-associated biomass concentrations at each side port measured. The associated biomass concentrations was compared to those measured during the 17.5 pore volume side port sampling event to assess whether liquid-phase biomass samples were able to accurately reflect biomass distribution within the column. The biomass concentrations measured from the extracted solid phase (*pceA* gene copies/g sediment) and the liquid phase (*pceA* gene copies/mL) are compared in Figure 7.10. Although the measured biomass concentration ranges are

very different, on the order of 10^7 *pceA* gene copies/g sediment versus 10^9 *pceA* gene copies/mL, the respective biomass concentration trends are similar, with both biomass concentrations increasing over the first four sampling ports (i.e., the source zone) and remaining relatively constant over the remaining seven ports (i.e., the plume region). Based on this result, it may be inferred that liquid biomass samples are sufficient to characterize microbial distributions within the biocolumn.
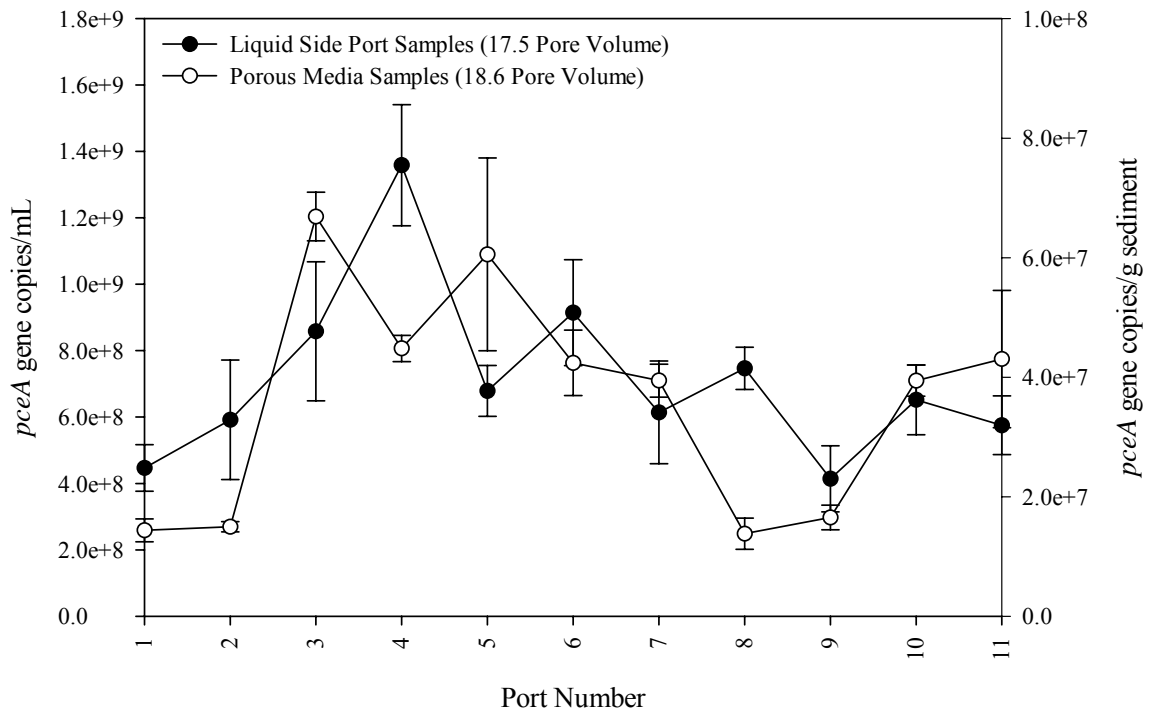
Figure 7.10: Comparison of biomass concentrations from liquid samples following 17.5 pore volumes of flushing and extracted from column porous media following 18.6 pore volumes of flushing for experiment SM-Mixed. Port 1 is nearest the influent while port 11 is nearest the effluent.

7.2.3.2 Experiment SM-Pure

The NAPL dissolution phase of experiment SM-Pure was conducted for a period of 11.5 pore volumes of flushing with pyruvate-amended mineral salts media following

the establishment of a pure PCE-DNAPL source zone over the first 10 cm of the biocolumn. The column effluent was sampled daily for chlorinated ethene concentrations, biomass, and pH (pH data not shown). In addition, the side ports located along the column length were sampled for chlorinated ethenes and biomass following 11.5 pore volumes of column operation during the NAPL dissolution phase.

Effluent chlorinated ethene concentrations measured over the course of SM-Pure are shown in Figure 7.11a, with the arrow indicating the time at which the side ports were sampled. The total expected chlorinated ethene concentration (PCE, TCE, and *cis*-DCE) in the absence of biologically-enhanced mass transfer from the NAPL is shown in Figure 7.11a as a dashed line. This value was assumed to be equal to the equilibrium solubility of PCE, approximately 1,200 μM (200 mg/L). Effluent PCE concentrations increased to values near solubility following 1.7 pore volumes of operation and remained at this level for the remainder of the experiment. Both TCE and *cis*-DCE were observed in the effluent; however concentrations were low, with TCE values ranging between 0 and 2 μM and *cis*-DCE increasing to just 7 μM following 11.5 pore volumes of flushing with pyruvate-amended media. Given the modest dechlorination product concentrations observed, the maximum biological enhancement factor (total effluent chlorinated ethene concentration divided by the expected total concentration in the absence of dissolution enhancement) reached a value of only 1.09, much of which was due to the measured PCE effluent concentrations occasionally exceeding solubility, indicating an absence of dissolution enhancement. Taken together, the effluent results indicate that little dechlorination activity, either directly in the PCE-DNAPL source zone or the down-gradient plume region, was ongoing in the column.
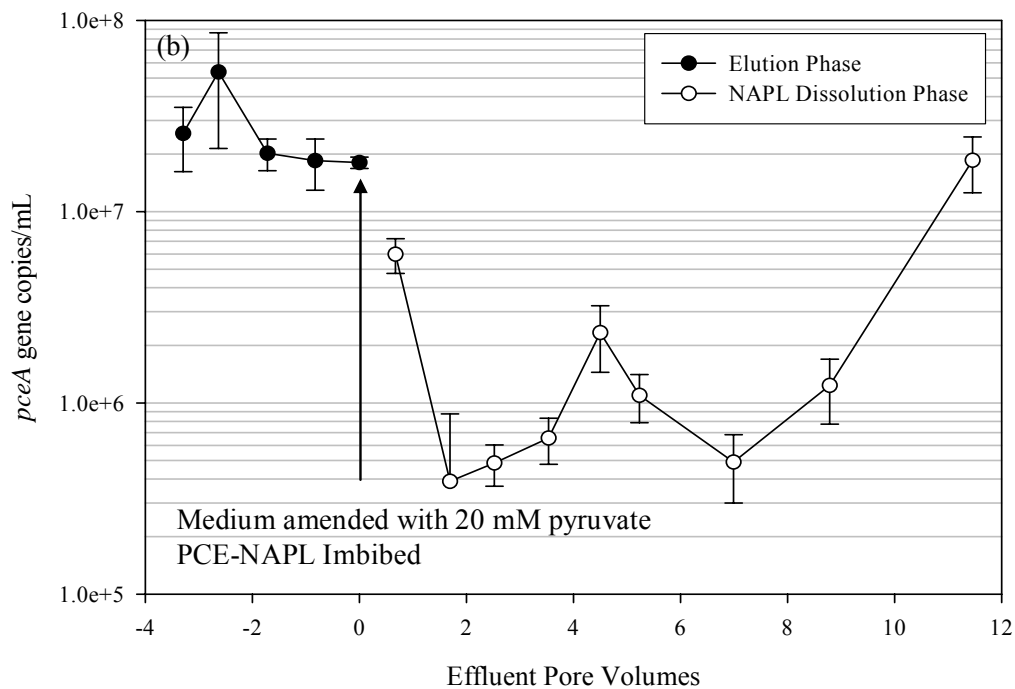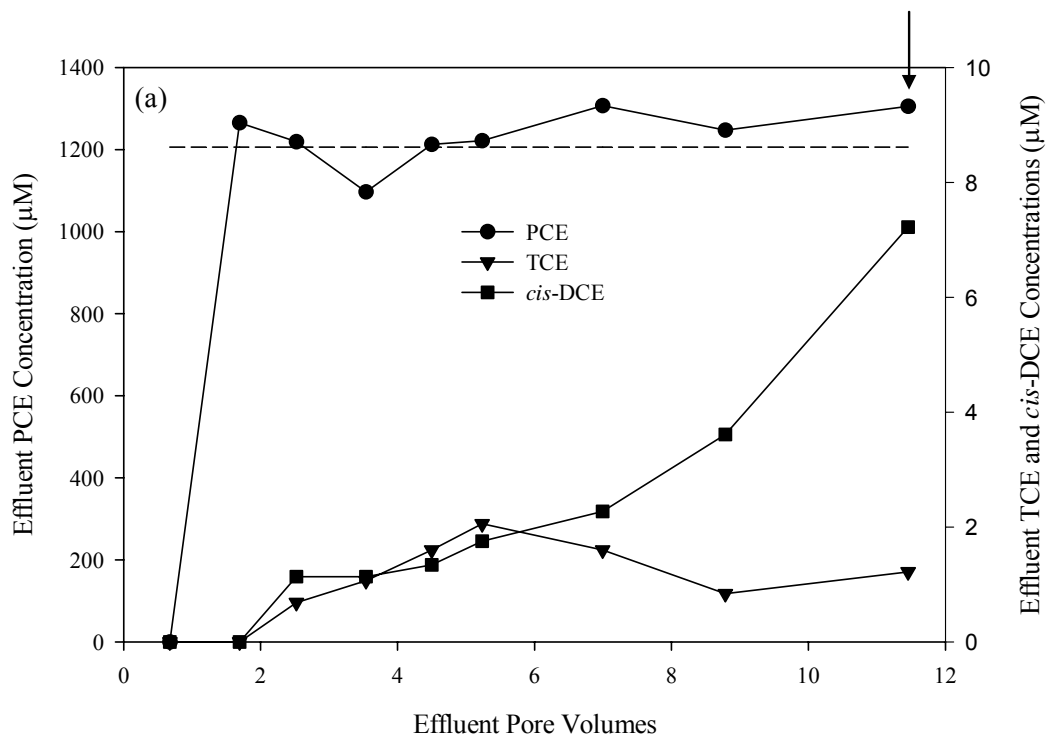
Figure 7.11: Effluent chlorinated ethene (a) and biomass (b) concentrations measured during NAPL dissolution phase of experiment SM-Pure. Arrow indicates side port sampling event.

During experiment SM-Pure the column effluent was also sampled for biomass, with the measured effluent biomass concentrations (in units of $pceA$ gene copies/mL) for both the elution and NAPL dissolution phases of the experiment shown in Figure 7.11b. Following imbibition with the PCE-DNAPL, effluent biomass concentrations decreased by nearly 2 orders-of-magnitude, from approximately 2.0×10^8 $pceA$ gene copies/mL to 5.0×10^6 $pceA$ gene copies/mL, and remained relatively constant until just prior to the conclusion of the experiment. The final effluent sample taken showed a possible rebound of biomass concentration to pre-NAPL values, but it is unclear if this is significant. In general, the observed decrease in effluent biomass signifies a decline in *S. multivorans* population within the biocolumn, a result consistent with toxic effects to the microorganisms due to the elevated PCE concentrations present in the system (see e.g., Nambi et al. 2003).

A single series of side port samples were taken during SM-Pure following 11.5 pore volumes of flushing with pyruvate-amended medium. The side ports were sampled for both chlorinated ethenes and biomass, and the respective concentration profiles are shown in Figures 7.12a and 7.12b. PCE concentrations throughout the column were at elevated concentrations, often exceeding the expected solubility value of 1,206 μM (200 mg/L). It is unclear why the PCE concentrations exceed solubility, potential explanations may include some component of the pyruvate-amended mineral salts medium acting to enhance the contaminant solubility. While PCE concentrations measured at the side ports were high, dechlorination daughter products (i.e., TCE and *cis*-DCE) were only present at very low concentrations, not exceeding 8 μM at any point within the column. In addition, biomass concentrations in the column ranged from 1.0×10^6 $pceA$ gene copies/mL to
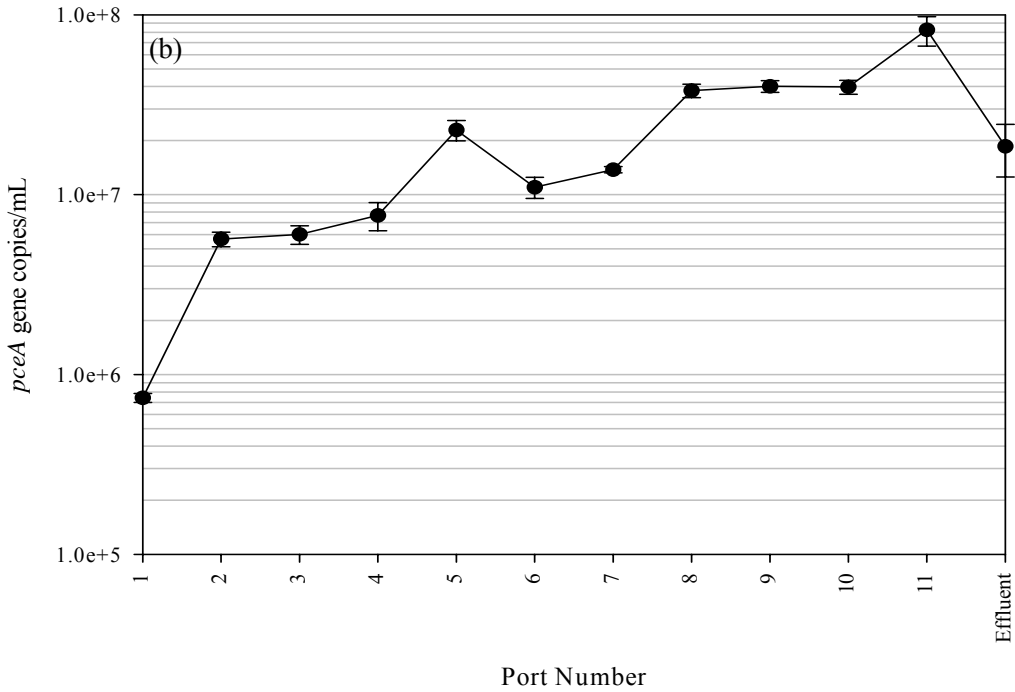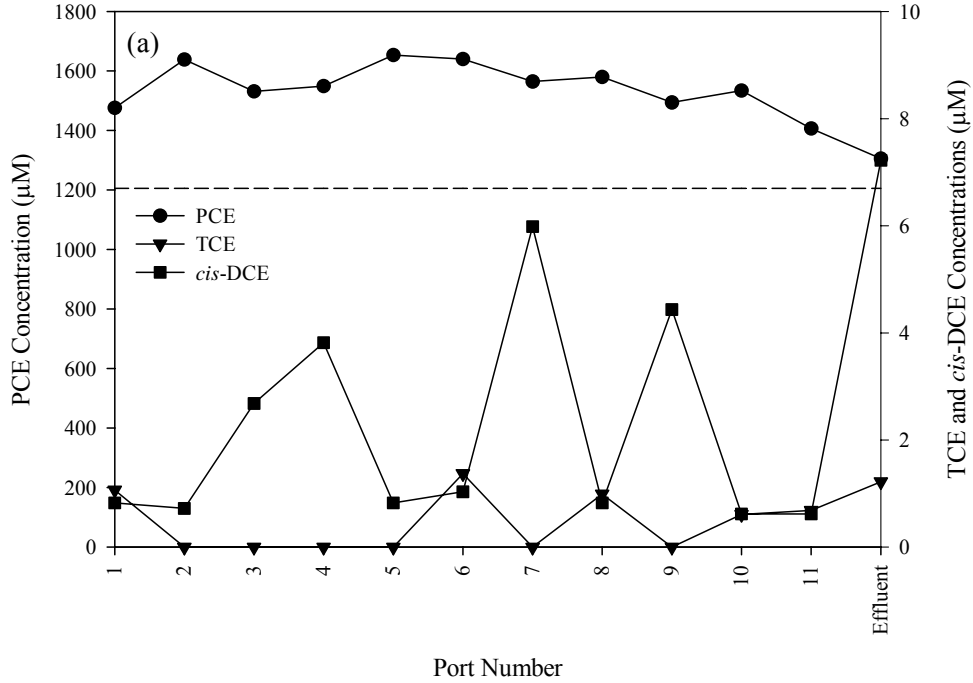
Figure 7.12: Side port chlorinated ethene (a) and biomass (b) concentrations for experiment SM-Pure following 11.5 pore volumes of flushing. Port 1 is nearest the influent while port 11 is nearest the effluent.

1.0x10^8 *pceA* gene copies/mL. While the concentrations increased down-gradient from the PCE-DNAPL source zone (Ports 1 and 2), they remained significantly lower than those observed during experiment SM-Mixed (1.0x10^9 *pceA* gene copies/mL), which when taken with the lack of dechlorination products observed indicates that microbial activity throughout the entire column was severely limited when the pure PCE-DNAPL was present.

7.2.4 Cumulative Chlorinated Ethene Recovery and Mass Transfer Enhancement

Cumulative chlorinated ethene recoveries, both on a molar as well as percent basis, for experiment SM-Mixed are shown in Figure 7.13a and summarized in Table 7.3. A total of 7,630 μmol of chlorinated ethenes (i.e., PCE, TCE, *cis*-DCE, and *trans*-DCE) were recovered over the course of SM-Mixed, representing approximately 53% recovery of the PCE initially present in the column following NAPL imbibition (14,400 μmol). Of the chlorinated ethenes recovered, the majority (7,470 μmol) was *cis*-DCE, with trace amounts of PCE (80 μmol), TCE (10 μmol), and *trans*-DCE (70 μmol) also recovered from the column effluent. The total chlorinated ethene recovery during SM-Mixed was significantly greater than the expected PCE mass recovery under abiotic conditions. Assuming an initial aqueous PCE solubility of 50 mg/L, accounting for changing NAPL composition with PCE mass depletion, and assuming equilibrium mass transfer at the operation flow rate of the column (0.25 mL/min), the expected abiotic mass recovery following 18.5 pore volumes of column operation was 1,640 μmol. This is significantly lower than the actual chlorinated ethene recovery, implying the occurrence of biological mass transfer enhancement. The enhancement factor was quantified by dividing the experimental cumulative mass recovery by the expected abiotic mass recovery. As

243

shown in Figure 7.13b, the mass transfer enhancement factor for SM-Mixed was approximately unity (i.e., no enhancement) for the first 5 pore volumes of operation, before rapidly increasing to a maximum value of approximately 4.7 following 10 pore volumes of operation, where it remained until termination of flow through the column. This is comparable to previously reported literature results (see e.g., Cope and Hughes 2001, Yang and McCarty 2002) where enhancement in column experiments ranged from 3 to 6.

Table 7.3: Chlorinated ethene mass recoveries and mass transfer enhancement factors for *S. multivorans* biocolumn experiments.

Biocolumn Parameter	SM-Mixed	SM-Pure
Initial PCE Loading (µmol)	14,400	87,010
Total Chlorinated Ethenes Recovered (µmol) [%]	7,630 [53.0]	5,640 [6.5]
PCE Recovered (µmol) [%]	80 [0.6]	5,610 [6.4]
TCE Recovered (µmol) [%]	10 [0.1]	10 [0.06]
cis-DCE Recovered (µmol) [%]	7,470 [51.9]	20 [0.04]
trans-DCE Recovered (µmol) [%]	70 [0.4]	0 [0]
Expected Abiotic PCE Recovered (µmol) [%]	1,640 [11.4]	5,430 [6.2]
Maximum Mass Transfer Enhancement Factor	4.74	1.04
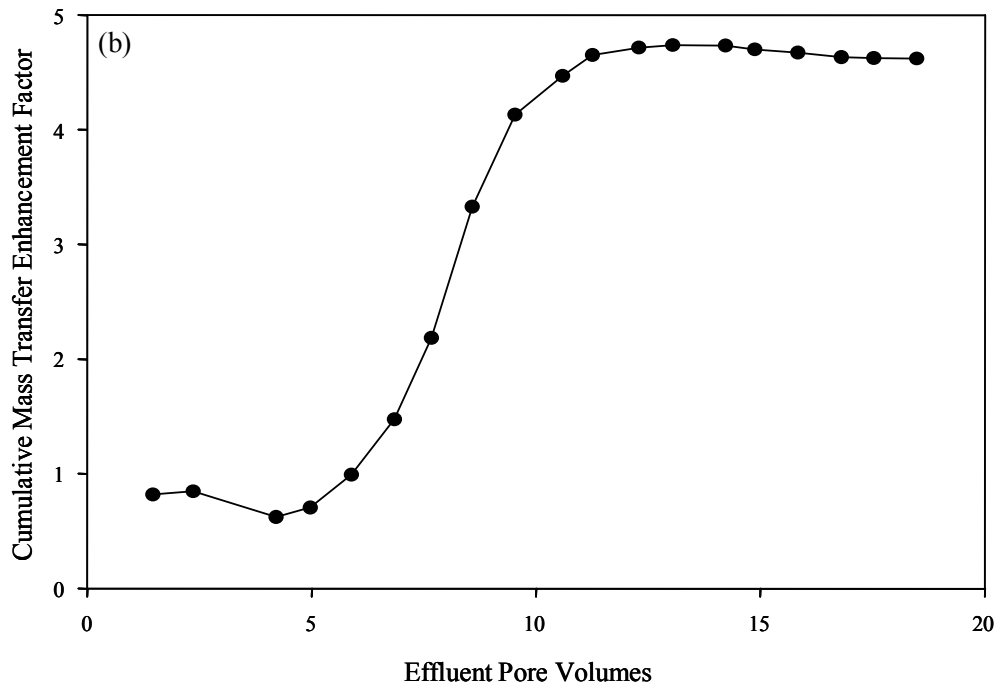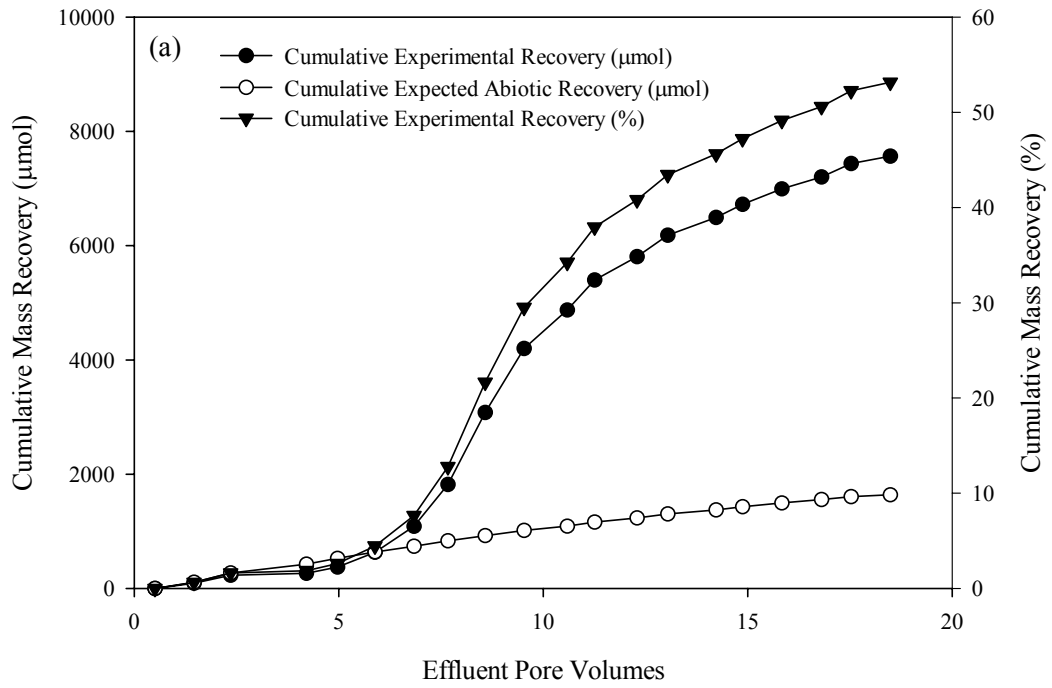
Figure 7.13: Cumulative chlorinated ethene molar recovery (a) and cumulative mass transfer enhancement factor (b) for experiment SM-Mixed.

Chlorinated ethene recovery (both molar and percentage) for experiment SM-Pure is shown in Figure 7.14a. Overall chlorinated ethene was during SM-Pure was low, with 5,640 μmol (6.5%) of the PCE initially present in the column following imbibition of the pure PCE-DNAPL recovered over the 11.5 pore volumes of column operation. PCE, TCE, and *cis*-DCE were all recovered, the majority of which was PCE (5,610 μmol, see Table 7.3) rather than dechlorination daughter products, indicating that dechlorination activity within SM-Pure was limited. In addition, the experimental cumulative chlorinated ethene recovery during SM-Pure was not significantly greater than the expected recovery under abiotic conditions (5,430 μmol), assuming an aqueous PCE solubility of 200 mg/L and equilibrium mass transfer. The similarity between the experimental and expected mass recoveries demonstrates the absence of significant biological mass transfer enhancement within the biocolumn during SM-Pure. This was confirmed by quantifying a mass transfer enhancement factor for SM-Pure, as shown in Figure 8.14b. The enhancement factor was approximately one over the course of column operation, indicating that the limited occurrence (or absence) of biologically-enhanced dissolution of the pure PCE-DNAPL.
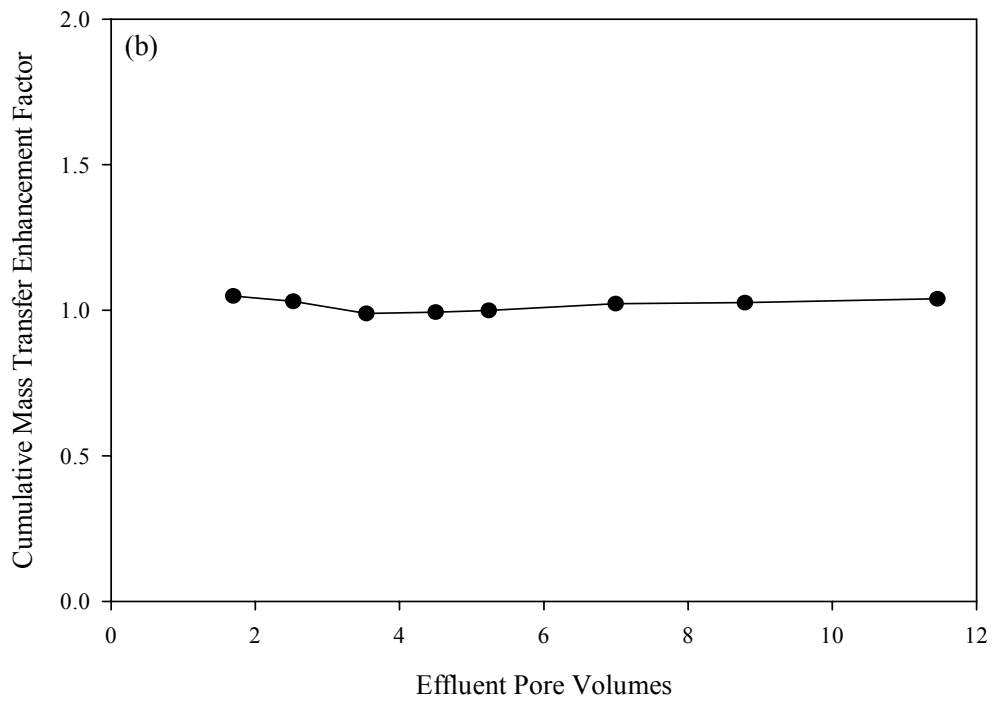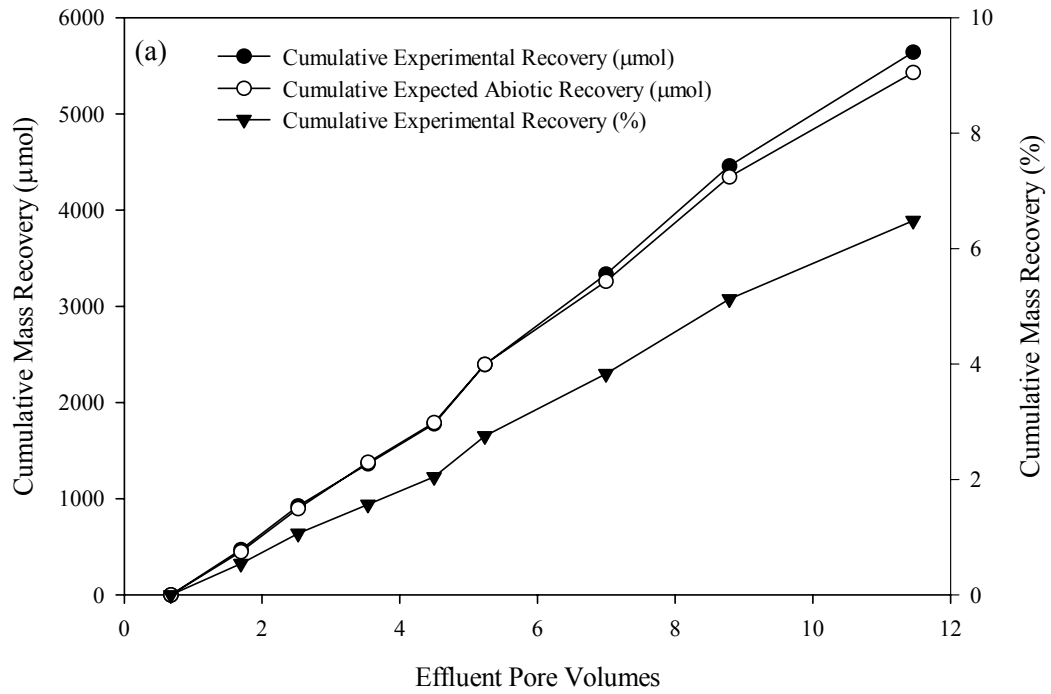
Figure 7.14: Cumulative chlorinated ethene molar recovery (a) and cumulative mass transfer enhancement factor (b) for experiment SM-Pure.

7.3 Summary and Conclusions

Results from the biocolumn experiments presented here are among the strongest evidence to date linking growth of microbial species capable of reductive dechlorination with enhanced dissolution of PCE from a NAPL source zone. Quantitative PCR permitted monitoring of *S. multivorans* populations (via the *pceA* gene) both *in situ* along the column length and in the column effluent. During experiment SM-Mixed, where aqueous phase PCE concentrations were moderate (approximately 300 μM or 50 mg/L), PCR results clearly demonstrated a several order-of-magnitude increase in effluent biomass following NAPL imbibition and initiation of flushing with pyruvate-amended medium. Side port sample results demonstrated that increasing biomass concentrations within the PCE-NAPL source zone coincided with increasing concentrations of dechlorination products (i.e., *cis*-DCE), implying the presence of active *S. multivorans* populations within the source zone. However, experiment SM-Pure, characterized by aqueous PCE concentrations near saturation (1,200 μM or 200 mg/L),s produced little evidence of *S. multivorans* growth and activity, both in the biocolumn effluent and along the column profile. While this result is somewhat disappointing, it is important to remember that this experiment represented a "worst case" scenario (i.e., the highest possible aqueous phase PCE concentration) and it is unlikely that PCE concentrations measured at field site will reach these levels. For more realistic concentrations such as those in SM-Mixed, a significant (4.7-fold) cumulative enhancement of NAPL dissolution was achieved, with enhancement sustained (albeit at decreasing levels) throughout the entire experiment. Hence, bioaugmentation or biostimulation of a PCE-NAPL source zone may be an effective tertiary treatment strategy for accelerated mass

recovery and control of post-treatment plume development, particularly in scenarios where primary treatment can reduce effluent concentrations to levels non-toxic to the microorganisms, for example the surfactant flushing strategies previously described in Chapters 5 and 6 of this work.

CHAPTER 8

QUANTITATIVE PCR CORRELATES MICROBIAL ACTIVITY

AND DISTRIBUTION WITH ENAHNCED CONTAMINANT

DISSOLUTION FROM A PCE-NAPL SOURCE ZONE

PART 2: BIO-DECHLOR INOCULUM

8.1 Introduction

Numerous aggressive *in situ* treatments (e.g., surfactant and cosolvent flushing, thermal treatment, air sparging, chemical oxidation) have been investigated as methods for accelerating contaminant mass recovery from DNAPL source zones (Stroo et al. 2003). While some field tests of these technologies have reported DNAPL mass recoveries in excess of 90% (Londergan et al. 2001, Hasegawa et al. 2000), it is generally recognized that NAPL recoveries on the order of 60-70% are a more likely remedial outcome (Stroo et al. 2003, NRC 2004, Brooks et al. 2004, Holmzer et al. 2000, Jawitz et al. 2000, Rao et al. 1997, Soga et al. 2004). Resulting post-treatment dissolved-phase contaminant concentrations within, and emanating from, DNAPL source zones will likely exceed drinking water standards (Soga et al. 2004, Sale and McWhorter 2001) and removal of NAPL mass remaining post-treatment may require considerable periods of time, particularly when contaminant dissolution is limited due to its distribution within the source zone porous media (Christ et al. 2005a). A promising strategy for the efficient detoxification and recovery of contaminant mass present following aggressive physicochemical treatment is the use of microbial reductive dechlorination, via either biostimulation or bioaugmentation.

250

Reductive dechlorination involves the sequential reduction of PCE to TCE, *cis*-DCE, vinyl chloride, and ethene. If dechlorination occurs metabolically, the process, although often requiring introduction of an external electron donor into the source zone, may be an efficient mechanism for PCE bioremediation. PCE may be converted to *cis*-DCE by a number of phylogenetic groups, including *Dehalobacter, Sulfurospirillum, Desulfuromonas, Desulfitobacterium,Clostridium bifermentans* strain DPH-1, and *Geobacter* (see Christ et al. 2005a). These organisms are incapable of complete dechlorination to ethene (Löffler et al. 2003) and may generate toxic intermediates within the subsurface. Dechlorination beyond *cis*-DCE to vinyl chloride (VC) and ethene is limited to members of the *Dehaolcoccoides* group (Löffler and Edwards 2006), and since no *Dehaolcoccoides* isolate is capable of growth using all chlorinated ethenes as electron acceptors (Löffler and Edwards 2006) successful PCE dechlorination to ethene requires the presence of multiple dechlorinating organisms.

It has generally been believed that toxic effects would preclude reductive dechlorination at aqueous PCE concentrations near saturation or within PCE-DNAPL source zones (Robertson and Alexander 1996). Recently, however, PCE dechlorination has been demonstrated in batch systems at PCE concentrations near saturation (Nielson and Keasling 1999, Yang and McCarty 2000) as well as in the presence of PCE-DNAPL (Carr et al. 2000). Dechlorination performance during batch studies was sufficiently promising to warrant further investigation, with a number of column studies conducted to evaluate microbial reductive dechlorination activity within a DNAPL source zone. Dechlorination activity with mixed PCE-to-ethene dechlorinating cultures was observed by both Cope and Hughes (2001) and Yang and McCarty (2002); however activity stalled

at vinyl chloride for the former and *cis*-DCE for the latter. Despite the lack of complete dechlorination, contaminant dissolution from the columns was enhanced by factors from 3-fold (Yang and McCarty 2002) to 6-fold (Cope and Hughes 2001), indicating that decreases in source zone longevity may be possible through reductive dechlorination. A number of technical obstacles, including column bio-clogging (Yang and McCarty 2002), partitioning of dechlorination products into the DNAPL (Adamson et al. 2004), and pH toxicity effects (Cope and Hughes 2001) were apparent, and no information is available regarding microbial populations and distributions within the columns.

Recent experimental efforts have focused on utilizing recently developed molecular tools to link microbial growth and population distribution with reductive dechlorination either within, or down-gradient from, a DNAPL source zone. In Chapter 7 of this work, effluent and side port samples (chlorinated ethene and biomass) from a 1-D biocolumn containing a mixed NAPL comprised of 0.25 mol/mol PCE in hexadecane clearly linked growth of microbial species capable of reductive dechlorination with enhanced dissolution of PCE from a NAPL source zone. While the ability to link growth to dechlorination was promising, the culture used in this work, *Sulfurospirillum multivorans*, is incapable of dechlorination beyond *cis*-DCE. A study evaluating bioaugmentation of a 2-D aquifer cell containing a pure PCE-DNAPL with a mixed PCE-to-ethene culture was conducted by Sleep et al. (2006). Effluent measurements demonstrated significant (3-fold) maximum PCE dissolution enhancement. In addition, ethene production was observed, coincident with growth of *Dehalococcoides* in the vicinity of and down-gradient from the PCE-DNAPL source zone.

The goal of this study was to further the work described in Chapter 7, evaluating microbial reductive dechlorination activity and distribution in the vicinity of a PCE-NAPL source zone. Instead of a pure dechlorinating culture (*S. multivorans*), a mixed microbial consortium (Bio-Dechlor INOCULUM, BDI) capable of complete PCE conversion to ethene was inoculated into the 1-D biocolumn. A single experiment was conducted, with a mixed NAPL (0.25 mol/mol PCE in hexadecane) imbibed into the source zone. As before, the biocolumn featured uniform (and known) initial PCE-NAPL and biomass distributions. Molecular tools were used to quantify and track microbial species of interest within the biocolumn. Effluent chlorinated ethene and biomass concentrations were monitored daily to evaluate reductive dechlorination performance down-gradient from the biologically-active PCE-NAPL source zone. Periodic side port samples were also taken to monitor chlorinated ethene and biomass concentration profiles within the biocolumn, and the cumulative chlorinated ethene recovery was determined and compared to expected abiotic recovery to evaluate biological contaminant mass transfer enhancement.

8.2 Results and Discussion

The BDI biocolumn experiment was conducted in the one-dimensional (1-D) column described in Chapter 3. At the conclusion of column packing, inoculation, and microbial community establishment, the biocolumn was imbibed with a mixed NAPL comprised of 0.25 mol/mol PCE in hexadecane and having an aqueous PCE solubility of 300 μM (50 mg/L). Following NAPL source zone establishment, the biocolumn was flushed with reduced mineral salts medium amended with 20 mM lactate and chlorinated ethene and biomass concentrations monitored. Weekly side port sampling events were

also conducted and the samples analyzed for chlorinated ethene and/or biomass concentrations. In addition, cumulative PCE mass recovery was determined based on effluent chlorinated ethene results, along with biological mass transfer enhancement factors. It should be noted that a number of relevant dechlorinating organisms are present in BDI, including *Dehalobacter*, *Geobacter*, and *Dehalococcoides* species. This research will focus only on analysis of *Dehalococcoides* populations; *Dehalobacter* and *Geobacter* results will be presented in Ben Amos's PhD dissertation (expected in May 2007).

8.2.1 Microbial Community Establishment and NAPL Imbibition

Once packed and inoculated, the BDI biocolumn was maintained under the condition of zero aqueous-phase flow for a period of approximately 24 hours to promote microbial community establishment within the column porous media. Reduced mineral salts medium was then flushed through the column at a nominal flow rate of 0.25 mL/min to elute unattached biomass. It was assumed that minimal growth and/or decay of the microbial community was ongoing during this phase of the experiment, a reasonable belief given that the mineral salts medium was not amended with a carbon source, electron donor, or electron acceptor. Daily samples were taken during the microbial community establishment portion of the BDI biocolumn experiment. DNA was extracted from the samples and analyzed using real time PCR to quantify the numbers of relevant organisms (i.e., *Dehalobacter*, *Geobacter*, and *Dehalococcoides* species) eluted from the biocolumn.

Duration of the elution phase of the BDI biocolumn experiment was 3.3 pore volumes, during which time the reduced mineral salts medium was not amended with

lactate. Effluent *Dehalococcoides* (*Dhc*) cell copies per milliliter eluted from the biocolumn as a function of the total effluent pore volume is shown in Figure 8.1a. The quantity of eluted *Dhc* cells was relatively high for the first 1.6 pore volumes of flushing, ranging from $4.6\text{x}10^7$ to $1.3\text{x}10^8$ cells/mL. These values were comparable to the quantity of *Dhc* present in the BDI inoculum ($1.8\text{x}10^8$ cells/mL), indicating that a significant fraction of the biomass initially present in the biocolumn was eluted. After 1.6 pore volumes of operation, effluent *Dhc* cell counts decreased by nearly two orders-of-magnitude for the remainder of the elution phase. Based on the effluent *Dhc* cell quantities, the cumulative percentage of *Dhc* cells eluted from the BDI biocolumn was estimated (Figure 8.1b). The quantity of *Dhc* initially present in the biocolumn was estimated based on the inoculum biomass density ($1.8\text{x}10^8$ cells/mL) and the liquid pore volume of the biocolumn (410 mL). Cumulative effluent *Dhc* cells eluted from the biocolumn were divided by this value to obtain an estimate of the percentage of *Dhc* recovered from the column, assuming that no microbial growth or decay was occurring. Recovery of *Dhc* was observed to rapidly increase to a value of nearly 90% following 1.6 pore volumes of column operation, where it remained for the remainder of the microbial elution phase. Hence, the fraction of *Dhc* attached and/or retained within the biocolumn of was relatively small, unlike for *S. multivorans* (see Chapter 7), with approximately 10% of the *Dhc* biomass initially present during packing retained.
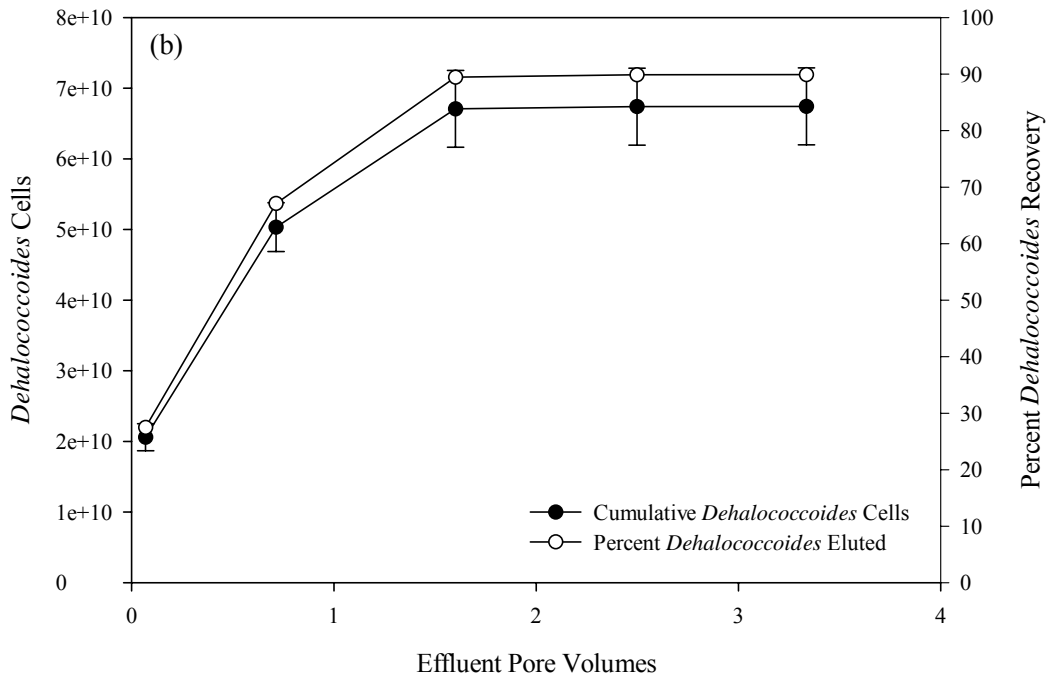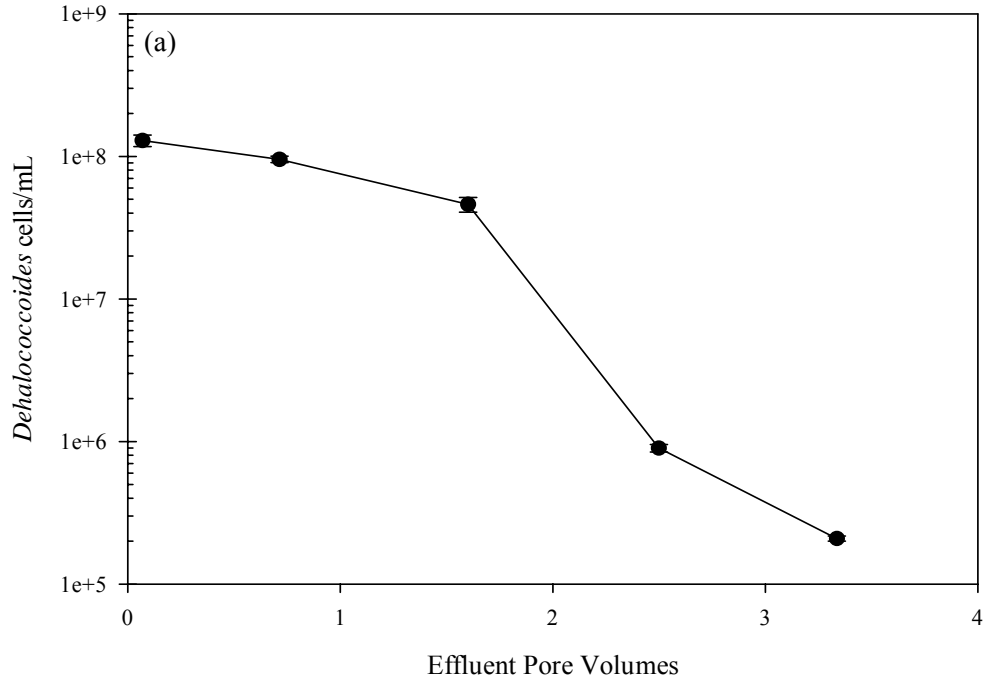
Figure 8.1: Effluent *Dehalococcoides* cells/mL (a) and cumulative *Dehalococcoides* cells recovered (b) as a function of pore volumes flushed during microbial elution phase of BDI biocolumn experiment.

Following the elution phase of the BDI experiment, a mixed NAPL comprised of 0.25 mol/mol PCE in hexadecane was imbibed with over the bottom 10 cm of the column. The mixed NAPL had a density of 0.86 g/cm^3 and yielded an equilibrium PCE solubility of slightly greater than 300 μM (50 mg/L). A mixed NAPL was selected for use in the BDI based on results from *S. multivorans* columns (see Chapter 7) indicating that, for the experimental conditions present in the biocolumn, reductive dechlorination in the presence of pure PCE-DNAPL was unlikely to occur. A total of 16 mL (1.66 mL of PCE) were imbibed over the first 10 cm of column length and the residual PCE-NAPL saturation within the column source zone was estimated to be 23.4%, given the overall pore volume of the column during the BDI experiment (410 mL). Distribution of the PCE-NAPL within the source zone was reasonably uniform over the first 10 cm of the column (i.e., before the second sampling port), although some NAPL fingering was observed between Ports 2 and 3. The experimental conditions for the BDI biocolumn experiment are summarized in Table 8.1.

Table 8.1: Summary of conditions for BDI biocolumn experiment.

Biocolumn Parameter	BDI Biocolumn
Column Pore Volume (mL)	410
NAPL Composition	Mixed[a]
NAPL Density (g/cm^3)	0.86
Equilibrium PCE Solubility (μM) [mg/L]	300 [50]
NAPL Injection Volume (mL)	16
Source Zone NAPL Saturation (%)	23.4

a: 0.25 mol/mol PCE in hexadecane

During the NAPL dissolution phase of the BDI biocolumn experiment, flushing was conducted using reduced mineral salts medium amended with 20 mM lactate to act as a carbon source and electron donor. The NAPL dissolution phase was operated for a totally period of 38.4 pore volumes, at a nominal aqueous-phase flow rate of 0.25 mL/min (1.1 day residence time) for the first 21.6 pore volumes and 0.1 mL/min (2.8 day residence time) for the remaining 16.8 pore volumes of flushing. Effluent samples were collected every 1 or 2 days, depending on the operational flow rate, and analyzed for chlorinated ethenes, biomass, and organic acids. In addition, the biocolumn side ports were sampled approximately weekly (at 8.7, 14.0, 20.3, 27.8, and 33.8 pore volumes of operation) and analyzed for chlorinated ethenes and biomass. Results from both the effluent and side port samples are presented below.

Measured effluent chlorinated ethene concentrations during the NAPL dissolution phase of the BDI biocolumn experiment are shown in Figure 8.2. The arrows in the figure denote the occurrence of side port sampling events, and the solid and dashed vertical lines correspond to an approximate 22 hour interruption of aqueous flow into the column and a decrease in the aqueous flow rate from 0.25 mL/min to 0.1 mL/min, respectively. The horizontal dashed line in Figure 8.2 corresponds to concentrations values on the left y-axis and is the expected total chlorinated ethene concentration in the column effluent (PCE, TCE, *cis*-DCE, *trans*-DCE, VC, and ethene) in the absence of biological mass transfer enhancement of PCE from the mixed NAPL. This value was initially expected to be equal to the equilibrium solubility of PCE from the mixed NAPL

(300 µM or 50 mg/L) and decrease over time as the NAPL was depleted of PCE, thereby lowering the PCE mole fraction in the organic phase.

Limited dechlorination activity was observed in the BDI biocolumn for approximately the first 3.5 pore volumes of operation (see Figure 8.2). While PCE concentrations were somewhat lower than the expected value of 300 µM, ranging from 200 to 250 µM, indicating some dechlorination, TCE (40 µM), *cis*-DCE (20 µM), and VC (<5 µM) concentrations were relatively low and ethene was not detected. Following this period of limited dechlorination, the next 7 pore volumes of operation (up to 10.5 total pore volumes) was characterized by nearly complete conversion of PCE to *cis*-DCE. Effluent *cis*-DCE concentrations ranged from 250 to 280 µM, indicating the absence of biological enhancement of PCE dissolution during this phase of the experiment. In addition, ethene was not detected in the effluent and VC concentrations were observed to steadily increase over the 7 pore volumes of flushing (from 5 µM to 40 µM), although the concentrations were much lower than those observed for *cis*-DCE.

Upon reaching 10.5 total pore volumes of flushing, *cis*-DCE concentrations in the biocolumn effluent increased to values significantly greater than the expected total chlorinated ethene concentration, eventually reaching a maximum value of approximately 2,600 µM following 18.6 pore volumes of flushing. This is indicative of PCE dissolution enhancement within the biocolumn source zone. Vinyl chloride production increased slightly during the phase of column operation prior to reaching a nominal steady-state value ranging from 40 to 50 µM, and no ethene was detected. A large spike in effluent VC concentration (up to approximately 200 µM) was observed at 18.6 pore volumes of operation, however, corresponding to a 22 hour cessation of aqueous-phase flow through

259

the column. Presence of this spike implies that the residence time within the column (1.1 days at a flow rate of 0.25 mL/min) was insufficient to dechlorinate large amounts of *cis*-DCE to VC (and potentially ethene). The maximum total chlorinated ethene (i.e., *cis*-DCE and VC) concentration in the biocolumn effluent was approximately 2,800 μM, which while somewhat lower than maximum effluent *cis*-DCE concentrations observed during experiment SM-Mixed (3,500 μM, see Chapter 7), nonetheless represents a 13.7-fold increase in total chlorinated ethene concentration over the expected total concentration (estimated to be 205 μM at 18.6 pore volumes of operation). During an additional 3.6 pore volumes of operations at 0.25 mL/min (22.2 total pore volumes), *cis*-DCE concentrations decreased from 2,600 μM to 1,700 μM.

At this point in the BDI biocolumn experiment, the aqueous-phase flow rate was lowered from 0.25 mL/min to 0.1 mL/min to increase the residence time in the column from 1.1 to 2.8 days and promote increased VC productions (and optimally ethene production). During this portion of the NAPL dissolution phase, effluent *cis*-DCE concentrations showed an initial increase, as could be expected due to the increased residence time allowing for additional reductive dechlorination to occur in the source zone. This was followed by a rapid decrease in *cis*-DCE concentrations to values less than 5 μM after 29.2 pore volumes of operation, consistent with depletion of PCE from the mixed NAPL. Vinyl chloride concentrations following the decrease in operational flow rate showed a strong upward trend for the duration of flushing prior to depletion of PCE from the NAPL, at which point they rapidly decreased to less than 5 μM. It must also be noted that the maximum effluent VC concentration (300 μM) remained significantly lower than *cis*-DCE concentrations, even with an increase in the column

residence time. No ethene production was initially detected at the lower flow rate. However, once the mixed NAPL was depleted of PCE and *cis*-DCE and VC concentrations decreased to 5 μM or less, limited amounts of ethene (less than 20 μM) were detected in the biocolumn effluent. While somewhat limited, this evidence suggests that accumulation of *cis*-DCE at high concentrations may act to inhibit significant dechlorination to VC and ethene. At this point, a VC pulse was injected into the biocolumn to monitor VC-dechlorination activity following source zone depletion. Results from the pulse are discussed in detail in section 8.2.3 of this work.

Periodic pH measurements were taken during the NAPL dissolution phase of the BDI biocolumn (data not shown). While the pH trends were not as clear as those demonstrated for the *S. multivorans* mixed-NAPL biocolumn (see Figure 7.5), they nonetheless demonstrated a decrease in pH with increasing concentrations of PCE dechlorination daughter products. The decrease was attributed to the release of hydrochloric acid (HCl) during each step of the reductive dechlorination process, with DCE and VC production expected to generate two or three moles of HCl per mole of PCE dechlorinated, respectively. Given a maximum effluent chlorinated ethene concentration of 2,800 μM (2,600 μM of *cis*-DCE and 200 μM of VC), generation of up to 5,800 μM of HCl was possible. Even given the high buffering capacity of the reduced mineral salts medium, the HCl production decreased the column effluent pH from an initial value greater than 7.2 to a minimum of 6.77. This pH reduction was comparable to that observed in the *S. multivorans* mixed-NAPL biocolumn, which was not unexpected given the similar levels of *cis*-DCE production. It is therefore likely that, had operational conditions within the biocolumn not been altered, a decrease in BDI performance (e.g.,

261

cis-DCE and VC concentration) similar to that observed for *S. multivorans* would have occurred. This is of particular importance for the *Dehalococcoides* species present in BDI, which are generally only capable of growth over narrow pH ranges (7.2-7.4, see He et al. 2003a, 2003b). The pH reduction in the biocolumn effluent may therefore partially explain the relative lack of VC production observed, although other factors may have contributed.
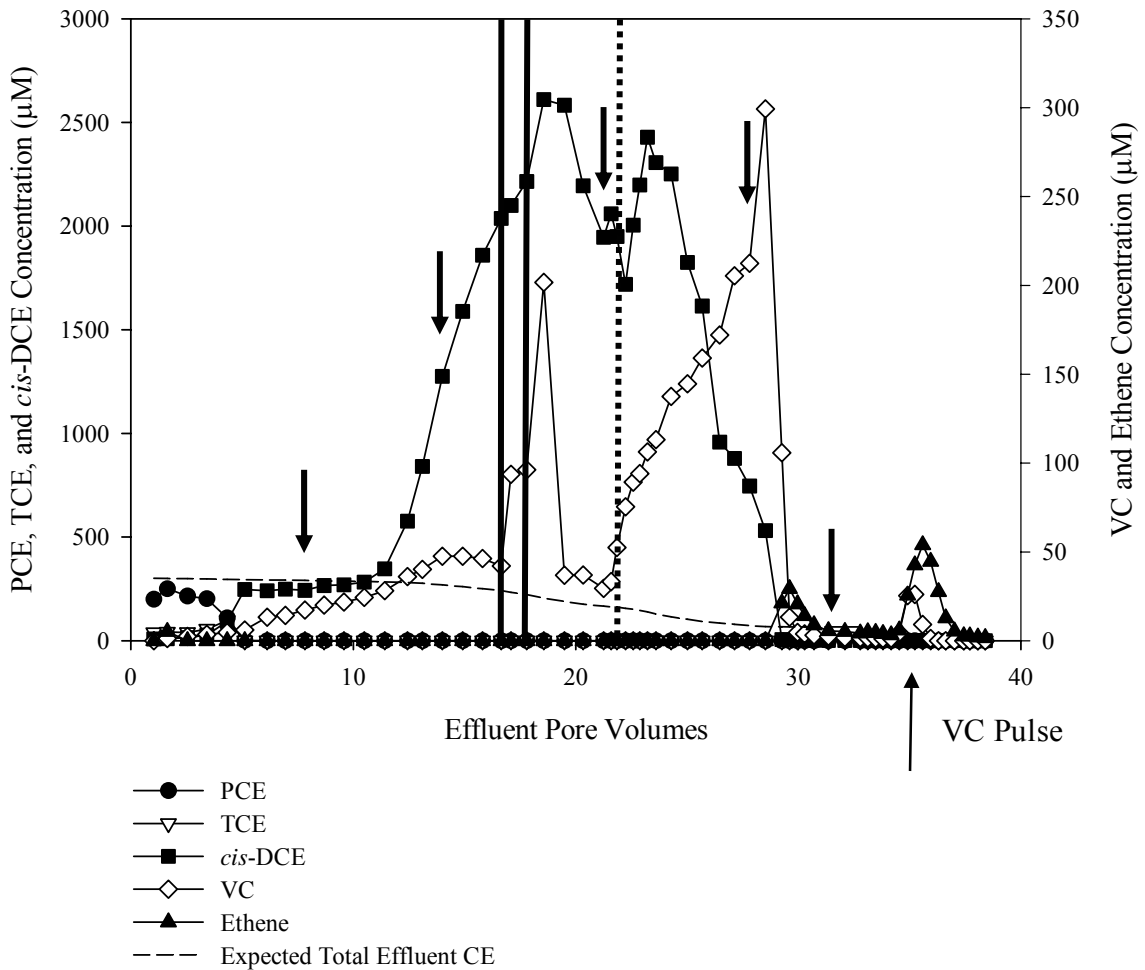
Figure 8.2: Effluent chlorinated ethene concentrations measured during the NAPL dissolution phase of the BDI biocolumn experiment. Solid vertical lines denote 22 hour flow interruption, dashed vertical line denotes reduction in aqueous flow rate to 0.1 mL/min, and arrows indicate side port sampling events.

Effluent *Dhc* cell quantities were also monitored over the duration of the NAPL dissolution phase of the BDI biocolumn experiment. Measured *Dhc* quantities are shown in Figure 8.3, with the filled and open circle representing concentrations during the elution and NAPL dissolution phases of the experiment, respectively. *Dehalococcoides* quantities in the biocolumn effluent approximately ranged from 5×10^5 to 1×10^6 cells/mL over the first 20 pore volumes of flushing during NAPL dissolution phase. These values are comparable to those observed near the conclusion of the elution phase of the experiment, and significantly lower than the inoculum *Dhc* loading (1.8×10^8 cells/mL). The relatively low *Dhc* quantities present in the biocolumn effluent over the first 20 pore volumes operation coincided with the limited *cis*-DCE degradation products (i.e., VC and ethene) observed during this time, where no ethene was observed and VC concentrations were below 50 μM (see Figure 8.2). Effluent *Dhc* increased to 4.3×10^7 cells/mL, approaching the initial biocolumn *Dhc* loading, by pore volume 28 of the NAPL dissolution phase. This increase corresponded to a decrease in operational flow rate of the column from 0.25 mL/min to 0.1 mL/min as well as a significant increase in effluent VC concentration (up to 300 μM, see Figure 8.2). The mixed NAPL became depleted from the biocolumn at this point, and effluent *Dhc* concentration decreased until the cessation of flushing, although concentrations at the conclusion of the NAPL dissolution phase were greater than those at the beginning. Based on the measured effluent *Dhc* cell quantities and the volume of medium flushed through the biocolumn, it was estimated that 1.9×10^{11} *Dhc* cells were recovered from the biocolumn over the course of the NAPL dissolution phase. This value is much greater than the *Dhc* loading in the biocolumn at

the beginning of the NAPL dissolution phase (7.5×10^{10} cells), providing evidence of ongoing *Dehalococcoides* growth within the column.
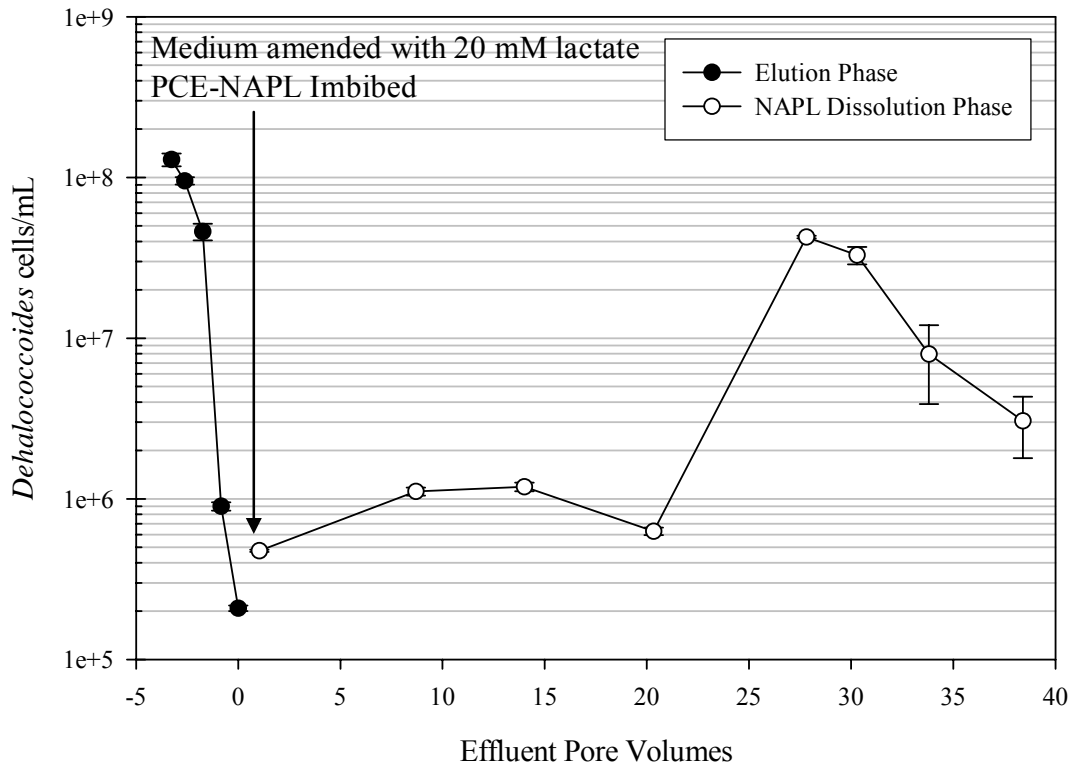
Figure 8.3: Effluent *Dehalococcoides* cell quantities measured during NAPL dissolution phase of BDI biocolumn experiment. The arrow indicates NAPL imbibition and start of flushing with lactate-amended media.

Side ports samples were first taken following 8.7 pore volumes of flushing with lactate-amended medium. The samples were analyzed for chlorinated ethenes (but not biomass), and the resulting concentration profiles are shown in Figure 8.4. Port 1 in Figure 8.4 is located at the bottom of the column (i.e., within the NAPL source zone and nearest the influent medium), and the dashed line represented the expected total chlorinated ethene concentration in the absence of biological mass transfer enhancement. PCE concentrations in Ports 1-3, coinciding with the NAPL source zone, were

comparable to the assumed total chlorinated ethene concentration in the absence of mass transfer enhancement (290 μM). The absence of significant amounts of *cis*-DCE within the NAPL source zone (Ports 1-3) indicated that biological mass transfer enhancement at this time was limited. PCE concentration was much lower in Port 4 and not detected by Port 5, however, with near stoichiometric conversion to *cis*-DCE. Increasing amounts of VC were also detected throughout the plume region of the biocolumn (Ports 4-11) at very low concentrations (less then 20 μM). It is therefore clear that while microbial populations capable of dechlorination were present within the BDI biocolumn, they were largely unable to colonize the mixed NAPL source zone prior to 8.7 pore volumes of column operation with lactate-amended media.
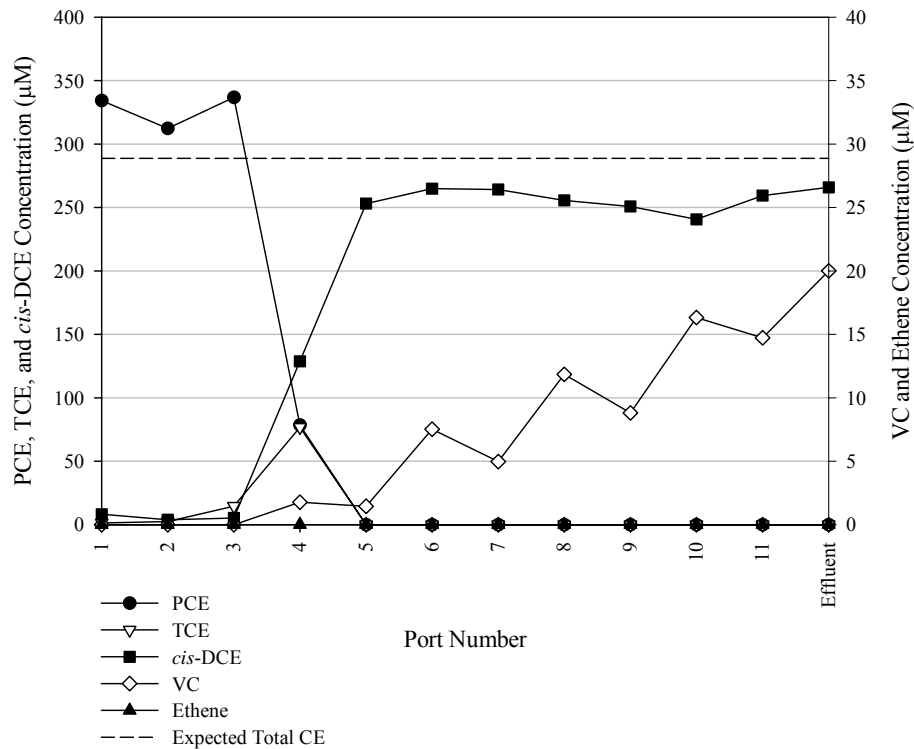
Figure 8.4: Side port chlorinated ethene concentrations for BDI biocolumn experiment following 8.7 pore volumes of flushing. Dashed line is expected total chlorinated ethene concentration. Port 1 is nearest the influent while port 11 is nearest the effluent.

The second series of BDI biocolumn side port samples were taken following 14.0 pore volumes of flushing, and the chlorinated ethene concentration and *Dehalococcoides* cell quantity profiles are shown in Figures 8.5a and 8.5b, respectively. PCE concentrations within the mixed NAPL source zone (Ports 1-3) remained near the expected total chlorinated ethene concentration (270 μM). Elevated TCE (100 μM) and *cis*-DCE (1,500 μM) concentrations were also observed in Ports 1-3, indicating the onset of dechlorination activity within the mixed NAPL source zone. In addition, the increased *cis*-DCE levels imply that biological mass transfer enhancement was occurring within the source zone. Complete PCE dechlorination in the source zone was not observed, however, and dechlorination stalled at *cis*-DCE, with no VC observed over the first 3 sampling ports. PCE and TCE were not detected beyond Port 3, and *cis*-DCE concentrations remained relatively stable over the plume region of the column, coinciding with effluent samples (Figure 8.2) characterized by *cis*-DCE concentrations significantly exceeding the expected total chlorinated ethene concentration. In addition, limited VC production was observed in the plume region of the biocolumn. While VC concentration never exceeded 50 μM, they were significantly higher than those observed following 8.7 pore volumes of column operation (see Figure 8.4). Ethene was not detected at any port within the biocolumn following 14 pore volumes of operation. *Dehalococcoides* cell quantities were less than approximately 1×10^5 cells/mL in the source zone (Figure 8.5b, Ports 1-3), corresponding to the observed absence of VC from chlorinated ethene samples taken at these ports. Quantities of *Dhc* cells from samples taken within the plume region (Ports 4-11) were up to two orders-of-magnitude greater than those observed in source zone, generally paralleling VC production within this region of the biocolumn.

Figure 8.5: Side port chlorinated ethene concentrations (a) and *Dehalococcoides* cell quantities (b) for BDI biocolumn experiment following 14.0 pore volumes of flushing. Dashed line is expected total chlorinated ethene concentration. Port 1 is nearest the influent while port 11 is nearest the effluent.

267

Chlorinated ethene profiles observed in the side port samples following 20.3 pore volumes of operation (Figure 8.6a) were in general comparable to those seen at 14.0 pore volumes. PCE concentrations within the source zone significantly exceeded the expected chlorinated ethene concentration (270 versus 180 µM), and both TCE and *cis*-DCE were observed at relatively high concentrations within the source zone, all demonstrating that mass transfer enhancement and reductive dechlorination were ongoing within the mixed NAPL source zone. Both PCE and TCE were completely dechlorinated to *cis*-DCE by Port 4. Interestingly, PCE, TCE, and *cis*-DCE concentrations measured at Port 1 were very low, less than 10 µM for PCE and TCE and 60 µM for *cis*-DCE. While it is difficult to draw strong conclusions based on results from a single data point, the results are consistent with complete PCE depletion from the mixed NAPL up-gradient of the first sampling port. Some VC production was also observed in the source zone, although quantities were small (less than 5 µM) and dechlorination generally remained stalled at *cis*-DCE. Plume region VC production was comparable to that observed during the 14.0 pore volume sampling event, steadily increasing throughout the column length but never reaching values greater than 40 µM, and ethene was not detected at any sampling port. Side port *Dhc* cell quantities generally increased over the length of the biocolumn (Figure 8.6b), coinciding with increasing VC levels throughout the column. Source zone (Ports 1-3) cell quantities following 20.3 pore volumes of flushing with lactate-amended medium ranged $1x10^5$ to $5x10^5$ cells/mL, up to an order-of-magnitude greater than those observed following 14.0 pore volumes of flushing, indicating limited colonization of the source zone by *Dhc*. Plume region *Dhc* cell quantities were comparable at 14.0 and 20.3 pore volumes, as might be expected given the similarities between the plume VC profiles.
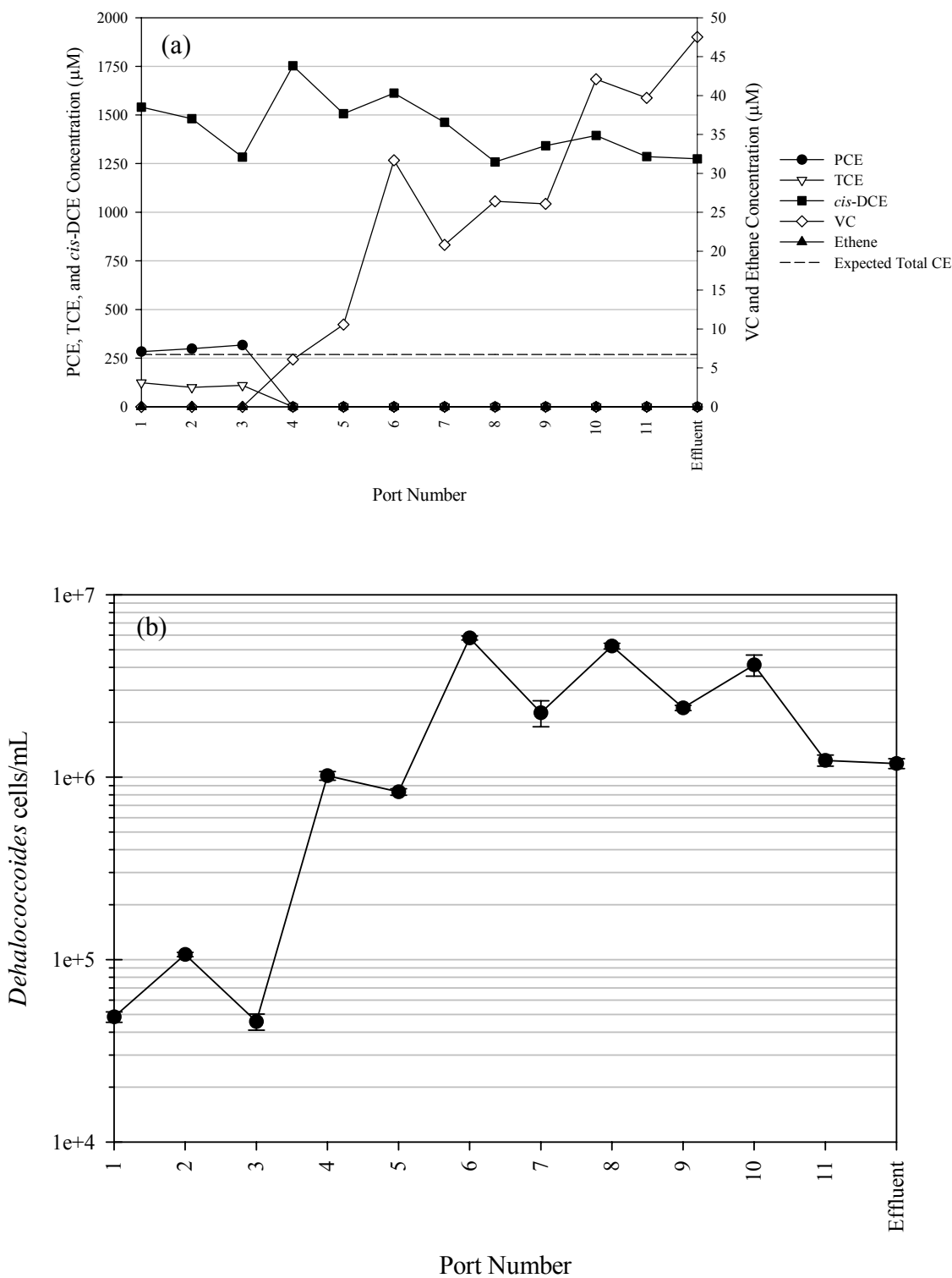
Figure 8.6: Side port chlorinated ethene concentrations (a) and *Dehalococcoides* cell quantities (b) for BDI biocolumn experiment following 20.3 pore volumes of flushing. Dashed line is expected total chlorinated ethene concentration. Port 1 is nearest the influent while port 11 is nearest the effluent.

Prior to complete depletion of PCE from the source zone NAPL, a series of side port samples were taken following 27.8 pore volumes of flushing, with the resulting chlorinated ethene profiles are shown in Figure 8.7a. Neither PCE nor TCE were detected within the mixed NAPL source zone during the 27.8 pore volume sampling event. While it is possible that the compounds were being completely dechlorinated to *cis*-DCE and thus not detected, this is unlikely given the low *cis*-DCE concentrations observed, particularly in Ports 1 and 2. A more probable explanation is that PCE had been depleted from the mixed NAPL, at least up-gradient of Port 2. Some *cis*-DCE was observed at the trailing edge of the NAPL source zone (i.e., Port 3), implying PCE depletion from the NAPL may not have occurred in a spatially uniform manner. In addition, *cis*-DCE concentration at Port 3 was significantly lower than concentrations in the plume region. Given that *cis*-DCE production in the plume was not occurring due to the lack of a suitable electron acceptor (i.e., PCE or TCE), it is therefore reasonable to suspect that this spatial non-uniformity was transient and the elevated levels of *cis*-DCE in the plume region were unlikely to be sustained. This is consistent with results from coinciding effluent samples (see Figure 8.2) that demonstrated rapidly decreasing *cis*-DCE concentrations consistent with PCE depletion from the mixed NAPL. While some VC production in the source zone was observed, concentrations were low. Plume VC production was significantly greater than that observed at 20.3 pore volumes, however, rapidly increasing to greater than 200 μM in the biocolumn effluent. The increase in VC generation was attributed in part to the reduction in aqueous flow rate to 0.1 mL/min, compared to 0.25 mL/min during the 20.3 pore volume sampling event. VC concentrations remained much lower than *cis*-DCE concentrations at corresponding

sampling ports, and ethene was once again not observed at any location. Following 27.8 pore volumes of operation, *Dhc* cell quantities within the biocolumn ranged from approximately 1×10^6 cells/mL within the source zone to 2×10^7 cells/mL near the column exit (Figure 8.7b). *Dehalococcoides* quantities increased over the length of the cell, again coinciding with increasing VC concentrations. In addition, from comparing Figures 8.6b and 8.7b it is clear that *Dhc* values at 27.8 pore volumes were somewhat higher than those observed at 20.3 pore volumes. As such, it is likely that the increased levels of VC present in the biocolumn at pore volume 27.8 were due to a combination of increased aqueous phase residence time as well as an increase in the amount of biomass available to reductively dechlorinate *cis*-DCE.

A final series of side port samples were taken following 33.8 pore volumes of flushing, corresponding to complete depletion of PCE from the source zone, resulting in the chlorinated ethene concentration profiles shown in Figure 8.8a. Neither PCE nor TCE were detected at any point within the column. In addition, *cis*-DCE was not observed within column source zone (Ports 1-3); the absence of PCE, TCE, and *cis*-DCE over the first three sampling ports is indicative of complete depletion of PCE from the NAPL. Low levels of VC (less than 3 μM) were detected within the biocolumn source zone and attributed to bleed of VC that had back-partitioned into the (predominately hexadecane) NAPL remaining within the source zone. Both *cis*-DCE and VC were detected at concentrations below 5 μM in the column effluent; given that *cis*-DCE was not detected prior to Port 11 and the VC present in the source zone was dechlorinated by Port 3, the source generating these compounds in the effluent is unclear. Ethene was also detected throughout the column length, increasing from approximately 5 μM within the
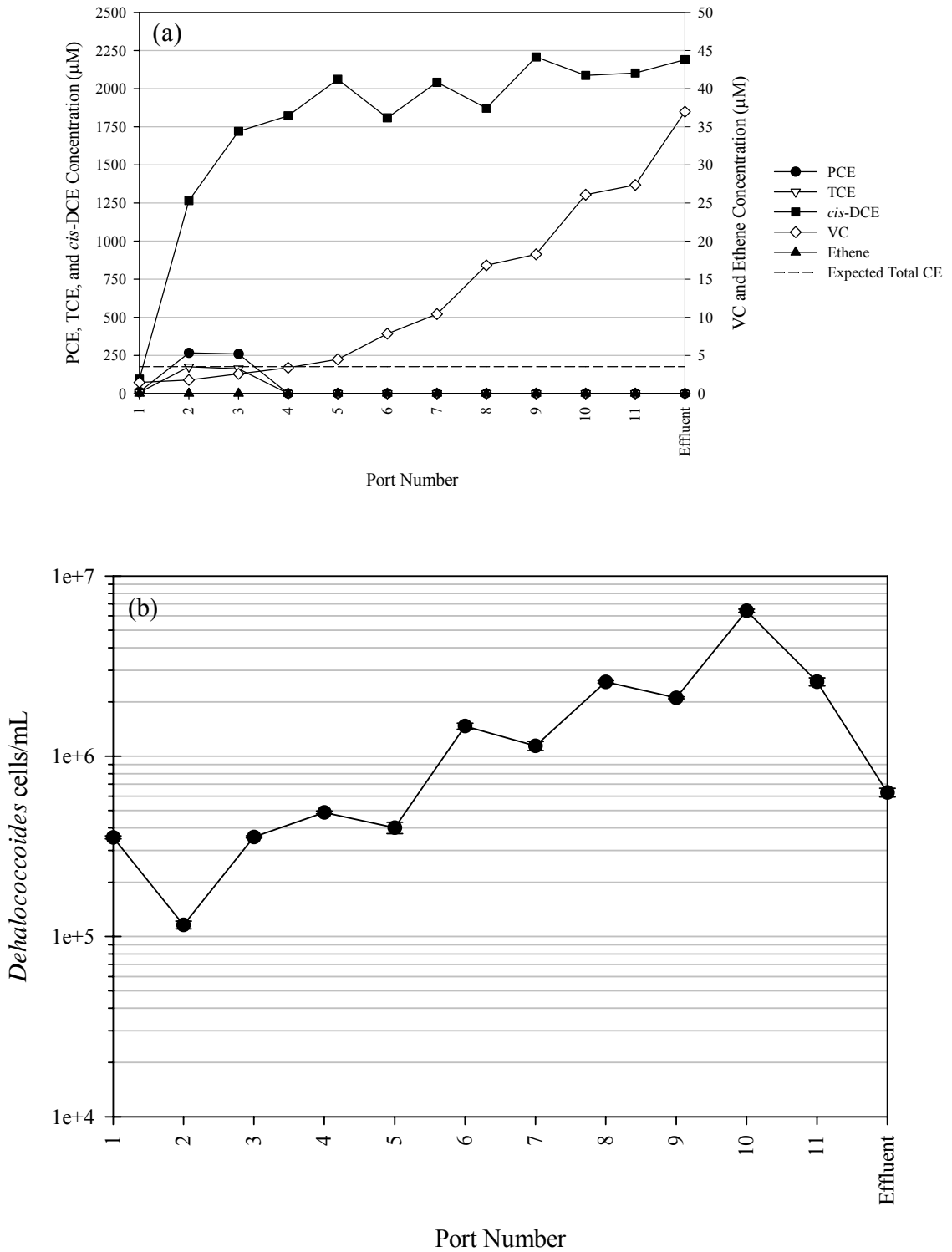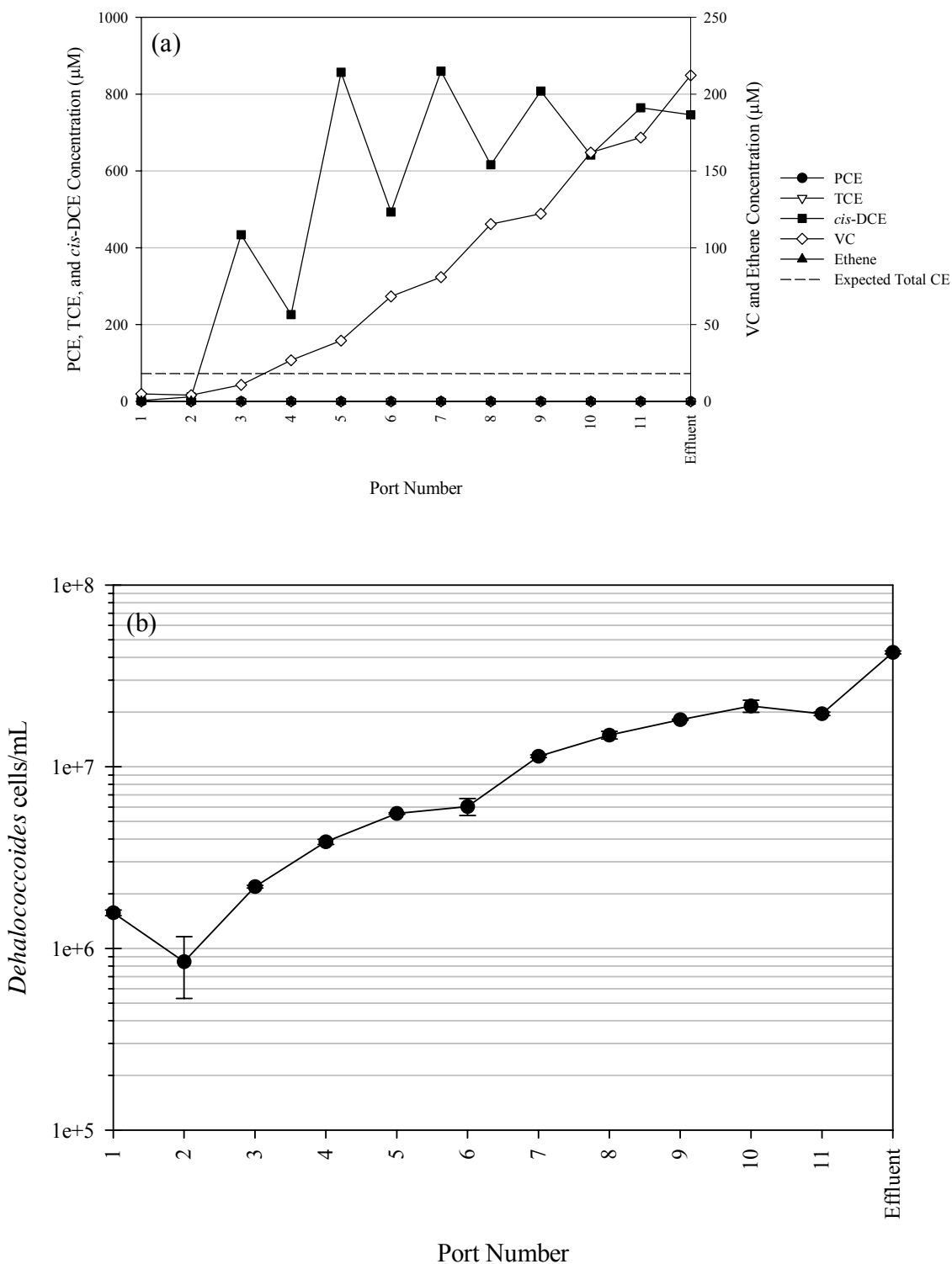
Figure 8.7: Side port chlorinated ethene concentrations (a) and *Dehalococcoides* cell quantities (b) for BDI biocolumn experiment following 27.8 pore volumes of flushing. Dashed line is expected total chlorinated ethene concentration. Port 1 is nearest the influent while port 11 is nearest the effluent.
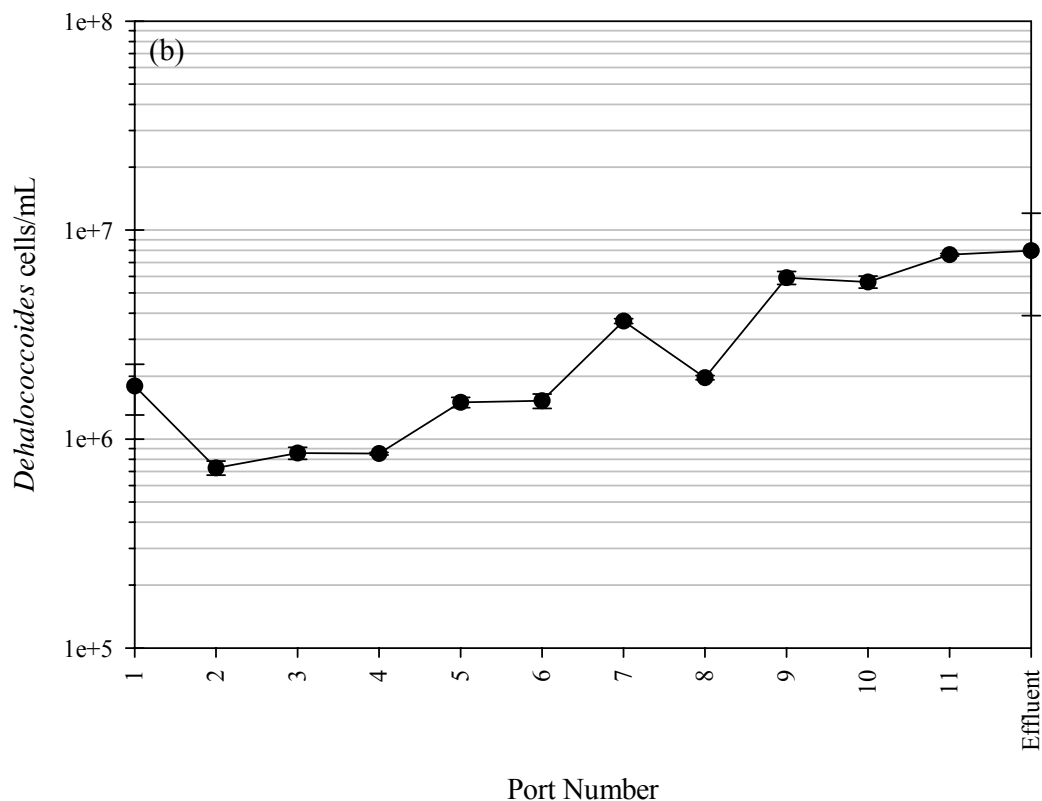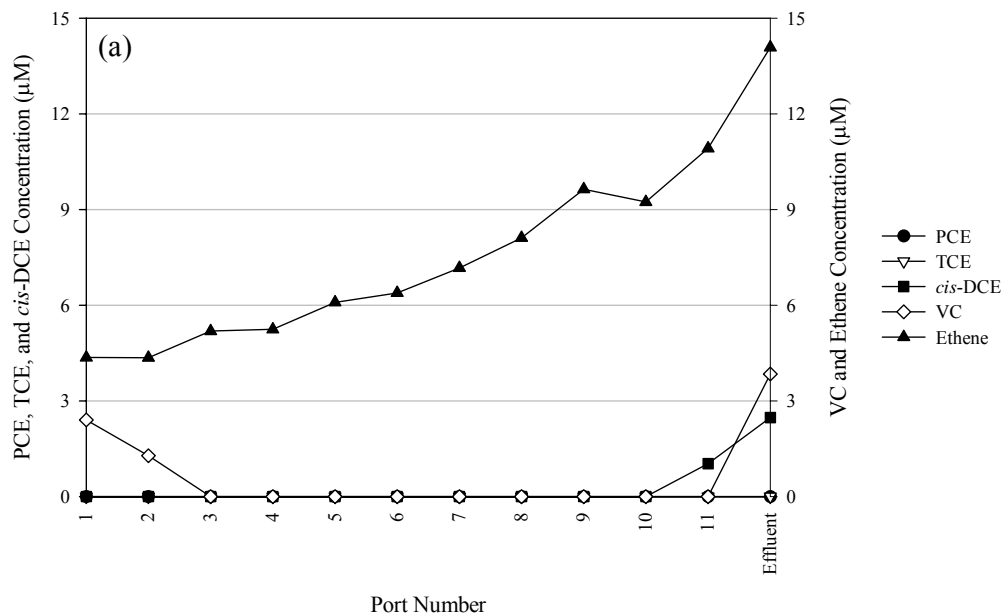
Figure 8.8: Side port chlorinated ethene concentrations (a) and *Dehalococcoides* cell quantities (b) for BDI biocolumn experiment following 33.8 pore volumes of flushing. Dashed line is expected total chlorinated ethene concentration. Port 1 is nearest the influent while port 11 is nearest the effluent.

273

source zone to nearly 15 μM in the effluent. The steadily increasing ethene concentration was attributed to dechlorination of low levels of VC dissolving either from the NAPL (within the source zone) or gas bubbles present in the down-gradient plume region of the biocolumn. *Dehalococcoides* was present in the column in quantities ranging from approximately $1x10^6$ cells/mL to $1x10^7$ cells/mL (Figure 8.8b), increasing with increasing ethene concentration. The *Dhc* quantities following 33.8 pore volumes of flushing were somewhat lower than those at pore volume 27.8 (Figure 8.7b), presumably due to a reduction in the amount of electron acceptor (i.e., *cis*-DCE and VC) available for dechlorination.

8.2.3 NAPL Dissolution: Vinyl Chloride Pulse

Given the onset of ethene production coinciding with PCE depletion from the mixed NAPL and decreasing *cis*-DCE and VC concentrations in the column effluent, it was hypothesized that microbial communities capable of ethene generation were present in the BDI biocolumn but inactive due to ambient conditions. To test this, a pulse of vinyl chloride-spiked influent media was injected into the biocolumn and the effluent monitored for VC and dechlorination products (i.e., ethene). Results of the VC pulse test are shown with the rest of the NAPL dissolution phase of the column experiment in Figure 8.2, and an exploded view providing greater resolution is presented in Figure 8.9. The VC-spiked influent medium was injected over an approximate 1.1 pore volumes of operation (32.8 to 33.9 total pore volumes). During injection, VC concentration within the influent was periodically monitored and decreased from 97.5 to 62.4 μM due to changes in the influent medium reservoir headspace and VC sorption to the reservoir

septum. Based on the measured concentrations, a total of 34.6 μmol of VC were injected into the biocolumn during the pulse.

Biocolumn effluent VC and ethene concentrations began to increase to values above background levels following 34.5 pore volumes of flushing. Vinyl chloride concentrations increased to a maximum value of 26.1 μM (at 35.2 pore volumes) and returned to background levels by 35.9 total pore volumes of column operation. The maximum observed ethene concentration was significantly higher than that of VC (53.9 μM at 35.6 pore volumes of operation) and ethene remained above background levels for a much longer duration. For both VC and ethene, spreading of the breakthrough curves indicate that some chlorinated ethene retardation was ongoing in the biocolumn. This was attributed to partitioning of VC and ethene into both the residual NAPL within the column source zone as well as the discrete gas bubbles that formed within the biocolumn during operation. Unfortunately, experimental conditions precluded estimation of the NAPL and gas volumes present in biocolumn, thereby preventing detailed analysis of the chlorinated ethene breakthrough curves. Based on the breakthrough curve results, total chlorinated ethene mass recoveries were estimated to be 10.2 μmol of VC and 34.2 μmol of ethene, respectively. The mass recoveries were corrected to account for background chlorinated ethene levels, which were assumed to be constant values of 1.33 μM for VC and 4.16 μM for ethene. The corrected mass recoveries were 7.6 μmol of VC and 26.1 μmol of ethene, resulting in a total recovery of 33.7 μmol. The total recovery was 97.4% of the VC present in the influent pulse, 75.6% of which was ethene, compared to 21.8% VC. This validates the hypothesis that VC dechlorination to ethene is possible under the biocolumn experimental conditions. In addition, it is likely that an increase in the column

residence time would result in additional VC dechlorination. *Dehalococcoides* was detected in the biocolumn effluent immediately prior to and following the VC pulse (33.8 and 38.4 pore volumes, respectively) at similar concentrations of approximately 5×10^6 cells/mL. In addition, cell quantities along the column profile following 38.4 pore volumes of flushing (data not shown) were nearly identical to those measured at pore volume 33.8 (Figure 8.8b).
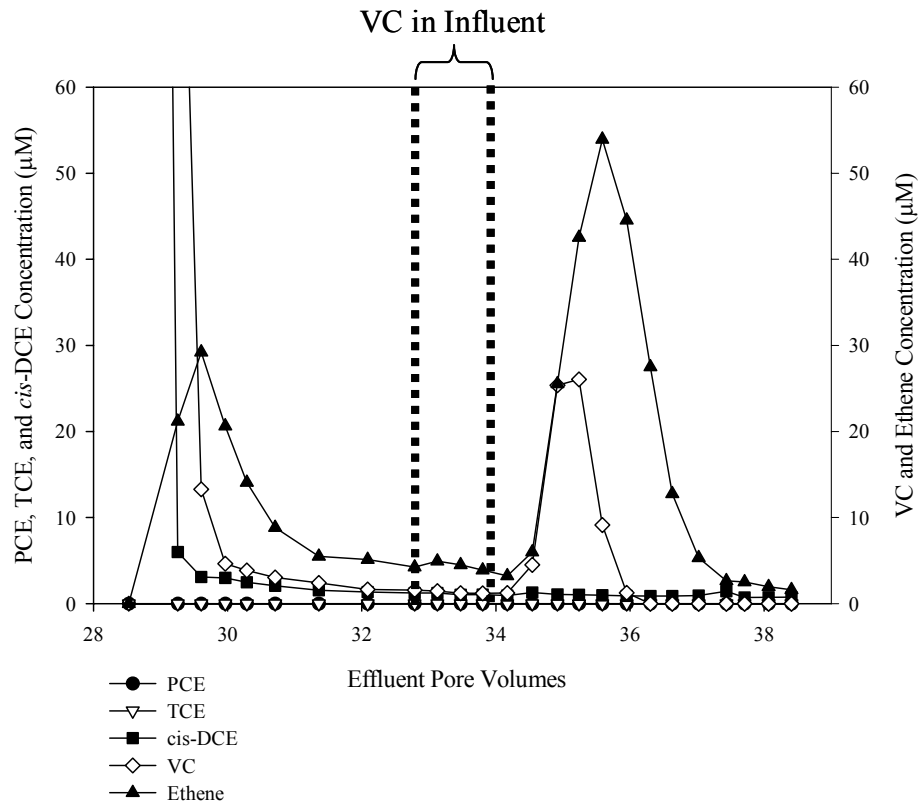
Figure 8.9: Effluent chlorinated ethene concentrations measured during the vinyl chloride pulse of the NAPL dissolution phase of the BDI biocolumn experiment. Dashed lines denote injection of VC-spiked influent media.

8.2.4 Cumulative Chlorinated Ethene Recovery and Mass Transfer Enhancement

Cumulative molar (and percentage) chlorinated ethene recovery for the BDI biocolumn experiment is summarized in Table 8.2, and the overall cumulative mass recovery curve is plotted in Figure 8.10. Including PCE, TCE, *cis*- and *trans*-DCE, VC, and ethene, 13,480 total μmol of chlorinated ethenes were recovered from the biocolumn effluent. The primary chlorinated ethene constituent present in the effluent was *cis*-DCE, which comprised 76.8% of the PCE initially present in the column (12,503 μmol). PCE and VC were also recovered from the column in significant (albeit much smaller) quantities, 340 μmol (2.1%) and 790 μmol (4.8%), respectively. Only trace amounts of TCE (100 μmol, 0.6%), *trans*-DCE (30 μmol, 0.2%), and ethene (20 μmol, 0.1%) were recovered from the column. The relatively low total amount of ethene recovered from the biocolumn is consistent with stalling of dechlorination at *cis*-DCE and/or VC, a phenomenon previously reported under comparable experimental conditions (see e.g., Cope and Hughes 2001, Yang and McCarty 2002).

Total overall mass recovery of the 16,320 μmol of PCE initially present in the column (including all dechlorination daughter products was 82.6%. The relatively low observed mass recovery was somewhat surprising given the previously discussed anecdotal evidence indicating that PCE had been depleted from the mixed NAPL. A number of explanations for this relatively low mass recovery have been postulated. They include mass losses occurring via NAPL sorption to the side port septa, the observed mobilization of the NAPL around the bottom end cap of the biocolumn, losses (both NAPL and aqueous) during the side port sampling events, and back-partitioning of *cis*-DCE, VC, and ethene into the residual hexadecane within the biocolumn source zone.

Taken together, the number of possible mass loss mechanisms highlights the complexity of the biocolumn system, implying that the observed recovery is not necessarily a disappointing result.

Table 8.2: Chlorinated ethene mass recoveries and mass transfer enhancement factors for BDI biocolumn experiment.

Biocolumn Parameter	BDI Biocolumn
Initial PCE Loading (μmol)	16,320
Total Chlorinated Ethenes Recovered (μmol) [%]	13,480 [82.6]
PCE Recovered (μmol) [%]	340 [2.1]
TCE Recovered (μmol) [%]	100 [0.6]
cis-DCE Recovered (μmol) [%]	12,530 [76.8]
trans-DCE Recovered (μmol) [%]	30 [0.2]
VC Recovered (μmol) [%]	790 [4.8]
Ethene Recovered (μmol) [%]	20 [0.1]
Expected Abiotic PCE Recovered (μmol) [%]	2,610 [16.0]
Maximum Mass Transfer Enhancement Factor Range	9.34-21.0
Cumulative Mass Transfer Enhancement Factor Range	3.47-5.17[a]

a: Range at depletion of PCE from mixed NAPL

The expected abiotic PCE mass recovery from the biocolumn following 32.8 pore volumes of flushing during the NAPL dissolution phase, coinciding with PCE depletion from the mixed NAPL, was estimated to be 2,610 μmol, or 16.0% of the PCE initially present in the source zone. The abiotic mass recovery was estimated assuming an initial aqueous PCE solubility of 50 mg/L (300 μM) and equilibrium mass transfer at both biocolumn flow rates (0.25 mL/min and 0.1 mL/min), accounting for changes in the mixed NAPL composition (i.e., PCE mole fraction) with PCE mass depletion. The expected abiotic recovery was much lower than the actual chlorinated ethene recovery measured in the biocolumn effluent (see Figure 8.10), indicating that biological mass transfer enhancement was occurring. In an effort to quantify the extent of enhancement,
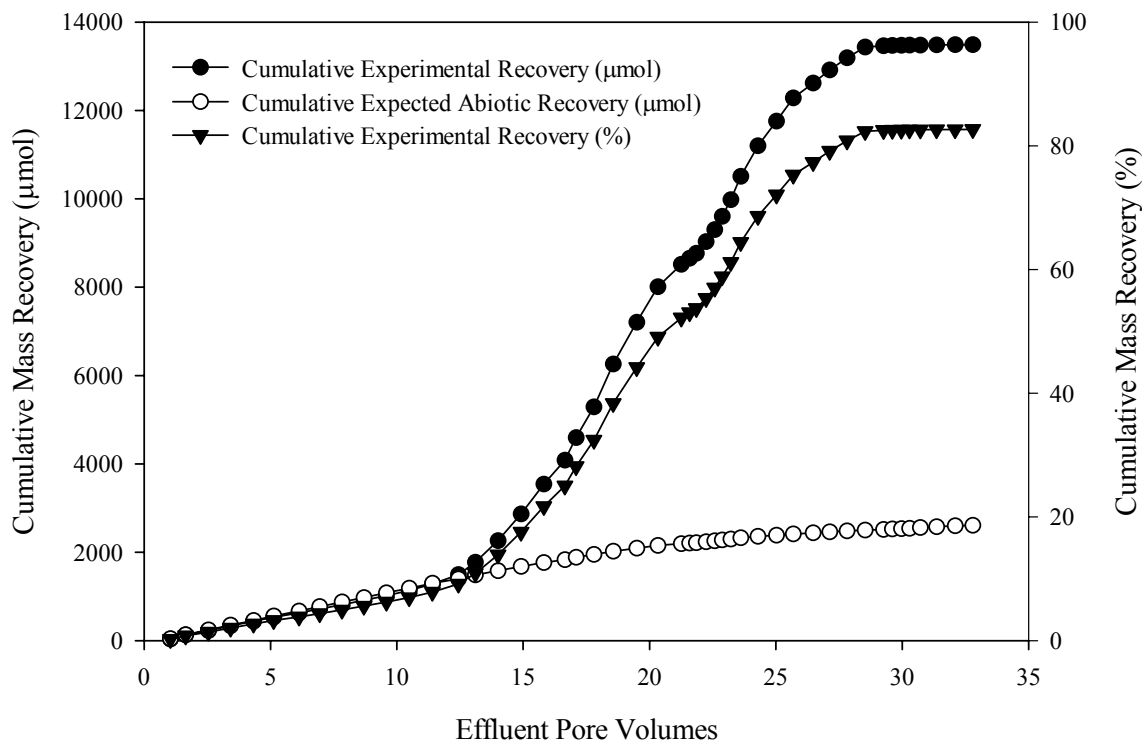
Figure 8.10: Overall cumulative chlorinated ethene molar recovery for BDI biocolumn experiment.

two metrics were evaluated, the effluent mass transfer enhancement factor (Figure 8.11a) and the cumulative mass transfer enhancement factor (Figure 8.11b). The effluent mass transfer enhancement factor was estimated by dividing the total measured chlorinated ethene concentration by expected abiotic concentration for a given effluent sample. Conversely, the cumulative mass transfer enhancement factor is based on the total (i.e., cumulative) chlorinated ethene recovered from the biocolumn at a given point divided by the expected total abiotic recovery. Both enhancement factors are presented as a range based on an assumption regarding the calculation of the expected abiotic values. For the uncorrected enhancement factors (open circles in both Figures), PCE concentration was assumed to remain at a constant saturation value of 300 μM (i.e., constant PCE mole

279

fraction in the NAPL). In calculating he corrected factors (filled circles) the PCE mole fraction was adjusted based on the cumulative chlorinated ethene recovery from the biocolumn, resulting in decreasing PCE saturation values as a function of mass recovery. These two assumptions were made to provide enhancement factors ranging from conservative (uncorrected) to optimistic (corrected). In reality, it is likely that the actual mass transfer enhancement factors fall somewhere within this range.

At the onset of mass transfer enhancement (following approximately 10.5 pore volumes of flushing), the effluent enhancement rapidly increased from initial values near unity, reaching maximum values ranging from 9.34 (uncorrected) to 21.0 (corrected). A large jump in corrected effluent enhancement was observed following reduction of the aqueous flow rate to 0.1 mL/min at 21.6 pore volumes of operation, indicating that the corrected effluent factor may give unrealistically high values, particularly when PCE depletion from the mixed NAPL became significant. The cumulative enhancement factor range observed during the BDI biocolumn experiment was much more limited, ranging from 3.47 to 5.17 following 32.8 pore volumes of operation, or at the point of complete PCE depletion from the mixed NAPL. These values are comparable to those measured in the mixed-NAPL *S. multivorans* column experiment (SM-Mixed, see Chapter 7) as well as literature results (see e.g., Cope and Hughes 2001, Yang and McCarty 2002). In addition, the relative "smoothness" of the cumulative enhancement factors compared to the effluent factors and the smaller range between the corrected and uncorrected factors indicate that the cumulative factor may be a more appropriate measurement of mass transfer enhancement than the more commonly reported effluent values.
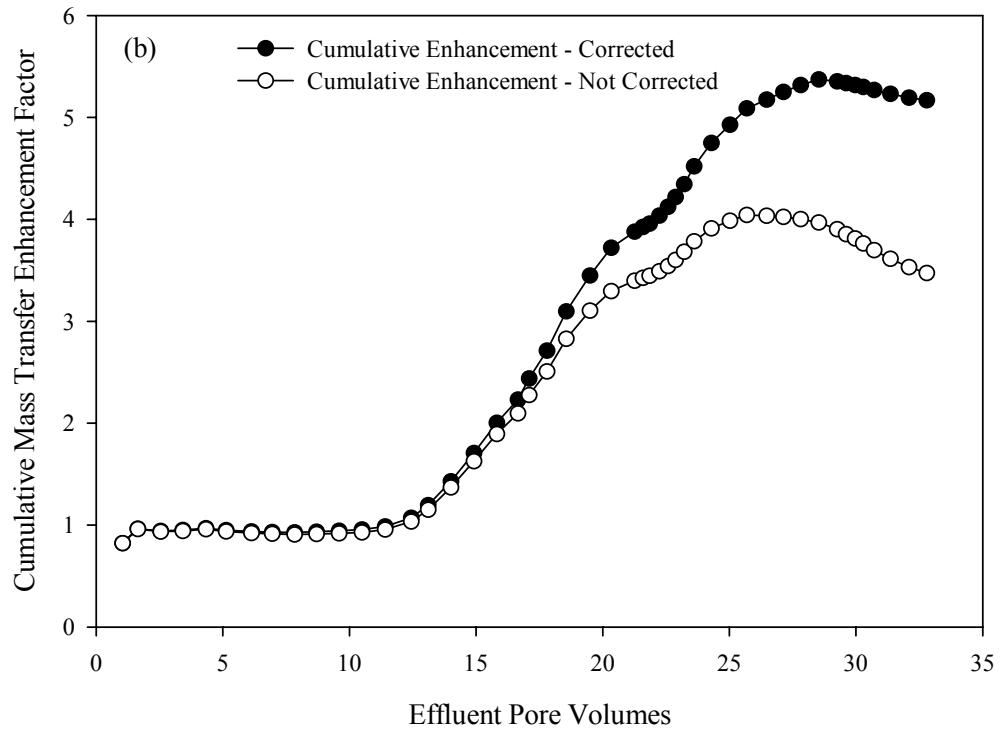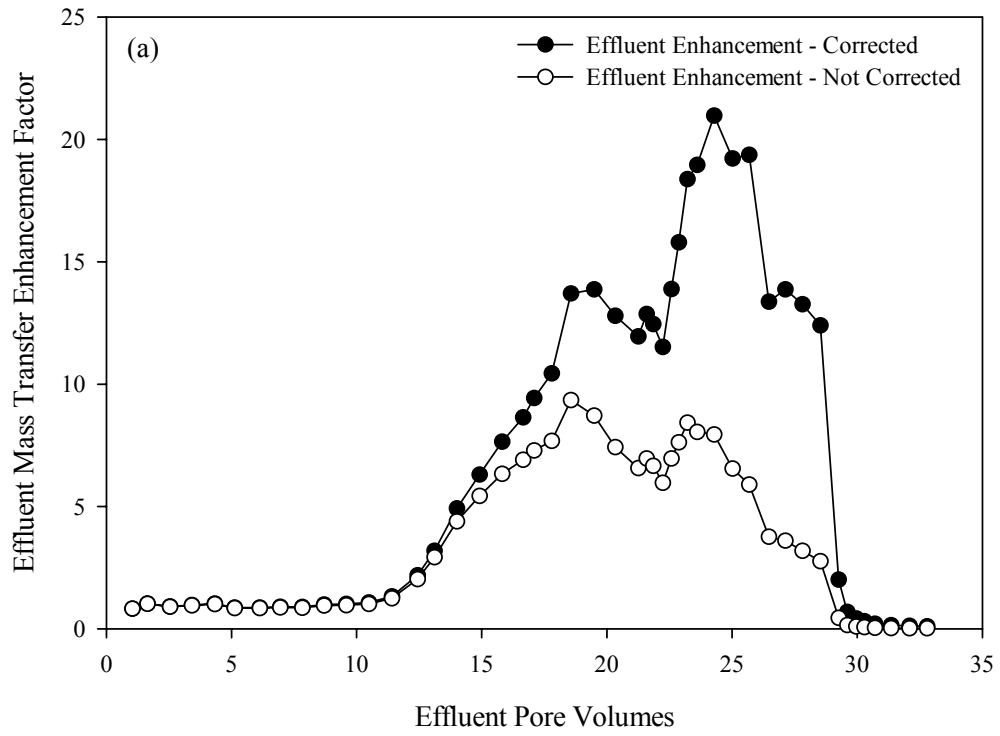
Figure 8.11: Effluent (a) and cumulative (b) mass transfer enhancement factors for BDI biocolumn experiment.

8.3 Summary and Conclusions

Enhancement of PCE dissolution from a mixed NAPL (0.25 mol/mol PCE in hexadecane) was evaluated in a 1-D biocolumn inoculated with BDI, a mixed microbial consortium capable of complete dechlorination of PCE to ethene. Experimental results demonstrated significant PCE dissolution enhancement and provided evidence linking growth of *Dehalococcoides* species with production of VC and ethene. Effluent chlorinated ethene concentrations increased to values significantly greater than the expected value in the absence of mass transfer enhancement (approximately 300 μM or 50 mg/L) following approximately 11 pore volumes of flushing with lactate-amended medium, indicating that the source zone was colonized by dechlorinating organisms. PCE dechlorination generally stalled at *cis*-DCE, although lowering the aqueous flow rate from 0.25 mL/min to 0.1 mL/min stimulated production of up to 200 μM VC. *Dehalococcoides* populations increased with increasing VC levels, both in the column effluent as well as in samples taken from side ports along the column profile. No ethene was detected in the effluent until PCE was depleted from the source zone and *cis*-DCE concentrations were reduced to low levels, indicating that high *cis*-DCE concentrations may be inhibitory to subsequent dechlorination. Cumulative enhancement of PCE-NAPL dissolution was comparable to that observed for the experiment SM-Mixed (see Chapter 7), ranging from 3.5 to 5.2, depending on the assumptions used in calculating abiotic dissolution. Results from the BDI biocolumn indicate that accelerated mass recovery and complete PCE detoxification may be possible via bioaugmentation or biostimulation of a PCE-NAPL source zone, provided *cis*-DCE concentrations are not inhibitory. Future research will focus on BDI bioaugmentation of a 2-D aquifer cell containing a non-

uniform distribution of pure PCE-DNAPL. The objective of this research will be to evaluate PCE dissolution enhancement and distribution of relevant microbial populations in a more realistic setting, where factors such as dilution can act to lower chlorinated ethene concentrations (particularly PCE and *cis*-DCE) to levels that will not inhibit microbial activity, ideally resulting in production of ethene.

CHAPTER 9

CONCLUSIONS AND RECOMMENDATIONS

This research focused on the implications of partial mass recovery from DNAPL source zones. Particular attention was paid to (a) evaluating post-treatment effluent concentration and mass flux following surfactant-based source zone treatments and (b) assessing the potential for microbial reductive dechlorination to be used as an efficient tertiary source zone treatment following surfactant flushing. Results from a series of two-dimensional (2-D) aquifer cell experiments demonstrated that TCE recovery when using a nonionic surfactant (Tween 80) formulation designed to solubilize TCE was comparable to that using an anionic surfactant (Aerosol MA) formulation designed to displace the TCE-DNAPL. TCE recovery after flushing with 2.5 pore volumes of 4% Tween 80 ranged from 66% for pool-dominated source zones to 85% for ganglia-dominated source zones. This supports the consideration of Tween 80 (or similar surfactants) for remediation of TCE source zones. This is especially true for scenarios where aggressive mass removal is combined with enhanced in situ bioremediation of residual contamination given published results indicating that complete microbial reductive dechlorination to ethene is possible in the presence of nonionic surfactants. DNAPL distribution will affect SEAR treatment selection, however, with solubilization becoming less favorable with increasing extents of DNAPL pooling.

The effects of partial PCE-DNAPL source zone mass removal on down-gradient plume concentrations and mass flux were evaluated in a 2-D aquifer cell, with sequential pulses of 4% Tween 80 surfactant solution used to achieve mass recovery. Initial PCE-DNAPL distribution within the source zone was demonstrated to play a key role in mass recovery and subsequent effluent mass flux reductions. Ganglia-dominated source zones required substantial (greater than 70%) mass removal prior to observation of effluent

mass flux reductions. Conversely, less mass removal (50%) was required to achieve mass flux reductions ranging from 50-65% for source zones characterized by high-saturation PCE-DNAPL pools. These results indicate that partial DNAPL mass removal from a source zone may be an effective remedial strategy. This is particularly true for source zone DNAPL distributions characterized by extensive pooling.

In addition to partial source zone mass removal, the implications of surfactant-based DNAPL recovery mechanism (i.e., solubilization, mobilization, and density modified displacement) were also investigated. Analysis of 2-D aquifer cell results indicated that immiscible displacement can be an efficient mechanism for PCE-DNAPL recovery, with observed PCE recovery efficiencies ranging from 0.19 to 0.41 g PCE/g surfactant. For surfactant formulations capable of complete DNAPL displacement, mass recovery and post-treatment effluent concentration reduction were both near 80%, with the PCE not recovered present as high saturation pools located either just above or within the aquifer cell lower confining layer, similar to post-treatment distributions observed at the conclusion of surfactant-enhanced solubilization. Thus, immiscible displacement may be a highly efficient and effective mechanism for remediation of DNAPL source zones, provided care is taken during design of the surfactant formulation and flushing system to limit mobilization of DNAPL into previously uncontaminated aquifer regions.

A promising treatment for residual DNAPL that is not recovered by an aggressive physicochemical treatment (i.e., surfactant flushing) is microbial reductive dechlorination. Column experiments were conducted to evaluate the activity and distribution of *Sulfurospirillum multivorans*, an organism capable of PCE to *cis*-DCE dechlorination, in the vicinity of a PCE-NAPL source zone. Experimental results were able to link growth of *S. multivorans* with enhanced dissolution of PCE from the NAPL source zone. In the presence of a mixed NAPL (equilibrium PCE concentration of 300 μM), PCR analysis of side port biomass samples demonstrated that increasing biomass concentrations within the PCE-NAPL source zone coincided with increasing *cis*-DCE

concentrations. In addition, a 4.7-fold cumulative enhancement of NAPL dissolution was achieved. Conversely, little evidence of *S. multivorans* growth and activity was observed in a column imbibed with pure PCE-DNAPL (equilibrium PCE concentration of 1,200 μM). Hence, PCE-DNAPL source zone bioremediation may be an effective polishing treatment, particularly if coupled with treatments such as surfactant flushing that may be capable of reducing aqueous PCE concentrations to non-toxic levels.

Complete PCE conversion to ethene is a primary remedial objective of microbial reductive dechlorination. As such, an additional column experiment was conducted to evaluate the distribution and activity of a mixed microbial consortium (Bio-Dechlor INOCULUM, BDI) capable of transforming PCE to ethene in the presence of a mixed NAPL (0.25 mol/mol PCE in hexadecane). Following a short lag period, source zone colonization by dechlorinating isolates was observed, along with enhanced PCE dissolution from the NAPL source zone. Chlorinated ethene concentrations during and immediate following this lag period also indicated that source zone dechlorination activity is required for dissolution enhancement. Mass transfer enhancement ranged from 4-fold to 20-fold, depending on the assumptions made in estimating abiotic dissolution. The large range of calculated enhancement factors demonstrates the difficulty in accurately estimating this parameter. In addition, dechlorination in the column generally stalled at *cis*-DCE (low levels of VC and ethene), implying that elevated *cis*-DCE concentrations may be adversely impact subsequent dechlorination steps.

The ganglia to pool ratio (GTP) was developed as a metric for evaluating source zone DNAPL distribution. Because source distribution was observed to be a key factor in down-gradient aqueous plume development following surfactant flushing, the GTP was incorporated into upscaled mass transfer equations correlating mass flux reductions and source zone mass recovery. As a result, the applicability and usefulness of the GTP must be evaluated. Further partial mass recovery studies at high GTP values (i.e., ganglia-dominated distributions) would allow the upscaled mass transfer correlations to

286

be refined to more accurately represent effluent mass behavior under these conditions. In addition, an attempt should be made to rectify the large difference between experimental (0.25-1.5) and numerical (2-20) GTP values in order to increase the robustness of the GTP approach. Finally, the potential for applying the GTP (or related) approach at pilot- or field-scale should be considered.

The results of this research are among the most complete data set to date relating partial mass recovery and post-treatment effluent mass flux. It would be beneficial to compare the experimental results to those obtained from complementary computational studies. A comparison would potentially allow more complete description of mass flux reduction curves as a function of source zone mass recovery, particularly since each experimental data set contains relatively few data points. Directly comparing experimental and numerical data may also allow refinement of the upscaled mass transfer correlations, improving their predictive utility for source zones containing predominately NAPL ganglia.

In addition to comparing 2-D aquifer cell experimental data and modeling results, a comparison between the 1-D biocolumn data generated during this work and values predicted by numerical modeling should be attempted. A successfully developed computational study would represent some of the first work directly modeling biomass and dissolution enhancement in the immediate vicinity of a NAPL source zone. This could provide critical insight into design of future bioremediation systems, especially if the model could be coupled to source zone distributions more complex than those present in the biocolumn.

In an effort to experimentally link complex source zone distributions with microbial reductive dechlorination, activity, spatial distribution, and down-gradient plume development should be evaluated in 2-D aquifer cells containing a PCE-DNAPL source zone and inoculated with BDI. Light transmission analysis of the PCE-DNAPL distribution, along with chlorinated ethene sampling and quantitative PCR measurement

of reductive dechlorination species could potentially link microbial growth and enhanced NAPL dissolution in a spatially complex system. A 2-D system is a more realistic representation of the subsurface than the 1-D biocolumn, and experiments in such a system could provide information on PCE-DNAPL dissolution enhancement factors and dechlorination endpoints that are more relevant at the field-scale. In addition, an experimental investigation of the possible synergistic effects of combined remedies such as surfactant flushing with a nonionic surfactant (i.e., Tween 80) and reductive dechlorination should be undertaken.

REFERENCES

Abriola, L. M., C. A. Ramsburg, K. D. Pennell, F. E. Löffler, M. Gamache, and E. A. Petrovskis. 2003. Post-Treatment Monitoring and Biological Activity at the Bachman Road Surfactant-Enhanced Aquifer Remediation Site. In *Pre-prints of Extended Abstracts of the American Chemical Society*, Washington, DC, 921-927.

Abriola, L. M., C. D. Drummond, L. D. Lemke, K. M. Rathfelder, K. D. Pennell, E. Petrovskis, and G. Daniels. 2001. Surfactant Enhanced Aquifer Remediation: Application of Mathematical Models in the Design and Evaluation of a Pilot-Scale Test. In *Groundwater Quality 2001, Pre-prints of the Third International Conference on Groundwater Quality*, University of Sheffield, United Kingdom, 6-8.

Abriola, L. M., T. J. Dekker, and K. D. Pennell. 1993. Surfactant-Enhanced Solubilization of Residual Dodecane in Soil Columns. 2. Mathematical Modeling. *Enviorn. Sci. Technol.*, **27**, 2341-2351.

Abriola, L. M., W. E. Condit, and M. A. Cowell. 2000. Influence of Soil Texture on Rate-Limited Micellar Solubilization. *J. Environ. Eng.*, **126**, 39-46.

Advanced Applied Technology Demonstration Facility (AATDF). 1997. *Technology Practices Manual for Surfactants and Cosolvents.* Rice University, Energy and Environmental Systems Institute, Houston, TX.

Adamson, D. T., J. M. McDade, and J. B. Hughes. 2003. Inoculation of a DNAPL Source Zone to Initiate Reductive Dechlorination of PCE. *Environ. Sci. Technol.*, **37**, 2525-2533.

Adamson, D. T., D. Y. Lyon, and J. B. Hughes. 2004. Flux and Product Distribution During Biological Treatment of a Tetrachloroethene Dense Non-Aqueous Phase Liquid. *Environ. Sci. Technol.*, **38**, 2021-2028.

Adeel, Z. and R. G. Luthy. 1995. Sorption and Transport Kinetics of a Nonionic Surfactant Through an Aquifer Sediemnt. *Environ. Sci. Technol.*, **29**, 1032-1042.

Amyx, J. W., D. M. Bass, and R. L. Whiting. 1960. *Petroleum Reservoir Engineering Physical Properties*. McGraw-Hill Book Co. Inc., New York, NY.

Annable, M. D., P. S. C. Rao, K. Hatfield, W. D Graham, A. L. Wood, and C. G. Enfield. 1998. Partitioning Tracers for Measuring Residual NAPL: Field-Scale Test Results. *J. Env. Engr.*, **124**, 498-503.

Attwood, D. and A. T. Florence. 1983. *Surfactant Systems: Their Chemistry, Pharmacy, and Biology*. Chapman and Hall, New York, NY.

Basel, M. D. and C. H. Nelson. 2000. Overview of In Situ Chemical Oxidation: Status and Lessons Learned. In *Treating Dense Nonaqueous-Phase Liquids (DNAPLs): Remediation of Chlorinated and Recalcitrant Compounds*, G.B. Wickramanayake, A.R. Gavaskar, and N. Gupta (Eds.). Battelle Press, Columbus, OH. 117-124.

Battelle. 2001. *Seventh Interim Report on the IDC Demonstration at Launch Complex 34, Cape Canaveral Air Station*, Interagency DNAPL Consortium, www.getf.org/file/dnapl/1779.pdf.

Bear, J. 1972. *Dynamics of Fluids in Porous Media*. Dover Pubilications, Mincola, NY.

Bergmann, J. G. and J. Sanik, Jr. 1957. Determination of Trace Amounts of Chlorine in Naphtha. *Anal. Chem.*, **29**, 241-243.

Bourrel, M. and R. S. Schechter. 1988. Surfactant Science Series v. 30: *Microemulsions and Related Systems*. Marcel Dekker, Inc., New York, NY.

Boving, T. B., Wang, X., and M. L. Brusseau. 1999. Cyclodextrin-Enhanced Solubilization and Removal of Residual-Phase Chlorinated Solvents from Porous Media. *Environ. Sci. Technol.*, **33**, 764-770.

Boving, T. B. and M. L. Brusseau. 2000. Solubilization and Removal of Residual Trichloroethene from Porous Media: Comparison of Several Solubilizing Agents. *J. Contam. Hydrol.*, **42**, 51-67.

Bradford, S. A. and F. J. Leij. 1995. Fractional Wettability Effects on Two- and Three-Fluid Capillary Pressure-Saturation Relations. *J. Contam. Hydrol.*, **20**, 89-109.

Bradford, S. A. and F. J. Leij. 1996. Predicting Two- and Three-Fluid Capillary Pressure-Saturation Relationships of Porous Media with Fractional Wettability. *Water Resour. Res.*, **32**, 251-259.

Bradford, S. A., R. A. Vendlinski, and L. M. Abriola. 1999. The Entrapment and Long-Term Dissolution of Tetrachloroethylene in Fractional Wettability Porous Media. *Water Resour. Res.*, **35**, 2955-2964.

Brooks M. C., M. D. Annable, P. S. C. Rao, K. Hatfield, J. W. Jawitz, W. R. Wise, A. L. Wood, and C. G. Enfield. 2004. Controlled Release, Blind Test of DNAPL Remediation by Ethanol Flushing. *J. Contam. Hydrol.*, **69**, 281-297.

Butler, E. C. and K. F. Hayes. 1998. Micellar Solubilization of Nonaqueous Phase Liquid Contaminants by Nonionic Surfactant Mixtures: Effects of Sorption, Partitioning and Mixing. *Water Res.*, **32**, 1345-1354.

Carr, C. S., S. Garg, and J. B. Hughes. 2000. Effect of Dechlorinating Bacteria on the Longevity and Composition of PCE-Containing Nonaqueous Phase Liquids under Equilibrium Dissolution Conditions. *Environ. Sci. Technol.*, **34**, 1088-1094.

Chang, Y. C., M. Hatsu, K. Jung, Y. S. Yoo, and K. Takamizawa. 2000. Isolation and Characterization of a Tetrachloroethylene Dechlorinating Bacterium, *Clostridium bifermentans* DPH-1. *J. Biosci. Bioeng.*, **89**, 489-491.

Chen, G., G. E. Hoag, P. Chedda, F. Nadim, B. A. Woody, and G. M. Dobbs. 2001. The Mechanism and Applicability of In Situ Oxidation of Trichloroethylene with Fenton's Reagent. *J. Haz. Mat.*, **87**, 171-186.

Cherry J. A., S. Feenstra, and D. M. Mackay. 1997. Developing rational goals for in situ remedial technologies. In *Subsurface Restoration*, C. H. Ward, J. A. Cherry, and M. R. Scalf (Eds.). Ann Arbor Press, Chelsea, MI, 75–98.

Childs, J. D., E. Acosta, R. Knox, J. H. Harwell, and D. A. Sabatini. 2004. Improving the Extraction of Tetrachloroethylene from Soil Columns Using Surfactant Gradient Systems. *J. Contam. Hydrol.*, **71**, 27-45.

Christ, J. A., C. A. Ramsburg, L. M. Abriola, K. D. Pennell, and F. E. Löffler. 2005a. Coupling Aggressive Mass Removal with Microbial Reductive Dechlorination for Remediation of DNAPL Source Zones: A Review and Assessment. *Environ. Health Persp.*, **113**, 465-477.

Christ, J. A., L. D. Lemke, and L. M. Abriola. 2005b Comparison of Two-Dimensional and Three-Dimensional Simulations of Dense Nonaqueous Phase Liquids (DNAPLs): Migration and Entrapment in a Nonuniform Permeability Field. *Water Resour. Res.*, **41**, W01007.

Christ, J. A., C. A. Ramsburg, K. D. Pennell, and L. M. Abriola. 2006. Numerical Evaluation of Upscaled Mass Transfer Coefficients for Estimation of DNAPL Source-Zone Mass Discharge. *Water Resour. Res.* (*in review*).

Chu, M., P. K. Kitanidis, and P. L. McCarty. 2003. Effects of Biomass Accumulation on Microbial Enhanced Dissolution of a PCE Pool: A Numerical Simulation. *J. Contam. Hydrol.*, **65**, 79-100.

Cohen, R. M. and J. W. Mercer. 1993. *DNAPL Site Evaluation*. C.K. Smoley, Boca Raton, FL.

Cole, J. R., B. Z. Fathepure, and J. M. Tiedje. 1995. Tetrachloroethene and 3-Chlorobenzoate Activities are Co-Induced in *Desulfomonile tiedjei* DCB-1. *Biodegradation*, **6**, 167-172.

Coleman, N. V., T. E. Mattes, J. M. Gossett, and J. C. Spain. 2002a. Biodegradation of *cis*-Dichloroethene as the Sole Carbon Source by a β-Proteobacterium. *Appl. Environ. Microbiol.*, **68**, 2726-2730.

Coleman, N. V., T. E. Mattes, J. M. Gossett, and J. C. Spain. 2002b. Phylogenetic and Kinetic Diversity of Aerobic Vinyl Chloride-Assimilating Bacteria from Contaminated Sites. *Appl. Enviorn. Microbiol.*, **68**, 6162-6171.

Cope, N. and J. B. Hughes. 2001. Biologically-Enhanced Removal of PCE from NAPL Source Zones. *Environ. Sci. Technol.*, **35**, 2014-2021.

Darnault, C. J. G., J. A. Throop, D. A. DiCarlo, A. Rimmer, T. S. Steenhuis, and J. −Y. Parlange. 1998. Visualization by Light Transmission of Oil and Water Contents in Transient Two-Phase Flow Fields. *J. Contam. Hydrol.*, **31**, 337-348.

Dekker, T. J. and L. M. Abriola. 2000a. Influence of Field-Scale Heterogeneity on the Infiltration and Entrapment of Dense Nonaqueous Phase Liquids in Saturated Formations. *J. Contam. Hydrol.*, **42**, 187-218.

Dekker, T. J. and L. M. Abriola. 2000b. The Influence of Field-Scale Heterogeneity on the Surfactant-Enhanced Remediation of Entrapped Nonaqueous Phase Liquids. *J. Contam. Hydrol.*, **42**, 219-251.

Delshad, M., G. A. Pope, L. Yeh, and F. J. Holzmer. 2000. Design of the Surfactant Flood at Camp Lejeune. In *Treating Dense Nonaqueous-Phase Liquids (DNAPLs): Remediation of Chlorinated and Recalcitrant Compounds*, Wickramanayake, G. B., A. R. Gavaskar, and N. Gupta (Eds.). Battelle Press, Columbus, OH, 203-210.

Diallo, M. S., L. M. Abriola, and W. J. Weber, Jr. 1994. Solubilization of Nonaqueous Phase Liquid Hydrocarbons in Micellar Solutions of Dodecyl Alcohol Ethoxylates. *Environ. Sci. Technol.*, **28**, 1829-1837.

Dwarakanath, V. 1997. Characterization and Remediation of Aquifers Contaminated by Nonaqueous Phase Liquids Using Partitioning Tracers and Surfactants. Dissertation, Department of Petroleum and Geosystems Engineering, The University of Texas at Austin.

Dwarakanath, V., K. Kostarelos, G. A. Pope, D. Shotts, and W. H. Wade. 1999. Anionic Surfactant Remediation of Soil Columns Contaminated by Nonaqueous Phase Liquids. *J. Contam. Hydrol.*, **38**, 465-488.

Falta, R. W., C. M. Lee, S. E. Brame, E. Roeder, J. T. Coates, C. Wright, A. L. Wood, and C. G. Enfield. 1999. Field Test of High Molecular Weight Alcohol Flushing for Subsurface Nonaqueous Phase Liquid Remediation. *Water Resour. Res.*, **35**, 2095-2108.

Falta, R. W., P. S. C. Rao, and N. Basu. 2005. Assessing the Impacts of Partial Mass Depletion in DNAPL Source Zones. I. Analytical Modeling of Source Strength Functions and Plume Response. *J. Contam. Hydrol.*, **78**, 259-280.

Fathepure, B. Z. and S. A. Boyd. 1988. Reductive Dechlorination of Perchloroethylene and the Role of Methanogens. *FEMS Microbiol. Lett.*, **49**, 149-156.

Fetter, C. W. 1999. *Contaminant Hydrogeology*. Prentice-Hall, Inc., Upper Saddle River, NJ.

Field, J. A. and T. E. Sawyer. 2002. High-Performance Liquid Chromatography Diode Array Detection of Trichloroethene and Aromatic and Aliphatic Anionic Surfactants Used for Surfactant-Enhanced Aquifer Remediation. *J. Chromatogr. A.*, **893**, 253-260.

Feenstra, S., J. A. Cherry, and B. L. Parker. 1996. Conceptual models for the behavior of dense non-aqueous phase liquids (DNAPLs) in the subsurface. In *Dense Chlorinated Solvents and Other DNAPLs in Groundwater*, J. F. Pankow and J. A. Cherry (Eds.), Waterloo Press, Guelph, Ontaria, Canada, 53-88.

Fortin, J., W. A. Jury, and M. A. Anderson. 1997. Enhanced Removal of Trapped Non-Aqueous Phase Liquids from Saturated Soil Using Surfactant Solutions. *J. Contam. Hydrol.*, **24**, 247-267.

Fountain, J. C., A. Klimel, M. G. Beikirch, and T. M. Middleton. 1991. The Use of Surfactants for In Situ Extraction of Organic Pollutants from a Contaminated Aquifer. *J. Hazard. Mater.*, **28**, 295-311.

Fountain, J. C., R. C. Starr, T. Middleton, M. Beikirch, C. Taylor, and D. Hodge. 1996. A Controlled Field Test of Surfactant-Enhanced Aquifer Remediation. *Ground Water*, **34**, 910-916.

Gerritse, J., V. Renard, P. Gomes, P. A. Lawson, M. D. Collins, and J. C. Gottschal. 1996. *Desulfitobacterium* sp. strain PCE1, an Anaerobic Bacterium that can Grow by Reductive Dechlorination of Tetrachloroethene or Ortho-Chlorinated Phenols. *Arch. Microbiol.*, **165**, 132-140.

Gierke, J. S., C. L. Wojick, and N. J. Hutzler. 1999. Field Test of Air Sparging Coupled with Soil Vapor Extraction. In *ACS Symposium Series*, *Vol. 725*, Oxford University Press, Oxford, England, 153-166.

Gossett, J. M. 1987. Measurement of Henry's Law Constants for C1 and C2 Chlorinated Hydrocarbons. *Environ. Sci. Technol.*, **21**, 202-208.

Hasegawa, M. H., B. J. Shau, D. A. Sabatini, R. C. Knox, J. H. Harwell, R. Lago, and L. Yeh. 2000. Surfactant-Enhanced Subsurface Remediation of DNAPLs at the Former Naval Air Station Alameda, California. In *Treating Dense Nonaqueous-Phase Liquids (DNAPLs): Remediation of Chlorinated and Recalcitrant Compounds*, Wickramanayake, G.B., A.R. Gavaskar, and N. Gupta (Eds.). Battelle Press, Columbus, OH, 219-226.

Hassanizadeh, S. M. and W. G. Gray. 1990. Mechanics and Thermodynamics of Multiphase Flow in Porous Media Including Interfacial Boundaries. *Adv. Water Resour.*, **13**, 169-186.

He, J., Y. Sung, M. E. Dollhopf, B. Z. Fathepure, J. M. Tiedje, and F. E. Löffler. 2002. Acetate Versus Hydrogen as Direct Electron Donors to Stimulate the Microbial Reductive Dechlorination Process at Chloroethene-Contaminated Sites. *Environ. Sci. Technol.*, **36**, 3945-3952.

He, J., K. M. Ritalahti, M. R. Aiello, and F.E. Löffler. 2003a. Complete Detoxification of Vinyl Chloride by an Anaerobic Enrichment Culture and Identification of the Reductively Dechlorinating Population as a *Dehalococcoides* Species. *Appl. Environ. Microbiol.*, **69**, 996-1003.

He. J., K. M. Ritalahti, K.-L. Yang. S. S. Koenigsberg, and F. E. Löffler. 2003b. Detoxification of Vinyl Chloride to Ethene Coupled to Growth of an Anaerobic Bacterium. *Nature*, **243**, 62-65.

Heron, G., S. Carroll, and S. G. Nielson. 2005. Full-Scale Removal of DNAPL Constituents Using Steam-Enhanced Extraction and Electrical Resistance Heating. *Ground Water Monitoring and Remediation*, **25**, 92-107.

Higgins, I. J., D. J. Best, and R. C. Hammond. 1980. New Findings in Methane-Utilizing Bacteria Highlight Their Importance in the Biosphere and Their Commercial Potential. *Nature*, **286**, 561-564.

Holliger, C., D. Hahn, H. Harmsen, W. Ludwig, W. Schumacher, B. Tindall, F. Vazquez, N. Weiss, and A. J. B. Zehnder. 1998 *Dehalobacter restrictus* gen. nov. and sp. nov., a Strictly Anaerobic Bacterium that Reductively Dechlorinates Tetra- and Trichloroethene in an Anaerobic Respiration. *Arch. Microbiol.* **169**, 313-321.

Holzmer, F. J., G. A. Pope, and L. Yeh. 2000. Surfactant-Enhanced Aquifer Remediation of PCE DNAPL in Low-Permeability Sand. In *Treating Dense Nonaqueous-Phase Liquids (DNAPLs): Remediation of Chlorinated and Recalcitrant Compounds*, Wickramanayake, G.B., A.R. Gavaskar, and N. Gupta (Eds.). Battelle Press, Columbus, OH, 211-218.

Huh, C. 1979. Interfacial-Tensions and Solubilizing Ability of a Microemulsion Phase that Coexists with Oil and Brine. *J. Colloid Interface Sci.*, **71**, 408-426.

Hunt, J. R., N. Sitar, and K. S. Udell. 1988. Nonaqueous Phase Liquid Transport and Cleanup. 2. Experimental Studies. *Water Resour. Res.*, **24**, 1259-1269.

Imhoff, P. T., S. N. Gleyzer, J. F. McBride, L. A. Vancho, I. Okuda, and C. T. Miller. 1995. Cosolvent Enhanced Remediation of Residual Dense Nonaqueous Phase Liquids: Experimental Investigation. *Environ. Sci. Technol.*, **29**, 1966-1976.

Jackson, R. E., H. W. Meinardus, and T. W. Griffin. 2003. Discussion of a Comparison of Field Techniques for Confirming Dense Nonaqueous Phase Liquids. *Ground Water Monitoring and Remediation*, **23**, 28-30.

Jawitz, J. W., R. K. Sillan, M. D. Annable, P. S. C. Rao, and K. Warner. 2000. In Situ Alcohol Flushing of a DNAPL Source Zone at a Dry Cleaner Site. *Eniviron. Sci. Technol.*, **34**, 3722-3729.

Jawitz, J.W., M.D. Annable, P.S.C. Rao, and R.D. Rhue. 2001. Evaluation of Remediation Performance and Cost for Field-Scale Single-Phase Microemulsion (SPME) Flushing. *J. Environ. Sci. Health*, **A36**, 1437-1450.

Jawitz, J. W., A. D. Fure, G. G. Demmy, S. Berglund, and P. S. C. Rao. 2005. Groundwater Contaminant Flux Reduction Resulting from Nonaqueous Phase Liquid Mass Reduction. *Water Resour. Res.,* **41**, W10408.

Jin, M., M. Delshad, V. Dwarakanath, D. C. McKinnery, G. A. Pope, K. Sepehrnoori, and C. E. Tillburg. 1995. Partitioning Tracer Test for Detection, Estimation, and Remediation Performance Assessment of Subsurface Nonaqueous Phase Liquids. *Water Resour. Res.*, **31**, 1201-1211.

Kaslusky, S. F. and K. S. Udell. 2002. A Theoretical Model of Air and Steam Co-Injection to Prevent the Downward Migration of DNAPLs During Steam-Enhanced Extraction. *J. Contam. Hydrol.*, **55**, 213-232.

Kibbey, T. C. G., C. A. Ramsburg, K. D. Pennell, and K. F. Hayes. 2002. Implications of Alcohol Partitioning Behavior for in situ Density Modification of Entrapped Dense Nonaqueous Phase Liquids. *Environ. Sci. Technol.*, **23**, 104-111.

Knox, R.C., B.J. Shau, D.A. Sabatini, and J.H. Harwell. 1999. Field Demonstration Studies of Surfactant-Enhanced Solubilization and Mobilization at Hill Air Force Base, Utah. In *Innovative Subsurface Remediation: Field Testing of Physical, Chemical, and Characterization Technologies*, Brusseau, M.L., D.A. Sabatini, J.S. Gierke, and M.D. Annable (Eds.). American Chemical Society, Washington, District of Columbia.

Koenigsberg, S. S. and W. Farone. 1999. The Use of Hydrogen Release Compound (HRC™) for CAH Bioremediation. In *Engineered Approaches for In Situ Bioremediation of Chlorinated Solvent Contamination*, Leeson, A. and B. C. Alleman (Eds.). Battelle Press, Columbus, OH. 67-72.

Kueper, B. H. and E. O. Frind. 1991. Two-Phase Flow in Heterogeneous Media. 1. Model Development. *Water Resour. Res.*, **27**, 1049-1057.

Lemke, L. D., L. A. Abriola, and P. Goovaerts. 2004. DNAPL Source Zone Characterization: Influence of Hydraulic Property Correlation on Predictions of DNAPL Infiltration and Entrapment. *Water Resour. Res.*, **40**, W01511.

Lenhard, R. J., T. G. Johnson, and J. C. Parker. 1993. Experimental Observations of Nonaqueous-Phase Liquid Subsurface Movement. *J. Contam. Hydrol.*, **12**, 79-101.

Letterman, R. D. (ed.). 1999. *Water Quality and Treatment*. 5th Ed. McGraw-Hill, Inc., New York, NY, 1.4-1.17.

Löffler, F. E., R. A. Sanford, and J. M. Tiedje. 1996. Initial Characterization of a Reductive Dehalogenase from *Desulfitobacterium chlororespirans* Co23. *Appl. Envrion. Microbiol.*, **62**, 3809-3813.

Löffler, F. E., J. E. Champine, K. M. Ritalahti, S. J. Sprague, and J. M. Tiedje. 1997. Complete Reductive Dechlorination of 1,2-Dichloropropane by Anaerobic Bacteria. *Appl. Environ. Microbiol.*, **63**, 2870-2875.

Löffler, F. E., J. M. Tiedje, and R. A. Sanford. 1999. Fraction of Electrons Consumed in Electron Acceptor Reduction and Hydrogen Threshold as Indicators of Halorespiratory Physiology. *Appl. Environ. Microbiol.*, **65**, 4049—4056.

Löffler, F. E., J. R. Cole, K. M. Ritalahti, and J. M. Tiedje. 2003. Diversity of Dechlorinating Bacteria. In *Dehalogenation: Microbial Processes and Environmental Applications*, Häggblom, M. M. and I. D. Bossert (Eds.). Kluwer Academic, New Your, NY.

Löffler, F. E. and E. A. Edwards. 2006 Harnessing Microbial Activities for Environmental cleanup. *Curr. Opin. Biotechnol.*, **17**, 274-284.

Londergan, J. T., H. W. Meinardus, P. E. Mariner, R. E. Jackson, C. L. Brown, V. Dwarakanath, G. A. Pope, J. S. Ginn, and S. Taffinder. 2001. DNAPL Removal from a Heterogeneous Alluvial Aquifer by Surfactant-Enhanced Aquifer Remediation. *Ground Water Monitoring and Remediation*, **21**, 57-67.

Longino, B. L. and B. H. Kueper. 1995. Use of Upward Gradients to Arrest Downward Dense, Nonaqueous Phase Liquid (DNAPL) Migration in the Presence of Solubilizing Surfactants. *Can. Geotech. J.*, **32**, 296-308.

Loverde, L. 1997. *Effect of Rate-Limited Interfacial Tension Reductions on the Displacement of Residual NAPLs During Surfactant Flushing*. MS Thesis, School of Civil and Environmental Engineering, Georgia Institute of Technology.

Lunn, S. R. D. and B. H. Kueper. 1997. Removal of Pooled Dense, Nonaqueous Phase Liquid from Saturated Porous Media Using Upward Gradient Alcohol Floods. *Water Resour. Res.*, **33**, 2207-2219.

Lunn, S. R. D. and B. H. Kueper. 1999a. Risk Reduction During Chemical Flooding: Preconditioning DNAPL Density In Situ Prior to Recovery by Miscible Displacement. *Environ. Sci. Technol.*, **33**, 1703-1708.

Lunn, S. R. D. and B. H. Kueper. 1999b. Manipulation of Density and Viscosity for the Optimization of DNAPL Recovery by Alcohol Flooding. *J. Contam. Hydrol.*, **38**, 427-445.

MacDonald, J. A. and M. C. Kavanaugh. 1994. Restoring Contaminated Groundwater: An Achievable Goal? *Environ. Sci. Technol.*, **28**, 362A-368A.

MacKinnon, L. K. and N. R. Thomson. 2002. Laboratory-Scale In Situ Chemical Oxidation of a Perchloroethylene Pool Using Permanganate. *J. Contam. Hydrol.*, **56**, 49-74.

Mackey, D. M. and J. A. Cherry. 1989. Groundwater Contamination: Pump-And-Treat Remediation. *Environ. Sci. Technol.*, **23**, 630-636.

Major, D., M. L. McMaster, E. E. Cox, E. A. Edwards, S. M. Dworatzek, E. R. Hendrickson, M. G. Starr, J. A. Payne, and L. W. Buonamici. 2002. Field Demonstration of Successful Bioaugmentation to Achieve Dechlorination of Tetrachloroethene to Ethene. *Environ. Sci. Technol.*, **36**, 5106-5116.

Martel, R., P.J. Gelinas, and J.E. Desnoyers. 1998a. Aquifer Washing by Micellar Solutions: 1. Optimization of Alcohol-Surfactant-Solvent Solutions. *J. Contam. Hydrol.*, **29**, 319-346.

Martel, R., R. Lefebvre, and P.J. Gelinas. 1998b. Aquifer Washing by Micellar Solutions: 2. DNAPL Recovery Mechanisms for an Optimized Alcohol-Surfactant-Solvent Solution. *J. Contam. Hydrol.*, **30**, 1-31.

Martel, R., P.J. Gelinas, and L. Saumure. 1998c. Aquifer Washing by Micellar Solutions: 3. Field Test at the Thouin Sand Pit (L' Assomption, Quebec, Canada). *J. Contam. Hydrol.*, **30**, 33-48.

Mayer, A. S., L. Zhong, and G. A. Pope. 1999. Measurement of Mass-Transfer Rates for Surfactant-Enhanced Solubilization of Nonaqueous Phase Liquids. *Environ. Sci. Technol.*, **33**, 2965-2972.

Maymo-Gatell, X., Y.-T. Chien, J. M. Gossett, and S. H. Zinder. 1997. Isolation of a Bacterium that Reductively Dechlorinates Tetrachloroethene to Ethene. *Science*, **30**, 33-48.

McGuire, T. and J. B. Hughes. 2003. Effects of Surfactants on the Dechlorination of Chlorinated Ethenes. *Environmental Toxicology and Chemistry*, **22**, 2630-2638.

McWhorter, D. B. and J. D. Nelson. 1979. Seepage in the Partially Saturated Zone Beneath Tailings Impoundments. *Mining Eng.*, **April**, 432-439.

McWhorter, D. B. and T. C. Sale. 2003. Reply to Comment by P. S. C. Rao and J. W. Jawitz on "Steady State Mass Transfer from Single-Component Dense Nonaqueous Phase Liquids in Uniform Flow Fields". *Water Resour. Res.*, **39**, 1069.

Meinardus, H.W., V. Dwarakanath, J. Ewing, G.J. Hirasaki, R.E. Jackson, M. Jin, J.S. Ginn, J.T. Londergan, C.A. Miller, and G.A. Pope. 2002. Performance Assessment of NAPL Remediation in Heterogeneous Alluvium. *J. Contam. Hydrol.*, **54**, 173-193.

Mercer, J. W. and R. M. Cohen. 1990. A Review of Immiscible Fluids in the Subsurface: Properties, Models, Characterization, and Remediation. *J. Contam. Hydrol.*, **6**, 107-163.

Middleman, S. 1998. *An Introduction to Fluid Dynamics*. John Wiley & Sons, Inc., New York, NY.

Miller, C. T., E. H. Hill III, and M. Moutier. 2000. Remediation of DNAPL-Contaminated Subsurface Systems Using Density Motivated Mobilization. *Enviorn. Sci. Technol.*, **34**, 719-724.

Morrow, N. R. 1990. Wettability and Its Effect on Oil Recovery. *J. Petrol. Technol.*, **December**, 1476-1484.

Mravik, S. C., R. K. Sillan, A. L. Wood, and G. W. Sewell. 2003. Field Evaluation of the Solvent Extraction Residual Biotreatment Technology. *Environ. Sci. Technol.*, **37**, 5040-5049.

Nambi, I. M., C. J. Werth, R. A. Sanford, and A. J. Valocchi. 2003. Pore-Scale Analysis of Anaerobic Halorespiring Bacterial Growth along the Transverse Mixing Zone of an Etched Silicon Pore Network. *Environ. Sci. Technol.*, **37**, 5617-5624.

National Research Council (NRC). 1997. *Innovations in Ground Water and Soil Cleanup: From Concept to Commercialization.* The National Academy Press, Washington, DC.

National Research Council (NRC). 2004. *Contaminants in the Subsurface: Source Zone Assessment and Remediation.* The National Academies Press, Washington, DC. 372.

Neumann, A., H. Scholz-Muramatsu, and G. Diekert. 1994. Tetrachloroethene Metabolism of *Dehalospirillum multivorans. Arch. Microbiol.*, **162**, 295-301.

Nielson, R. B. and J. D. Keasling. 1999. Reductive Dechlorination of Chlorinated Ethene DNAPLS by a Culture Enriched from Contaminated Groundwater. *Biotechnol. Bioeng.*, **62**, 160-165.

Pankow, J. F. and J. A. Cherry. 1996. *Dense Chlorinated Solvents and other DNAPLs in Groundwater: History, Behavior, and Remediation.* Waterloo Press, Portland, OR.

Parker, J. C. and E. Park. 2004. Modeling Field-Scale Dense Nonaqueous Phase Liquid Dissolution Kinetics in Heterogeneous Aquifers. *Water Resour. Res.*, **40**, W051091.

Pennell, K. D., L. M. Abriola, and W. J. Weber. 1993. Surfactant-Enhanced Solubilization of Residual Dodecane in Soil Columns. 1. Experimental Investigation. *Environ. Sci. Technol.*, **27**, 2332-2340.

Pennell K. D., M. Jin, L. M. Abriola, and G. A. Pope. 1994. Surfactant Enhanced Remediation of Soil Columns Contaminated by Residual Tretrachloroethylene. *J. Contam. Hydrol.*, **16**, 35-53.

Pennell, K. D., G. A. Pope, and L. M. Abriola. 1996. Influence of Viscous and Bouyancy Forces on the Mobilization of Residual Tetrachloroethylene During Surfactant Flusing. *Environ. Sci. Technol.*, **30**, 1328-1335.

Pennell, K. D., A. M. Adinolfi, L. M. Abriola, and M. S. Diallo. 1997. Solubilization of Dodecane, Tetrachloroethylene, and 1,2-Dichlorobenzene in Micellar Solutions of Ethoxylated Nonionic Surfactants. *Environ. Sci. Technol.*, **31**, 1382-1389.

Pennell, K. D. and L. M. Abriola. 1997. Surfactant Enhanced Aquifer Remediation: Fundamental Processes and Practical Implications. *In* Bioremediation: Principles and Practice, Volume 1., S.K. Sikdar and R.L. Irvine (Eds.), Technomic Publ., Lancaster, PA. p. 693-750.

Pennell, K. D. 2000. United States Patent Number 6,099,206: Density Modified Displacement to Remediate Contaminated Aquifers. Assigned to the Georgia Institute of Technology.

Pennell, K. D., Pavlostathis, S. G., Karagundux, A., and D. H. Yeh. 2001. Influence of Nonionic Surfactants on the Bioavailability of Hexachlorobenzene to Microbial Reductive Dechlorination. In *Chemicals in the Environment: Fate, Impacts, and Remediation*, R. L. Lipnik, R. P. Mason, M. L. Phillips, and C. U. Pittman (Eds.), Oxford Press, New York, NY. 449-466

Pope, G. A. and W. H. Wade. 1995. Lessons From Enhanced Oil Recovery Research for Surfactant-Enhanced Aquifer Remediaion. In *ACS Symposium Series 594*, American Chemical Society, Washington, DC. 142-160.

Powers, S. E., C. O. Loureiro, L. M. Abriola, and W. J. Weber. 1991. Theoretical Study of the Significance of Nonequilibrium Dissolution of Nonaqueous Phase Liquids in Subsurface Systems. *Water Resour. Res.*, **27**, 463-477.

Powers, S. E., L. M. Abriola, and W. J. Weber, Jr. 1992. An Experimental Investigation of Nonaqueous Phase Liquid Dissolution in Saturated Subsurface Systems: Steady State Mass Transfer Rates. *Water Resour. Res.*, **28**, 2691-2705.

Powers, S. E. 1992. Dissolution of Nonaqueous Phase Liquids in Saturated Subsurface Systems. Doctoral Thesis, The University of Michigan.

Ramsburg, C. A. and K. D. Pennell. 2001. Experimental and Economic Assessment of Two Surfactant Formulations for Source Zone Remediation at a Former Dry Cleaning Facility. *Ground Water Monitoring and Remediation, ***21**, 68-82.

Ramsburg, C. A. and K. D. Pennell. 2002a. Density-Modified Displacement for Dense Nonaqueous-Phase Liquid Source-Zone Remediation: Density Conversion Using a Partitioning Alcohol. *Environ. Sci. Technol.*, **36**, 2082-2087.

Ramsburg, C. A. and K. D. Pennell. 2002b. Density-Modified Displacement for DNAPL Source Zone Remediation: Density Conversion and Recovery in Heterogeneous Aquifer Cells. *Environ. Sci. Technol.*, **36**, 3176-3187.

Ramsburg, C. A. 2002. Development of Surfactant-Based Immiscible Displacement Technologies for Remediation of Aquifers Contaminated with Dense Non-Aqueous Phase Liquids. Dissertation, School of Civil and Environmental Engineering, Georgia Institute of Technology.

Ramsburg, C. A., K. D. Pennell, T. C. G. Kibbey, and K. F. Hayes. 2003. Use of a Surfactant-Stabilized Emulsion to Deliver 1-Butanol for Density-Modified Displacement of Trichloroethene. *Environ. Sci. Technol.*, **37**, 4246-4253.

Ramsburg, C. A., K. D. Pennell, T. C. G. Kibbey, and K. F. Hayes. 2004a. Refinement of the Density-Modified Displacement Method for Efficient Treatment of Tetrachloroethene Source Zones. *J. Contam. Hydrol.*, **74**, 105-131.

Ramsburg, C. A., L. M. Abriola, K. D. Pennell, F. E. Löffler, M. Gamache, B. K. Amos, and E. A. Petrovskis. 2004b. Stimulated microbial reductive dechlorination following surfactant treatment at the Bachman Road site. *Environ. Sci. Technol.*, **38**, 5902-5914.

Ramsburg, C. A., K. D. Pennell, L. M. Abriola, G. Daniels, C. D. Drummond, M. Gamache, H.-L. Hsu, E. A. Petrovskis, K. M. Rathfelder, J. L. Ryder, and T. P. Yavaraski. 2005. Pilot-Scale Demonstration of Surfactant-Enhanced PCE Solubilization at the Bachman Road Site. 2. System Operation and Evaluation. *Environ. Sci. Technol.*, **39**, 1791-1801.

Rao, P. S. C., M. D. Annable, R. K. Sillan, D. Dai, K. Hatfield, W. D. Graham, A. L. Wood, and C. G. Enfield. 1997. Field-Scale Evaluation of In Situ Cosolvent Flushing for Enhanced Aquifer Remediation. *Water Resour. Res.*, **33**, 2673-2686.

Rao, P. S. C. and J. W. Jawitz. 2003. Comment on "Steady State Mass Transfer from Single-Component Dense Nonaqueous Phase Liquids in Uniform Flow Fields". *Water Resour. Res.*, **39**, 1068.

Rathfelder, K. M., L. M.Abriola, T. P. Taylor, and K. D. Pennell. 2001. Surfactant Enhanced Recovery of Tetrachloroethylene from a Porous Medium Containing Low Permeability Lenses 2. Numerical Simulation. *J. Contam. Hydrol.*, **48**, 351-374.

Reeves, P. C. and M. A. Celia. 1996. A Functional Relationship Between Capillary Pressure, Saturation, and Interfacial Area as Revealed by a Pore-Scale Network Model. *Water Resour. Res.*, **32**, 2345-2358.

Riddick, J. A. and W. B. Bunger. 1970. *Techniques of Chemistry. Vol. 2, Organic Solvents: Physical Properties and Methods of Purification 3rd ed.*, Weissberger, A. Ed., Wiley-Interscience, New York, NY, 1041.

Ritalahti, K. M., R. Krajmalnik-Brown, and F. E. Löffler. 2001. *Dehalococcoides* Species are the Dominant Vinyl Chloride-Dechlorinating Bacteria in Anaerobic Environments. Unpublished presentation at the 6th International Symposium on *In Situ* and On-Site Bioremediation, 4-7 June 2001.

Robertson, B. K. and M. Alexander. 1996. Mitigation of Toxicity to Permit Bioremediation of Constituents of Nonaqueous-Phase Liquids. *Environ. Sci. Technol.*, **24**, 2066-2070.

Rogers, B. and B. E. Logan. 2000. Bacterial Transport in NAPL-Contaminated Porous Media. *J. Environ. Eng*., **126**, 657-666.

Rosen, M. J. 1989. *Surfactants and Interfacial Phenomena*, 2nd ed. Wiley Interscience, New York, NY.

Ruith, M. and E. Meiburg. 2000. Miscible Rectiliniear Displacements with Gravity Override. Part 1. Homogeneous Porous Medium. *J. Fluid Mech.*, **420**, 225-257.

Sabatini, D. A., R. C. Knox, J. H. Harwell, and B. Wu. 2000. Integrated Design of Surfactant Enhanced DNAPL Remediation: Efficient Supersolubilization and Gradient Systems. *J. Contam. Hydrol.*, **45**, 99-121.

Sale, T. C. and D. B. McWhorter. 2001. Steady State Mass Transfer from Single-Component Dense Nonaqueous Phase Liquids in Uniform Flow Fields. *Water Resour. Res.*, **37**, 393-404.

Schroth, M. H., S. J. Ahearn, J. S. Selker, and J. D. Istok. 1996. Characterization of Miller-Similar Silica Sands for Laboratory Hydrology Studies. *Soil Science Society of America Journal*, **60**, 1331-1339.

Schroth, M. H., M. Oostrom, T. W. Wietsma, and J. D. Istok. 2001. In-Situ Oxidation of Trichloroethene by Permanganate: Effects on Porous Medium Hydraulic Properties. *J. Contam. Hydrol.*, **50**, 79-98.

Schmidt, R. J. Gudbjerg, T. O. Sonnenborg, and K. H. Jensen. 2002. Removal of NAPLs from the Unsaturated Zone Using Steam: Prevention of Downward Migration by Injecting Mixtures of Steam and Air. *J. Contam. Hydrol.*, **55**, 233-260.

Schwarzenbach, R. P., P. M. Gschwend, and D. M. Imboden. 2003. *Environmental Organic Chemistry*. John Wiley & Sons, Inc., Hoboken, NJ.

Schwille, F. 1984. Migration of Organic Fluids Immiscible with Water in the Unsaturated Zone. In *Pollutants in Porous Media*, B. Yaron, G. Dagen, and J. Goldshmid (Eds.). Springer-Verlag, Berlin, Germany. 27-48

Schwille, F. 1988. *Dense Chlorinated Solvents in Porous and Fractured Media*. Translated by J.F. Pankow. Lewis Publishers, Boca Raton, FL, xiii-xvi.

Shah, D. O. and R. S. Schecter. 1977. *Improved Oil Recovery y Surfactant and Polymer Flooding*. Academic Press, Inc. New York, NY.

She, H. Y. and B. E. Sleep. 1999. Removal of Perchloroethylene From a Layered Soil System by Steam Flushing. *Ground Water Monitoring and Remediation*, **19**, 70-77.

Shiau, B.-J., D. A. Sabatini, and J. H. Harwell. 1994. Solubilization and Microemulsification of Chlorinated Solvents Using Direct Food Additive (Edible) Surfactants. *Ground Water*, **32**, 806-814.

Shim, H., D. Ryoo, P. Barbieri, and T. K. Wood. 2001. Aerobic Degradation of Mixtures of Tetrachloroethylene, Trichloroethylene, Dichloroethylenes, and Vinyl Chloride by Toluene-*o*-Xylene Monooxygenase of *Pseudomonas stutzeri* OX1. *Appl. Microbiol. Biotechnol.*, **56**, 265-269.

Sleep, B. E., D. J. Seeperad, K. Mo, C. M. Heidorn, L. Hrapovic, P. L. Morrill, M. L. McMaster, E. D. Hood, C. Lebron, B. S. Lollar, D. W. Major, and E. A. Edwards. 2006. Biological Enhancement of Tetrachloroethene Dissolution and Associated Microbial Community Changes. *Environ. Sci. Technol.*, **40**, 3623-3633.

Soga, K., J. W. E. Page, and T. H. Illangasekare. 2004. A Review of NAPL Source Zone Remediation Efficiency and the Mass Flux Approach. *J. Haz. Mat.*, **110**, 13-27.

Sung, Y., K. M. Ritalahti, R. A. Sanford, J. W. Urbance, S. J. Flynn, J. M. Tiedje, and F. E. Löffler. 2003 Characterization of Two Tetrachloroethene-Reducing, Acetate-Oxidizing Anaerobic Bacteria, and Their Description as *Desulfuromonas michiganensis* sp. nov. *Appl. Environ. Microbiol.*, **69**, 2964-2974.

Sung, Y., K. E. Fletcher, K. M. Ritalahti, R. Apkarian, N. Ramos-Hernández, R. A. Sanford, N. M. Mesbah, F. E. Löffler. *Geobacter lovleyi* sp. nov. strain SZ, a Novel Metal-Reducing and Tetrachloroethene-Dechlorinating Bacterium. *Appl. Environ. Microbiol.*, **72**, 2775-2782.

Stroo, H. F., M. Unger, C. H. Ward, M. C. Kavanaugh, C. Vogel, A. Leeson, J. A. Marqusee, and B. P. Smith. 2003. Remediating Chlorinated Solvent Source Zones. *Environ. Sci. Technol.*, **37**, 225A-230A.

Taylor, T. P. 1999. Characterization and Surfactant Enhanced Remediation of Organic Contaminants in Saturated Porous Media. Dissertation, School of Civil and Environmental Engineering, Georgia Institute of Technology.

Taylor, T. P., K. D. Pennell, L. M. Abriola, and J. H. Dane. 2001. Surfactant Enhanced Recovery of Tetrachloroethylene From a Porous Medium Containing Low Permeability Lenses 1. Experimental Studies. *J. Contam. Hydrol.*, **48**, 325-350.

Taylor, T. P., K. M. Rathfelder, K. D. Pennell, and L. M. Abriola. 2003. Effects of Ethanol Addition on Micellar Solubilization and Plume Migration During Surfactant Enhanced Recovery of Tetrachloroethene. *J. Contam. Hydrol.*, **50**.

Tchelepi, H. A. 1994. *Viscous Fingering, Gravity Segregation and Permeability Heterogeneity in Two-Dimensional and Three-Dimensional Flows*. Dissertation,

Department of Petroleum Engineering, School of Earth Sciences, Stanford University.

Teel, A. L., C. R. Warberg, D. A. Atkinson, and R. J. Watts. 2001. Comparison of Mineral and Soluble Iron Fenton's Catalysts for the Treatment of Trichloroethylene. *Wat. Res.*, **35**, 977-984.

Tidwell, V. C., and R. J. Glass. 1994. X-Ray and Visible Light Transmission for Laboratory Measurement of Two-Dimensional Saturation Fields in Thin-Slab Systems. *Water Resour. Res.*, **30**, 2873-2882.

United States Environmental Protection Agency (USEPA). 1990. *Handbook, Ground Water, Volume 1: Ground Water and Contamination*. Office of Research and Development, EPA 625/6-90/016a, EPA, Washington, DC.

United States Environmental Protection Agency (USEPA). 1995. *In Situ Remediation Technology Status Report: Thermal Enhancements*. Office of Solid Waste and Emergency Response. EPA 542-K-94-009.

United States Environmental Protection Agency (USEPA). 1998. *Field Applications of In Situ Remediation Technologies: Chemical Oxidation*. Office of Solid Waste and Emergency Response. EPA 542-R-98-008.

United States Environmental Protection Agency (USEPA). 2000. *Abstracts of Remediation Case Studies, Volume 4*. Federal Remediation Technologies Roundtable. EPA 542-R-00-006.

United States Environmental Protection Agency (USEPA). 2003. *The DNAPL remediation challenge: Is there a case for source depletion?*, EPA 600-R-03-143.

United States Geological Survey (USGS). 1998. Estimated Use of Water in the United States in 1995. U.S. Geological Survey Circular 1200, Reston, VA, 6-14.

van Genuchten, M. T. 1980. A Closed Form Equation for Predicting the Hydraulic Conductivity of Unsaturated Soils. *Soil Sci. Soc. Am. J.*, B44B, 892-898.

West, C. C. 1992. Surfactant-Enhanced Solubilization of Tetrachloroethylene and Degradation Products in Pump and Treat Remediatin. In *ACS Symposium Series 491*, D.A. Sabatini and R.C. Knox (Eds.). American Chemical Society. Chapter 12.

Willson, C. S., J. T. Hall, C. T. Miller, and P. T. Imhoff. 1999. Factors Affecting Bank Formation During Surfactant-Enhanced Mobilization of Residual NAPL. *Environ. Sci. Technol.*, **32**, 2440-2446.

Winsor, P. A. 1954. *Solvent Properties of Amphiphilic Compounds*. Butterworth, London, U.K.

Wolin, F. A., M. J. Wolin, and R. S. Wolfe. 1963. Formation of Methane by Bacterial Extracts. *J. Biol. Chem.*, **238**, 2882-2886.

Wood, A. L., C. G. Enfield, F. P. Espinoza, M. Annable, M. C. Brooks, P. S. C. Rao, D. Sabatini, and R. Knox. 2005. Design of Aquifer Remediation Systems: (2) Estimating Site-Specific Performance and Benefits of Partial Source Removal, *J. Contam. Hydrol.*, **81**, 148-166.

Xu, S. and S. A. Boyd. 1995. Cationic Surfactant Sorption to a Vermiculitic Subsoil via Hydrophobic Bonding. *Environ. Sci. Technol.*, **29**, 312-320.

Yang, Y. and P. L. McCarty. 2000. Biologically Enhanced Dissolution of Tetrachloroethene DNAPL. *Environ. Sci. Technol.*, **34**, 2979-2984.

Yang, Y. and P. L. McCarthy. 2002. Comparison Between Donor Substrates for Biologically Enhanced Tetrachloroethene DNAPL Dissolution. *Environ. Sci. Technol.*, **36**, 3400-3404.

Yeh, D. H., Pennell, K. D., and S. G. Pavlostathis. 1999. Effect of TWEEN Surfactants on Methanogenesis and Microbial Reductive Dechlorination of Hexachlorobenzene. *Eviron. Toxicol. Chem.*, **18**, 1408-1416.

Zhu, J. and J. F. Sykes. 2004. Simple Screening Models of NAPL Dissolution in the Subsurface. *J. Contam. Hydrol.*, **72**, 245-258.

Zimmerman, J. B., T. C. G. Kibbey, M. A. Cowell, and K. F. Hayes. 1999. Partitioning of Ethoxylated Nonionic Surfactants into Nonaqueous-Phase Organic Liquids: Influence on Solubilization Behavior. *Environ. Sci. Technol.*, **33**, 169-176.

Zoh, K.-D. and M. K. Stenstrom. 2002. Fenton Oxidation of Hexahydro-1,3,5-Triazine (RDX) and Octahydro-1,3,5,7-Tetrazocine (HMX). *Water Resour. Res.*, **36**, 1331-1341.

VITA

ERIC JOHN SUCHOMEL

Eric John Suchomel was born to parents Tom and Sue Suchomel in June 1979. He was born in Casper, Wyoming and lived there for 2 years, before moving with his family to Douglas, Wyoming. He was valedictorian of the 1997 graduating class of Douglas High School. Mr. Suchomel attended the University of Iowa beginning in August 1997, where he pursued a degree in chemical engineering. At the University of Iowa, he was inducted into Omega Chi Epsilon, a chemical engineering honor society, and was named to the president's list in each of his eight semesters of attendance. Mr. Suchomel also served as an undergraduate research assistant in the laboratory of Dr. Jerald Schnoor. He earned a Bachelor of Science in Engineering degree with high distinction from the University of Iowa in May 2001. Mr. Suchomel began attending the Georgia Institute of Technology in August 2001 as an Institute Fellow and received as Master of Science in Environmental Engineering in May 2004. His research topic was a comparison of surfactant-based DNAPL remediation strategies. He has continued his research and academic endeavors at Georgia Tech, pursuing a doctoral degree in environmental engineering with a minor in chemical engineering. While at Georgia Tech, Mr. Suchomel has served the Association of Environmental Engineers and Scientists (AEES) as a vice president (2002-2003) and president (2003). In recognition of his research and academic accomplishments and service, he was named the 2004 AEES Outstanding Doctoral Candidate. Mr. Suchomel's recreational interests include running, hiking, and baseball.